Balochistan Journal of Engineering & Applied Sciences (BJEAS)

HEC Recognized in "Y" Category

Volume 6, No. 1

June 2023

Balochistan University of Engineering & Technology, Pakistan

Email: editor.bjeas@buetk.edu.pk

p-ISSN: 2518-2706

This Publication has been partially funded by the Higher Education Commission (HEC), Islamabad
Which highly acknowledge

Balochistan Journal of Engineering & Applied Sciences (BJEAS)

BJEAS is a biannual research journal published by the Balochistan University of Engineering and Technology (BUET) Khuzdar, through the Office of Research, Innovation and Commercialization (ORIC). It is dedicated to the dissemination of research among institutions, universities, researchers, and students with the promotion of quality on national and international levels as its main objectives.

BUETK is a renowned degree awarding institute of Engineering and Technology dedicated to providing quality education and promoting research activities in Pakistan and on international levels as well. It is a public-sector university established by the Government of Pakistan in 1987 and is approved and recognized by Higher Education Commission (HEC) of Pakistan and Pakistan Engineering Council (PEC).

Guidelines for Authors

BJEAS seeks to publish research papers that identify, extend, or unify scientific knowledge and research pertaining to engineering and applied sciences.

The researchers/ authors are requested to submit well-researched and original unpublished papers, not already submitted to another journal for publication. Papers are accepted after approval through a process of double-blind peer-reviewed by independent reviewers.

Patron-in-Chief's Message

I am delighted to have the opportunity to share a few thoughts at the time of publication of the upcoming issue of BJEAS. In this era of technological advancements, it is necessary that research work carried out in various engineering and sciences disciplines is recognized and propagated properly. BJEAS is a step towards disseminating high-quality research nationally as well as globally while maintaining the unique recognition of Balochistan. I believe that this Journal will become a hallmark of research in the future. As Patron-in-Chief, I will ensure that BJEAS remains in line with rapidly shifting scientific communication landscape, while also maintaining and intensifying the high standards of academic excellence.

I sincerely hope that research articles published by BJEAS will provide insightful and stimulating information to readers and scholars that will shape our future and lead the way to extraordinary discoveries.

Prof. Engr. Dr. Maqsood Ahmed
Vice Chancellor
Balochistan UET, Khuzdar

Aims of Journal

BJEAS is a quality publication of peer-reviewed and refereed journal from diverse fields in sciences, Engineering and Technologies that emphasizes new research, development and their applications. BJEAS provides an open-access forum for scientists, scholars, researchers and engineers to exchange their research work, technical notes & surveying results among professionals through print and online publications.

Scope of Journal (but not limited to)

- Applied science
- Mathematics
- Electrical engineering
- Computer engineering
- Electronic engineering
- Optical engineering
- Power engineering
- Mechanical engineering
- Acoustical engineering
- Manufacturing engineering
- Thermal engineering
- Vehicle engineering
- Automotive engineering
- Aerospace engineering
- Bioprocess engineering
- Food engineering
- Aquaculture engineering
- Applied engineering
- Automation/Control systems/Robotics
- Computer-aided drawing and design
- Construction
- Electronics
- Manufacturing
- Graphics
- Biological engineering
- Nanotechnology
- Genetic engineering
- Biomedical engineering
- Biological organisms
- Biochemical engineering
- Protein engineering
- Tissue engineering
- Energy engineering
- Building services engineering
- Manufacturing engineering
- Industrial engineering
- Systems engineering
- Component engineering
- Textile engineering
- Construction engineering
- Reliable engineering
- Safety engineering
- Nano engineering
- Mechatronics
- Petroleum engineering
- Chemical engineering

Review Policy of Journal

This journal has zero tolerance against plagiarism. All submitted papers are scanned through an Approved Plagiarism detection software as per HEC guidelines. After plagiarism check, the papers are reviewed under double-blind peer review process.

Submission and acceptance of papers depend upon the response of the reviewers. Plagiarism checking, and review process may take from four weeks to eight weeks depending upon the response from the reviewers and compliance from authors. After satisfactory review, the Editorial Board accepts the paper for publication and an acceptance letter is issued to the author(s).

INTERNATIONAL EDITORIAL ADVISORY BOARD

NATIONAL EDITORIAL ADVISORY BOARD

EDITORIAL REVIEWER BOARD

TABLE OF CONTENTS

Volume 4 No. 1 June 2023

Balochistan Journal of Engineering & Applied Sciences (BJEAS) – (p-ISSN: 2518-2706
Volume 6, No.1

Arduino based Fault Location in under-Ground Power Cables

Saeed Ahmed Shaikh[1], Abdul Hameed Soomro[1], Assad Ullah Khauhwar[1], Dureshahwarana[3], Satish Kumar Jeswani[3]
[1]Faculty, Department of Electrical Engineering, Quaid-e-Awam University of Engineering Science and Technology Nawabshah Campus Larkana, Sindh Pakistan
[3]Students, Department of Electrical Engineering, Quaid-e-Awam University of Engineering Science and Technology Nawabshah Campus Larkana, Sindh Pakistan
Correspondence Author: Abdul Hameed Soomro, Email: abdul.hameed@quest.edu.pk

***Abstract*—The electrical power system consists of different components, such as alternators, motors, transformers, transmissions, and distribution lines. From these components, the lines are the major components that supply the electrical power to consumers for utilization. The overhead and underground systems are approaches to power transmission and distribution systems. The overhead power system is affected by natural disasters, snowfall, storms, heavy rains, wind, and earthquakes. Overhead lines are harmful for humans and also for animals. Overhead lines contaminate the natural beauty of the environment, especially streets. The underground lines are not affected by natural environmental disasters, keep the environment clean, and are not harmful to humans or animals under fault conditions. The main drawback of underground lines is that they lie deep underground and are not visible, so whenever a fault occurs, repairmen will have to dig up the whole area where the cables are lying to search for the fault point. More time and energy are required to detect and locate the fault and also correct it. In the past, several methods were applied, such as the tracer technique, terminal technique, sectionalizing, and thumping, but due to their drawbacks, an Arduino-based fault detection system and its location are proposed in this research paper to analyse the fault in the different phases of underground transmission lines and display it on an LCD. It will result in reduced maintenance costs and ease in locating faults in the transmission and distribution underground lines. The prototype of a fault locator based on Arduino was developed in the laboratory of QUEST Campus Larkana.**

Index Terms: Arduino, Underground Fault, Fault Location

I.INTRODUCTION

The electrical power system consists of different components, such as transformers, transmission and distribution lines, etc. From these components, the lines are the major components that supply the electrical power to consumers for utilisation [1]. The transmission and distribution lines are badly affected by the fault [2]. Overhead lines and underground power systems are the two basic approaches to transmitting and distributing electrical power [3]. The overhead power system is affected by natural disasters, snowfall, storms, heavy rains, wind, and earthquakes [4]. Overhead lines are harmful for humans and also for animals [5], and they affect the natural beauty of the environment, especially streets [6]. The underground power system is most reliable, has a lower maintenance cost, less transmission and distribution losses, and is free from snowfall, wind, and earthquakes [7, 8]. The world is moving towards an underground power transmission and distribution system to deliver reliable power to consumers [9]. Pakistan's large cities and some areas have underground power systems [10]. The drawback of underground power systems is that if faults occur, they will not be easy to repair and trace out [11]. In the past, several methods were applied, such as the tracer technique, terminal technique, sectionalizing, and thumping, but due to their drawbacks [12], such as the tracer technique, electromagnetic signals or audible signals are taken through walking on a cable line, where faults occur, which will result in time consumption, revenue loss, and an increase in labour costs [13]. In the terminal technique, one end terminal of the cable or both ends of the cable terminals are tested through a test set [14]. In sectionalizing, the cables are required to be cut into sections or subsections; each section is tested with an ohmmeter or high-voltage insulation resistance [15]. In thumping, a high voltage is required, which results in a high current being produced to make enough noise to hear [16]. In control centres, large alarms and SMS are received during fault conditions, and the operator analyses the data to make a decision [17]. If a fault occurs in distribution lines, then it is necessary to locate the fault urgently to restore the supply [18]. The electrical power system network is more complex, so it is necessary to install a proper fault locator to locate the fault in the underground system in order to save time and revenue [11]. Most transmission companies still rely on the circuit indicators to locate the fault in the underground power system [19]. Although fault indicators are the most reliable means for fault location, the technical team and petrol teams are still physically in the vehicle and inspect the device for longer hours to detect the faulty section of their underground transmission system [20]. In this research study, the prototype on the QUEST campus in Larkana based on Arduino for monitoring the underground power system for the location of faults on the LCD is presented and validated under different fault distances, which results in a reduced time for locating the fault and carrying out the maintenance to restore the supply in the minimum amount of time [21]. Figure 01 shows the block diagram of the proposed system.

A. Motivation

In the current scenario, developing countries are replacing the overhead power system with an under-ground system due to the lower chance of a fault occurring and the greater reliability of the overhead power system, but if a fault occurs, it is necessary to trace it out within a short

period of time; otherwise, it will result in revenue loss to the utility company and increase the labour cost [9]. Pakistan's large cities and some areas have underground power systems [10]. In this research study, the Arduino UNO device is utilised to trace out the underground fault without waste of time, and continuity of supply will be maintained within the shortage period [11].

B. Related work

The tracer technique of fault was presented by Hassoun et al. in 2000 [22], but this technique will result in time-consuming, revenue-loss, and an increase in labour costs [13]. In 2011, Liu et al. presented the terminal technique [23], in which one end terminal of the cable or both ends of the cable terminals are tested through a test set. Linli et al. presented their research in 2012 on the sectionalizing method, but in this technique, the cables are required to be cut into sections or subsections, and each section is tested with an ohmmeter or high-voltage insulation resistance [15]. In 2014, Ali et al. presented the thumping method for fault location [24], but in this method, a high voltage is required, which results in a high current being produced to make enough noise to hear [16]. In 2018, Samapatharaja et al. presented research on IOT-based fault location [14], but the authors only located the single-phase fault. In 2020, Arifin et al. presented research on the location of a fault through Arduino but tested it under a fault up to a fixed distance [25].

C. Problem Statement

It has been seen from a literature survey that the methods such as thumbing, terminal technique, and tracer technique presented in past research are not appropriate for the location of the fault, resulting in a reduction in revenue for the utility company, high labour costs, and more time to locate the fault 22–24]. Research was carried out in 2020 through Arduino, but the performance was analysed in different phases, but accuracy was not considered [25].

1.1 Problem Solution

In this research study, the prototype of Arduino is developed and analysed for performance through applications where Arduino is installed at the same distance of fault and at different distances of fault to measure accuracy because such a device is the selection as compared to the other techniques discussed in the literature review to locate the fault in underground power cables [25].

D. Contribution

In this research paper, each author has contributed equally to developing the prototype of the Arduino for fault location in an underground system, involving no conflict of interest.

E. Organization of Research Paper

Section 2 describes the Arduino,
Section 3 describes the Methodology,
Section 4 describes the Results and discussions,
Section 5 describes the conclusions.

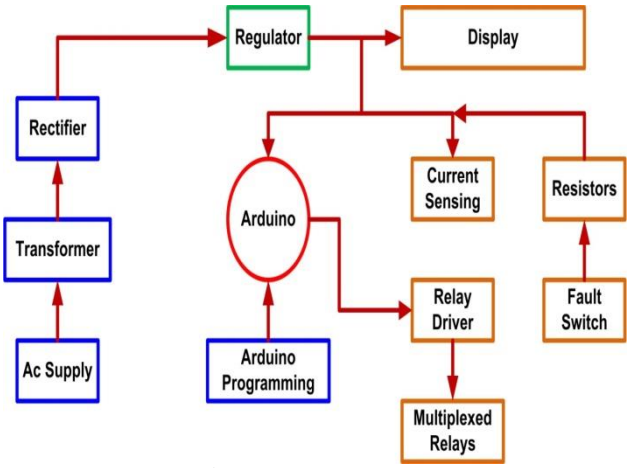

Fig. 01 Block diagram of Proposed System

II. ARDUINO UNO

Arduino UNO is an open-supply platform to develop projects based on electronics [26]. It consists of a microcontroller and a software bit used in laptops with programming [27]. The Arduino is more famous for the right reasons and does not require a piece of separate hardware that will load new code onto the board, so we can use the USB cable [28]. Finally, Arduino provides the latest thing that breaks out the capabilities of the microcontroller [29]. Figure 02 shows the hardware model of Arduino.

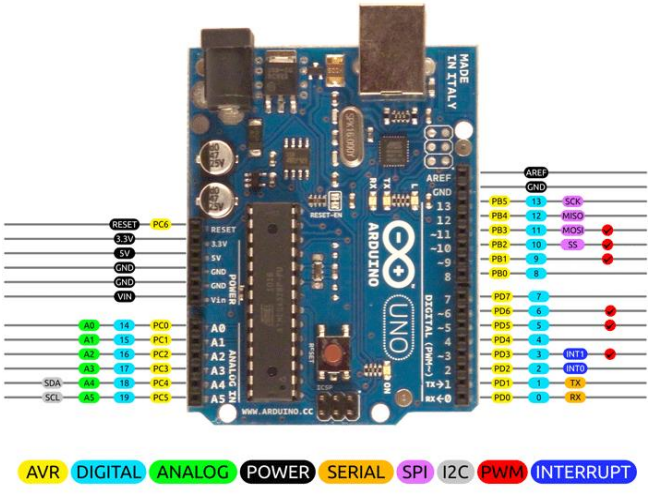

Fig. 02 Hardware Model of Arduino

A. Arduino Ide

The software used to programme an Arduino is called Arduino E. Arduino IDE is open-source software available for research purposes [30, 31]. This Arduino IDE can be downloaded to one's laptop or computer based on the operating system. The Arduino IDE can be programmed in both java and C++ languages. Arduino is connected to a computer or laptop through its USB data cables [32]. Arduino IDE has features such as compile, upload, save, and open and has multiple libraries for all types of sensors. The compile option is used to feature check the programmeme; the upload button is used to upload or dump code to the Arduino board; the save option is used to save the particular programmeme

to a specified file; and the open feature allows the user to open pre-written code from files [33].

B. *Components of Arduino*

The different components are used [29] in Arduino, such as relays. The relay is a sensing device; under normal operating conditions, the contacts of the relay are closed. When the relay contact is opened, power is supplied to the circuit. When the relay is switched off, it will produce voltage spikes that will be harmful, so diodes and resistors are connected to overcome this problem. Vero board is an original prototyping board made of copper-clad laminate and available in both-sided format. On the Vero board, we can easily fix the components and wires for the development of prototype circuits. The resistor consists of two leads and has no polarity, so we can connect from either side. Resistors are used to limit the flow of current. An LCD is used to display the data. It has 16 columns and two rows. A potentiometer is a manually adjustable resistor with three terminals. Two terminals are connected to the end of the resistive element, and the third terminal is connected to a sliding contact, also known as a wiper. We can adjust the resistance of the potentiometer by rotating the wiper. An adapter is used to convert the AC into a DC supply. It is a mechanical switch that slides from ON to OFF position to allow the current in control circuits without any need for a cut wire. An LED is a semiconductor light source that emits light when current flows through it. A rectifier is used to convert DC into AC.

III. METHODOLOGY

This research study is based on Ohm's law. If low-voltage DC is applied to the feeder and through series resistors, the current would vary depending upon the location of the fault in the cable, as the resistance is proportional to the distance. Whenever a fault occurs in a cable, the Arduino detects and displays it on the LCD, and a buzzer produces an alarm to alert and prompt field workers to take immediate action. In this model, two lines of fault and three phases of fault are considered. All types of faults will display on the LCD screen. In the first stage, DC power of 12 volts is supplied, and with the help of a voltage regulator, the 12 volts are regulated to 5 volts of DC power. This 5V DC is used to deliver power to the Arduino. Now this 12-volt power supply will flow in a line-to-line circuit and also in a line-to-ground circuit, which is attached in parallel with the line-to-line circuit. Now, if we switch on any switch, it will show on the LCD. If a fault occurs in the red phase at a distance of 6 km, then ultimately the red bulb will turn off, as we can see on the LCD. The fault switches have two positions: the no fault position (NF) and the fault position (F). The LM7805 transmission module is used to step down the flow of power and give it to the relay module. The relay module works on a cycle; if a fault occurs, it will operate automatically within one second and display it on the LCD. In this method, the Arduino Uno controls the whole system through the indication of three different bulbs that show R-Y-B loads through a 1-channel relay, as shown in Figure 3, and Figure 4 shows the flow chart of the Arduino-based fault location.

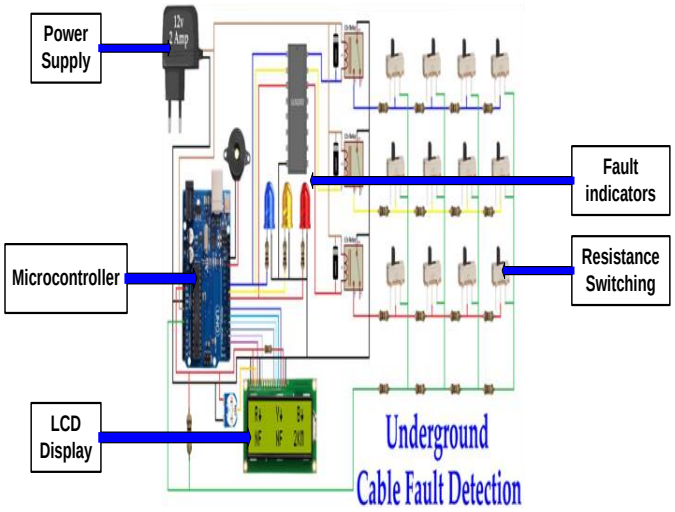

Fig. 3 Arduino based fault location.

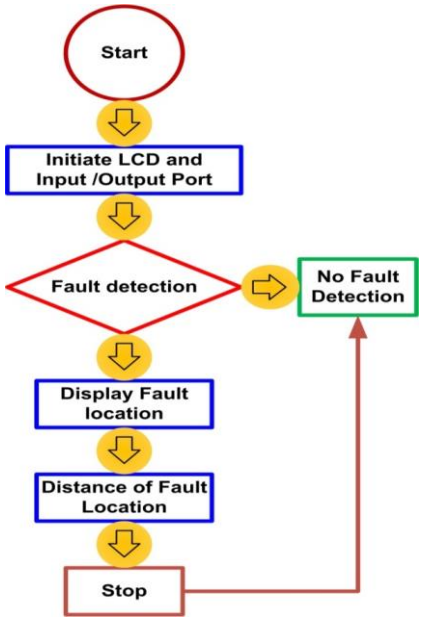

Fig. 4 Flow chart of Arduino UNO

A. *results and discussions*

Resistors are used in transmission lines. If there is no fault at any phase, the LCD will display NF (no fault). When faults occur in the red phase, the LCD will display the fault in terms of KM in the red phase. The second switch is used to indicate the fault in the red phase, the third switch is used to indicate the yellow phase, and the fourth switch is used to indicate the fault in the blue phase on the LCD.

B. *Accuracy of Arduino at Different Distances*

In this stage, the fault is applied in the red phase, and the LED is switched on to display the fault on the LCD. In this condition, we have applied a fault beyond the actual distance of the fault and measured the accuracy of the proposed system. We have seen that the accuracy of Arduino is not 100% even with small changes, and the results are tabulated in Table 1.

C. *Accuracy of Arduino at the same distance*

In this stage, the fault is applied in the red phase, and the LED is switched on to display the fault on the LCD. In

this condition, we have applied a fault at the same distance and measured the accuracy of the proposed system. We have seen that the accuracy of Arduino is 100%, and the results are tabulated in Table 2. Prototype design and working are shown in figures 5 and 6.

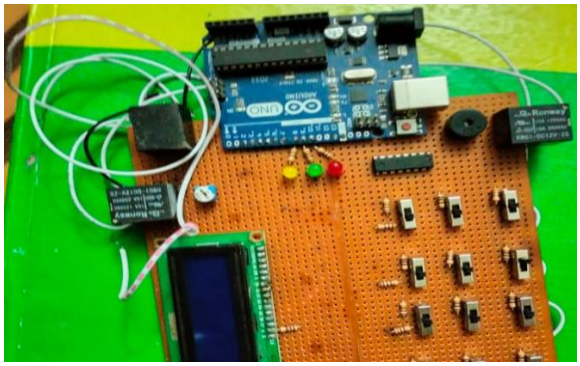

Fig. 5 Design of Prototype of proposed system

Fig. 6 Working of Prototype of proposed system

Table 01 location of Fault at Different distance

S.No	Actual Fault Distance	Fault Distance	Accuracy %
1	30 km	29.8 km	99.33
2	40 km	39.2 km	98
3	50 km	51.7 km	96.6
4	40 km	40.2 km	99.50
5	50 km	54.3 km	91.4

Table 02 location of Fault at Same distance

S.No	Actual Fault Distance	Fault Distance	Accuracy 1
1	20 km	20.0 km	100
2	30 km	30.0 km	100
3	40 km	40.0 km	100
4	50 km	50.0 km	100

D. Discussion

It has been seen from the results that the Arduino-based technique is a better approach to locating the fault in an underground power system. The accuracy depends on the fault distance; if the fault distance is small or large, the accuracy will vary, but if the fault distance is the same as the actual distance, the accuracy of the fault location will be 100%.

IV. CONCLUSIONS

This research study is proposed to detect the accurate location of the fault in the underground cables from the feeder end in km by using an Arduino microcontroller. The Arduino microcontroller is based on the output of the cable resistance. Relay helps to separate the faulty line from the healthy line. In this model, line-to-line, line-to-ground, double-line-to ground, three-phase-balanced faults occur, and the system detects this fault and displays it on the LCD. Considerable efforts were taken to locate the fault in an underground cable power infrastructure, but due to the drawbacks of past technologies, a simple ohm's law-based technology such as Arduino-based fault location was designed and developed in the laboratory of QUEST campus Larkana to analyse the performance under the same and different fault distances. This research study results in easily clearing the faults, high efficiency, a reduction in the time duration of excavation, and reduced cost.

ACKNOWLEDGMENT

We are thankful to QUEST Campus Larkana to provide facility for developing the Prototype of Arduino for underground fault location.

REFERENCES

[1] A. H. Bagdadee and L. Zhang, "A review of the smart grid concept for electrical power system," *Research Anthology on Smart Grid and Microgrid Development*, pp. 1361-1385, 2022.

[2] P. S. Kundur and O. P. Malik, *Power system stability and control*: McGraw-Hill Education, 2022.

[3] A. Hermann, T. V. Jensen, J. Østergaard, and J. Kazempour, "A complementarity model for electric power transmission-distribution coordination under uncertainty," *European Journal of Operational Research*, vol. 299, pp. 313-329, 2022.

[4] A. Z. El Dein, O. E. Gouda, M. Lehtonen, and M. M. Darwish, "Mitigation of the Electric and Magnetic Fields of 500-kV Overhead Transmission Lines," *IEEE Access*, vol. 10, pp. 33900-33908, 2022.

[5] K. O. Papailiou and G. L. Ford, "Overhead Transmission Line Asset Sustainment Investment," in *Power System Assets: Investment, Management, Methods and Practices*, ed: Springer, 2022, pp. 273-285.

[6] I. Blinov, I. O. Zaitsev, and V. V. Kuchanskyy, "Problems, methods and means of monitoring power losses in overhead transmission lines," in *Systems, Decision and Control in Energy I*, ed: Springer, 2020, pp. 123-136.

[7] A. Prasad, J. B. Edward, and K. Ravi, "A review on fault classification methodologies in power transmission systems: Part—I," *Journal of electrical systems and information technology*, vol. 5, pp. 48-60, 2018.

[8] A. A. Khan, N. Malik, A. Al-Arainy, and S. Alghuwainem, "A review of condition monitoring of underground power cables," in *2012 IEEE International Conference on Condition Monitoring and Diagnosis*, 2012, pp. 909-912.

[9] C. L. Bak and F. F. da Silva, "High voltage AC underground cable systems for power transmission–A review of the Danish experience, part 1," *Electric Power Systems Research*, vol. 140, pp. 984-994, 2016.

[10] M. S. Shaikh, M. M. Ansari, M. A. Jatoi, Z. A. Arain, and A. A. Qader, "Analysis of underground cable fault techniques using MATLAB simulation," *Sukkur IBA Journal of Computing and Mathematical Sciences*, vol. 4, pp. 1-10, 2020.

[11] R. M. Asif, S. R. Hassan, A. U. Rehman, A. U. Rehman, B. Masood, and Z. A. Sher, "Smart underground wireless cable fault detection and monitoring system," in *2020 International Conference on Engineering and Emerging Technologies (ICEET)*, 2020, pp. 1-5.

[12] S. Dheeban, S. N. Muthu, and L. Krishnaveni, "IoT Based Underground Cable Fault Detection," *Smart Grids and Microgrids: Technology Evolution*, pp. 273-294, 2022.

[13] R. Rengaraj, G. Venkatakrishnan, S. Shalini, R. Subitsha, S. Suganthi, and S. S. Carolyn, "Identification and classification of faults in underground cables–A review," in *IOP Conference Series: Materials Science and Engineering*, 2021, p. 012018.

[14] N. Sampathraja, L. A. Kumar, V. Kirubalakshmi, C. Muthumaniyarasi, and K. V. Murthy, "IoT based underground cable fault detector," *International Journal of Mechanical Engineering and Technology*, vol. 8, pp. 1299-1309, 2018.

[15] B. Lanz and E. Sanchez, "Is Fault Location Killing Our Cable Systems?," in *2016 IEEE/PES Transmission and Distribution Conference and Exposition (T&D)*, 2016, pp. 1-5.

[16] N. Murugan, J. Senthil Kumar, T. Thandapani, S. Jaganathan, and N. Ameer, "Underground cable fault detection using internet of things (IoT)," *Journal of Computational and Theoretical Nanoscience*, vol. 17, pp. 3684-3688, 2020.

[17] A. J. Pansini, *Electrical distribution engineering*: River Publishers, 2020.

[18] R. P. K. Naidu and S. Meikandasivam, "Power quality enhancement in a grid-connected hybrid system with coordinated PQ theory & fractional order PID controller in DPFC," *Sustainable Energy, Grids and Networks*, vol. 21, p. 100317, 2020.

[19] N. Roshan, R. A. K. Langah, and S. Ayoob, "Underground Cable Fault Distance Locator over GSM Technology," *iKSP Journal of Emerging Trends in Basic and Applied Sciences*, vol. 1, pp. 1-7, 2021.

[20] E. Bjerkan, "Efficient fault management using remote fault indicators," in *CIRED 2009-20th International Conference and Exhibition on Electricity Distribution-Part 1*, 2009, pp. 1-4.

[21] B. Sarker, S. Y. Radin, S. H. Zahedee, and T. T. I. Shanto, "Arduino based power system protection," Brac University, 2021.

[22] S. Hassoun, T. McBride, and D. A. Russell, "Development of perfluorocarbon tracer technology for underground leak location," *Journal of Environmental Monitoring*, vol. 2, pp. 432-435, 2000.

[23] C.-W. Liu, T.-C. Lin, C.-S. Yu, and J.-Z. Yang, "A fault location technique for two-terminal multisection compound transmission lines using synchronized phasor measurements," *IEEE Transactions on Smart Grid*, vol. 3, pp. 113-121, 2011.

[24] M. S. Ali, A. H. Abu Bakar, H. Mokhlis, H. Arof, and H. Azil Illias, "High- impedance fault location using matching technique and wavelet transform for underground cable distribution network," *IEEJ Transactions on Electrical and Electronic Engineering*, vol. 9, pp. 176-182, 2014.

[25] F. M. Arifin, M. Hasan, I. Mahyudin, and S. Arshad, "Development of fault distance locator for underground cable detection," in *Journal of Physics: Conference Series*, 2020, p. 012014.

[26] S. A. Arduino, "Arduino," *Arduino LLC*, vol. 372, 2015.

[27] Y. A. Badamasi, "The working principle of an Arduino," in *2014 11th international conference on electronics, computer and computation (ICECCO)*, 2014, pp. 1-4.

[28] D. Kushner, "The making of arduino," *IEEE spectrum*, vol. 26, pp. 1-7, 2011.

[29] A. A. Galadima, "Arduino as a learning tool," in *2014 11th International Conference on Electronics, Computer and Computation (ICECCO)*, 2014, pp. 1-4.

[30] L. Louis, "working principle of Arduino and u sing it," *International Journal of Control, Automation, Communication and Systems (IJCACS)*, vol. 1, pp. 21-29, 2016.

[31] M. Fezari and A. Al Dahoud, "Integrated development environment "IDE" for Arduino," *WSN applications*, pp. 1-12, 2018.

[32] N. Zlatanov, "Arduino and open source computer hardware and software," *J. Water, Sanit. Hyg. Dev*, vol. 10, pp. 1-8, 2015.

[33] O. Amestica, P. Melin, C. Duran-Faundez, and G. Lagos, "An experimental comparison of Arduino IDE compatible platforms for digital control and data acquisition applications," in *2019 IEEE CHILEAN Conference on Electrical, Electronics Engineering, Information and Communication Technologies (CHILECON)*, 2019, pp. 1-6.

Balochistan Journal of Engineering & Applied Sciences (BJEAS) – (p-ISSN: 2518-2706
Volume 6, No.1

Numerical Analysis of Non-Newtonian Fluid Flows Through an Annulus Occupied With Or Without Porous Materials

Rahim Bux Khokhar[1], Afaque Ahmed Bhutto[2], Iftikhar Ahmed Bhutto[3], Abdullah Mengal[4], Fozia Shaikh[1], Asif Ali Shaikh[1,5]
[1,2]Department of Basic Sciences and Related Studies, Mehran University of Engineering and Technology, Jamshoro - 76062, Pakistan
[2]Department of Basic Sciences and Related Studies, Quaid e Awam University of Engineering, Science and Technology, Larkana campus - 77150, Pakistan.
[3]Department of Mathematics Sukkur IBA University, Pakistan.
[5]Department of Mathematics, Near East University, 99138 Mersin, Turkey.
Corresponding Author: afaq_bhutto@quest.edu.pk

***Abstract*—Fluid flow modeling in complex geometries through porous media has fascinated and challenged applied mathematicians and engineers for decades. It has great importance in various industries, including petroleum, food processing, and pharmaceuticals. This study looks at how non-Newtonian inelastic fluids behave in an annulus that is filled with a medium that lets fluids pass through it. The medium can combine and separate flow regimes. The finite element approach with the Taylor-Galerkin/Pressure-Correction scheme is used in this work. The flow consists of two reversible configurations inside a porous material-filled annulus with a sudden gap. Variations in flow rates, inertia intensification, and porosity are examined in this study.**

***Keywords*—** *Finite Element Mesh, Uniform Conformal Mapping, Mixing And Separating Flows, Annular System*

I. INTRODUCTION

Due to numerous industrial and practical applications, research on the flow of non-Newtonian inelastic fluids through intricate channels and pipes containing porous or non-porous mediums has recently attracted significant attention from engineers and scientists. Specifically in oil and gas industrial applications like improved recovery of petroleum, dripping operations, thermal insulation, porous bearing, solar cells, radiators, nuclear reactors, compacted bed reactors, biomechanics, chromatography, food, pharmaceuticals, biotechnology, screening processes, geothermal engineering, and many others [1–3]. Utilising inelastic fluids, which have extremely complicated rheological behaviour, may be a challenging element in many procedures. According to the literature, various researchers [1–4] have examined the hydrodynamic properties and thermal behaviour of inelastic flows via porous channels. The constitutive model was utilised for viscoelastic simulations, a category of shear-thinning (PTT), to computationally represent the consequences of shear-thinning impacts on alterations in space size between appended parallel plates. In essence, shear thinning is a natural characteristic of many fluids, including lubricants and polymers [5], and has continued to be an important and fascinating subject in the realm of CFD, which is often utilised in industries.

Several studies have been conducted on how mixing and reversing flows of non-Newtonian inelastic fluids behave in circular pipes [1][28]. The impact of inertia on such flow structure, and pressure transition are of particular interest. The critical role of inertia is revealed by observing the flow and behavior of fluid inside the pipe/channel [2, 6, 9-13]. Th–13]. lude the production of flow transitions and the emergence of singularities at steep bends [16]. Due to its importance for several real-world applications, the behavior behaviour flows in complicated domains is of particular interest [7, 8]. The mixing and separating flow of extremely elastic fluids was studied by Baloch [9] adopt[9], a time-dependent finite element method with Taylor-Petrov-Galerkin algorithms [10, 15]. He additionally applied the pressure-correction method to incompressibility to achieve second-order accuracy.

In recent years, modern high-speed computer technology has progressed to the point where complex numerical algorithms have been designed. International organizations have strengthened the practical use of computer simulations to evaluate complex fluid dynamics in a region with permeable materials [13]. Due to its capacity for performing constraint-based simulations, the Computational Fluid Dynamics (CFD) method is anticipated to manifest a specific feature. Significant advancements have been made in the previous three decades in our understanding of numerical uncertainties and flow types, including unsteady and turbulent [14]. Mathematical representation of the flow phenomena involving both mixing and separation, combined with additional adjustments, see the initial work of [11, 14], solved experimentally and numerically adopting numerical technique analyses by Baloch et al. [9].

The main motivation behind the present work is to formulate, estimate, and analyze a numerical approach to address the transient hydrodynamics characteristics involved in mixing and separating non-Newtonian inelastic fluids inside an annular gap filled with or without a porous media. Wide parameter ranges of inertia are explored using a sophisticated computational method, and relative flow rates are of relevance to this study.

A. *Problem specification*

A schematic representation of the two-dimensional annular system under investigation is shown in Figure 1(a). The horizontal annular pipe or conduit has an inner pipe with a radius of Ri that fits within the outer pipe with a radius of Ro. A two-dimensional axisymmetric computational domain is assumed to have a length of 23R and a non-dimensional thickness of α = 0.0245, where R is the inner pipe's characteristic radius. The separation with the width β =3L is produced at the wall of the inner pipe at the centre in such a way that fluid is mixing and separating in both pipes. A small-radius inner pipe is included in the sizable conduit domain, creating twin inlets and outlets. Figure 1(b) shows a finite element mesh on the domain under consideration. IDEAS software and FORTRAN programming are employed to discretize the flow domain in the computational domain, utilising triangular components produced by uniform conformal mapping. The mesh provides a total of 5049 elements, 19057 nodes, and 73953 degrees of freedom to be used in the analysis.

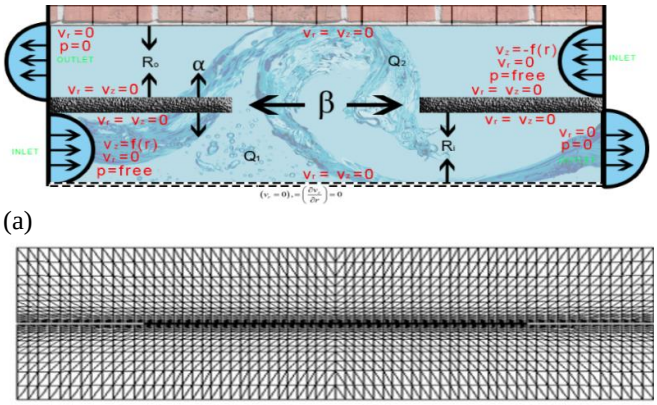

(a)

(b)

Fig. 1 (a) Geometry of mixing and unraveling fluid flows in a tubular pipe, (b) Finite element mesh.

To understand the behaviour of an inelastic non-Newtonian fluid, a few models (Bird-Carreau and Power Law) have been examined. The impact of the fluid's functional viscosity in a pipe is examined in relation to the shear rate. By changing the number and modifying the stream rates in the external tube, increasing degrees of inertia are introduced. This makes it possible to examine how inertia affects flow patterns and pressure differences.

B. *Mathematical Formulation*

In an annular, permeable medium, two-dimensional axisymmetric non-Newtonian incompressible fluid is flowing in a pipe while the flow is fully established at both inlets. The abrupt imposition of a pressure gradient causes the fluid flow to be erratic. The equations of continuity and generalised momentum balance (Darcy-Brinkman), which control flow, are used to develop a mathematical model of the flow by taking cylindrical polar coordinates into account.

$$\frac{1}{r}\frac{\partial}{\partial r}(rv_r)+\frac{\partial v_z}{\partial z}=0 \quad (1)$$

r- component:

$$\rho\left(\frac{\partial v_r}{\partial t}+v_r\frac{\partial v_r}{\partial r}+v_z\frac{\partial v_r}{\partial z}\right)=\left(\frac{1}{r}\frac{\partial}{\partial r}(r\tau_{rr})-\frac{\tau_{\theta\theta}}{r}+\frac{\partial}{\partial z}\tau_{rz}\right)-\frac{\partial p}{\partial r}-\frac{\mu}{\rho\kappa}v_r \quad (2a)$$

z- component:

$$\rho\left(\frac{\partial v_z}{\partial t}+v_r\frac{\partial v_z}{\partial r}+v_z\frac{\partial v_z}{\partial z}\right)=\left(\frac{1}{r}\frac{\partial}{\partial r}(r\tau_{rz})+\frac{\partial}{\partial z}\tau_{zz}\right)-\frac{\partial p}{\partial z}-\frac{\mu}{\rho\kappa}v_z \quad (2b)$$

Where v_z and v_r are velocity components, p is pressure, ρ is density and μ signifies the thickness of fluid stuff, t is time, and κ is the permeability of porous media. The shear and normal stress components are articulated in the following form [17]:

$$\tau_{rr}=2\mu(\dot{\gamma})\frac{\partial v_r}{\partial r} \quad (3)$$

$$\tau_{rz}=\mu(\dot{\gamma})\left\{\frac{\partial v_r}{\partial z}+\frac{\partial v_z}{\partial r}\right\} \quad (4)$$

$$\tau_{zz}=2\mu(\dot{\gamma})\frac{\partial v_z}{\partial z} \quad (5)$$

$$\tau_{\theta\theta}=2\mu(\dot{\gamma})\frac{v_r}{r} \quad (6)$$

here, γ and $\mu(\dot{\gamma})$ are the shear rate and the functional viscosity of the fluid respectively.

C. *.Initial and boundary conditions*

The initial and boundary conditions are essential for presenting a well-posed flow of fluid in a pipe problem specification. To provide a precisely formulated problem statement for the fluid flow in a pipe, it must incorporate suitable prerequisites. To provide v_0 at starting value of time, the following initial condition is used:

$$v_r(r,z,t)=v_r^0(r,z,0) \quad (7)$$

$$v_z(r,z,t)=v_z^0(r,z,0) \quad (8)$$

$$p(r,z,t)=p^0(r,z,0) \quad (9)$$

Where,

$$\nabla\cdot v^0=0 \quad (10)$$

The suitable boundary conditions on Γ as:

$$v=g_1(x,t)\ on\ \Gamma_1 \quad (11)$$

$$(\sigma.n)=g_2(x,t)\ on\ \Gamma_2 \quad (12)$$

Where, $v\cong(v_r,v_z)$

Here the enfolding domain is the unit apparent normal to the boundary, signifies the velocity vector stipulated on, allocates the traction vector articulated on, and is the Cauchy's stress tensor. It should be noted that mixed velocity-traction boundary conditions are also possible. Finally, if diminishing tractions are enforced, the specified velocity must meet consistency conditions.

In order to prevent indefiniteness or a fluid dynamic discrepancy, a consistent pressure datum must be provided up to an arbitrary constant in this situation. On solid walls, the no-slip condition is mandated, while the Dirichlet condition and Neumann condition for the axial component are mandated on the axis of symmetry.

D. *Numerical scheme*

The simulation methods are based on convergence rate, efficiency, and robustness. According to published research [9, 17, 18], semi-implicit procedures are preferable for explicit systems, which have a sluggish rate of convergence. Generally, implicit approaches are employed to improve numerical stability; nevertheless, these methods are not computationally more expensive.

E. Taylor–Galerkin/Pressure–Correction Scheme

A multi-stage finite element method is the preferred approach here. In the initial phase of the approach, a pressure-correction technique (Taylor-Galerkin) was used for non-Newtonian fluids [19]. The present investigation has been taken into consideration in order to achieve second-order correct solutions in accordance with the theories of [20] and to build on the work of [21]. The momentum equation was improved by adding Darcy's term to a FORTRAN computer programme for flow through porous material that was constructed based on the Taylor-Galerkin/pressure-correction method. A fully discrete system is derived by defining appropriate finite-dimensional subspaces of The equations are solved using a mixed velocity-pressure formulation after being spatially discretized using the Galerkin weighted residual approach. Piecewise quadratic and piecewise linear functions are used to portray velocity and pressure over a triangular mesh subdivision. The equations estimate the velocity (,) and pressure p over each element.

The main idea behind this plan is to find a way to use an expensive and pretty accurate transient scheme to find both temporary and permanent solutions to problems with fluid flow. The approach uses Taylor series expansions to produce temporal discretization. The Lax-Wendroff approximation technique is used to ensure the second-order temporal correctness of the desired results. The approach additionally encapsulates temporal derivatives and consistent spatial derivatives' higher-order precision. Compared to the Euler-Galerkin and Finite Difference approaches, the algorithm significantly improves accuracy and stability [19].

Chorin first proposed the pressure-correction/projection approach in 1968 [22], and Fortin et al. explicitly presented it in 1971 [23]. The pressure and velocity fields are decoupled, and a linearized momentum study is usually used to obtain second-order precision and stability [24, 25]. The semi-implicit approach is recommended for situations with considerable diffusion-dominated flows since it is noticed as numerically accurate, computationally effective, and reliable.

F. Semi-implicit time-stepping scheme

A semi-implicit time-stepping method is a numerical approach that offers the solution of partial differential equations (PDEs) with stiff and non-stiff components. This approach seeks to produce exact results using three Jacobi mass-matrix iterations. Conventional time steps are used when applying a semi-implicit technique to the Newtonian. Literature [26] suggests that a relative increment tolerance of 10^{-1} times the time step should be allowed in order to obtain steady-state solutions. Studies have shown that semi-implicit approaches have higher rates of convergence than explicit methodologies [27].

The details of the discrete semi-implicit equations that incorporate Darcy's component are as follows:

Stage–1(a):

$$\left[\frac{2}{\Delta t}M+\frac{1}{Re}\left(\frac{S_{rr}}{2}+\frac{M}{D_a}\right)\right]\left(V_{r,j}^{n+\frac{1}{2}}-V_{r,j}^{n}\right)=\left[-\frac{1}{Re}\{S_{rr}+S_{rz}\}V_{r,j}-J_1^{\dagger}P_k\right]^{n}-N(V)V_{r,j}^{n}-\frac{1}{ReD_a}MV_{r,j}^{n}. \quad (13)$$

Stage–1(b):

$$\left[\frac{1}{\Delta t}M+\frac{1}{Re}\left(\frac{S_{rr}}{2}+\frac{M}{D_a}\right)\right]\left(V_{r,j}^{*}-V_{r,j}^{n}\right)=\left[-\frac{1}{Re}\{S_{rr}+S_{rz}\}V_{r,j}-J_1^{\dagger}P_k^{n}\right]^{n}-N(V)V_{r,j}^{n+\frac{1}{2}}-\frac{1}{ReD_a}MV_{r,j}^{n}. \quad (15)$$

$$\left[\frac{1}{\Delta t}M+\frac{1}{Re}\left(\frac{S_{zz}}{2}+\frac{M}{D_a}\right)\right]\left(V_{z,j}^{*}-V_{z,j}^{n}\right)=\left[-\frac{1}{Re}\{S_{rz}^{\dagger}+S_{zz}\}V_{z,j}-J_2^{\dagger}P_k^{n}\right]^{n}-N(V)V_{z,j}^{n+\frac{1}{2}}-\frac{1}{ReD_a}MV_{z,j}^{n}. \quad (16)$$

Stage–2:

$$K(Q^{n+1})=-\frac{2}{\Delta t}\left(J_1V_{r,j}+J_2V_{z,j}\right). \quad (17)$$

Stage–3:

$$M\left({V_{r,j}}^{n+1}-{V_{r,j}}^{*}\right)=\frac{\Delta t}{2}{J_1}^{\dagger}(p^{n+1}-p^{n}). \quad (18)$$

$$M\left({V_{z,j}}^{n+1}-{V_{z,j}}^{*}\right)=\frac{\Delta t}{2}{J_2}^{\dagger}(p^{n+1}-p^{n}). \quad (19)$$

Where $S=\int\left\{\frac{\partial\phi_i}{\partial x}\frac{\partial\phi_j}{\partial x}+\frac{\partial\phi_i}{\partial y}\frac{\partial\phi_j}{\partial y}\right\}d\Omega$ is a momentum diffusion matrix, $M=\int\phi_i\phi_j\,rd\Omega, is\ a\ mass\ matrix$, $J_1=\int\frac{\partial\psi_i}{\partial x}\phi_j\,d\Omega$ and $J_2=\int\frac{\partial\psi_i}{\partial y}\phi_j\,d\Omega$ are divergence/pressure gradient matrix and $K=\int\left\{\frac{\partial\psi_{ki}}{\partial x}\frac{\partial\psi_{kj}}{\partial x}+\frac{\partial\psi_{ki}}{\partial y}\frac{\partial\psi_{kj}}{\partial y}\right\}d\Omega$ is a stiffness matrix for pressure, where † is matrix transpose. V^n, V^*, V^{n+1} are nodal vectors of velocity field, the pressure p^n, p^{n+1}, and the time interval Δt is (t_n, t_{n+1}). V_j^n, is a nodal velocity vector at t_n time, V_j^* is an intermediate non-divergence-free velocity vector and $V_j^{n+1}$is a divergence-free velocity vector at time stept_{n+1}. In the above-mentioned equations, the pressure vector is p_k^n, and $Q^{n+1}=\ p_k^{n+1}-p_k^n$ is a pressure difference vector.

C. Finite Element Discretization

The collection of equations (13) to (19) is discretized in the spatial domain using a variational formulation that makes use of a weighted approach.

The shape and weight functions are specified in Hilbert spaces which correspond to subsets of the two-dimensional Euclidean space $\Omega\subset\Re^2$. Explicitly, we focus on scalar-valued functions and associated first-order derivatives in the Hilbert space $H^1(\Omega)^2$ and the vector-valued Sobolev space for second-order derivatives of functions that are integrable square in the $L^2(\Omega)$ norm. Finite element approximation is established on such function spaces. The method described above is a typical one for discretizing and approximating the relevant equations.

$$V=\left\{u^n\subset H^1(\Omega)^2\,\middle|\,u\Gamma_1=b\right\}, \quad (20)$$

$$V_0=\{v\subset H^1(\Omega)^2|u\Gamma_1=0\}. \quad (21)$$

The conventional inner product for demonstrating integrable square functions is presented as follows:

$$\langle f,g\rangle=\int_\Omega f(x)\,g(x)d\Omega. \quad (22)$$

Assume that $L^2(\Omega)$ h is a scalar Hilbert space where functions can be square-integrated:

$P = \{q \subset L^2(\Omega)^d\}.$ (23)

The set of equations (13 - 19) suggests a weak formulation of the problem. The following semi-discrete variational forms are projected at several stages:

Stage–1a:

$$\left(\left(\frac{2}{\Delta t} - \frac{1}{2Re}\nabla^2 + \frac{1}{2\text{Re D}_a}\right)\left(v^{n+\frac{1}{2}} - v^n, v\right)\right) = \left(\frac{1}{\text{Re}}\nabla^2 v - (v.\nabla)v - \frac{1}{\text{Re D}_a}v, v\right) - (\nabla p, q) \quad (24)$$

Stage–1b:

$$\left(\frac{1}{\Delta t} - \frac{1}{2\text{Re}}\nabla^2 + \frac{1}{\text{Re D}_a}\right)(v^* - v^n, v) = \left(\frac{1}{\text{Re}}\nabla^2 v - \frac{1}{\text{Re D}_a}v, v\right)^n - (\nabla p, q)^n - \left(v.\nabla v^{n+\frac{1}{2}}, v\right) \quad (25)$$

Stage–2:

$$\theta\nabla^2(p^{n+1} - p^n, q) = \frac{1}{\Delta t}(\nabla . v^*, v) \quad (26)$$

Stage–3:

$$\frac{2}{\Delta t}(v^{n+1} - v^*, v) = -\nabla(p^{n+1} - p^n, q) \quad (27)$$

To establish a discrete system for the problem that properly characterizes the finite-dimensional subspaces. Adopting a weighted residual approach in which the weighted function is designed to be equal to the shape function, the aforementioned equation (23) is spatially discretized. Piecewise quadratics and piecewise linear over tessellations of a triangular mesh are the shape functions used to calculate the velocity and pressure components, respectively.

On introducing the approximate results of primitive parameters, $u(x,y,t), v(x,y,t)\ and\ p(x,y,t)$, on the finite spaces of the below functions:

$u(x,y,t) \cong \sum_{j=1}^{6} U_j^n(t)\,\Phi_j(x,y)$ (28)

$v(x,y,t) \cong \sum_{j=1}^{6} V_j^n(t)\,\Phi_j(x,y)$ (29)

$p(r,z,t) \cong \sum_{k=1}^{3} P_k(t)\psi_k(r,z)$ (30)

Here, shape functions ψ_k and Φ_j are linear and quadratic respectively. The completely discrete system's compact matrix is defined as:

Stage–la:

$$\left[\left\{\frac{2M}{\Delta t} - \frac{1}{Re}\left(\frac{S}{2} + \frac{M}{D_a}\right)\right\}\left(V^{n+\frac{1}{2}} - V^n\right) = \left[-\frac{1}{Re}(SV_j) + j_1^{\dagger}P_k - N(V)V_j - \frac{1}{Re\,D_a}MV_j\right]^n \quad (31)$$

Stage–lb:

$$\left[\frac{M}{\Delta t} - \frac{1}{Re}\left(\frac{S}{2} + \frac{M}{D_a}\right)\right](V^* - V^n) = \left[-\frac{1}{Re}(SV_j) + j_2^{\dagger}P_k - \frac{1}{Re\,D_a}MV_j\right]^n - N(V)V_j^{\,n+\frac{1}{2}} \quad (32)$$

Stage–2:

$$K(p^{n+1} - p^n) = -\frac{2}{\Delta t}JV_j^{\,*} \quad (33)$$

Stage–3:

$$\frac{2M}{\Delta t}\left(V_j^{\,n+1} - V_j^{\,*}\right) = J^{\dagger}(p^{n+1} - p^n) \quad (34)$$

Where V^n, V^*, V^{n+1} are nodal vectors of velocity field, the pressure p^n, p^{n+1}, and the time interval Δt is (t_n, t_{n+1})

D. Stream function

Fluid dynamics analysis requires a thorough grasp of flow structures. Using stream functions, it is possible to compute the flow structure in a two-dimensional coordinate system and gain insightful quantitative information. Multiple stream functions are needed for each dimensional component of a three-dimensional coordinate system. Stream functions are helpful resources for mathematical analysis, demonstrating flow structure, and transferring significant physical significance. By visualising the flow field with respect to local velocity vectors, streamlines are employed to understand the solid edges of a flow. They are particularly helpful for quantitatively evaluating recirculation zones. When modelling fluid flow problems using basic variables, the development of stream functions becomes significant. The flow pattern may be clearly and succinctly visualised using this method. Before producing streamlines from one node region to another, the stream function has to be established. The stream function may be described by a series of curves that pass through the flow structure. Throughout a steady-state flow field, the variance of fluid particles with a single streamline or path line is consistent. In both a Cartesian and a cylindrical polar coordinate system, the stream function satisfies Poisson's equation. A suitable vector potential for incompressible two-dimensional flow, denoted as 'Ψ,' as follows:

$$V = \nabla \times \Psi. \quad (35)$$

Where,$\Psi = \{0,0,\ \Psi\}$ represents the stream function.

The velocity components are considered to be distributed along the axial and radial directions within an axisymmetric cylindrical polar coordinate system (r, z). This choice is made due to the fact that Cartesian coordinates, which are a specific type of axisymmetric frames of reference, are utilised in the computation process. The relationship between the stream function (r,z) and the velocity components can be described as follows, as stated in reference [9].

$$\frac{1}{r}\frac{\partial \Psi}{\partial r} = -v_z\ and\ \frac{1}{r}\frac{\partial \Psi}{\partial z} = v_r. \quad (36)$$

For computation employing pseudo time stepping procedure, abovementioned (36) suggests the subsequent technique:

$$\frac{\partial \Psi}{\partial t} = \left(\frac{\partial^2 \Psi}{\partial r^2} + \frac{\partial^2 \Psi}{\partial z^2}\right) - r\frac{\partial v_z}{\partial r} - v_z + r\frac{\partial v_r}{\partial z}. \quad (37)$$

Offers some calculations by r gives equation (37) becomes:

$$\frac{1}{r}\frac{\partial \Psi}{\partial t} = \frac{1}{r}(\nabla^2 \Psi) - \frac{\partial v_z}{\partial r} - \frac{v_z}{r} + \frac{\partial v_r}{\partial z}. \quad (38)$$

When forward time stepping along the Δt step is applied to determine time derivative of equation (38), the following difference configuration of equation (38) emerges:

$$\frac{1}{r}\left(\frac{\Psi^{n+1} - \Psi^n}{\Delta t}\right) = \frac{1}{r}(\nabla^2 \Psi^n) - \frac{\partial v_z}{\partial r} - \frac{v_z}{r} + \frac{\partial v_r}{\partial z}. \quad (39)$$

Operating weighted residual technique, weak form of equation (39) turns into:

$$\frac{1}{\Delta t}\int_\Omega \frac{w}{r}(\Psi^{n+1} - \Psi^n)\,r d\Omega = \int_\Omega \frac{w}{r}(\nabla^2 \Psi^n)\,r d\Omega - \int_\Omega w\frac{\partial v_z}{\partial r} r d\Omega - \int_\Omega w\frac{v_z}{r} r d\Omega + \int_\Omega w\frac{\partial v_r}{\partial z} r d\Omega. \quad (40)$$

A finite element approximation will be:

$$(\Psi, v_r, v_z) = \sum_{i=1}^{N}\left(\Psi_j, V_r^j, V_z^j\right)\Phi_i(r,z). \quad (41)$$

Here, Φ_j is the quadratic basis function on nodal point j, and stream function'Ψ_j'. The radial and axial velocity elements are described by$\left(V_r^j, V_z^j\right)$ in r and $z$directions distinctly.

Performing the Galerkin approximation, during that the weight function (wi) is considered to correspond the shape function (Φ_i), is illustrated here:

$\sum_{i=1}^{N} w_i(x) = \sum_{i=1}^{N} \Phi_i\,(x).$ (42)

provides:

$\frac{1}{\Delta t}\int_\Omega \Phi_i\Phi_j d\Omega\Delta\Psi_j^{n+1} = \int_\Omega \Phi_i\left(\nabla^2\Phi_j\right) d\Omega\Psi_j^n -$
$\int_\Omega \Phi_i \frac{\partial\varphi_j}{\partial r} r d\Omega\, v_z^j - \int_\Omega \Phi_i\Phi_j\, d\Omega v_z^j + \int_\Omega \Phi_i \frac{\partial\Phi_j}{\partial z} r d\Omega\, v_r^j$.(43)

By applying Green's theorem to carry out integration and relying on Dirichlet boundary conditions, it is possible to reduce the second derivatives of equation (43), which may be written as:

$\frac{1}{\Delta t}\int_\Omega \Phi_i\Phi_j d\Omega\Delta\Psi_j^{n+1} = -\int_\Omega \frac{\partial\Phi_i}{\partial r}\frac{\partial\Phi_j}{\partial r} + \frac{\partial\Phi_i}{\partial z}\frac{\partial\Phi_j}{\partial z} d\Omega\Psi_j^n -$
$\int_\Omega \Phi_i \frac{\partial\Phi_j}{\partial r} r d\Omega\, v_z^j - \int_\Omega \Phi_i\Phi_j\, d\Omega v_z^j + \int_\Omega \Phi_i \frac{\partial\Phi_j}{\partial z} r d\Omega\, v_r^j$. (44)

The semi-implicit and explicit variants of equation (44) are represented as matrices and vectors as follows:

$\frac{1}{\Delta t} M\Delta\Psi_j^{n+1} = -S\Psi_j^n - D_1 v_z^j - M v_z^j + D_2 v_r^j$, (45)

$\left(\frac{1}{\Delta t} M + \frac{S}{2}\right)\Delta\Psi_j^{n+1} = -S\Psi_j^n - D_1 v_z^j - M v_z^j + D_2 v_r^j$. (46)

In equations (45) and (46), $D_1$and D_2 are symbolized as velocity gradient matrices with entries:

$\int \Phi_i \frac{\partial\Phi_j}{\partial r} r d\Omega$ and $\int \Phi_i \frac{\partial\Phi_j}{\partial z} r d\Omega$.

G. Results and Discussions

The Power law and the Carreau models, two distinct inelastic models, have had their effects compared. The values of N (power law index), absorbency 1, viscidness 1, permeability, and null shear viscidness are changed to increase inertia, with Reynolds numbers ranging from -for each non-Newtonian fluid flow domain, the power law ranges from 0.9 to 0.7 to track the behaviour of shear thinning. The numerical findings for a pipe filled with porous materials are demonstrated using streamline calculations, and graphs of the pressure differential versus rising Reynolds numbers are also shown.

H. Blending and Segregation of Non-Newtonian Fluid Streams in a Porous Media-Occupied Pipe (Power Law Model)

The outcomes of the inelastic power law reveal a rise in inertia. Figure 2 presents streamline projections and non-Newtonian fluid flows for equal and unequal stream rates, with an adapting power law index shifting from The study investigates the effects of mixing and separating concerning different flow rates and the power law. To examine the impacts of permeability on pressure disparity for flow rates, the permeability value varied alongside changes in the power law index. Top of Form

I. The influence of inertia on flow structure

The steady state illustrates streamline functions for equal and unequal stream rates in the internal pipe and the external cylinder, respectively, depicted in Figures These results are obtained with increasing Reynolds numbers ranging from, accompanied by a variation in the power law index. Like Newtonian fluids, the fluid has been pumped into the inner pipe in the usual direction. Notably, a line of symmetry and an inverse flow in the inner pipe have also been observed. It is noteworthy that altering the power law or increasing the Reynolds number does not appear to affect inertia.

When the power law index is high, changing the stream rates in the external pipe has specific influences on inertia, as clarified in Figure; however, for other declining values, as shown in Figures, such effects vanish. Figure illustrates that a vortex forms at the junction space in the outer cylinder when Re = 1, but dissipates when it increases to at, and stream rate is By altering flow rates or examining the power law index, no further evident impacts of inertia on flow structure have been identified.

In a similar way, Newtonian fluids in a conduit, whether porous or non-porous, flow unidirectionally. Due to a numerical error, only a small number of reverse flows were seen in the internal tube travelling towards the exit region close to the symmetry line. Only an inner pipe in the separating gap is used to mix fluids. In all instances of varying flow speeds and rising inertia values, mixing and separation were observed. No other clear effect of varying flow rate in an external cylinder has been observed in this study.

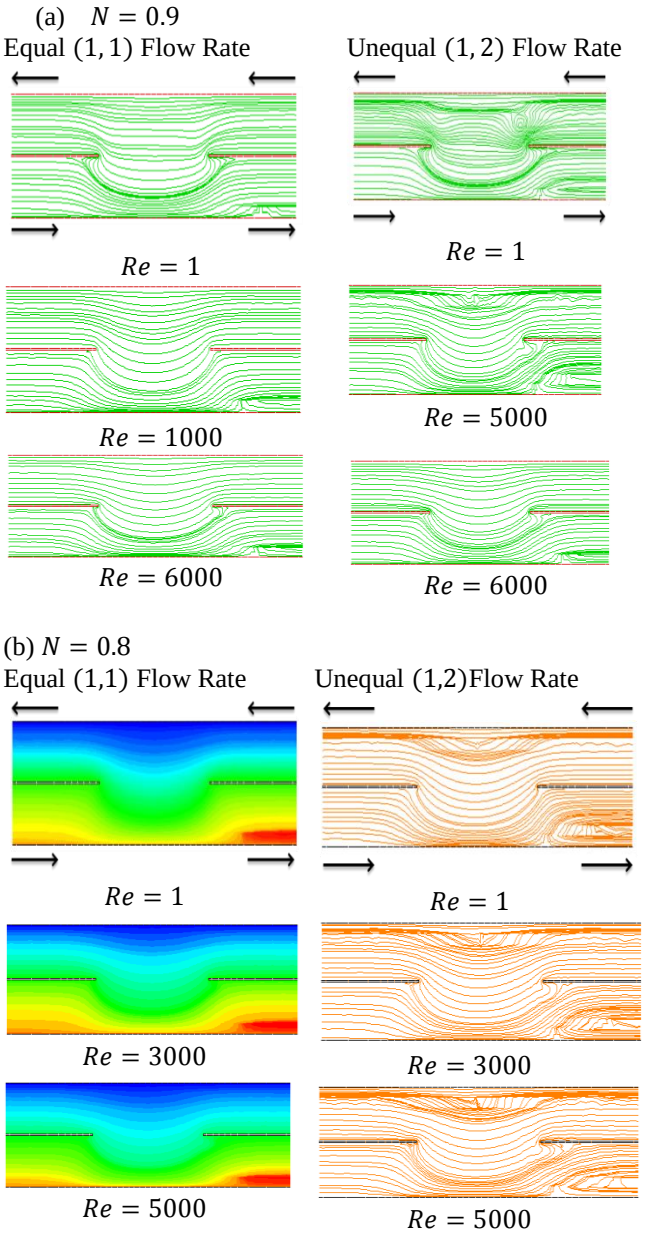

(c) $N = 0.7$

Equal $(1,1)$ Flow Rate Unequal $(1,2)$ Flow Rate

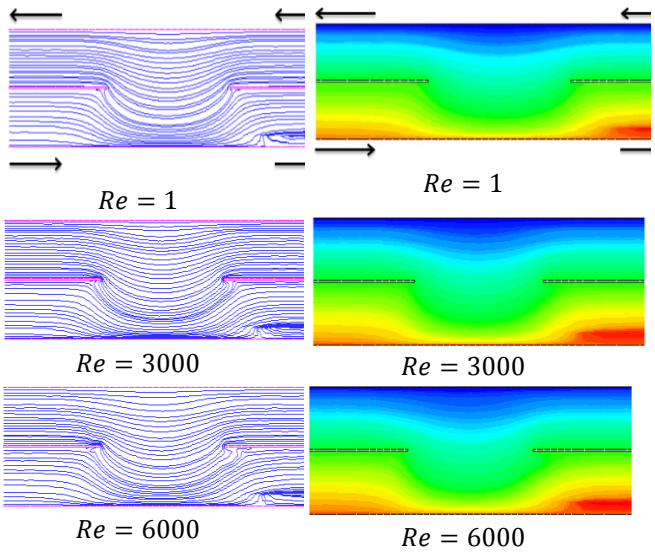

Fig. 2. Restructure function of non-Newtonian fluid streams for Power law model below the variable of power law index from 0.9 *to* 0.7 with growing Re number from 1 *to* 6000, For equal $(1,1)$ and unequal $(1,2)$ stream rates.

J. Impact of altering flow rates and permeability on pressure

Figures and illustrations illustrate the impact of non-Newtonian fluid flow on pipe pressure within a porous medium and present the relative flow rate. Under varying permeability values from, the highest and lowest mounted pressures for both flow rates at are and, respectively. Similarly, for flow rates at, the maximum and minimum scaled pressures are and, respectively, with permeability values ranging from. Likewise, the greatest and minimum scaled pressures for flow rates at are and, respectively, with a constant permeability for all progressing inertia values.

Switching the power law from 0.9 to 0.7, the absorptivity from 0.1 to 0.0001, and the Reynolds number from 1 to 6000 will all be used to track the impacts of evolving flow rates on pressure differential. According to this study, pressure elevates when flow rates alter. The pressure difference also results from a reduction in permeability. When the permeability decreases from 0.1 to 0.001 and the power law index, as shown in Figure 3(a), the pressure climbs up at Re=1 and 10 by maintaining Darcy's number at 1. Figure 3 (at) illustrates the pressure rise when the permeability is changed from 0.001 to 0.0001 while maintaining the same power law index. Again, the pressure grows as the permeability falls from at to 1000. According to Figure 3 (at), pressure increases when permeability varies from 0.001 to 0.0002 in circumstances of an unequal flow rate. When absorptivity was originally fixed at the power law index, there was no significant change in pressure difference. While permeability was altered from 0.001 to 0.0001, pressure increased in the same manner as when shown in Figure 3. In comparison to both flow rates, the pressure difference changes the least when the less permeable domain is N = 0.8, and the trend tends to be linear.

Due to a constant value of permeability, Figure 3(a) was unable to depict the effects on the pressure of altering flow rates and a power law index from 0.8 to 0.7. By partitioning the vertical axis into its smaller units of scaled pressure and flow rates at N = 0.7, its impacts are depicted in Figure 3(b). When N=0.7, which indicates there is no discernible influence of pressure, permeability remains constant with an increase in Reynolds number, however, inertia values grow steadily. Pressure differences result from fluctuating flow rates and permeability values as well as rising inertia.

(a) (b)

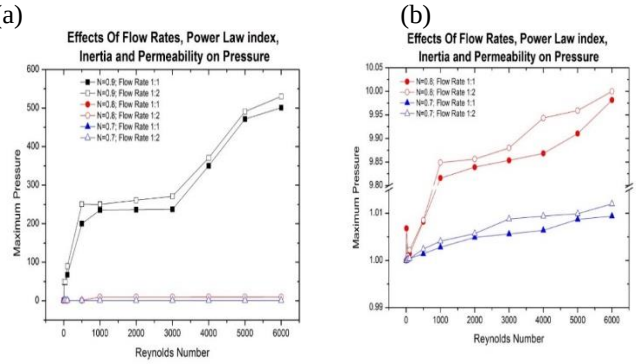

Fig. $3(a) - (b)$. Pressure difference 0.9 *to* 0.7 and with getting higher Re number 1 *to* 6000.

K. Blending and Segregation of Non-Newtonian Fluid Flows in a Porous Media-Occupied Pipe (Bird-Carreau model)

Bird Carreau's inelastic model served as the basis for the numerical calculations. This model considers both equal and unequal flow rates within the external pipe and internal pipe, which are filled with porous materials. Figure 4 illustrates the streamline projections of non-Newtonian fluid flows, showcasing the impact of increasing inertia and changing the power law index from 0.9 to 0.7. The study investigates how variations in flow rate and power law index affect mixing and separating phenomena. Additionally, the presence of porous media enables a comparison of inertial effects with those that the power law model predicts.

L. Impact of inertia on flow structure

Figures 4(a)–4(c) show non-Newtonian effects to observe the effects of inertia on flow structures in pipes filled with porous medium when there are equal and unequal flow rates. Variations in stream rates or rising Reynolds numbers together with decreasing power law index values have not been shown to have any effect on inertia in pipes filled with porous medium. The Reynolds number rises for both flow rates, as shown, from 1 to 6000, while the power law index reduces from 0.9 to 0.7, correspondingly. Similar streams have been forced into the internal pipe from either side of the external cylinder in the region leading up to the symmetry line, and some reversal flows have also been seen in the interior tube leading down to the downstream exit.

It was discovered that Bird Carreau had no impact on the inertia caused by pressure; however, the power law model has a very slight inertia effect. The same unidirectional flows apply as they did in the power law model. Changes in the power law index have no effect. Whatever the cause, no evidence of inertia has been found. The flow has not been

impacted by rising inertia, changing flow rates, or variations in the power law index or permeability values. A cross stream has been observed in an internal pipe at the departure portion.

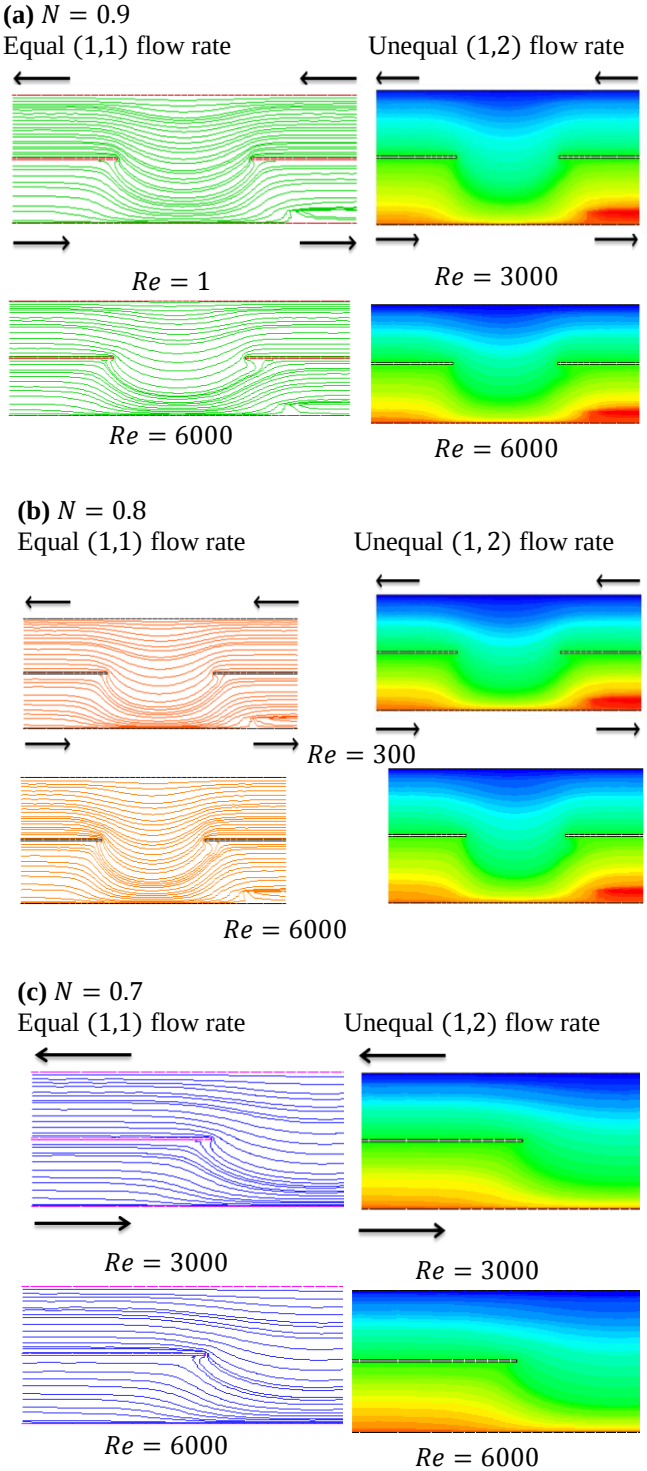

Fig. 4. Restructure role of non-Newtonian fluid streams for Bird Carreau model below altering values of power law index from 0.9 *to* 0.7 with rising Re number from $Re = 1$ *to* 6000, from highest to lowest. For equal $(1, 1)$ and unequal $(1, 2)$ stream rates,

M. Impacts of Power Law and Bird Carreau model on pressure when pipes are occupied without porous media.

The disparities between the implications of Bird Carreau and power law caused by pressure by a surge in the Re for streams of non-Newtonian fluids are demonstrated in Figure 5. As pipes are packed with a non-porous medium, the Reynolds number has been computed from $Re = 1\ to\ 200$ for an equal $(1, 1)$ stream rate. For Re up to 50, there is no discernible variance with rising pressure. Power law has a greater impact on pressure than the Bird-Carreau model. When scaled pressure is increased, the Bird-Carréau model exhibits a linear trend, but the Power law exhibits a non-linear trend beyond $Re = 150$. While the Bird Carreau model exhibits no discernible influences in inertia, power laws have considerable inertia impacts on flow behavior. The same tendencies have been seen in non-Newtonian streams after a tube contains non-porous medium, and pressure climbs with altering values of Re, similar to prior cases addressed.

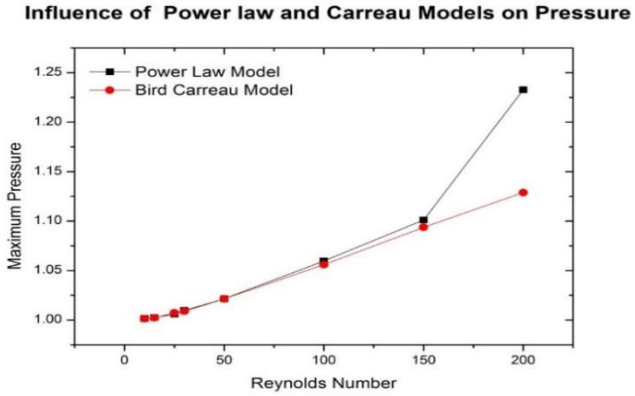

Figure 5. Relationship of Power Law and Bird Carreau model on pressure.

II. Concluding Remarks

This study concludes that:

- Numerical simulations of Bird-Carreau and Power law rheological models for combining and separating flow conditions in inner and outer circular pipes were conducted.
- The Taylor-Galerkin/Pressure-Correction finite element method was shown to be accurate and consistent in execution and predictions.
- The power law model described inertia effects on flow structure well at small Reynolds numbers, which disappeared at higher power law index values.
- The Bird Carreau model has no influence on inertia when altering power law index values or stream rates.
- Blending and segregation flows in tubes packed with porous material exhibited minimal inertial effects for both the Power Law and Bird Carreau models.
- Various numerical inaccuracies were found in the flows.
- Different mixing and separating flow circumstances had an impact on absorbency, power law index, and stream rates in a pipe.
- Pressure in the outer cylinder increased with flow rate and power law index changes.
- Permeability values affected pressure linearly, with higher permeability leading to higher pressure.
- Inertia and flow had greater impacts on pressure compared to the power law model, as opposed to the

Bird-Carreau model, where pressure was not significantly impacted.

REFERENCES

[1] S. Kakac, B. Kilkis, F. Arinic, "Convective Heat and Mass transfer in Porous media", Kulwer, Netherlands, 1991.

[2] D. A. Nield, A. Bejan, "Convection in Porous Media", Springer–Verlag, New York, 1999

[3] S. Kakac, B. Kilkis, F. Arinic, "Convective Heat and Mass transfer in Porous media", Kulwer, Netherlands, 1991.

[4] V. G. Ramanathan, "Estimating pressure drop in two-Phase flow through porous media",1-4, 2009.

[5] Shaikh, F., Shah, S. F., Siddiqui, A. M., & Kumar, L. (2022). Application of recursive approach of pseudoplastic fluid flow between rotating coaxial cylinders. *Alexandria Engineering Journal*, *61*(10), 7823-7832.

[6] R. B. Khokhar, "Numerical Modelling of Mixing and Separating of Fluid Flows through Porous Media," 2018.

[7] A. A. Bhutto, S. F. Shah, R. B. Khokhar, K. Harijan, and M. Hussain, "To Investigate Obstacle Configuration Effect on Vortex Driven Combustion Instability," 2023.

[8] A. A. Bhutto, K. Harijan, M. Hussain, S. F. Shah, and L. Kumar, "Numerical simulation of transient combustion and the acoustic environment of obstacle vortex-driven flow," *Energies*, vol. 15, no. 16, p. 6079, 2022.

[9] A. Baloch, P. Townsend, and M. F. Webster, "On the simulation of highly elastic complex flows," *J. Nonnewton. Fluid Mech.*, vol. 59, no. 2–3, pp. 111–128, 1995.

[10] D. M. Hawken, H. R. Tamaddon- Jahromi, P.Townsend, and M. F. Webster, "A Taylor Galerkin- based algorithm for viscous incompressible flow," *Int. J. Numer. Methods Fluids*, vol. 10, no. 3, pp. 327–351, 1990.

[11] Cochrane, T., Walters, K. & Webster, M. F.(1981),On newtonian and non-newtonian flow incomplex geometries, Philosophical Transactionsof the Royal Society of London. Series A, Mathematical and Physical Sciences, vol.301, no.1460, pp.163-181.

[12] Afonso, A. M., Alves, M. A., Poole, R. J.,Oliveira, P. J. & Pinho, F. T. (2011),Viscoelastic flows in mixing-separating cells, Journal of Engineering Mathematics, vol.71, no.1, pp.3-13.

[13] Echendu, S. O. S., Belblidia, F., TamaddonJahromi, H. R. & Webster, M. F.(2011),Modelling with viscous and viscoplastic materials under combining and separating flow configurations, Mechanics of Time-Dependent Materials, vol.15, no.4, pp.407-428.

[14] Cochrane, T., Walters, K. & Webster, M. F. (1982), Newtonian and non-newtonian flow near a re-entrant corner, Journal of Non-Newtonian Fluid Mechanics, vol.10, no.1-2, pp.95- 114.

[15] Shaikh, F., Shaikh, A. A., Hincal, E., & Qureshi, S. (2023). Comparative analysis of numerical simulations of blood flow through the segment of an artery in the presence ofstenosis. *Journal of Applied Mathematics and Computational Mechanics*, *22*(2).

[16] Khokhar, R. B., Chen, Y. K., Calay, R. K. andXu, Y. (2013), Numerical scheme to simulatecombined mixing and separating flow in achannel, Applied Mechanics and Materials, Vols.(303-306), pp. 2798-2805.

[17] Solangi, M. A., Khokhar, R. B. and Baloch,A. (2013), A FEM Study for Non-Newtonianbehaviour of blood in plaque depositedcapillaries: analysis of blood flow structure,Mehran University Research Journal ofEngieering and Technology, vol. 32 (2), pp. 27728

[18] Hawken, D. M., .Tamaddon-Jahromi, H. R.,Townsend, P. & And Webster, M. F. (1990),A taylor-galerkin-based algorithm for viscous incompressible flow, International Journal for Numerical Methods in Fluids, vol.10, no.3, pp.327-351.

[19] Townsend, P. & Webster, M. F. (1987),An algorithm for the three-dimensional transient simulation of non-newtonian fluid flows, Proc. Int. Conf. Num. Meth. Eng: Theory and Applications, pp.T12/1-

[20] Donea, J., Quartapelle, L. & Selmin, V. (1987),An analysis of time discretization in the finite element solution of hyperbolic problems, Journal of Computational Physics, vol.70, no.2, pp.463-499

[21] Van Kan, J. (1986),A second-order accurate pressure-correction scheme for viscous incompressible flow, SIAM Journal on Scientific and Statistical Computing, vol.7, no.3, pp.870-891.

[22] Chorin, A. J. (1968),Numerical solution of the navier-stokes equations, Math. Comp., vol.22pp.745-762.

[23] Fortin, M., Peyret, R. & Temam, R. (1971),Lecture notes in physics, Springer vol.8pp.337- 382

[24] Kan, J. V. (1986),A second-order accurate pressure-correction scheme for viscous incompressible flow, SIAM Journal on Scientific and Statistical Computing, vol.7, no.3, pp.870-891.

[25]` Peyret, R. & T. D. Taylor (1985),Computational methods for fluid flow, The SAO/NASA Astrophysics Data System (ADS)

[26] E. O. Carew, P. Townsend, and M. F. Webster, "Taylor- Galerkin algorithms for viscoelastic flow: application to a model problem," *Numer. Methods Partial Differ. Equ.*, vol. 10, no. 2, pp. 171–190, 1994.

[27] F. shaikh, M.S. chandio and Z. kalhoro (2016) "Numerical Simulation of Blood Flow through a Segment of an Artery with Single Stenosis ", *Sindh University Research Journal - SURJ (Science Series)*, 48(3)

[28] Khokhar, R. B., Bhutto, A. A., Siddiqui, N. F., Shaikh, F., & Bhutto, I. A. (2023). Numerical analysis of flow rates, porous media, and Reynolds numbers affecting the combining and separating of Newtonian fluid flows.

Balochistan Journal of Engineering & Applied Sciences (BJEAS) – (p-ISSN: 2518-2706
Volume 6, No.1

Maximizing Efficiency and Sustainability with Smart Solar Street Lights Control

AssadUllah Khauhwar[1], Saeed Ahmed Shaikh[1], Abdul Hameed Soomro[1], Imtiaz Ali Laghari[1],
[1]Faculty, Department of Electrical Engineering, Quaid-e-Awam University of Engineering Science and Technology Nawabshah Campus Larkana, Sindh Pakistan
Corresponding Author: Hameed Soomro, Email: abdul.hameed@quest.edu.pk

***Abstract*—In modern times, the rise of nighttime crime rates due to people working late at night prompted the recommendation of installing solar-powered street lighting systems with effective control and monitoring systems. This type of lighting system not only saved money but also reduced the need for human labour by utilising LDR sensors. With the increasing global focus on environmental issues, energy-efficient technologies emerged, including those that aimed to reduce energy consumption for lighting, especially for large-scale projects such as street lighting. LED lights, with their longer lifespan and lower maintenance requirements, were considered a more cost-effective and eco-friendly alternative to traditional HID lights for public lighting systems. However, many public lighting systems continued to rely on outdated standards and technologies, and there was a need for new methods and technologies that could save costs and reduce CO2 emissions. Although solar photovoltaic panels were frequently used in street lighting systems, their lack of intelligent performance was a significant limitation. Therefore, automating these systems became crucial to reducing energy consumption and improving overall efficiency.**

Keywords*—*Solar System, Street Lighting, Control System

I. INTRODUCTION

As urbanization continues to grow, the demand for efficient street lighting systems is becoming increasingly important. However, traditional street lighting systems are often inefficient, expensive, and require high maintenance [1]. A new solution that has emerged to address these issues is the concept of smart street lighting systems [2]. These systems are designed to optimize energy consumption, lower maintenance costs, and improve public safety by utilizing advanced technologies such as sensors, communication networks, and data analytics [3]. By automatically adjusting lighting levels based on factors such as pedestrian or vehicle traffic and ambient light levels, these systems can significantly reduce energy consumption and light pollution [4]. Moreover, they can detect and report any issues with the lighting infrastructure, allowing for swift maintenance and repair [5]. Smart street lighting systems provide a range of benefits, including improved energy efficiency, cost savings, and the creation of more sustainable and livable cities [6]. In this article, we will examine the features and potential applications of a smart street lighting control system, highlighting the concept's benefits. Smart street lighting control systems are becoming increasingly popular as cities seek to reduce their energy consumption and increase the efficiency of their infrastructure [7]. One of the key advantages of smart street lighting is that it enables remote control and monitoring of individual lights, allowing for more targeted and efficient lighting [8]. Several studies have highlighted the potential of Smart Street lighting control systems to reduce energy consumption and improve public safety [9]. For example, a study by A. Hussain and M. Hassan found that smart street lighting systems could reduce energy consumption by up to 50% compared to traditional street lighting systems [10]. This is achieved through features such as automatic dimming and switching, which ensure that lights are only on when needed and at the appropriate brightness level. In addition to energy savings, Smart Street lighting control systems can also improve public safety [11]. For example, a study by S. S. S. Sarma and A. K. Barua noted that smart street lighting systems can help reduce crime rates by providing better illumination in high-crime areas [12]. By incorporating sensors and cameras, these systems can also detect and respond to suspicious activity, further enhancing public safety. Wireless sensor networks (WSNs) are an essential component of Smart Street lighting control systems, enabling real-time communication and coordination between individual lights [13]. A study by A. de Oliveira and M. R. Pinto highlighted the importance of WSNs in optimizing energy consumption and reducing maintenance costs [14]. By providing real-time data on lighting levels, traffic patterns, and other factors, WSNs can enable smart street lighting systems to respond dynamically to changing conditions [15]. Another key feature of Smart Street lighting control systems is data analytics [16]. By collecting and analyzing data on energy usage, traffic patterns, and other factors, these systems can identify opportunities for further energy savings and optimization [17]. A study by H. Alamri et al. explored the potential of data analytics in smart street lighting systems, highlighting the benefits of predictive maintenance, early fault detection, and energy-efficient scheduling [18]. In conclusion, smart street lighting control systems have the potential to revolutionize the way we illuminate urban environments [19]. By reducing energy consumption, improving public safety, and enabling targeted and efficient lighting, these systems can create more sustainable, efficient, and livable cities [20].

I. PROBLEM STATEMENT

Many cities are facing the challenge of high expenses on street lighting, especially due to the significant power consumption of sodium vapour lamps [21]. The existing manual system of turning the lights on and off in the evening and

morning results in a lot of energy waste [14]. Energy efficiency is a crucial factor in reducing the high cost of energy consumption, particularly electricity, which accounts for around 20% of the world's electrical energy usage [22]. Efficient lighting can significantly contribute to energy savings. The increase in population and traffic congestion has led to the utilisation of new technologies, such as solar cell technology, to reduce energy waste and protect the environment [23]. Therefore, the shift towards smart street light control systems has become necessary to address these issues.

A. *Objective of this research study*

The main objective of this research is to take care of the environment by employing a novel strategy that uses solar photovoltaic panel street lighting systems to reduce energy consumption [24]. When traditional lighting systems like incandescent or compact fluorescent lamps are replaced by light-emitting diode (LED) lights without changing the installation of the electrical system, the proposal aims to save energy, have a high luminous efficacy, and have a long useful life, but new technology in lighting street systems with solar systems can reduce the cost of installing wired connections for sensors [25].

Section 2 describes the Solar Street Light
Section 3 describes the Methodology
Section 4 describes the results
Section 5 describes the Conclusions

B. *Solar Street Light*

Solar power is a type of renewable energy. Solar street lights are now common along the sides of roads, as shown in Fig. 1 [24]. Photovoltaic cells make up the solar street lights, which use the sun's energy during the day. The battery contains photovoltaic cells that convert solar energy into electrical energy [26]. The lamp automatically starts at night and uses electricity that is already stored in the battery. The battery is refilled during the day, and the process continues every day [27]. The street light automatically turns off when the sun is shining because the LDR sensor detects the presence of surrounding light [25]. The LDR signals the microcontroller to turn on the street light at night when there is no light. An assembly of photovoltaic cells mounted in a framework for the purpose of producing energy is known as a solar cell panel, photo-voltaic (PV) module, or solar panel [28]. The rechargeable battery then stores the solar energy. Solar lights use the battery's energy to operate when darkness falls.

A relay is a switch that controls the connection or disconnection of another circuit by using an electrical signal to operate an electromagnet instead of manual control. Relays are frequently used to isolate the controller from the device, as devices can operate on both AC and DC, but microcontrollers that send signals typically operate on DC. Thus, relays are used to bridge this gap. [29]. In this study, we use two types of resistors: a fixed resistor and a variable resistor. Two terminals make up a variable resistor, which is also known as an adjustable resistor, and one of the terminals is a sliding or moving contact that is commonly referred to as a wiper [28]. LEDs are semiconductor light sources that combine a P-type semiconductor with an N-type semiconductor, which has a higher electron concentration and a higher hole concentration [24], so we have recommended the LED rather than sodium lamps. Photoresistors, also known as light-dependent resistors, are commonly used in electric circuits to measure the level of light. It is simple to use this kind of photoresistor in circuit designs to show the resistance to changes in light level [13]. An LDR is a passive device without a PN junction, which is the primary distinction between a phototransistor and an LDR. When there is complete darkness, the LDR response to a light occurs within milliseconds, but when there is no light, it takes up to a second or longer to reach the final resistance level, so we use an LDR sensor to detect the intensity to turn on or off the street lights [30]. To support and connect electronic components, conductive pathways, tracks, or signal traces are etched from copper sheets and laminated onto a non-conductive substrate on a printed circuit board (PCB). These pathways provide both mechanical support and electrical connections for the components. [31]. The components of a street light are shown in Fig. 2 [28]. The street light based on a solar system is shown in Fig. 3 [14], and the circuit connection diagram of the proposed system is shown in Fig. 4 [28].

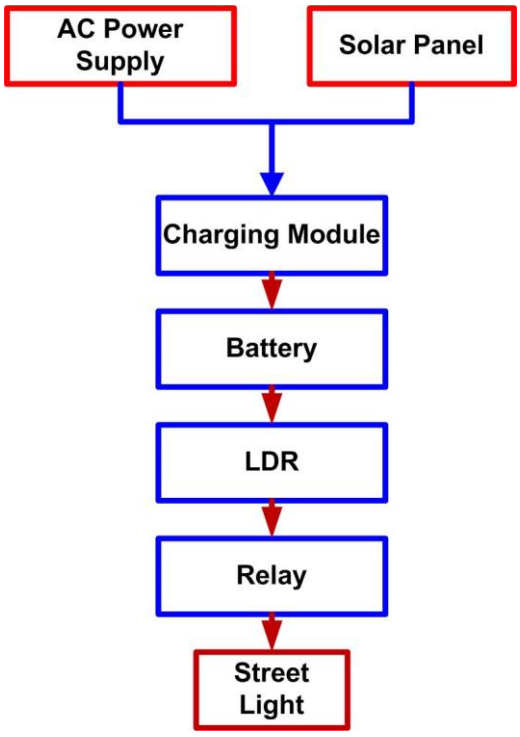

Fig. 2 Components of street light

Fig. 3 Street light based on Solar System

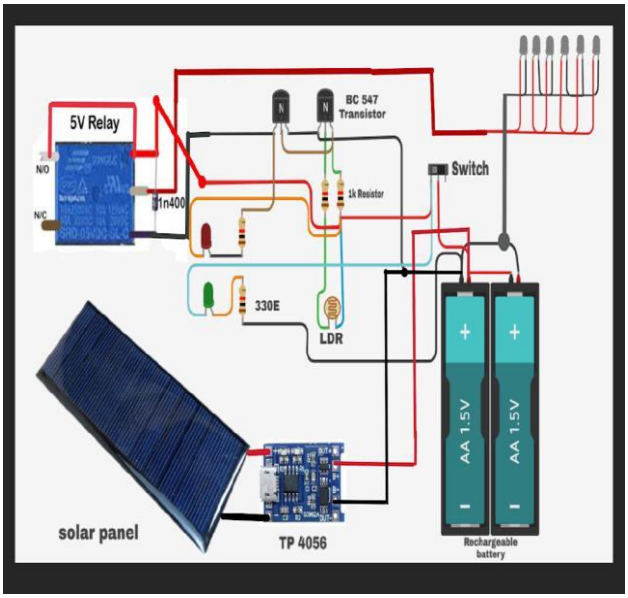

Fig. 4 Circuit diagram of proposed System

II. Methodology

The simulation model is shown in Fig. 5. In the first instant, we made the connection of transistors labelled with Q1-BC547 (NPN) and Q2-BC547 (NPN). The emitter pin of both transistors is connected to the -ve terminal of the battery, and a wire is connected between the transistor Q1's collector pin and the transistor Q2's base. A 1KΩ resistor is connected between the positive terminal of the battery PCB and the transistor Q1's collector pin. The positive terminal of the battery PCB is connected to the base terminal of the transistor Q1 using the Light Dependent Resistor (LDR) is connected. A 330Ω resistor is placed between the negative terminal of the battery PCB and the base pin of the transistor Q1. The anode terminal of an LED (light-emitting diode) is connected to the collector pin of transistor Q2 with a resistor of 330Ω across the positive terminal of the battery PCB. The straightforward circuit is now ready for testing. See the output by connecting the 6V to 9V battery terminals to the circuit. The LED glows when you block light from hitting the light-dependent resistor (LDR).

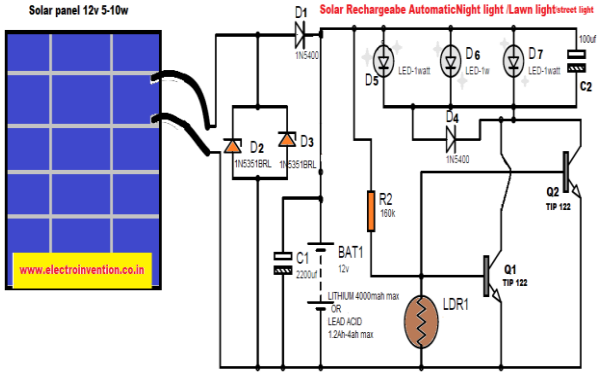

Fig. 5 Simulated diagram of proposed System

III. Results and Discussions

Measurements were taken to determine the charge time and discharge time of a battery with a capacity of 27 watt-hours at a single location using time measurements. These measurements were recorded and analyzed. Additionally, the brightness of a lamp was measured in lumens, and the results are presented in Table 1.

Table. 1. Charge and Discharge Time with Lumens

Type	Capacity	Discharge Time	Charge Time	Lumens-M
Lamp-1 (100-LED)	6.40 W	4-Hours	4-Hours	199
Lamp-2 (50-LED)	3.21 W	7-Hours	4-Hours	120

Table 1 displays the lumens for all the lamps used in the experiment. It was observed that the handmade lamp (1) had the highest light intensity compared to the commercially available lamp (2), despite carrying approximately the same power. Therefore, lamp (1) was deemed better than lamp (2) and subsequently chosen as the superior option. Meanwhile, Table 2 showcases the ideal results obtained from the formula utilised for measuring the charge time and discharge time of a battery with a capacity of 27 watts.

$$\text{Charge Time} = \frac{\text{Ahx Tolerance}}{\text{Charge rate}} \quad (1)$$

Where Ah is Ampere-hour removed×50% and Tolerance is from source

$$\text{Discharge Time} = \frac{\text{Battery Ah x Battery voltage}}{\text{Applied Load w}} \quad (2)$$

Table.2. Charge and Discharge Time

Type	Discharge Time	Charge Time
Lamp-1 (100-LED)	4.35-Hours	3.15-Hours
Lamp-2 (50-LED)	8.9-Hours	3.15-Hours

The following Graph shows the relationship between intensity of light with time:

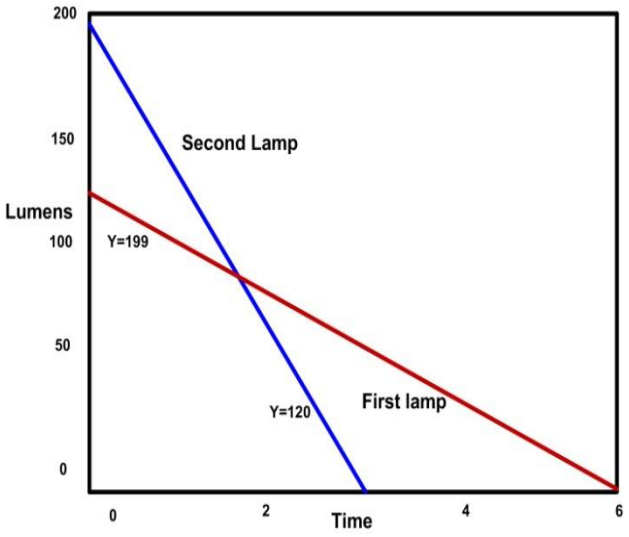

Fig. 6 Intensity of light with Time

Upon investigating the data, it was observed that there was a correlation between the intensity of light and time. Specifically, when the battery was fully charged, the intensity of light was at its maximum. As the charge of the battery

gradually decreased, the intensity of light also decreased correspondingly.

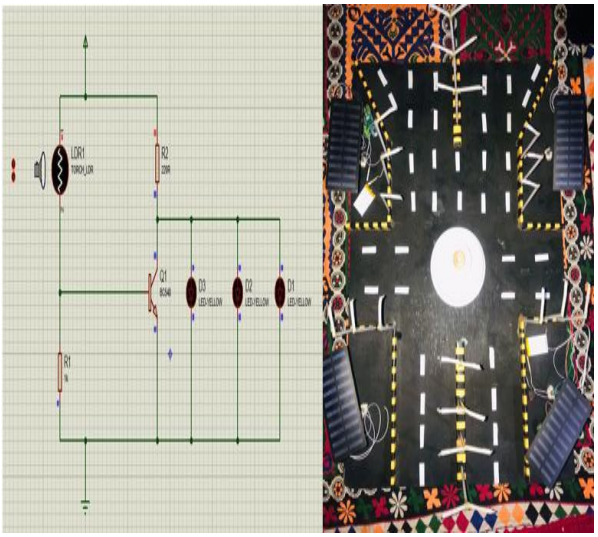

Fig. 7 Street Light during Day Time

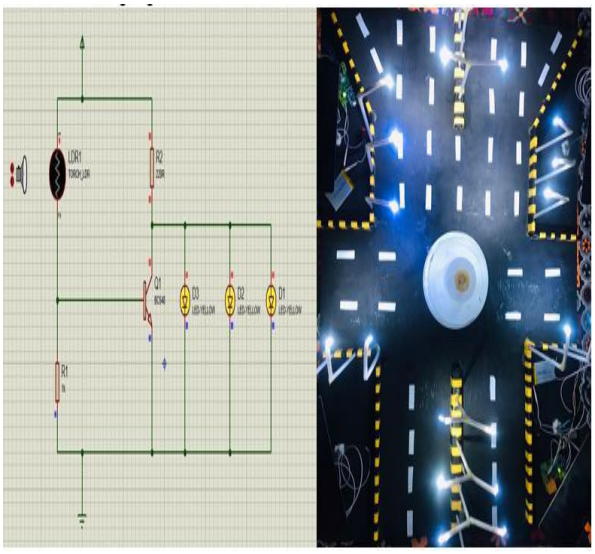

Fig. 8 Street light during Night Time

IV. CONCLUSIONS

The automatic street lights project is a highly effective, safe, and eco-friendly way to conserve energy, providing a solution for two of the biggest global challenges: energy preservation and incandescent lamp disposal. By utilising statistical data, the project can potentially reduce electrical energy consumption on highways by over 40%. Although there may be some initial costs and maintenance requirements, these can be minimised through the use of advanced equipment and strategic resource planning. Furthermore, the benefits of using LED lights, such as their long lifespan, cool light emission, lack of harmful substances, and quick switching capabilities, far outweigh any drawbacks. With low initial costs and long-term advantages, a return on investment is assured. Additionally, the project can be utilised in various other settings, such as factories, campuses, and large shopping mall parking lots. It can also serve as a surveillance tool on corporate campuses and in industries.

REFERENCES

[1] V. Chandrasekhar and N. Vishwanathan, "Soft Switched Full- Bridge DC-DC LED Driver For Street Lighting," *Optik*, vol. 273, p. 170430, 2023.

[2] C. Chiatti, C. Fabiani, and A. L. Pisello, "Toward the energy optimization of smart lighting systems through the luminous potential of photoluminescence," *Energy*, vol. 266, p. 126346, 2023.

[3] M. Füchtenhans, C. H. Glock, E. H. Grosse, and S. Zanoni, "Using smart lighting systems to reduce energy costs in warehouses: A simulation study," *International Journal of Logistics Research and Applications*, vol. 26, pp. 77-95, 2023.

[4] S. Yu, L. S. Shi, L. Zhang, Z. Liu, and Y. Tu, "A solar optical reflection lighting system for threshold zone of short tunnels: Theory and practice," *Tunnelling and Underground Space Technology*, vol. 131, p. 104839, 2023.

[5] Z. Chen, C. Sivaparthipan, and B. Muthu, "IoT based smart and intelligent smart city energy optimization," *Sustainable Energy Technologies and Assessments*, vol. 49, p. 101724, 2022.

[6] E. Dizon and B. Pranggono, "Smart streetlights in Smart City: a case study of Sheffield," *Journal of Ambient Intelligence and Humanized Computing*, pp. 1-16, 2022.

[7] C. Badgaiyan and P. Sehgal, "Smart street lighting system," *International Journal of Science and Research*, vol. 4, pp. 271-274, 2015.

[8] Y. M. Yusoff, R. Rosli, M. U. Karnaluddin, and M. Samad, "Towards smart street lighting system in Malaysia," in *2013 IEEE Symposium on Wireless Technology & Applications (ISWTA)*, 2013, pp. 301-305.

[9] S. C. Suseendran, K. B. Nanda, J. Andrew, and M. B. Praba, "Smart street lighting system," in *2018 3rd International Conference on Communication and Electronics Systems (ICCES)*, 2018, pp. 630-633.

[10] D. Jin, C. Hannon, Z. Li, P. Cortes, S. Ramaraju, P. Burgess, *et al.*, "Smart street lighting system: A platform for innovative smart city applications and a new frontier for cyber-security," *The Electricity Journal*, vol. 29, pp. 28-35, 2016.

[11] G. Gagliardi, M. Lupia, G. Cario, F. Tedesco, F. Cicchello Gaccio, F. Lo Scudo, *et al.*, "Advanced adaptive street lighting systems for smart cities," *Smart Cities*, vol. 3, pp. 1495-1512, 2020.

[12] M. Mahoor, F. R. Salmasi, and T. A. Najafabadi, "A hierarchical smart street lighting system with brute-force energy optimization," *IEEE Sensors Journal*, vol. 17, pp. 2871-2879, 2017.

[13] F. S. El-Faouri, M. Sharaiha, D. Bargouth, and A. Faza, "A smart street lighting system using solar energy," in *2016 IEEE PES Innovative Smart Grid Technologies Conference Europe (ISGT-Europe)*, 2016, pp. 1-6.

[14] P. V. Parkash and D. Rajendra, "Internet of things based intelligent street lighting system for smart city," *International journal of innovative research in science, engineering and technology*, vol. 5, 2016.

[15] G. Shahzad, H. Yang, A. W. Ahmad, and C. Lee, "Energy-efficient intelligent street lighting system using traffic-adaptive control," *IEEE Sensors Journal*, vol. 16, pp. 5397-5405, 2016.

[16] P. Mohandas, J. S. A. Dhanaraj, and X.-Z. Gao, "Artificial neural network based smart and energy efficient street lighting system: A case study for residential area in Hosur," *Sustainable Cities and Society*, vol. 48, p. 101499, 2019.

[17] K. Arun Bhukya, S. Ramasubbareddy, K. Govinda, and T. Aditya Sai Srinivas, "Adaptive mechanism for smart street lighting system," in *Smart Intelligent Computing and Applications: Proceedings of the Third International Conference on Smart Computing and Informatics, Volume 2*, 2020, pp. 69-76.

[18] R. Carli, M. Dotoli, and E. Cianci, "An optimization tool for energy efficiency of street lighting systems in smart cities," *IFAC-PapersOnLine*, vol. 50, pp. 14460-14464, 2017.

[19] N. Yoshiura, Y. Fujii, and N. Ohta, "Smart street light system looking like usual street lights based on sensor networks," in *2013 13th International Symposium on Communications and Information Technologies (ISCIT)*, 2013, pp. 633-637.

[20] P. Veena, P. Tharakan, H. Haridas, K. Ramya, R. Joju, and T. Jyothis, "Smart street light system based on image processing," in *2016 International Conference on Circuit, Power and Computing Technologies (ICCPCT)*, 2016, pp. 1-5.

[21] D. Nuttall, R. Shuttleworth, and G. Routledge, "Design of a LED street lighting system," 2008.

[22] S. Palanisamy, Z. Rahiman, and S. Chenniappan, "Introduction to Smart Power Systems," *Artificial Intelligence- based Smart Power Systems*, pp. 1-13, 2023.

[23] R. Ciriminna, F. Meneguzzo, L. Albanese, and M. Pagliaro, "Solar street lighting: a key technology en route to sustainability," *Wiley Interdisciplinary Reviews: Energy and Environment*, vol. 6, p. e218, 2017.

[24] N. S. M. Aung and Z. H. Myint, "Design of stand-alone solar street lighting system with LED," *International journal of scientific engineering and technology research*, vol. 3, pp. 3518-3522, 2014.

[25] M. Wadi, A. Shobole, M. R. Tur, and M. Baysal, "Smart hybrid wind-solar street lighting system fuzzy based approach: Case study Istanbul-Turkey," in *2018 6th International Istanbul Smart Grids and Cities Congress and Fair (ICSG)*, 2018, pp. 71-75.

[26] G. Liu, "Sustainable feasibility of solar photovoltaic powered street lighting systems," *International Journal of Electrical Power & Energy Systems*, vol. 56, pp. 168-174, 2014.

[27] O. D. Cota and N. M. Kumar, "Solar energy: a solution for street lighting and water pumping in rural areas of Nigeria," in *Proceedings of International Conference on Modelling, Simulation and Control (ICMSC-2015)*, 2015, pp. 1073-1077.

[28] M. Fathi, A. Chikouche, and M. Abderrazak, "Design and realization of LED Driver for solar street lighting applications," *Energy procedia*, vol. 6, pp. 160-165, 2011.

[29] W. Sutopo, I. S. Mardikaningsih, R. Zakaria, and A. Ali, "A model to improve the implementation standards of street lighting based on solar energy: A case study," *Energies*, vol. 13, p. 630, 2020.

[30] A. Khalil, Z. Rajab, M. Amhammed, and A. Asheibi, "The benefits of the transition from fossil fuel to solar energy in Libya: A street lighting system case study," *Applied Solar Energy*, vol. 53, pp. 138-151, 2017.

[31] M. Dalla Costa, L. Schuch, L. Michels, C. Rech, J. Pinheiro, and G. Costa, "Autonomous street lighting system based on solar energy and LEDs," in *2010 IEEE International Conference on Industrial Technology*, 2010, pp. 1143-1148.

Balochistan Journal of Engineering & Applied Sciences (BJEAS) – (p-ISSN: 2518-2706
Volume 6, No.1

Enhancing Diesel Generator Efficiency- Best Practices for Optimized Operation

Abdul Hameed Soomro[2], Saeed Ahmed Shaikh[2], Muhammad Waseem[3], NaseebUllah[3], Awais Ahmed[3], Zainab Junejo[3], Tayab Bajkani[3]
[2]Faculty, Department of Electrical Engineering, Quaid-e-Awam University of Engineering Science and Technology Nawabshah Campus Larkana, Sindh Pakistan
[3]Students, Department of Electrical Engineering, Quaid-e-Awam University of Engineering Science and Technology Nawabshah Campus Larkana, Sindh Pakistan
Corresponding Author: Abdul Hameed Soomro, Email: abdul.hameed@quest.edu.pk

***Abstract*—Large consumers are extensively utilising diesel generators as a backup in case of electricity failure due to their availability and consistent operation, but their low efficiency and consumption of a large amount of fuel come from the limitations of diesel generators. The improved efficiency will result in lower fuel consumption, a lower cost of operation, and greater sustainability. The main objective of this study is to improve the efficiency of a diesel generator with a lower fuel cost. Different types of methods were presented for the improvement of diesel generator efficiency, power output, and fuel consumption, such as turbo charging, variable geometry turbo charging, and cylinder deactivation. The system based on solar, wind, and battery systems can be utilised for efficiency improvement, monitoring of load demand, speed of the engine, and fuel consumption, but this system incorporates more than one energy source, which results in a large maintenance cost. In this research study, we have analysed the efficiency of a 50KVA diesel generator installed at QUEST, Campus Boys Hostels, through the development of a simulation model in MATLAB software under load variations.**

Index Terms: *Diesel Generator, Generator Efficiency, optimized operations*

I. INTRODUCTION

Diesel generators are widely used as a reliable source of backup power in various industries, including hospitals, data centres, and manufacturing facilities, but they consume significant amounts of fuel and produce high levels of greenhouse gas emissions [1]. Therefore, improving the efficiency of diesel generators has become a critical issue in recent years [2]. Several methods have been proposed to improve the efficiency of diesel generators. One method is the use of advanced fuel injection systems. These systems use advanced injectors and control systems to optimise the fuel injection process, resulting in improved combustion efficiency and reduced emissions [3]. A study conducted by Wang et al. (2016) demonstrated that using an advanced fuel injection system reduced fuel consumption by up to 20% and lowered emissions by up to 40% [4]. The method is the use of variable speed drives (VSDs), which allow the diesel generator to adjust its engine speed to match the load demand, resulting in reduced fuel consumption and improved efficiency. A study by Bione et al. (2019) found that the use of VSDs reduced fuel consumption by up to 30% and improved the efficiency of the diesel generator by up to 15% [5]. Cylinder deactivation is another method that can be used to improve the efficiency of diesel generators [6]. This technology allows the engine to deactivate some cylinders when the load demand is low, resulting in reduced fuel consumption and improved efficiency. A study by Gao et al. (2018) found that cylinder deactivation technology improved the fuel economy of a diesel generator by up to 12%. Exhaust gas recirculation (EGR) is a method of reducing nitrogen oxide emissions by recirculating exhaust gas back into the engine [7], and this method can also improve the efficiency of the diesel generator by reducing the amount of fuel needed for combustion. A study by Bione et al. (2019) found that the use of EGR reduced nitrogen oxide emissions by up to 80% and improved the efficiency of the diesel generator by up to 10%. [8]. Maintenance and cleaning of the diesel generator can also improve its efficiency. Regular maintenance activities such as changing the oil, cleaning the air filters, and tuning the engine can ensure that the generator operates at peak efficiency [9]. A study by Carvalho et al. (2021) found that regular maintenance activities improved the efficiency of the diesel generator by up to 5% [10]. Renewable energy integration is another method that can be used to improve the efficiency of diesel generators [11]. Integrating renewable energy sources such as solar or wind power with the diesel generator can reduce the load demand on the generator, resulting in lower fuel consumption and improved efficiency [12]. A study by Li et al. (2019) found that the integration of solar power with a diesel generator reduced fuel consumption by up to 40% and improved the efficiency of the generator by up to 30% [13]. In conclusion, several methods have been proposed to improve the efficiency of diesel generators, including the use of advanced fuel injection systems, variable-speed drives, cylinder deactivation, exhaust gas recirculation, maintenance and cleaning, and renewable energy integration. These methods have been shown to reduce fuel consumption, lower emissions, and improve the efficiency of diesel generators in various contexts. In addition to the methods mentioned in the literature review, other methods can also be used to improve the efficiency of diesel generators. One such method is the use of hybrid energy systems, which combine two or more sources of energy, such as solar power, wind power, or batteries, with a diesel generator [14]. The use of a hybrid system can reduce reliance on the diesel generator and provide a more sustainable and efficient source of backup power [15]. A study by Singh et al. (2021) found that the integration of a solar-wind-battery hybrid system with a diesel generator reduced fuel consumption by up to 50% and improved the efficiency of the generator by up to 25% [16]. Another method is the use of waste heat recovery systems, which capture and reuse the heat generated by the diesel generator. The recovered heat can

be used for space heating, water heating, or to power a turbine or engine to generate additional electricity [17]. A study by Li et al. (2020) found that the use of a waste heat recovery system improved the efficiency of a diesel generator by up to 10% [18]. The use of advanced engine technologies such as lean-burn combustion and homogenous charge compression ignition (HCCI) can also improve the efficiency of diesel generators [19]. Lean-burn combustion uses a lean air-fuel mixture to reduce emissions and improve combustion efficiency, while HCCI uses a mixture of air and fuel that ignites spontaneously, resulting in improved efficiency and reduced emissions [20]. A study by Zhang et al. (2018) found that the use of HCCI technology improved the fuel economy of a diesel generator by up to 20% [21]. Lastly, the use of real-time monitoring and control systems can help improve the efficiency of diesel generators by optimising their operation based on real-time data [22]. These systems can monitor various parameters such as load demand, engine speed, and fuel consumption and adjust the operation of the generator accordingly [23]. A study by Duan et al. (2020) found that the use of a real-time monitoring and control system improved the efficiency of a diesel generator by up to 15% [24]. In summary, several methods can be used to improve the efficiency of diesel generators, including the use of hybrid energy systems, waste heat recovery systems, advanced engine technologies, and real-time monitoring and control systems. These methods can reduce fuel consumption, lower emissions, and improve the overall efficiency and sustainability of diesel generators, but they increase the cost of maintenance [25]. QUEST Campus Larkana was founded in 2010 with the aim of providing quality education to students. To meet the power requirements of the boy's hostel, a 50KVA generator was initially installed when the campus started its operations. As the campus expanded over the years with the induction of new student batches, one more boys hostel was manufactured and shared the load on this single 50KVA generator. In this research study, we have analysed the efficiency of a 50-kVA diesel generator installed at QUEST, a campus boy's hostel, through the development of a simulation model in MATLAB software under load variations. Figure 2 illustrates the efficiency improvement of using a VSDG rather than a fixed-speed one, especially at low loads [2].

Section 2 describes the diesel generator.
Section 3 describes the technical and economical aspects of diesel generators.
Section 4 describes the hostels at QUEST Campus Larkana.
Section 5 describes the methodology.
Section 6 describes the simulation results and discussions.
Section 7 describes the conclusions.

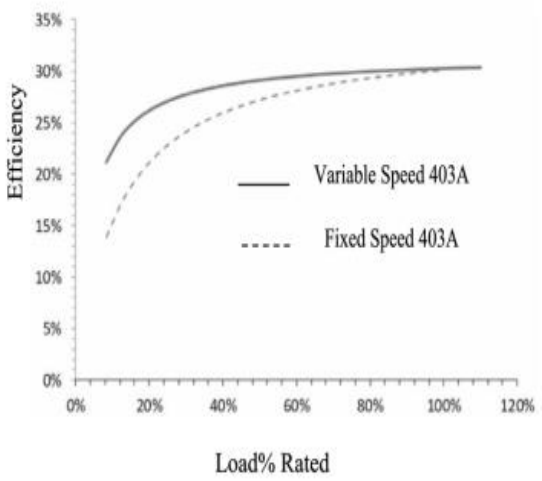

II. DIESEL GENERATOR

A diesel generator is a device that converts diesel fuel into electrical energy [1]. It is commonly used in areas where a reliable source of electricity is not available or as a backup power source in case of power outages [8]. The construction of a diesel generator involves several parts, including the engine, alternator, fuel system, and control panel [26]. The engine is the heart of the diesel generator and is responsible for converting the energy from the fuel into mechanical energy [27]. Diesel engines are typically more efficient and durable than gasoline engines, making them a popular choice for generators [28]. They use compression ignition, where the fuel is sprayed into the cylinder at high pressure and is ignited by the heat generated by the compression of the air in the cylinder [29]. The alternator is another important part of the diesel generator [30]. It converts the mechanical energy generated by the engine into electrical energy. The alternator consists of a rotor and a stator. The rotor is a rotating component that is driven by the engine, while the stator is a stationary component that produces the electrical current [31]. The fuel system is responsible for supplying diesel fuel to the engine. It includes components such as the fuel tank, fuel filter, fuel pump, and fuel injectors [32]. The fuel tank stores the diesel fuel, while the fuel filter removes any impurities from the fuel [8]. The fuel pump then pumps the clean fuel to the injectors, which spray the fuel into the cylinder [33]. The control panel is the part of the generator that allows the user to start and stop the generator, monitor its performance, and control its output [34]. It typically includes gauges for measuring the voltage, current, and frequency of the electrical output, as well as controls for starting and stopping the engine and adjusting the output [35]. In summary, a diesel generator is a reliable and efficient device that converts diesel fuel into electrical energy. Its construction involves several important parts, including the engine, alternator, fuel system, and control panel. Together, these parts work to provide a reliable source of power in areas where electricity is not readily available [36]. There are several ways to improve the efficiency of a diesel generator, including: Reducing Engine Load: The efficiency of a diesel generator can be improved by reducing the load on the engine. Reducing the number of electrical devices connected to the generator or using more effective

devices can achieve this. Increasing Compression Ratio: The compression ratio of a diesel engine can be increased to improve its efficiency. This can be done by changing the design of the engine or by using higher-quality fuel. Improving Fuel Quality: The efficiency of a diesel generator can be improved by using higher-quality fuel, such as low-sulphur diesel or biodiesel. Regular Maintenance: Regular maintenance of the diesel generator can help improve its efficiency. This includes cleaning or replacing air filters, checking fuel injectors, and keeping the engine well lubricated.

The efficiency, output power, fuel consumption, and load of a diesel generator can be calculated through equations (1-4) [9].Efficiency $= {}^{P_{out}}/_{P_{in}}$ (1)

Where

P_{in} is the input Power which is equal to Fuel Consumption x Fuel Energy Content

P_{out} is the output Power

$$P_o = V \times I \times Cos\emptyset \quad (2)$$

Where

P_o is the output Power, V is the voltage, and $Cos\emptyset$ is power factor

$$F_C = {}^{P_o}/_{SFC} \quad (3)$$

Where

F_C is the fuel consumption, P_{out} is the output power, and SFC is the specific power consumption

$$Load = {}^{P_o}/_{P_{rated}} \quad (4)$$

Where P_{rated} is the rated power which is the maximum power that the generator can produce.

III. TECHNICAL AND ECONOMICAL ASPECTS OF DIESEL GENERATOR

In a conventional DG, the DE operates at a consistent speed to deliver a predetermined mechanical torque for an electric power generator [1]. It does so without considering the fluctuations in electric load or engine efficiency [37]. On the other hand, the VSDG addresses these limitations by dynamically adjusting its operation to enhance efficiency while maintaining a balance between supply and demand [37]. Figure 1 depicts a performance analysis contrasting the VSDG and conventional DG across various climatic conditions [1].

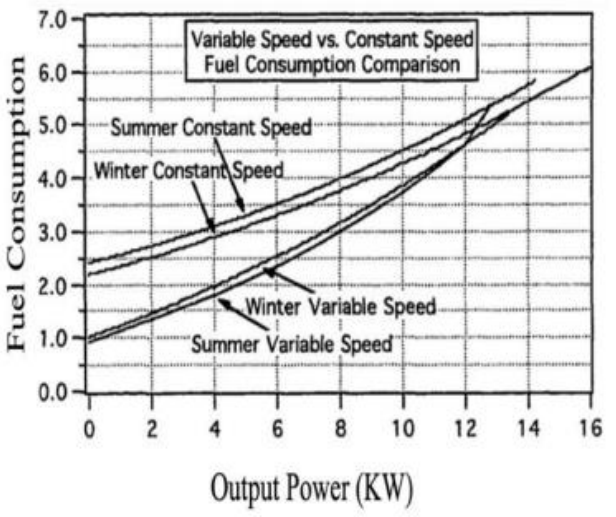

Fig 1. Performance Analysis VSDG and Conventional DG

A. Economic Improvement.

The comparison depicted in Figure 4 reveals that when the load decreases, a variable-speed diesel generator (VSDG) exhibits lower fuel consumption compared to a fixed-speed diesel generator (FSDG) [38]. In a study, it was observed that the brake-specific fuel consumption (BSFC) profile of an FSDG significantly increases when the electric load reaches 30–40% of its full load, whereas the VSDG maintains a nearly constant BSFC by synchronising the DE speed with the load. By allowing the DE to operate at its most efficient speed based on the load [39], the VSDG offers several advantages, including enhanced fuel efficiency based on load characteristics. Increased engine lifespan and extended time intervals between engine overhauls

Technical AspectsThe amount of current drawn from the generator varies with the load, while it is important to maintain constant voltage and frequency. During peak loads, the stator poles of the generator absorb a higher magnetic flux from the rotor windings. Consequently, the mechanical torque applied to the rotor shaft must increase to maintain the required fixed speed corresponding to a fixed voltage frequency and amplitude [40]. The DE crankshaft, which is solidly connected to the power generator's rotor, must provide sufficient mechanical torque to ensure the production of high-quality power. However, in an FSDG, as the load decreases, the DE crankshaft maintains a fixed speed with lower torque, resulting in reduced efficiency.

A. HOSTELS: QUEST CAMPUS LARKANA

QUEST Campus Larkana was founded in 2010 with the aim of providing quality education to engineering students in the fields of electrical, civil, mechanical, electronic, and computer systems. To meet the power requirements of the boy's hostel, a 50KVA generator was initially installed when the campus started its operations. As the campus expanded over the years with the induction of new student batches, one more boys hostel was manufactured and shared the load on this single 50KVA generator. There are ZA Bhutto and PTS hostels with a capacity of 500 student residences and 200 rooms. The facilities in the hostels are: outdoor games, TV

lounge, mosques, play ground, well-maintained study hall, and many other things. The overall load of hostels is 234.36 amperes, including water cooling machines and water pumping motors, and the capacity of generators is less than the required load. Figure 1 shows the front view of hostels. Figure 3 shows the 50KVA diesel generator at hostels.

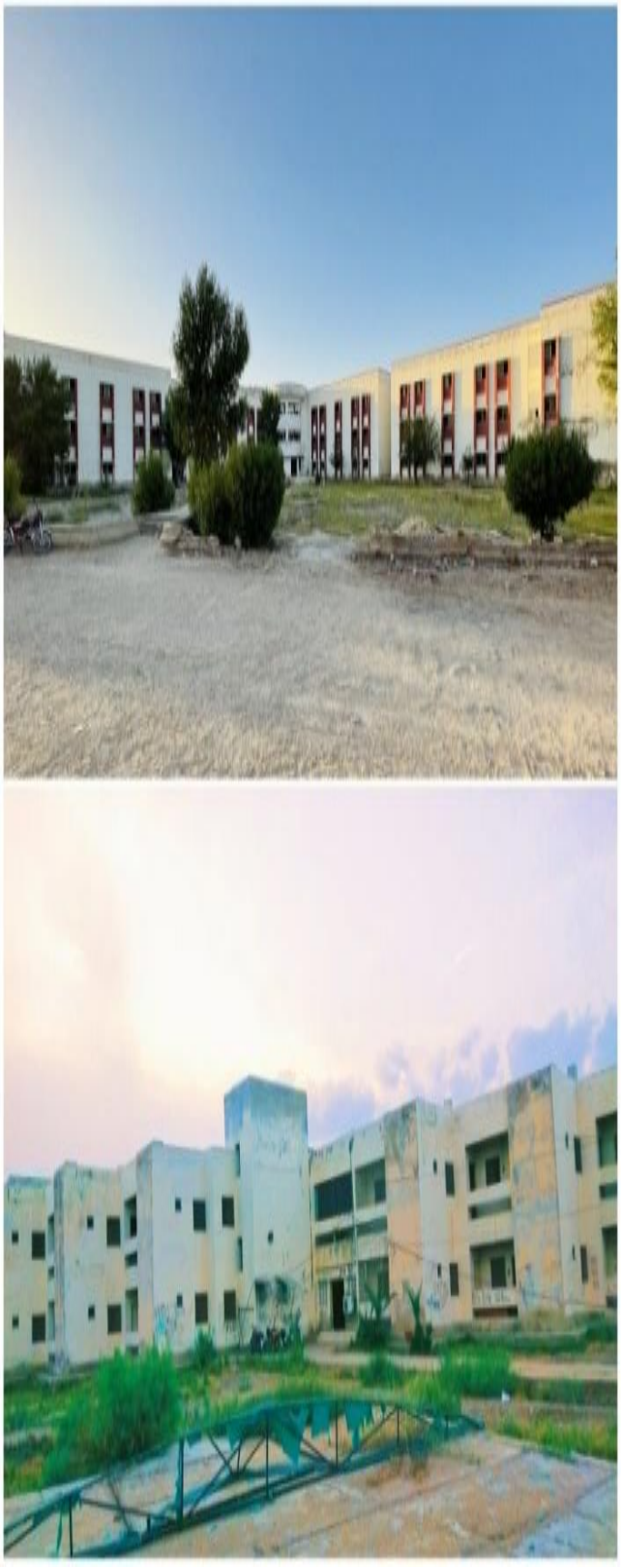

Figure 2. Front view of Hostels

Figure 3. 50KVA diesel generator at Hostels

IV. METHODOLOGY

The performance of a diesel generator operating under normal and overload condition, is assessed using a simulation model developed in MATLAB software. Figure 4 illustrates the generator simulation model, while Table I presents the generators' parameters.

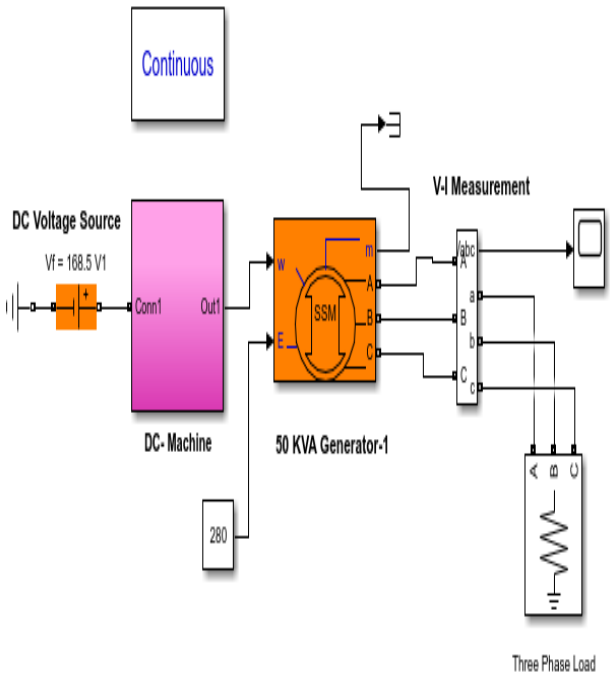

Fig 4. Matlab Model of Diesel Generator

Table I. Parameters of AC Generators

S.No	Generator Parameters	Value
1	Generator rating	50 KVA
2	Output voltage per phase	220 volts
3	Frequency	50 Hz
4	Inertia	$3.7e^3$
5	Pair of poles	2 Nos
6	Internal Resistance	0.0001 Ohm
7	Internal Inductance	0.05 Henry
8	DC Machine Field type	Wound
9	Armature Resistance of DC machine	24 Ohm
10	Field Resistance of DC machine	618 Ohm
11	Field Inductance of DC machine	0.05 Henry
12	Field Armature mutual inductance of DC machine	1.8 Henry
13	Initial Field Current of DC machine	0.3 Ampere

I. Simulation Results and Discussions

A. *Generator operating under normal load conditions (at 50 amperes)*

During the initial stage, the load of the PTS hostel was 50 amperes, which could be met with a single unit generator without any issues. The simulation results indicate that the generator was able to produce a stable 220-volt three-phase output without any oscillations and satisfactorily meet the load requirement. Figure 5 depicts the simulation results of the generator operating under normal load conditions.

Discussion

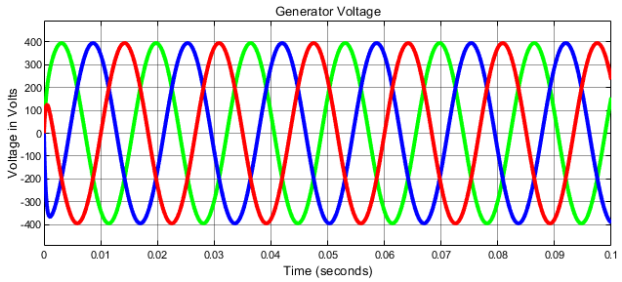

Fig. 5. Generator output voltage at 50A

B. *Generator operating under Normal Load condition (At 120Ampere)*

During this condition, the half one portion of 40 rooms of ZA Bhutto hostel were allotted to the students for residence then load of both hostels was increased from 50A to 120A. The simulation results indicate that the generator was able to produce a stable 220V without any oscillations and satisfactorily meet the load requirement. Figure 6 depicts the simulation results of the generator operating under normal load conditions.

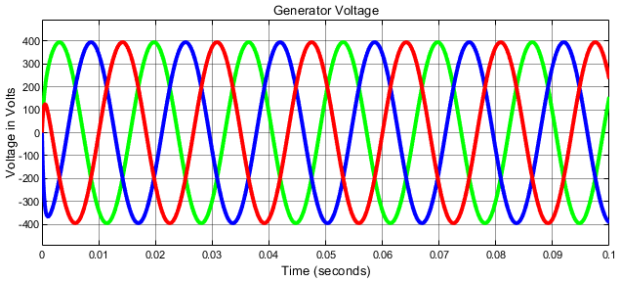

Fig. 6. Generator output voltage at 120A

C. *Generator operating under normal load condition (at 120 amperes)*

During this condition, half a portion of the 40 rooms of the ZA Bhutto hostel were allotted to the students for residence, and the load of both hostels was increased from 50A to 120A. The simulation results indicate that the generator was able to produce a stable 220V without any oscillations and satisfactorily meet the load requirement. Figure 6 depicts the simulation results of the generator operating under normal load conditions.

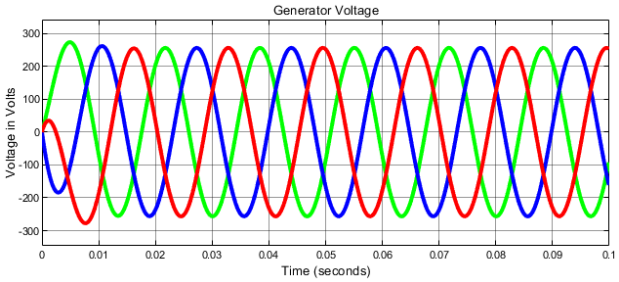

Fig. 7. Generator output voltage at 230A

According to existing literature, Pakistan is experiencing an increasing power crisis that is making it difficult for the industrial, public, and commercial sectors to maintain reliable operations of their equipment. Although solar systems are available, they can be costly and unreliable at night. As a result, an AC generator is often seen as the best option to bridge the energy gap between day and night. However, simulations have shown that a single-unit generator may not perform well under overload conditions, resulting in consumers receiving less voltage for utilisation and the generator overheating and shutting down. To address this issue, it is recommended to connect another generator of the same rating in parallel to ensure satisfactory performance under overload conditions. Table II provides simulation results for the operation of an AC generator.

Table. II. shows the simulation results of operation of AC generators operating alone and in parallel.

S. No	Load	Output Voltage of Generator
1	At 50 Ampere	400 Volts
2	At 120 Ampere	390 Volts
3	At 280 Ampere	280Volts

CONCLUSIONS

The efficiency and sustainability of diesel generators are essential concerns in various applications, including backup power sources for critical infrastructure and remote areas. This paper has provided a literature review of the methods for improving the efficiency of diesel generators, including engine modifications, fuel additives, hybrid energy systems, waste heat recovery systems, advanced engine technologies, and real-time monitoring and control systems. The review shows that several methods can be used to improve the efficiency of diesel generators, and each method has its advantages and disadvantages. Engine modifications, such as turbocharging and cylinder deactivation, can enhance the engine's performance and reduce fuel consumption and emissions. The use of fuel additives, such as biodiesel and ethanol, can also reduce emissions and improve combustion efficiency. Hybrid energy systems and waste heat recovery systems can provide a more sustainable and efficient source of backup power, while advanced engine technologies, such as lean-burn combustion and HCCI, can improve combustion efficiency and reduce emissions. Real-time monitoring and control systems can optimise the operation of diesel generators based on real-time data, improving efficiency and reducing fuel consumption and emissions. Further research is needed to optimise these methods and explore new technologies for improving the efficiency and sustainability of diesel generators. In summary, improving the efficiency of diesel generators is a critical issue for achieving sustainable energy production and reducing greenhouse gas emissions. The methods presented in this paper can serve as a guideline for enhancing the efficiency of diesel generators and providing a more sustainable and reliable source of backup power.

Acknowledgements

We are thankful to Dr. Abdul Hameed Soomro who support us to achieve this goal.

REFERENCES

[1] M. Mobarra, M. Rezkallah, and A. Ilinca, "Variable speed diesel generators: Performance and characteristic comparison," *Energies*, vol. 15, p. 592, 2022.

[2] R. Barbosa, M. Issa, S. Silva, and A. Ilinca, "Variable Speed Diesel Electric Generators: Technologies, Benefits, Limitations, Impact on Greenhouse Gases Emissions and Fuel Efficiency," *Journal of Energy and Power Technology*, vol. 4, pp. 1-21, 2022.

[3] A. K. Agarwal, V. Kumar, A. Jena, and A. Kalwar, "Fuel injection strategy optimisation and experimental performance and emissions evaluation of diesel displacement by port fuel injected methanol in a retrofitted mid-size genset engine prototype," *Energy*, vol. 248, p. 123593, 2022.

[4] X. Wang, Y. Qian, Q. Zhou, and X. Lu, "Modulated diesel fuel injection strategy for efficient-clean utilization of low-grade biogas," *Applied Thermal Engineering*, vol. 107, pp. 844-852, 2016.

[5] D. E. Batueva and J. E. Shklyarskiy, "Increasing efficiency of using wind diesel complexes through intellectual forecasting power consumption," in *2019 IEEE Conference of Russian Young Researchers in Electrical and Electronic Engineering (EIConRus)*, 2019, pp. 434-436.

[6] G. Musicco, "Development of simulation methodologies and analysis of advanced VVA and Cylinder Deactivation strategies for Diesel engines," Politecnico di Torino, 2019.

[7] J. Chen, X. Gao, L. Yan, and D. Xu, "Retracted Article: Computational fluid dynamics modeling of the millisecond methane steam reforming in microchannel reactors for hydrogen production," *RSC advances*, vol. 8, pp. 25183-25200, 2018.

[8] M. Issa, H. Ibrahim, R. Lepage, and A. Ilinca, "A review and comparison on recent optimization methodologies for diesel engines and diesel power generators," *Journal of Power and Energy Engineering*, vol. 7, p. 31, 2019.

[9] O. Khvatov and D. Kobyakov, "Increasing the efficiency of a diesel-generator power plant," *Russian Electrical Engineering*, vol. 91, pp. 742-748, 2020.

[10] V. H. L. Correia, R. P. de Abreu, and M. Carvalho, "Robustness within the optimal economic polygeneration system for a dairy industry," *Journal of Cleaner Production*, vol. 314, p. 127976, 2021.

[11] E. Oró, V. Depoorter, A. Garcia, and J. Salom, "Energy efficiency and renewable energy integration in data centres. Strategies and modelling review," *Renewable and Sustainable Energy Reviews*, vol. 42, pp. 429-445, 2015.

[12] H. A. Kazem, H. A. Al-Badi, A. S. Al Busaidi, and M. T. Chaichan, "Optimum design and evaluation of hybrid solar/wind/diesel power system for Masirah Island," *Environment, Development and Sustainability*, vol. 19, pp. 1761-1778, 2017.

[13] J. Lian, Y. Zhang, C. Ma, Y. Yang, and E. Chaima, "A review on recent sizing methodologies of hybrid renewable energy systems," *Energy Conversion and Management*, vol. 199, p. 112027, 2019.

[14] M. Jahangiri, O. Nematollahi, A. Haghani, H. A. Raiesi, and A. Alidadi Shamsabadi, "An optimization of energy cost of clean hybrid solar-wind power plants in Iran," *International Journal of Green Energy*, vol. 16, pp. 1422-1435, 2019.

[15] M. Shivaie, M. Mokhayeri, M. Kiani-Moghaddam, and A. Ashouri-Zadeh, "A reliability-constrained cost-effective model for optimal sizing of an autonomous hybrid solar/wind/diesel/battery energy system by a modified discrete bat search algorithm," *Solar Energy*, vol. 189, pp. 344-356, 2019.

[16] M. Suresh and R. Meenakumari, "An improved genetic algorithm-based optimal sizing of solar photovoltaic/wind turbine generator/diesel generator/battery connected hybrid energy systems for standalone applications," *International Journal of Ambient Energy*, vol. 42, pp. 1136-1143, 2021.

[17] A. T. Hoang, "Waste heat recovery from diesel engines based on Organic Rankine Cycle," *Applied energy*, vol. 231, pp. 138-166, 2018.

[18] J. Wang, X. Song, Y. Li, C. Zhang, C. Zhao, and L. Zhu, "Modeling and analysis of thermoelectric generators for diesel engine exhaust heat recovery system," *Journal of Energy Engineering*, vol. 146, p. 04020002, 2020.

[19] V. Rapp, N. Killingsworth, P. Therkelsen, and R. Evans, "Lean-burn internal combustion engines," *Lean Combustion*, pp. 111-146, 2016.

[20] J. Liu and C. E. Dumitrescu, "Lean-burn characteristics of a heavy-duty diesel engine retrofitted to natural-gas spark ignition," *Journal of Engineering for Gas Turbines and Power*, vol. 141, 2019.

[21] Y. Zhuang, Y. Qian, and G. Hong, "Lean burn performance of a spark ignition engine with an ethanol–gasoline dual injection system," *Energy & fuels*, vol. 32, pp. 2855-2868, 2018.

[22] C. Wang, Y. Liu, X. Li, L. Guo, L. Qiao, and H. Lu, "Energy management system for stand-alone diesel-wind-biomass microgrid with energy storage system," *Energy*, vol. 97, pp. 90-104, 2016.

[23] M. Y. Worku, M. A. Hassan, and M. A. Abido, "Real time energy management and control of renewable energy based

microgrid in grid connected and island modes," *Energies*, vol. 12, p. 276, 2019.

[24] P. Li, W. Sheng, Q. Duan, Z. Li, C. Zhu, and X. Zhang, "A Lyapunov optimization-based energy management strategy for energy hub with energy router," *IEEE Transactions on Smart Grid*, vol. 11, pp. 4860-4870, 2020.

[25] M. J. Khan, A. K. Yadav, and L. Mathew, "Techno economic feasibility analysis of different combinations of PV-Wind-Diesel-Battery hybrid system for telecommunication applications in different cities of Punjab, India," *Renewable and Sustainable Energy Reviews*, vol. 76, pp. 577-607, 2017.

[26] A. H. Soomro, S. A. A. Shah, A. Khauhwar, S. Talani, A. A. Solangi, T. Soomro, *et al.*, "Simulation based Analysis of Single Unit and Parallel Connected Three Phase AC Generator in QUEST Campus Larkana," *Sukkur IBA Journal of Emerging Technologies*, vol. 5, pp. 33-41, 2022.

[27] K. Mollenhauer, H. Tschöke, and K. G. Johnson, *Handbook of diesel engines* vol. 1: Springer Berlin, 2010.

[28] K. Reif, *Diesel engine management*: Springer, 2014.

[29] L. Guzzella and A. Amstutz, "Control of diesel engines," *IEEE Control Systems Magazine*, vol. 18, pp. 53-71, 1998.

[30] M. Canova, K. Sevel, Y. Guezennec, and S. Yurkovich, "Control of the start/stop of a diesel engine in a parallel HEV with a belted starter/alternator," SAE technical paper 0148-7191, 2007.

[31] M. G. Gouda and F. F. Haddix, "The alternator," *Distributed Computing*, vol. 20, pp. 21-28, 2007.

[32] J. Tickell, *From the fryer to the fuel tank: the complete guide to using vegetable oil as an alternative fuel*: Biodiesel America, 2003.

[33] N. Green, M. Mueller-Stoffels, and E. Whitney, "An Alaska case study: Diesel generator technologies," *Journal of Renewable and Sustainable Energy*, vol. 9, p. 061701, 2017.

[34] A. Mohammed, J. Pasupuleti, T. Khatib, and W. Elmenreich, "A review of process and operational system control of hybrid photovoltaic/diesel generator systems," *Renewable and Sustainable Energy Reviews*, vol. 44, pp. 436-446, 2015.

[35] A. Palamar and E. Pettai, "Control system for a diesel generator and ups based microgrid," *Rigas Tehniskas Universitates Zinatniskie Raksti*, vol. 27, p. 47, 2010.

[36] L. Luo, L. Gao, and H. Fu, "The control and modeling of diesel generator set in electric propulsion ship," *International Journal of Information Technology and Computer Science (IJITCS)*, vol. 3, p. 31, 2011.

[37] M. Asif and M. Iqbal, "Diesel consumption in a high penetration remote hybrid power system with a pumped hydro and battery storage," in *2013 IEEE Electrical Power & Energy Conference*, 2013, pp. 1-6.

[38] A. Shirneshan, M. Almassi, B. Ghobadian, A. Borghei, and G. Najafi, "Brake specific fuel consumption of diesel engine by using biodiesel from waste cooking oil," *World Sci. J*, vol. 1, pp. 45-52, 2013.

[39] M. Greig and J. Wang, "Fuel consumption minimization of variable-speed wound rotor diesel generators," in *IECON 2017-43rd Annual Conference of the IEEE Industrial Electronics Society*, 2017, pp. 8572-8577.

[40] A. Barakat, S. Tnani, G. Champenois, and E. Mouni, "Analysis of synchronous machine modeling for simulation and industrial applications," *Simulation Modelling Practice and Theory*, vol. 18, pp. 1382-1396, 2010.

Balochistan Journal of Engineering & Applied Sciences (BJEAS) – (p-ISSN: 2518-2706
Volume 6, No.1

Review of Water Management in Balochistan: Challenges, Policies, and Innovative Approaches

Jahanzaib Abdullhazai Kakar[1], Kabir Utmankhail Kakar[2] , Arshad Hussain Hashmi[3]
[1]Project Engineer, Sabagzai Dam Irrigation Department, Government of Balochistan
[2]Executive Engineer, Irrigation Department, Government of Balochistan
[3]Registrar, Pakistan Institute of Development Economics. Islamabad, Pakistan
Corresponding author: jhanzaib1232@gmail.com

***Abstract*—This review paper provides an overview of Balochistan, the largest province in Pakistan, and its water resources. Balochistan is a semi-arid to arid region with diverse hydrological features, including rivers, groundwater, and precipitation. The water resources in the province are mainly managed by the Water and Power Development Authority (WAPDA) and the Balochistan Water and Development Board (BWDB). The paper highlights the importance of water management in Balochistan for socio-economic progress, focusing on agriculture, drinking water supply, environmental sustainability, economic development, and social welfare. The study aims to identify the challenges and prospects related to water governance in Balochistan and evaluate existing policies and procedures. It covers various aspects of water management, including water resources, infrastructure, governance, demand and supply, and conservation. The paper discusses the surface water resources in Balochistan, such as rivers, dams, and reservoirs, as well as the significance of groundwater, particularly the Quetta Aquifer. It also emphasizes the impact of climate change on water resources in the region. Water quality issues, including salinity, arsenic contamination, and fluoride contamination, are addressed, and their effects on public health and agriculture are discussed. The challenges faced in water management include water scarcity, limited access to safe drinking water, poor infrastructure, climate change, and conflicting water demands. The paper suggests that a comprehensive approach integrating supply and demand management strategies is necessary to overcome these challenges. Various water management policies and strategies are examined, including the National Water Policy of Pakistan, the Provincial Water Management Strategy and Action Plan, irrigation and agriculture policies, and drinking water supply and sanitation policies. Community-based water management initiatives are also highlighted as an essential element of water management in Balochistan.**

I. A BRIEF OVERVIEW OF BALOCHISTAN AND ITS WATER RESOURCES

Balochistan constitutes the largest province of Pakistan in terms of area, encompassing around 44% of the nation's land area. The area is in the country's southwestern region and is adjacent to Afghanistan and Iran [1]. The hydrological features of the province are varied, encompassing deserts, mountains, plateaus, and coastal regions. The estimated population of Balochistan is around 12.3 million, which ranks it among the least populated provinces in Pakistan [2]. The water resources in Balochistan rely mainly on its rivers, groundwater, and precipitation. The region where the province is situated is semi-arid to arid, and it experiences frequent droughts[3].

The water resources management in the province is mainly carried out by the Water and Power Development Authority (WAPDA) and the Balochistan Water and Development Board (BWDB) [4].

The water supply of Balochistan indicates that the province's rivers primarily depend on rainfall, except for the Indus River, which serves as the province's eastern border. The Zhob, Bolan, Pishin, and Hingol are the primary rivers in Balochistan [5]. The province has several small dams and reservoirs that serve as water sources for drinking and irrigation. Groundwater is vital in providing water resources in Balochistan, especially in regions with little surface water. The Quetta Aquifer is the province's largest and most productive aquifer, and several other aquifers are in the area. Nonetheless, inadequate management practices and overexploitation have resulted in the depletion of groundwater levels and the degradation of water quality in certain regions [6].

The province typically receives an average annual rainfall of approximately 200-300 mm. Rainfall exhibits high variability; certain regions receive over 500 mm of precipitation while others receive less than 100 mm. Rainwater harvesting and conservation practices have succeeded in certain regions. These practices are being advocated as a viable and sustainable solution to address water scarcity issues in the province [7].

The water resources in Balochistan are crucial for the region's socio-economic progress and the welfare of its inhabitants. The management of water resources in the province is faced with several challenges that hinder sustainable practices. These challenges include inadequate facilities, poor infrastructure, and water scarcity. To tackle these challenges, a holistic and unified strategy for water management is necessary, encompassing improved policies, governance, and community involvement [8].

II. IMPORTANCE OF WATER MANAGEMENT IN BALOCHISTAN

Balochistan's economy heavily depends on agriculture, the primary livelihood source for most of its population. Nonetheless, it is evident that agriculture relies heavily on water resources, and water scarcity has significantly impacted agricultural output in the region. Efficient water management can enhance agricultural productivity, boost crop yields, and improve food security in the area [9].

A. *Drinking Water Supply*

Ensuring access to safe drinking water is a fundamental human right; however, many individuals in Balochistan are deprived of access to uncontaminated drinking water; it is reported by the Pakistan Council of Research in Water Resources (PCRWR) that more than 80% of water sources in

Balochistan are polluted with different contaminants, such as arsenic and fluoride. Effective hydrological practices can enhance the accessibility and purity of potable water in the region [10].

B. Environmental Sustainability

The ecosystem in Balochistan is delicate and can be quickly impacted by climate change, excessive use of natural resources, and unsustainable development methods. Effective water management is crucial for maintaining ecological balance, protecting biodiversity, and ensuring the sustainability of natural resources in the province [11].

C. Economic Development

Sufficient water resources are crucial for the advancement and prosperity of the economy. Hydrologically speaking, Balochistan exhibits significant potential for generating hydropower, which can serve as a sustainable and eco-friendly energy source for the region. Water resources support industrial growth, tourism, and other economic pursuits ([11].

D. Social Welfare

Effective water management is essential for ensuring the community's well-being in Balochistan. Better water management practices can positively impact poverty reduction, public health, and overall quality of life for the residents of this province. Implementing effective water management practices is imperative for ensuring Balochistan's sustainable development and promoting its populace's overall welfare. Resolving issues about water scarcity, pollution, and ineffective management necessitates collaborating with governmental bodies, non-governmental organizations, and the business community. Sustainable water management practices can enhance agricultural productivity, facilitate access to potable water, foster environmental sustainability, stimulate economic growth, and augment social welfare within the province [12].

III. PURPOSE AND SCOPE OF THE REVIEW PAPER

This study aims to discern the obstacles and prospects related to water governance in Balochistan while also assessing the efficacy of existing policies and procedures. The review paper encompasses various topics about water management in Balochistan, comprising various aspects.

A. Water Resources

This study investigates the accessibility and caliber of surface and groundwater reservoirs in Balochistan while evaluating the influence of climate change on said resources.

B. Water Infrastructure

This study assesses the sufficiency and efficacy of the hydrological infrastructure, encompassing hydroelectric dams, water storage facilities, and irrigation networks, within the region.

C. Water Governance

This study examines the institutional arrangements, legal frameworks, and policy instruments of water governance in Balochistan.

D. Water Demand and Supply

This study evaluates the current state of water demand and supply in Balochistan while analyzing the factors that impact water demand, including population growth, urbanization, and agricultural practices.

E. Water Conservation and Management

This study examines the current strategies and endeavours concerning water preservation and administration in Balochistan while pinpointing optimal practices and prospects for enhancement.

IV. WATER RESOURCES OF BALOCHISTAN

Balochistan, encompassing an area of around 347,190 square kilometres, is the most extensive province of Pakistan. The geographical location of the area in question is in the nation's southwestern region. It exhibits contiguous boundaries with Afghanistan to the north and northwest, Iran to the west, and the Arabian Sea to the south. The region of Balochistan is characterized by a climate that ranges from semi-arid to arid, and the availability of water resources is limited. The hydrological system of the province is intricate, comprising two primary sources of water, namely surface and groundwater resources [13].

A. Surface Water Resources

Balochistan has four primary rivers: the Zhob, Mula, Bolan, and Hingol. Nonetheless, these rivers exhibit ephemeral characteristics and have a limited flow duration following the monsoon season. The region also has several minor streams and nullahs, which serve as irrigation and livestock sustenance sources. Balochistan boasts numerous dams and reservoirs that serve as storage facilities for water, catering to the needs of irrigation, drinking, and industrial sectors. Several significant dams and reservoirs, such as Mirani Dam, Mangi Dam, Tangi Dam, and Tauseef Dam, are present in the region.

B. Groundwater Resources

In Balochistan, groundwater is the principal water source for drinking and irrigation. The region under consideration encompasses two primary aquifers: the Quetta aquifer and the Pishin Lora aquifer. The Quetta aquifer is the preeminent and most prolific subterranean water-bearing formation in Balochistan, catering to the water requirements of the urban center of Quetta and its environs. The excessive utilization of groundwater reserves has resulted in a reduction in water levels and degradation of water quality in certain regions. Furthermore, the escalating levels of salinity and fluoride concentration in groundwater present noteworthy health hazards to the populace [15].

C. Climate Change and Water Resources

The impact of climate change poses a considerable risk to the water resources of Balochistan. The region exhibits a high susceptibility to the consequences of climate change, encompassing amplified temperatures, reduced precipitation, and altered precipitation distribution. The alterations mentioned above have resulted in a reduction in both the quantity and caliber of water in certain regions within the province. The amplified occurrence and severity of anomalous weather phenomena, such as inundations and

dry spells, have likewise had detrimental impacts on Balochistan's hydrological reserves and biotic communities. The water resources in Balochistan are limited and encounter significant obstacles stemming from excessive utilization, alterations in climate patterns, and declining water purity. Implementing proficient water management strategies, encompassing conservation, infrastructure advancement, and governance, is imperative to guarantee the durability and accessibility of water resources for future cohorts in Balochistan [16].

D. Water quality issues: salinity, arsenic, and fluoride contamination

The management of water in Balochistan is faced with significant challenges related to water quality, particularly regarding salinity, arsenic, and fluoride contamination.

D.A. Salinity:

The issue of salinity is a significant concern in Balochistan, particularly in the southern regions of the province. The introduction of irrigation has resulted in the buildup of salts in both the soil and groundwater. Elevated salinity levels harm the quality of water used for irrigation, ultimately leading to a decrease in crop productivity. Additionally, the elevated salt concentration in potable water can potentially induce adverse health effects, such as hypertension, renal impairment, and cardiovascular ailments [17].

D.B. Arsenic Contamination

The escalation of arsenic contamination has become a significant issue in Balochistan, with a particular focus on the Quetta Valley. The pollution is predominantly attributed to inherent geological mechanisms and amplified by anthropogenic operations such as mining and drilling. Arsenic is a hazardous element that can potentially induce cutaneous lesions, respiratory distress, and diverse forms of malignancy [18].

D.C. Fluoride Contamination

The presence of fluoride in the groundwater resources of Balochistan is a notable concern regarding water quality in the region. Elevated concentrations of fluoride in potable water have the potential to induce dental and skeletal fluorosis, a debilitating ailment that adversely impacts the skeletal and dental systems [19].

The water quality concerns in Balochistan have significant ramifications for public health and agriculture. A holistic strategy encompassing surveillance, governance, therapy, and educational initiatives is imperative to tackle these concerns. Furthermore, promoting sustainable water management strategies that mitigate dependence on groundwater and encourage the utilization of alternative water sources can effectively tackle these issues in the foreseeable future.

V. WATER MANAGEMENT IN BALOCHISTAN FACES SEVERAL CHALLENGES THAT, INCLUDE

A. Water Scarcity and Uneven Distribution

Balochistan is a region within Pakistan characterized by a notably arid climate and limited availability of water resources. The region's arid and semi-arid climatic conditions, with restricted precipitation and snow thaw, have led to persistent water scarcity. The issue is further compounded by the inequitable allocation of water resources across various geographical areas and societal groups [3].

B. Limited Access to Safe Drinking Water

Providing safe drinking water poses a significant obstacle in Balochistan, particularly its rural regions. The restricted accessibility of potable water sources, coupled with inadequate sanitation practices, contributes to the dissemination of waterborne illnesses such as cholera, typhoid fever, and hepatitis[20].

C. Poor Infrastructure and Inadequate Facilities

The region of Balochistan exhibits a notable insufficiency in infrastructure, specifically in the domains of water supply and sanitation. Inadequate water supply systems, wastewater treatment facilities, and storage infrastructure result in substantial losses and waste of water resources [21].

D. Climate Change and Its Impact on Water Resources

The effects of climate change have further complicated the water management issue in Balochistan. The alterations in temperature and precipitation regimes have led to a decline in the quantity and quality of water resources, consequently elevating the incidence of severe meteorological phenomena such as floods and droughts [22].

E. Conflicting Water Demands and Competing Interests

The divergent water requirements of various sectors, such as agriculture, industry, and domestic consumption, frequently result in conflicting interests and the depletion of resources. The issue is further complicated by inadequate governance and institutional capacity to manage these conflicts effectively [23].

A comprehensive approach that integrates supply and demand management strategies is necessary to tackle these challenges. The recommended measures entail the implementation of tactics such as water conservation, water pricing reforms, infrastructure development, governance reforms, and public awareness campaigns. In addition, implementing various water-sourcing methods such as rainwater harvesting, groundwater recharge, and desalination can promote sustainable water management practices in Balochistan [24].

VI. WATER MANAGEMENT POLICIES AND STRATEGIES IN BALOCHISTAN

Implementing water management policies and strategies is of utmost importance in tackling the water management issues in Balochistan. Several pivotal policies and strategies encompass:

A. National Water Policy and Its Relevance to Balochistan

The National Water Policy of Pakistan serves as a comprehensive structure for the effective governance and advancement of water resources within the nation. The policy acknowledges the water management difficulties encountered in Balochistan and advocates for implementing sustainable water management approaches, such as

encouraging water conservation, rainwater harvesting, and groundwater recharge [24].

B. Provincial Water Management Strategy and Action Plan

The provincial government of Balochistan has formulated a comprehensive strategy and action plan for water management at the provincial level. This plan is intended to guide water management initiatives throughout the region. The approach, as mentioned above, centers on advancing sustainable water usage methodologies, enhancing water governance and institutional proficiency, creating alternative water reservoirs, and ameliorating accessibility to potable water and sanitation [25].

C. Irrigation and Agriculture Policies

The agriculture industry in Balochistan exhibits a significant reliance on irrigation, thereby rendering irrigation policies a crucial determinant in the management of water resources. The provincial administration has formulated policies to advance sustainable irrigation practices, which encompass adopting effective irrigation systems, promoting crop diversification, and encouraging water-efficient crops [26].

D. Drinking Water Supply and Sanitation Policies

The Balochistan government has also developed policies to improve safe drinking water and sanitation access. These policies focus on improving the quality and availability of drinking water sources, developing wastewater treatment facilities, and promoting hygiene and sanitation practices [27].

E. Community-Based Water Management Initiatives

In Balochistan, water management policies incorporate community-based initiatives as a crucial element. These endeavors entail the dynamic engagement of indigenous communities in administering and preserving aquatic resources. The initiatives, as mentioned earlier, have received governmental backing in capacity building, technical assistance, and financial aid ([27].

The successful implementation of policies and strategies necessitates a harmonized and unified methodology that encompasses the involvement of all relevant stakeholders, such as the government, communities, and private sector entities. Balochistan can ensure a secure and sustainable water future by promoting sustainable water management practices, enhancing governance and institutional capacity, and exploring alternative water sources.

VII. WATER GOVERNANCE AND INSTITUTIONAL FRAMEWORK

Implementing efficient water governance and developing institutional capacity are essential factors in tackling the water management issues prevalent in Balochistan [28]. Several fundamental elements of water governance and institutional framework in Balochistan comprise:

A. Role of Government Agencies

Water management in Balochistan involves the participation of various governmental entities, such as the Water and Power Development Authority (WAPDA), Balochistan Water and Drainage Board (BWDB), Public Health Engineering Department (PHED), among others. The agencies are responsible for strategizing, constructing, and overseeing the water resources and infrastructure within the province [29].

B. Institutional Setup and Coordination Mechanisms

The management of water in Balochistan is characterized by a complex institutional framework that involves the participation of various agencies and stakeholders. Establishing coordination mechanisms, such as the Provincial Water Council and the Provincial Water Resources Development Board, facilitates interagency coordination and stakeholder engagement [29].

C. Stakeholder Engagement and Participation

The attainment of successful water management initiatives in Balochistan is contingent upon implementing effective stakeholder engagement and participation. The government has implemented various measures to foster collaboration with nearby communities and other relevant parties, such as forming Water Users Associations and Community-Based Organizations (30].

D. Challenges in Water Governance and Institutional Capacity Building

Notwithstanding the endeavors to enhance water governance and institutional capacity development, several obstacles endure. Some factors contributing to this issue are the absence of specialized knowledge, insufficient financial resources, ineffective institutional collaboration, and restricted involvement of interested parties. Moreover, the frequent replacement of government officials and the resultant political instability may impede the continuity and efficacy of endeavors to manage water resources [31].

Resolving obstacles in water governance and enhancing institutional capacity necessitates a continuous endeavor by the government, private sector, and communities. The process entails enhancing technical proficiency, reinforcing institutional collaboration, augmenting stakeholder engagement, and guaranteeing sufficient financial support and resources. Balochistan can secure a viable water prospect for its populace and financial system by mitigating these obstacles [32].

VIII. INNOVATIVE APPROACHES TO WATER MANAGEMENT IN BALOCHISTAN

The implementation of novel strategies for water management is imperative in order to tackle the water management predicaments in Balochistan effectively. Several novel approaches that can be implemented include:

A. Rainwater Harvesting and Conservation

Although Balochistan experiences a scarcity of precipitation, it is possible to collect and preserve the available rainfall for future utilization. Implementing rainwater harvesting and conservation techniques, such as rooftop rainwater harvesting, can potentially augment the accessibility of water resources within the province [9].

B. Artificial Recharge of Groundwater

The excessive utilization of subterranean water reserves poses a noteworthy predicament in Balochistan. Artificially recharging groundwater is a novel technique that replenishes the aquifers with surplus surface water during the monsoon season. This methodology can facilitate the restoration of groundwater reserves and mitigate their exhaustion [33].

C. Water-use Efficiency and Conservation Practices

Enhancing water-use efficiency and conservation techniques can aid in mitigating water demand and augmenting water availability in Balochistan. Water-conserving technologies, such as drip irrigation, sprinkler irrigation, and laser land leveling, have the potential to enhance crop productivity while minimizing water usage [34].

D. Innovative Financing Mechanisms and Public-Private Partnerships

Inventive financing mechanisms and collaborations between the public and private sectors can facilitate the mobilization of resources and promote sustainable water management practices in Balochistan. Private sector investments in water supply and sanitation infrastructure can potentially enhance the accessibility of safe drinking water [35].

E. Role of Technology in Water Management

The utilization of technology can be deemed a crucial factor in the effective management of water resources in the region of Balochistan. The utilization of remote sensing and GIS-based methodologies can facilitate the monitoring of water resources and the development of water management strategies. Novel technological advancements, such as desalination plants powered by solar energy and water treatment facilities, have the potential to enhance the accessibility of potable water [36].

The implementation of novel methodologies for water management has the potential to tackle the water management predicaments encountered in Balochistan effectively. Implementing these strategies necessitates a concerted endeavor involving the cooperation of the public sector, corporate entities, and local populations. Through the implementation of novel strategies, Balochistan has the potential to establish a viable water future that is sustainable for both its populace and economy [36].

F. CASE STUDIES AND BEST PRACTICES

Examining effective water management strategies and transferable frameworks in Balochistan can reveal valuable insights and exemplary approaches that can be implemented in other geographical areas. The following are instances of efficacious water management strategies and community-driven water management endeavors in Balochistan.

G. Karez System

Examining effective water management strategies and transferable frameworks in Balochistan can reveal valuable insights and exemplary approaches that can be implemented in other geographical areas. The following are instances of efficacious water management strategies and community-driven water management endeavors in Balochistan [37].

H. The Chagai Rainwater Harvesting Project

The Balochistan Rural Support Program (BRSP) has launched the Chagai Rainwater Harvesting Project intending to mitigate water scarcity in the Chagai district of Balochistan [38].

I. The Community-Based Water Management Project

The Pakistan Poverty Alleviation Fund (PPAF) has launched the Community-Based Water Management Project intending to enhance water management in Balochistan. The project entails the community's engagement in strategizing, conceptualizing, and executing water management initiatives. The project has effectively enhanced water management methodologies in multiple communities located in Balochistan [39].

J. Solar-Powered Water Supply Schemes

Some solar-powered water supply initiatives have been executed in Balochistan to enhance the availability of potable water. The initiatives mentioned above employ pumps powered by solar energy to extract subsurface water resources and distribute them to local populations. The efficacy of the schemes in furnishing dependable and enduring water supply to geographically isolated and unconnected regions has been demonstrated [39].

Conducting a comprehensive analysis of effective water management strategies and community-driven initiatives in Balochistan can reveal transferable frameworks and optimal methodologies that can be implemented in other geographical areas. Implementing these practices enhances water management, and fosters increased community participation and ownership in water management activities.

CONCLUSION AND RECOMMENDATIONS

To summarize, managing water resources in Balochistan encounters substantial obstacles such as inadequate water supply, imbalanced allocation, insufficient infrastructure, and concerns regarding water quality. The challenges of climate change and competing water demands are further compounded, underscoring the imperative of implementing efficient water management policies and strategies. Notwithstanding, there exist prospects for pioneering methodologies, such as rainwater harvesting, artificial groundwater recharge, and water-use efficiency practices, to tackle these predicaments.

In order to enhance water management in Balochistan, some policy and institutional suggestions are imperative. Initially, executing the National Water Policy and Provincial Water Management Strategy and Action Plan with greater coordination and efficacy is imperative. Furthermore, it is imperative to prioritize community-based water management initiatives, as they foster community involvement and ownership in water management endeavors. Thirdly, it is imperative to enhance water governance and institutional capacity building utilizing augmenting stakeholder engagement, refining coordination mechanisms, and bolstering the capacity of government agencies.

The involvement of stakeholders and the development of their capacities are essential components for the effective

management of water resources in the region of Balochistan. The engagement of stakeholders can enhance comprehension of conflicting water demands and foster the creation of comprehensive water management policies and strategies. The capacity-building process can improve institutional and technical capacities, producing more professional and productive water management practices.

Water management in Balochistan entails several research priorities, including water quality monitoring, the effects of climate change on water resources, water-use efficiency practices, and community-based water management practices. Undertaking research in these domains can enhance comprehension of the obstacles and prospects for water governance in Balochistan and guide the formulation of policies and strategies grounded in empirical evidence.
To enhance water management in Balochistan, a comprehensive strategy that encompasses policy and institutional restructuring, stakeholder engagement and skill development, and inventive water management techniques is necessary. By adopting effective strategies and capitalizing on favorable circumstances, Balochistan can enhance its water management methodologies and guarantee the longevity and impartiality of its water resources for future cohorts.

REFERENCES

[1] Kundi, M. A. (2016). Pak-Afghan Borderland Interaction: Alone Together. *Margalla Papers, 20*(1).

[2] Khan, K. A. (2022). Water Scarcity and its Impact on the Agricultural Sector of Balochistan. *Journal of Public Policy Practitioners, 1*(1), 01-66.

[3] Ahmed, K., Shahid, S., Harun, S. b., & Wang, X.-j. (2016). Characterization of seasonal droughts in Balochistan Province, Pakistan. *Stochastic environmental research and risk assessment, 30*, 747-762.

[4] Johnson, S. H. (2019). Social and economic impacts of investments in ground water: lessons from Pakistan and Bangladesh *Irrigation Management in Developing Countries: Current Issues and Approaches* (pp. 179-216): Routledge.

[5] Basharat, M. (2019). Water management in the Indus Basin in Pakistan: challenges and opportunities. *Indus river basin*, 375-388.

[6] Watto, M. A., & Mugera, A. W. (2016). Groundwater depletion in the Indus Plains of Pakistan: imperatives, repercussions and management issues. International Journal of River Basin Management, 14(4), 447-458.

[7] Abdullah, S. M., Ahmed, S. I., Hussain, E., Hasan, F., & Ahmed, S. (2023). Drought assessment of a data-scarced watershed-Quetta Valley, Pakistan. Jordan Journal of Civil Engineering, 17(2), 310-321.

[8] Malik, S. M., Awan, H., & Khan, N. (2012). Mapping vulnerability to climate change and its repercussions on human health in Pakistan. Globalization and health, 8(1), 1-10.

[9] Ashraf, M., Arshad, A., Patel, P. M., Khan, A., Qamar, H., Siti-Sundari, R., . . . Babar, J. R. (2021). Quantifying climate-induced drought risk to livelihood and mitigation actions in Balochistan. *Natural Hazards, 109*, 2127-2151.

[10] Shah, S. A. (2017). The provision and violation of water rights (the case of Pakistan)–a human rights based approach Charting the Water Regulatory Future (pp. 167-194): Edward Elgar Publishing.

[11] Zhang, L., Xu, M., Chen, H., Li, Y., & Chen, S. (2022). Globalization, green economy and environmental challenges: state of the art review for practical implications. Frontiers in Environmental Science, 10, 199.

[12] Baloch, Q. B., Shah, S. N., Iqbal, N., Sheeraz, M., Asadullah, M., Mahar, S., & Khan, A. U. (2023). Impact of tourism development upon environmental sustainability: A suggested framework for sustainable ecotourism. Environmental Science and Pollution Research, 30(3), 5917-5930.

[13] Siddiqui, G.-u., & Siddiqui, Z. A. (2009). Balochistan: People and Culture. Al-Burz, 1(1), 38-56.

[14] Dolo, M. (2020). Water supply challenges in urban and rural areas of Eastern Cape.

[15] Durrani, I. H., Adnan, S., Ahmad, M., Khair, S., & Kakar, E. (2018). Observed long-term climatic variability and its impacts on the ground water level of Quetta alluvial. Iranian Journal of Science and Technology, Transactions A: Science, 42, 589-600.

[16] Otto, F. E., Zachariah, M., Saeed, F., Siddiqi, A., Kamil, S., Mushtaq, H., . . . Barnes, C. (2023). Climate change increased extreme monsoon rainfall, flooding highly vulnerable communities in Pakistan. Environmental Research: Climate, 2(2), 025001.

[17] Qureshi, A. S., McCornick, P. G., Qadir, M., & Aslam, Z. (2008). Managing salinity and waterlogging in the Indus Basin of Pakistan. Agricultural Water Management, 95(1), 1-10.

[18] Dawood, F., Akhtar, M. M., & Ehsan, M. (2021). Evaluating urbanization impact on stressed aquifer of Quetta Valley, Pakistan. Desalination and water treatment, 222, 103-113.

[19] Khalid, S. (2019). An assessment of groundwater quality for irrigation and drinking purposes around brick kilns in three districts of Balochistan province, Pakistan, through water quality index and multivariate statistical approaches. Journal of Geochemical Exploration, 197, 14-26.

[20] Khattak, N., Hassnain, S. R. U., Shah, S. W., & Mutlib, A. (2006). Identification and removal of barriers for renewable energy technologies in Pakistan. Paper presented at the 2006 International Conference on Emerging Technologies.

[21] Mohammed, J., & Farooq, S. U. (2002). The role of public sector in the economic development of Balochistan. The Dialogue, 3(4), 472-494.

[22] Ali, G., Hasson, S., & Khan, A. M. (2009). Climate change: Implications and adaptation of water resources in pakistan. Global Change Impact Studies Centre (GCISC): Islamabad, Pakistan.

[23] Hargrove, W. L., & Heyman, J. M. (2020). A comprehensive process for stakeholder identification and engagement in addressing wicked water resources problems. Land, 9(4), 119.

[24] Morelands, S., & Jasper, S. (2014). A comprehensive approach to operations in complex enviroments. Monterrey: Calhoun.

[25] Aftab, S. M., Siddiqui, R. H., & Farooqui, M. A. (2018). Strategies to Manage Aquifer Recharge in Balochistan, Pakistan: An Overview. Paper presented at the IOP Conference Series: Materials Science and Engineering.

[26] Asghar, S., Sasaki, N., Jourdain, D., & Tsusaka, T. W. (2018). Levels of technical, allocative, and groundwater use efficiency and the factors affecting the allocative efficiency of wheat farmers in Pakistan. Sustainability, 10(5), 1619.

[27] Griffiths, J., & Lambert, R. (2013). Free flow: reaching water security through cooperation: Unesco.

[28] Yasin, H. Q., Breadsell, J., & Tahir, M. N. (2021). Climate-water governance: a systematic analysis of the water sector resilience and adaptation to combat climate change in Pakistan. Water Policy, 23(1), 1-35.

[29] Price, G., Alam, R., Hasan, S., Humayun, F., Kabir, M. H., Karki, C., . . . Saran, S. (2014). Attitudes to water in South Asia: Royal Institute of International Affairs London.

[30] Hussain, N., Haque, A. U., & Baloch, A. (2019). Management theories: The contribution of contemporary management theorists in tackling contemporary management challenges. Yaşar Üniversitesi E-Dergisi, 14, 156-169.

[31] Pahl-Wostl, C. (2015). Water governance in the face of global change: Springer.

[32] Niemczynowicz, J. (1999). Urban hydrology and water management–present and future challenges. Urban water, 1(1), 1-14.

[33] Ahmed, M., & Hassan, M. (2020). Real Unemployment in Balochistan, Pakistan: Context, Issues and Way Forward. Pakistan Vision, 21(2).

[34] Qadir, M., Sharma, B. R., Bruggeman, A., Choukr-Allah, R., & Karajeh, F. (2007). Non-conventional water resources and opportunities for water augmentation to achieve food security in water scarce countries. Agricultural Water Management, 87(1), 2-22.

[35] Thiele, T., & Gerber, L. R. (2017). Innovative financing for the high seas. Aquatic Conservation: Marine and Freshwater Ecosystems, 27, 89-99.

[36] Bhatti, S. S., Khattak, M. U. K., & Roohi, R. (2008). Planning water resource management in Pishin-Lora river basin of Balochistan using GIS/RS techniques. Paper presented at the 2008 2nd International Conference on Advances in Space Technologies.

[37] Khattak, A. S. (2014). Mutual sustainability of Tubewell farming and aquifers: Perspectives from Balochistan, Pakistan: Springer.

[38] Qureshi, M. (2022). Balochistan Livestock Breeding Policy 2022 and Action Plan.

[39] Appell, V., & Baluch, M. S. (2004). Mitigating the effects of drought through traditional and modern water supply systems in Balochistan. Poverty Reduction through Improved Agricultural Water Management, 241.

Balochistan Journal of Engineering & Applied Sciences (BJEAS) – (p-ISSN: 2518-2706
Volume 6, No.1

Optimization of Solar Panels Output by Determining Tilt Angle for Khuzdar Region

Zahoor Ahmed, Raza Haider, Muhammad Ilyas and Attaullah Khidrani
Balochisatan Univeristy of Engineering and Technology Khuzdar
Corresponding author: razahaider@buetk.edu.pk

***Abstract*— Sun** is an imperishable **source of clean energy. Each day the sun releases about 385×10^{24} watts of energy in the shape of light and other forms of radiation. Today PV modules are being used in every home to convert sunlight into electricity. According to the World Green Building Council (WGBC) PV modules will completely replace traditional ways of generating electricity by 2050. Due to low literacy rate, people do not know the exact position of panels to avail maximum output power in Khuzdar Pakistan. The PV modules can deliver maximum output when there is a right angle between sunlight and the surface of the solar panel. As the position of the sun changes throughout the year, therefore a fixed panel on earth would not deliver maximum output. The panels are required to be titled accordingly. In this work, the tilt angle between the incident rays and panels for the Khuzdar (Pakistan) region are determined and presented. The achieved results shown significant improvement in output power of fixed panel through adjusting the title angles**

Index Terms*—Elevation angle, PV module, maximum solar power output, solar panel tilt angle.*

I. INTRODUCTION

THE ERA of larger central power stations is going to be ended soon due to their hazardous emissions and other negative effects to living organism and environment [1]. Sunlight has been found to be most suitable renewable source of cheap energy to replace conventional sources. A very small fraction of the energy that we get from sun is sufficient to meet all our power needs. The solar energy hits the earth in the form of enormous radiations. Nearly 1000 W/m^2 of solar energy falls on the earth surface on a clear sunny day. The each receive solar radiation per annum is about 6200 times greater than the demand of the entire population of the world [2]. The energy received from the sun is referred as solar energy. For domestic use, the sunlight is converted into electricity by using photovoltaic (PV) and for large scale generation concentrated glasses are applied to focus a large area of sunlight into a small beam [3]. Pakistan is facing severe energy crisis and spends 60% of their foreign exchange while importing the fossil fuels. To meet its requirement of energy, Pakistan imports averagely 380 thousand barrels of oil per day [4]. Pakistan's Natural Gas consumption is about 4.418 billion cubic feet per day [5, 6]. Pakistan is a sunny country. Most regions remain sunny throughout the year during the daytime. Particularly, most regions in Balochistan and Sindh provinces are exposed to sunlight for about 4402/4380 hours [7]. Secondly being at temperature zone, the day-time at regions situated in Balochistan and Sindh provinces are long and scorching where temperature goes as high as 54C°. Hence, we claim that solar and wind power plants are the sole, durable and everlasting source to replace conventional sources of power generation. The only thing on solar power generation at the domestic level is to educate the people how to exploit the maximum efficiency. Most people have fixed their PV panel with metallic frame over the roofs of their houses. The angle of the solar panel of your solar system is not the same everywhere but it varies from region to region and time to time. The solar modules provide maximum energy when they are accurately exposing to sunlight. [8]. The major limitation is that the angle between fixed PV panels and sunlight is also changing continuously which degrades the output power of the PV system. Hence to have an optimal angle, this problem needs to be countered. In literature different authors have presented different technique as a solution to this problem [9, 10]. Maximum Power Point Tracking (MPPT) is one the emerging area of the research to attain optimal power [11]. Various tracking algorithms are designed depends different conditions and environments [12, 13]. Each and every algorithms possess their pros and cons. The MPPT algorithms has structural limitations due to its complications and cost effect as well. Furthermore, the MPPT have significant advantages for commercial purposes. If a common man of underdeveloped country like Pakistan wants to utilize solar energy for home energy requirements, it is quite an expensive way to adopt these modern techniques. The most viable solution to address this problem is to calculate the tilt angle for PV panel while considering the position of the sun rays on certain area at various regular interval during a year. In the current research it is investigated that by adjusting and optimizing the position of the PV panel based on title will lead to increase the output power of the PV modules. Different techniques for different geographical locations have been used to find out optimal PV panel tilt angle [14] to [16].

In this paper, optimal tilt angles for Khuzdar, Pakistan lying at N 27°44'18.16″and E 66°38'36.09″are calculated for the twelve months starting from June 2021 to May 2022. Some statistics related to Khuzdar city have been provided by local meteorological department [17]. The measured tilt angles and the optimal output power of the panels are presented in tables and depicted in graph as well. The rest of paper is organized as Section II based on the concept of the various position of PV panel to measure the optimal tilt angle. Section III focuses on the presented research titled as case study which is based on the investigation and analysis of various parameters to identify the optimal tilt angle to attain the maximum power for Khuzdar,

Pakistan. Section IV concludes the current research work presented in the paper and comments on future perspectives.

II. CONCEPT

A. *Fixed and Adjustable Panel*

To make it further clear, here we provide an example of four different tracking systems as mentioned in Table I. The PV module is moved in four different positions throughout the year. *i.e*. (i) fixed at one position at some summer angle through the year (ii) fixed at some winter angle (iii) tilted four time in a year, as given below in Table I, (iv) adjusted daily at 90˚ toward the incident rays. The effect on output power of solar panel due its movement as per the given schedule in northern hemisphere are depicted in Fig.1 and tabulated in Table II. When the PV module is fixed at the full year angle, it gives 66 to 75% of the optimum power as compared to the case when you tilt your PV module daily [14]. In case if the PV module is fixed at a winter angle, it gives 39% (during the summer) to 95% (during the winter) of the optimum power. In case if the PV module is tilted four times a year as per the schedule provided in table-1, it gives 71 to 95% of the optimum power.

Fig.1. Four different scenarios of tilting the PV module

B. *Strategy to Measure the Optimal Angle for Solar*

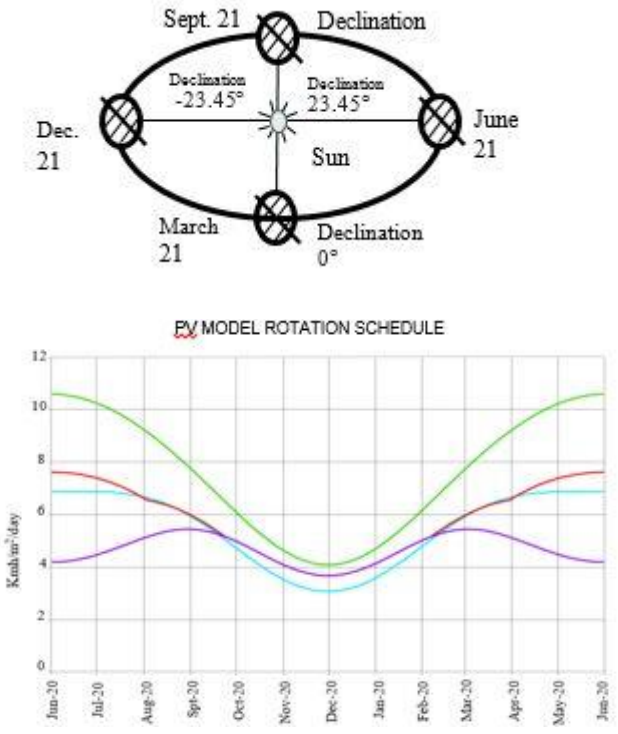

B. *Panel*

As the study is being done for Khuzdar, where a large ratio of the inhabitants are either illiterate or non-technical, we present a viable method for calculating the optimal solar panel angle for such a group of people. This method is providing optimum performance fixing the module in one position throughout the year or tilting blindly. The output attained from solar energy depends on latitude and the season. Hence the optimizing the tilt angle of the solar panel while considering the latitude and season of the season is challenging from research perspective to enhanced the power output. In current method, for PV panel for the optimum angle is adjusted twice a year. During winter, it is reckoned by summing 29° to the product of latitude and 0.9. For example, the latitude of Khuzdar is 27° so the tilt angle will be (27 × 0.9) + 29 = 53.3°. During summer, the tilt angle is obtained by subtracting 23.5° to the product of latitude and 0.9. Again, calculating it for Khuzdar region, it comes (27 × 0.9) – 23.5 = 0.8°. During spring and fall, simply subtract 2.5° from the latitude, *i.e*. (27-2.5 = 24. 5°) [18].

C. *Declination Angle (δ)*

As Declination Angle (D.A) denoted by (δ) is the angular distance between the equator and to the north or south of the sun. Due to orbital rotation of earth the declination is different in various season. The earth is tilted by 23.45°, so the D.A varies by +23.45° or -23.45° at solstices and remains 0° at the spring and fall equinoxes [18]. Fig.2 shows the different values of D.A at different season.

Fig.2. Different value of declination angle in various seasons

The mathematical expression for declination angle is defined as in (1), as

$$\delta = 23.45\frac{\pi}{180} sin\left[2\pi\left(\frac{284+d}{36.25}\right)\right] \quad (1)$$

Whereas δ is declination angle in (rads) and d shows the number of day of the year. (e.g, d = 33, on 2nd Feb).

D. *Hour Angle (ω)*

It is the angular distance between two meridians *i.e*. the meridian of the plane containing the sun and the meridian of the observer. The following mathematical expression are used to calculate the hour angle in (2) [18].

$$sin\ sin\ \omega = -\frac{coscos\ \alpha\ sin\ A_Z}{coscos\ \delta} \quad (2)$$

$$sin\ sin\ \omega = \frac{sinsin\ \alpha - sinsin\ \delta sinsin\ \phi}{coscos\ \delta\ coscos\ \phi} \quad (3)$$

In (2) and (3) the A_z shows the solar azimuth angle, α is the altitude angle and ϕ is the latitude of the observer. The solar azimuth angle (γ) is the angle of the sun rays and the north as measured clockwise around the observer's horizon can be expressed mathematically in (4) as [16].

$$sin\ sin\ \gamma = \frac{sinsin\ \varpi\ coscos\ \delta}{sin\theta_Z} = \frac{sinsin\ \varpi\ coscos\ \delta}{coscos\ \alpha} \quad (4)$$

E. *Elevation Angle*

An object above us always makes an angle between the horizontal and the line of sight to the object reffered as an elevation angle. It is evident that elevation angle is various round the day such as 0° at sunrise and sunset and 90° when sun is at right angle to the surface of the earth as described in (5) as [18].

$$\alpha = 90 + \phi - \delta \quad (5)$$

Where φ is the latitude of the solar module.

The power density of solar energy on the surface shall be maximum when tilted surface of the PV panel and sunlight at 90 ° to each other. The Fig. 3, is quite helpful to draw mathematical expression to compute the radiation incident on

the tilted surface (S_{module}) when the solar radiation measured on horizontal surface ($S_{horizontal}$) or the solar ray's perpendicular to the sun ($S_{incident}$) [15].

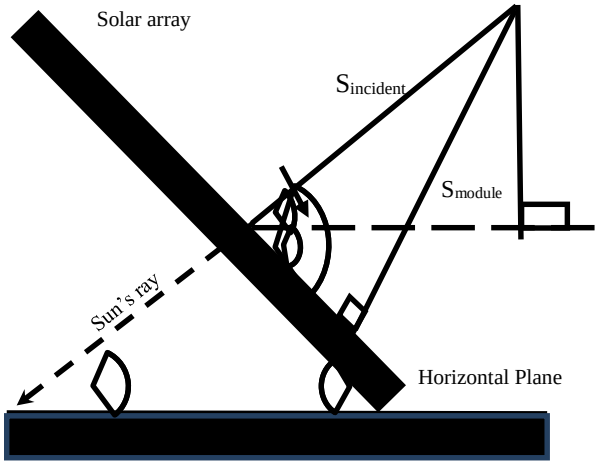

Fig.3. Incident rays of sun on tilted surface

The phenomena in Fig.3 can be expressed mathematically in (6) and (7) as,

$$S_{horizontal} = S_{incident} sin\alpha \quad (6)$$

$$S_{module} = S_{incident} sin(\alpha + \beta) \quad (7)$$

α is elevation angle defined and β is the tilt angle.

To find out the tilt angle (β), it is investigated to determine the incident energy of solar in warm climate of Khuzdar region having latitude N 27˚44'18.16˝and longitude E 66˚38'36.09˝for whole year. The variation in the elevation angle of incident rays of sun for twenty fours is negligible. In the current research interval of one hundred twenty hours (5days) is chosen to compute the optimum tilt angle. It can be seen from (7) that the solar panel energy may be equal to the maximum incident energy only if the sin $(\alpha + \beta)$ term is equal to 1, its mean the output would be maximum if the sum of α and β is 90. We know the value of α, and subtracting it from 90 gives us the value of the desired optimum tilt angle. The process is repeated every 5 days for calculation of β

III. CASE STUDY

To calculate the optimum tilt angle of PV panel data for Khuzdar city have been obtained from the meteorological department of Balochistan, Pakistan by personal visit and some from their official website. Table III shows the monthly maximum and minimum temperature and duration of sunlight from sunrise to sunset [17]. It is clear from the given data that the weather is sunny and clear throughout the year.

The tilt angle is calculated from June 2021 to May 2022 because of changing of elevation angle of the sun to attain maximum efficiency.

C. Tilt Angle from June (2021) to December (2021)

The Table IV shows the output power measured in (kwh/m^2/day) while adjusting the tilt angles for month of June, July, August, September, October, November and December of 2021 in district Khuzdar, province Balochistan of Pakistan. The interval amongst each measurement is five days to show the significant variations in the output power of PV panel.

To illustrate the graphical analysis of the output power from the solar panel and adjusting the tilt angle for the data in Table IV is shown in Fig.4, Fig.5, Fig. 6, Fig.7, Fig.8, Fig.9 and Fig.10 for month of June, July, August, September, October, November and December 2021 respectively.

TABLE III
MONTHLY MIN & MAX TEMPERATURE (OF KHUZDAR REGION FOR YEAR (2021-22)

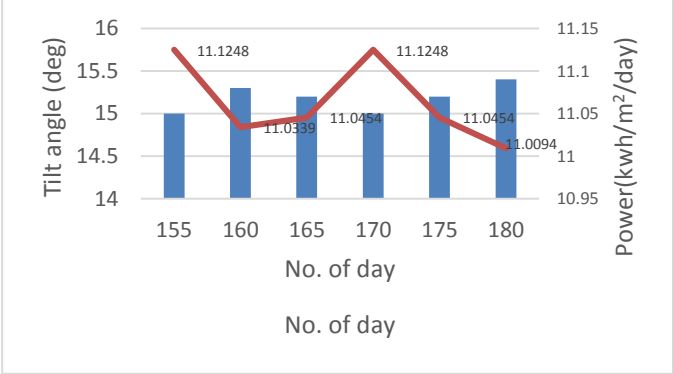

Fig.4. Tilt Angle for June vs. Output Power (kwh/m^2/day)

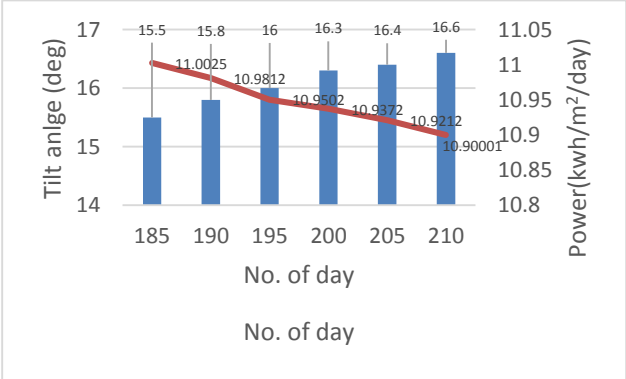

Fig.5. Tilt Angle for July vs. Output Power (kwh/m^2/day)

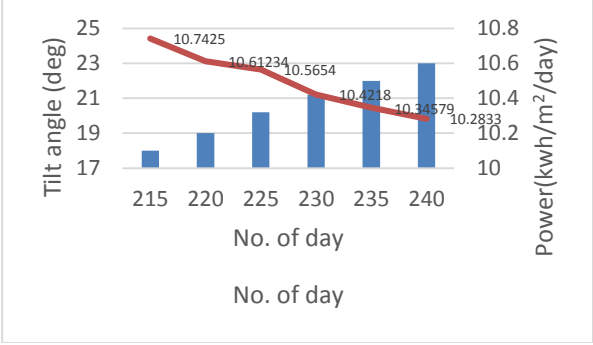

Fig.6. Tilt Angle for August vs. Output Power (kwh/m^2/day)

TABLE Iv
TILT ANGLE FOR JUNE

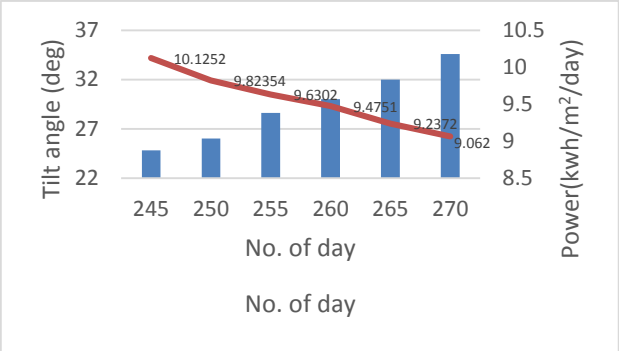

Fig.7. Tilt Angle for September vs. Output Power (kwh/m^2/day)

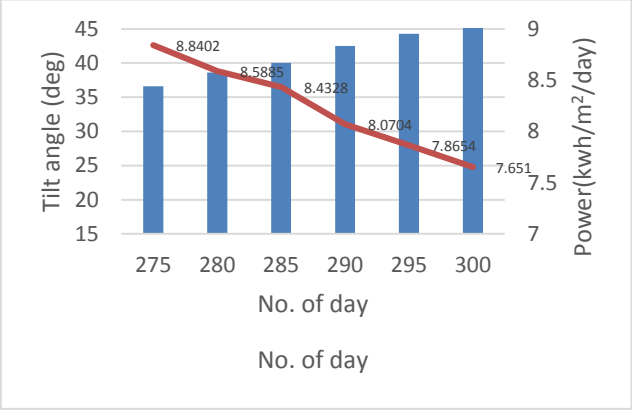

Fig.8. Tilt Angle for October vs. Output Power (kwh/m^2/day)

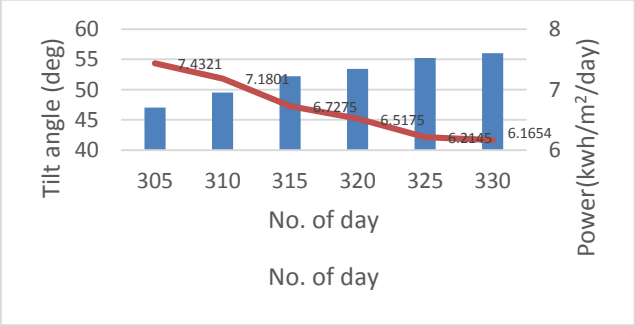

Fig.9. Tilt Angle for November vs. Output Power (kwh/m^2/day)

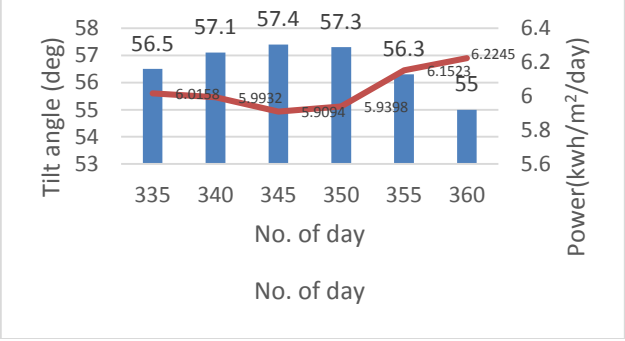

Fig.10. Tilt Angle for December vs. Output Power (kwh/m^2/day)

From the tabulated data, it can be seen that when the duration of daylight is decreasing, the solar irradiance also decrease exponentially, whereas resultantly the tilt angle of the solar panels is increase from June to December as show in Fig.4, Fig.5, Fig. 6, Fig.7, Fig.8, Fig.9 and Fig.10. Similarly irradiance is decrease from July to December leads to reduction in output power of the PV as shown in Table IV.

TABLE v
TILT ANGLE FOR JANUARY

D. Tilt Angle from January (2022) to May (2022

As the irradiance start to increase from January to June leads to enhancement in the output power of the PV panel and it can be seen that when the duration of daylight is increasing, the solar irradiance also increases exponentially, whereas resultantly the tilt angle of the solar panels is decreases as shown in Table V.

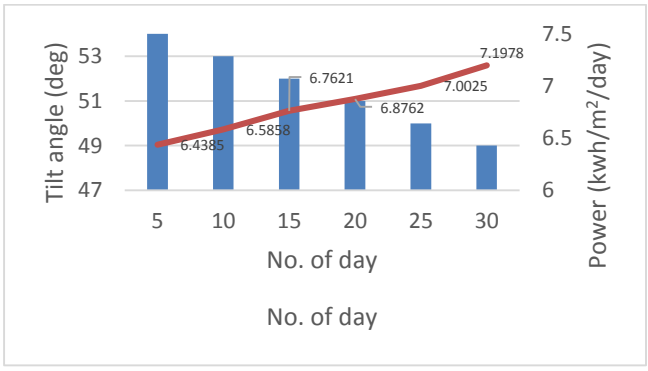

Fig.11. Tilt Angle for January vs. Output Power (kwh/m^2/day)

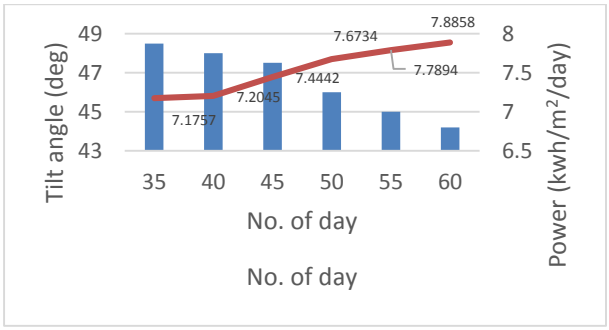

Fig.12. Tilt Angle for February vs. Output Power (kwh/m^2/day)

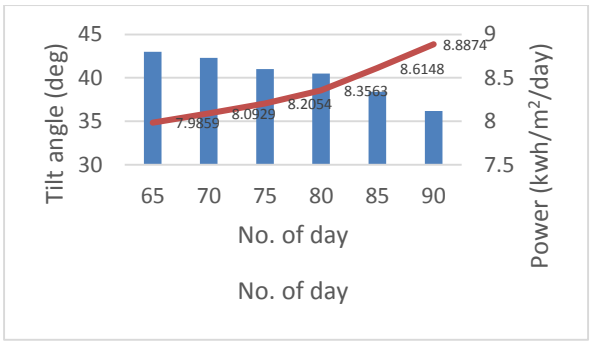

Fig.13. Tilt Angle for March vs. Output Power (kwh/m^2/day)

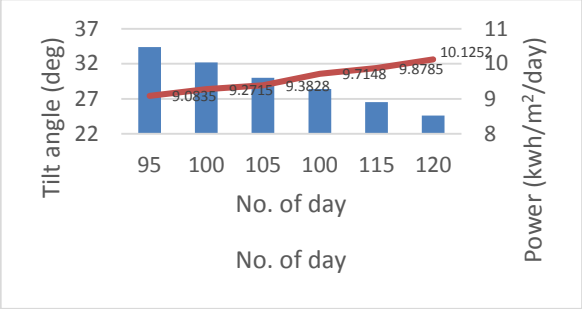

Fig.14. Tilt Angle for April vs. Output Power (kwh/m^2/day)

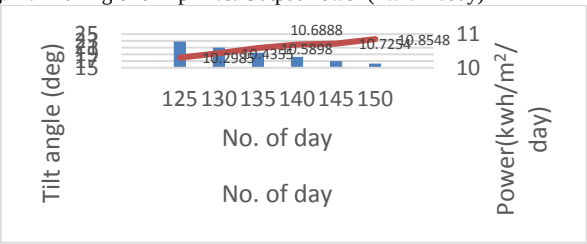

Fig.15. Tilt Angle for May vs. Output Power (kwh/m^2/day)

Fig. 16 shows the overall tilt angle for the whole year. It can be seen from the Fig.16 that the optimal angle goes up during the winter and comes down during the summer mainly due to the position of the sun in the sky.

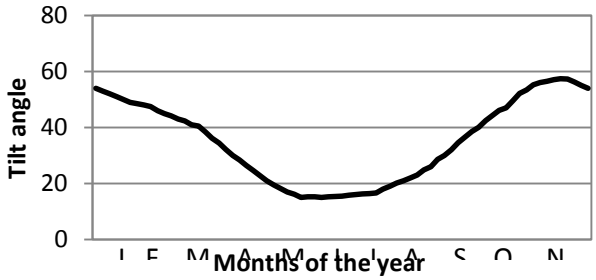

Fig.16. Tilt Angle of the year

IV. CONCLUSION

In this work, we have tried to find out the optimal tilt angle of the PV panel for a city situated in Pakistan, Khuzdar. Although, in literature we can find modern techniques like MPPT, but MPPT and all others modern techniques are expensive and complicated to be used by poor inhabitants of an underdeveloped country. Hence, we confined our work in providing the data to the local inhabitants and making them out how to adjust your frame according to the given tilt angles. From the deduced data, it can be seen that the tilt angle in summer is less than the angle in winter. From study, it is also learnt that optimal tilt angle varies as a function of latitude and weather. From our results, it has been proved that when the knowledge of advantage of tile angle is known to the inhabitants of this region, they can increase their annual power output of the PV panel by 6% to 29%. The same methodology can also be used in the other regions in Pakistan so that people may exploit maximum efficiency of PV panel installation. In future, this work can be carried out ahead to design such type of smart motor which can adjust the optimal tilt angle by sensing or inserting the specific longitude and latitude of that specific region.

ACKNOWLEDGMENT

The author is highly thankful to local meteorological department Khuzdar, provincial government of Balochistan for providing data relevant to the presented research.

REFERENCE

[1] Michael A. Geyer and William B. Stine, “Power From The Sun” Netbook Publisher, January 2001

[2] Volker Quaschning, “The Sun as an Energy Resource” Renewable Energy World 2003, pp. 90-93

[3] Olindo Isabella, Klaus Jäger, Arno Smets, René van Swaaij, and Miro Zeman, “Solar Energy: The Physics and Engineering of Photovoltaic Conversion, Technologies and Systems” UIT Cambridge Ltd.; 1st Edition, Apr. 2016

[4] National Electric Power Regulatory Authority (NEPRA) Anuunal Report 2021. [Online]. Available: https://nepra.org.pk/publications/Annual%20Reports.php

[5] https://www.ssgc.com.pk

[6] Abdul Lateef Kalwar and Siraj jamal siddiqui, “Leadership practices in corporate sector: a study of Sui southern gas company,” Journal of Grassroots, vol. 51, No. 2, December 2017.

[7] www.pmd.gov.pk

[8] Mohamed Nfaoui, Khalil El-Hami, “Extracting the maximum energy from solar Panels,” ELSEVIER, Energy report, volume. 4, pp. 536-545, Nov.2018.

[9] Manoj Kumar Sharma, Deepak Kumar, Sandeep Dhundhara, Dipesh Gaur and Yajvender Pal Verma, “optimal Tilt Angle Determination for PV Panels Using Real Time Data Acquisition,” Global Challenges, volume. 4, issue. 8 pp. 1-12, Feb. 2020.

[10] Ridha Ben Mansour, Meer Abdul Mateen Khan and Fahad Abdulaziz, “Optimizing the Solar PV Tilt Angle to Maximize the Power Output: A Case Study for Saudi Arabia” IEEE access, vol. 9, pp-15914-15928, 2021.

[11] Kundu, Shiena, Nikita Gupta, and Parmod Kumar, "Review of solar photovoltaic maximum power point tracking techniques," 7th India International Conference on Power Electronics (IICPE), IEEE, 2016.

[12] Trishan Eshram and Patrick L. Chapman, “Comparison of Photovoltaic Array Maximum Power Point Techniques,” IEEE Transaction on Energy Conversion, vol.22, no.2, pp. 439-449, June 2007.

[13] M. Shaneh, H. Shahinzadeh, M. Moazzami and Gharehpetian, G. B, “Optimal Sizing and Management of Hybrid Renewable Energy System for Highways Lighting,” International Journal of Renewable Energy Research (IJRER), vol. 8 No. 4, pp.2336-2349, December 2018.

[14] S. Muhammad Sami ur Rehman , Muhammad Ammar Nazeer, Zafar Iqbal, Muhammad Abdul Basit and Aqeel Ahmed, “Mathematical Analysis for Calculation of an optimum Tilt Angle of Solar Panels for Islamabad,” International Conference on Power Generation Systems and Renewable Energy Technologies (PGSRET), 10-12 September 2018, Islamabad, Pakistan.

[15] M.A.A. Mamun, M.M. Islam, M. Hasanuzzaman, Jeyraj Selvaraj, “Effect of tilt angle on the performance and electrical parameters of a PV module: Comparative indoor and outdoor experimental investigation,” Energy and Built Environment, vol. 3 issue. 3, pp-278-290, July 2022.

Balochistan Journal of Engineering & Applied Sciences (BJEAS) – (p-ISSN: 2518-2706
Volume 6, No.1

Numerical Simulation of Combustion Chamber Film Cooling Mechanism

Afaque Ahmed Bhutto[1], Sanaullah Memon[2], Iftikhar Ahmed Bhutto[3], Rahim Bux Khokhar[4], Asif Ali Shaikh[5]
[*1]Department of Basic Sciences and Related Studies, Quaid e Awam University of Engineering, Science and Technology, Larkana campus - 77150, Pakistan.
[2]Department of Basic Sciences and Related Studies, Mehran University of Engineering and Technology, SZAB campus, Khairpur, Pakistan
[3]Department of Mathematics Sukkur IBA University, Kandhkot Campus, Pakistan,
[4,5]Department of Basic Sciences and Related Studies, Mehran University of Engineering and Technology, Jamshoro - 76062, Pakistan
[5]Department of Mathematics, Near East University, 99138 Mersin, Turkey.
Corresponding author: afaq_bhutto@quest.edu.pk

***Abstract*— In liquid propellant rocket engines, film cooling is an integral part of the cooling process. During the internal flow of the propulsion system, it serves as a protective measure, shielding critical components from excessive heat. In recent years, advances in computational power have enabled advanced CFD tools to become more accurate and useful in predicting complex flows encountered in liquid-fueled engines. The purpose of this study is to evaluate the effectiveness of film cooling using CFD. In this study, numerical simulations were performed for air subsonic film cooling on a flat plate. Three different models were used for the steady-state simulations: SST k-ω, Realizable k-ε, and Spalart-Allmaras. Further, steady-state simulations were carried out using the SSTk-ω model with varying grid resolutions. The findings indicate that all three models, namely realizable k-ε, SST k-ω, and Spalart-Allmaras, demonstrate reasonable agreement with experimental data in terms of average performance. However, the realizable k-ε model is more accurate and provides better agreement with experimental data than the two other models. The SST k-ω model, when employed with different grid resolutions, also demonstrates agreement with experimental data. This solver performs extraordinarily well, effectively capturing film cooling efficiency degradation within the subsonic regime.**

Keywords: CFD, Scramjet Engine, Hypersonic Flow, Supersonic Comparison, Heat Load.

I. INTRODUCTION

The efficient cooling of components within combustion chambers is of paramount importance in modern propulsion systems, particularly in liquid propellant rocket engines [1][2]. The harsh operating conditions, including high temperatures and pressures, necessitate effective cooling strategies to ensure the longevity and performance of critical components. One such vital cooling technique is film cooling, which involves the injection of a cooler fluid (usually air) parallel to a heated surface to shield it from excessive heat. The study of film cooling effectiveness is essential for optimizing engine design and ensuring safe and reliable operation [3].

Combustion chambers play a critical role in jet engines, generating high-pressure, high-temperature gases through chemical reactions between fuel and oxidizer [4]. The design of combustion chambers thoroughly analyzed prior to their practical implementation. The feed system supplies high-pressure oxidizer and fuel to the combustion chamber of a liquid fuel jet engine [5]. In the combustion chamber, the mixture burned at a constant pressure, causing the combustion gases to flow through the turbine and nozzle of the combustion chamber [6]. The combustion gases of a scramjet engine are, delivered directly to the nozzle without passing through an intermediate turbine stage. Increasing chamber pressure causes exhaust gases to expand for a higher nozzle area ratio, resulting in increased performance. However, high heat flux accompanied by higher combustion chamber pressure [1][7][8]. Combustion dynamics phenomena emerge in numerous applications and frequently yield grave repercussions for the proper functioning of the apparatus. When these phenomena manifest within high-performance contrivances such as gas turbines, aero-engines, or stages of liquid rocket propulsion, they frequently culminate in operational breakdown, and in the most severe instances, total annihilation of the apparatus [9]. In numerous scenarios, these dynamic occurrences stem from an interconnection between combustion and the resonant acoustic modes inherent to the system. Oscillations of elevated frequency, entwined with transverse modes, amplify heat fluxes that surpass the designated heat transfer rates. This, in turn, leads to the liquefaction of chamber walls, resulting in subsequent system failure. In select cases, this chain of events can even prompt remarkable propulsion system detonations [10]. There are a number of processes involved in combustion instability, including injection, atomization, vaporization, mixing, and chemical kinetics, and limited information is available to predict the occurrence of combustion instability, despite several studies addressing the issue. The literature [11][12] and its references provide extensive reviews of the various processes influencing combustion instability.

An effective cooling system employed in the combustion chamber of a scramjet engine is essential for ensuring its structural integrity. The purpose of this mechanism is to shield the combustion chamber wall from the intense heat generated during the combustion process, thus maintaining the chamber at a low and safe temperature [13]. A film cooling system effectively lowers the temperature of the burning gases near the chamber walls by using a mixture of fuel and air or pure fuel in the injection process. The research conducted by Troti [14] examined the effectiveness of film cooling techniques in maintaining combustion chamber walls at high temperatures during the core flow. An analysis was conducted to compare the experimental and numerical results

of various film cooling prototypes and heat transfer factors. The numerical solver currently being used has been thoroughly verified and validated by Barbera Betti [15]. Verification and validation procedures included several test cases, including convergence and divergence nozzles, air subsonic film cooling, and helium/air supersonic/supersonic mixing layers. As a measure of the accuracy of numerical solvers for steady-state challenges. The overall computational model and the sub-models were also validated by comparing them with experimental data. It was considered essential to ensure that the theoretical spatial order of accuracy matched the spatial order achieved in solution verification, and that the numerical solution obtained from three different grid levels exhibited asymptotic grid convergence within the specified range as well [16].

Kirchberger [17] has done in his study investigation heat transfer, tests with kerosene and nitrogen have been conducted using gaseous and liquid film cooling models. The study was conducted in 2010 by Bogin Jr. al. [18] worked on the combustion process of the ignition quality tester with KIVA-3V by using CFD. The problem of the transient process in engines based on the combustion of liquid fuel has been studied. First attempt by India to create a "dynamic simulator for liquid-propellant rocket engines" called CRESP-LP-LP [3] in early 2000s. Currently, the University of Technology in Tehran has developed transient simulation tools. To investigate, the transient system in the combustion system, Several tests were conducted by Karimi et al.[19] CNES has tested AMESim platform in Europe for modeling and simulating the dynamics of these structures. The cooling of films has also been studied through experiments and numerical simulations. In rocket engine chambers, wall heat transfer is an important factor of research and design, particularly for chambers that use film cooling To better understand the flow field, the film cooling mechanism must be studied in detail. By doing so, it would be possible to accurately predict the chamber wall heat flux and optimize the design of rocket engine chambers [20].

The aim of this study to contribute to the understanding of film cooling efficiency by conducting a systematic numerical analysis utilizing the SST k-ω, Realizable k-ε, and S-A turbulence models. The assessment involves a grid-independent study with different grid resolutions, and the simulation results compared with experimental data. The findings from this study hold the potential to advance our understanding of film cooling mechanisms, providing valuable insights for the design and analysis of combustion chambers in liquid propellant rocket engines.

II. Mathematical Formulation

Computational Fluid Dynamics was utilized to simulate fluid stream and heat transfer in this study. The discretization approach was used to approximate the principal equations and their boundary terms as a system of linear equations. Heat transfer and fluid stream problems are solved mathematically by using the discretization method. Due to the advancements in CFD and the application of these techniques to industrial complexity, there is a growing demand for computational strategies that can accurately simulate flows in complex geometries. An ANSYS Fluent is considered to solve conservation equations for mass and momentum, it is suitable for simulations involving all types of fluids, whether steady-state or transient [21]. This study considers the conservation equation for combination of fraction and its variation in detail. To investigate these equations in detail, this study employs the non-premixed blend fraction combustion model. Following is the equation for mass conservation [22][23]:

$$\frac{\partial \rho}{\partial t} + \nabla.(\rho \vec{v}) = S_m \tag{1}$$

Where ρ is used to represent density and S_m represents the effect of source term for the velocity. This equation provides a generalized form of mass conservation for both incompressible and compressible fluids. This equation is expressed in the form of a 2D axis-symmetric equation, due to the geometry of the test case being 2D axisymmetric. As follows:

$$\frac{\partial v}{\partial t} + \frac{\partial}{\partial x}(\rho v_x) + \frac{\partial}{\partial r}(\rho v_r) + \frac{\rho v_r}{r} = S_m \tag{2}$$

momentum preservation is defined by,

$$\frac{\partial}{\partial t}(\rho \vec{v}) + \nabla.(\rho \vec{v}\vec{v}) = -\nabla p + \nabla.(\bar{\bar{\tau}}) + \nabla \vec{g} + \vec{F} \tag{3}$$

Where ρ is the density, $\vec{v}$ is the velocity, p is the pressure, $(\bar{\bar{\tau}})$ is the second order stress tensor, $\vec{g}$ is the gravity and external forces is denoted by $\vec{F}$.

$$\bar{\bar{\tau}} = \mu\left[\left(\nabla \vec{v} + \nabla \vec{v}^T - \frac{2}{3}\nabla.\vec{v} I\right)\right] \tag{4}$$

Where μ represent the dynamic viscosity of the fluid. Radial and axial momentum conservation equations are given by,

$$\frac{\partial}{\partial t}(\rho v_x) + \frac{1}{r}\frac{\partial}{\partial x}(r\rho v_x v_x) + \frac{1}{r}\frac{\partial}{\partial x}(r\rho v_r v_x) = -\frac{\partial \rho}{\partial x} + \frac{1}{r}\frac{\partial}{\partial x}\left[r\mu\left(2\frac{\partial v_x}{\partial x} - \frac{2}{3}(\nabla.\vec{v})\right)\right] + \frac{1}{r}\frac{\partial}{\partial r}\left[r\mu\left(\frac{\partial v_x}{\partial r} + \frac{\partial v_r}{\partial x}\right)\right] + F_x \tag{5}$$

$$\frac{\partial}{\partial t}(\rho v_r) + \frac{1}{r}\frac{\partial}{\partial x}(r\rho v_x v_r) + \frac{1}{r}\frac{\partial}{\partial r}(r\rho v_r v_r) = -\frac{\partial \rho}{\partial r} + \frac{1}{r}\frac{\partial}{\partial x}\left[r\mu\left(\frac{\partial v_r}{\partial x} + \frac{\partial v_x}{\partial r}\right)\right] + \frac{1}{r}\frac{\partial}{\partial r}\left[r\mu\left(2\frac{\partial v_r}{\partial r} - \frac{2}{3}(\nabla.\vec{v})\right)\right] - 2\mu\frac{v_r}{r^2} + \frac{2}{3}\frac{\mu}{r}(\nabla.\vec{v}) + \rho\frac{v_z^2}{r} + F_r \tag{6}$$

Equation (7) represents the conservation of energy [20],

$$\frac{\partial}{\partial t}(\rho E) + \nabla.\left(\vec{v}(\rho E + p)\right) = -\nabla.\left(\sum_j h_j J_j\right) + S_h \tag{7}$$

The SST k-ω model is similar to the standard k-ω model:

$$\frac{\partial}{\partial t}(\rho k) + \frac{\partial}{\partial x_i}(\rho k u_i) = \frac{\partial}{\partial x_j}\left(\Gamma_k \frac{\partial k}{\partial x_j}\right) + \tilde{G} - Y_k + S_K \tag{8}$$

And

$$\frac{\partial}{\partial t}(\rho\omega) + \frac{\partial}{\partial x_j}(\rho\omega u_j) = \frac{\partial}{\partial x_j}\left(\Gamma_\omega \frac{\partial \omega}{\partial x_j}\right) + G_\omega - Y_\omega + D_\omega + S_\omega \quad (9)$$

$$\Gamma_k = \mu + \frac{\mu_t}{\sigma_k} \quad (10)$$

Where, $\boldsymbol{\sigma_k}$ is the turbulent Prandtl number for k

$$\Gamma_\omega = \mu + \frac{\mu_t}{\sigma_\omega} \quad (11)$$

the turbulence viscosity calculated as follows:

$$\mu_t = \frac{\rho k}{\omega} \frac{1}{\max\left[\frac{1}{\alpha^*}, \frac{SF_2}{a_1 \omega}\right]} \quad (12)$$

Where S is denoted the rate magnitude:

$$\boldsymbol{\sigma_k} = \frac{1}{\frac{F_1}{\sigma_{k,1}} + \frac{1-F_1}{\sigma_{k,2}}} \quad (13)$$

$$\boldsymbol{\sigma_\omega} = \frac{1}{\frac{F_1}{\sigma_{\omega,1}} + \frac{1-F_1}{\sigma_{\omega,2}}} \quad (14)$$

$$\boldsymbol{\alpha^*} = \boldsymbol{\alpha^*_\infty} \frac{\boldsymbol{\alpha^*_0} + \left(\frac{Re_t}{R_k}\right)}{1 + \left(\frac{Re_t}{R_k}\right)} \quad (15)$$

The blending function F_1 and F_2 are defined as.

$$F_1 = \tanh(\Phi_1^4) \quad (16)$$

$$\Phi_1 = \min\left[\max\left(\frac{\sqrt{k}}{0.09\omega y}, \frac{500\mu}{\rho y^2 \omega}\right), \frac{4\rho k}{\sigma_{\omega,2} D_\omega^+ y^2}\right] \quad (17)$$

$$D_\omega^+ = max\left[2\rho \frac{1}{\sigma_{\omega,2}} \frac{1}{\omega} \frac{\partial k}{\partial x_j} \frac{\partial \omega}{\partial x_j}, 10^{-10}\right] \quad (18)$$

$$F_2 = tanh(\Phi_2^2) \quad (19)$$

$$\Phi_2 = max\left[2\frac{\sqrt{k}}{0.09\omega y}, \frac{500\mu}{\rho y^2 \omega}\right] \quad (20)$$

Production of k and ω defined by below equations, where $\tilde{G}_k$

3. Test case description

and G_w represents production factor of turbulence kinetic energy and ω respectively.

$$\widetilde{G_k} = \min(G_k, 10\rho B^* k\omega) \quad (21)$$

$$G_\omega = \frac{\alpha}{v_t} \tilde{G}_k \quad (22)$$

These above formulations differ SST K-ω model from a standard k-ω model. For the SST k-ω model is given below.

$$a_\infty = F_1 a_{\infty,1} + (1 - F_1) a_{\infty,2} \quad (23)$$

Where,

$$a_{\infty,1} = \frac{\beta_{i,1}}{\beta^*_\infty} - \frac{\kappa^2}{\sigma_{\omega,1}\sqrt{\beta^*_\infty}} \quad (24)$$

$$a_{\infty,2} = \frac{\beta_{i,2}}{\beta^*_\infty} - \frac{\kappa^2}{\sigma_{w,2}\sqrt{\beta^*_\infty}} \quad (25)$$

The expression "feasible" implies that the model satisfy certain numerical imperatives on the Reynolds stresses, reliable with the material science of choppiness streams. The feasible k-ε demonstrates contains an elective detailing for the fierce consistency. An altered transport condition for the dispersal rate ε, has been gotten from a correct condition for the vehicle of the mean square vorticity vacillation. Feasible k-ε display suggested by Shih et al [24] was planned to enhance insufficiencies of conventional k-ε models by receiving the accompanying a new vortex thickness recipe including a variable Cμ initially suggested by Reynolds. New model condition for scattering (ε) in light of the dynamic condition of the mean square vorticity variance. One constraint of feasible k-ε display is that it produces non-physical tempestuous viscosities in circumstance when the computational space contains both pivoting and stationary zones.

$$\frac{\partial}{\partial t}(\rho k) + \frac{\partial}{\partial x_j}(\rho k u_j) = \frac{\partial}{\partial x_j}\left[\left(\mu + \frac{\mu_t}{\sigma_k}\right)\frac{\partial k}{\partial x_j}\right] + G_k + G_b - \rho\varepsilon - Y_M + S_k \quad (26)$$

And

$$\frac{\partial}{\partial t}(\rho\epsilon) + \frac{\partial}{\partial x_j}(\rho\varepsilon u_j) = \frac{\partial}{\partial x_j}\left[\left(\mu + \frac{\mu_t}{\sigma_\varepsilon}\right)\frac{\partial \epsilon}{\partial x_j}\right] + \rho C_1 S_\varepsilon - \rho C_2 \frac{\varepsilon^2}{k + \sqrt{v\varepsilon}} + C_{1\varepsilon}\frac{\varepsilon}{k} C_{3\varepsilon} G_b + S_\varepsilon \quad (27)$$

Where $C_1 = max\left[0.43, \frac{\eta}{\eta+5}\right], \eta = S\frac{k}{\varepsilon}$, $S = \sqrt{2S_{ij}}Si_j$

A Spalart-Allmaras display settles the demonstrated transport condition for kinematic vortex (fierce) thickness. it display was specifically designed for aviation applications including divider-limited streams and has shown excellent results for limit layers exposed to antagonistic weight slopes. It is to deliver accurate predictions of boundary layer characteristics, such as turbulent kinetic energy and the wall shear stress. Moreover, the model can be used for flows with a wide range of pressure gradients at low computational cost [23].

The transport Equation for $\breve{v}$:

$$\frac{\partial}{\partial t}(\rho\tilde{v}) + \frac{\partial}{\partial x_i}(\rho\tilde{v}u_i) = G_v + \frac{1}{\sigma_{\tilde{v}}}\left[\frac{\partial}{\partial x_j}\left\{(\mu + \rho\tilde{v})\frac{\partial \tilde{v}}{\partial x_j}\right\} + C_{b2\rho}\left(\frac{\partial \tilde{v}}{\partial x_j}\right)^2\right] - Y_v + S_{\tilde{v}} \quad (28)$$

This paper examines a subsonic film cooling structure along a flat plate with respect to the evaluation of film cooling efficiency. An adiabatic wall is shielded from the mainstream hot flow by inserting cold air parallel to the wall [25]. The thickness of the splitter plate is not negligible in terms of slot height, and therefore it affects the flow downstream of the insertion of the film in the present study. A constant pressure of 1 bar is used in the numerical simulations conducted using ANSYS Fluent. Mainstream is air with a stagnation temperature of 462.92K and a velocity of 11.10 m/s. Once again, air is used in the film stream at a low temperature of 296.33K as opposed to the mainstream temperature at a high velocity of 24.70 m/s as opposed to the mainstream speed. It has been conducted by using three types of grids levels which are fine, medium, and coarse. CFD simulations for the turbulence models Spalart-Allmaaras and K-epsilon have also been performed. In this study, we have applied a least squares cell-based gradient of second order pressure and second order upwind momentum, as well as turbulence kinetic energy and specific dissipation rate for steady pressure-based coupled schemes. Data relating to fine, medium, and coarse SST k-ω has been compared with experimental data [26]. In addition, turbulence models SST K-ω, Spalart-Allmaaras and k-epsilon have been tested using experimental data.

B. Configuration Test case

In this study, retained a subsonic film cooling mechanism [27]. The geometrical details of present test case given below Figure 1. In this case required 2D axis planar geometry.

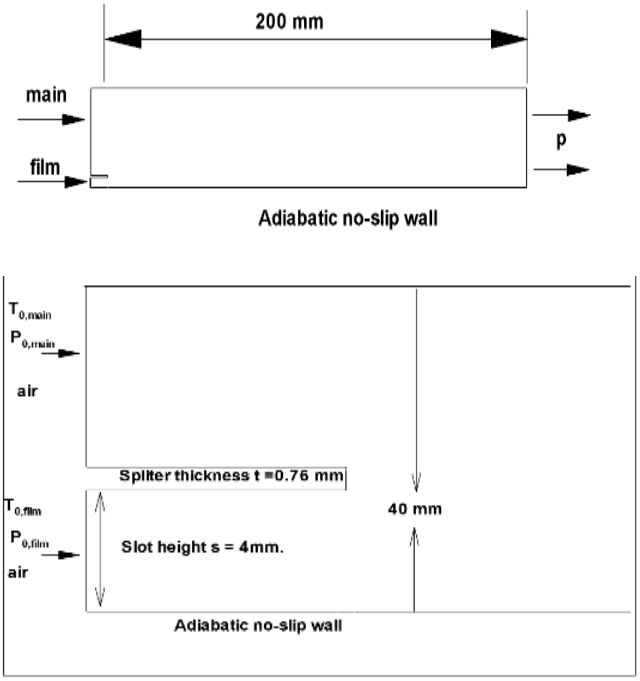

Figure 1: Geometrical detail and subsonic film cooling in combustor

C. Grid generation

Modelling and mesh generation for subsonic film cooling experimental test case has been done using Gridgen software, structure grid is made for present study. Steady 2D- axis planar is presented Figure 2.

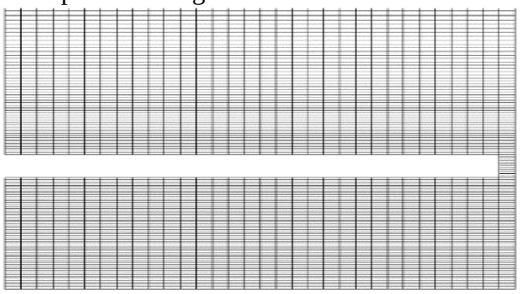

Bottom wall

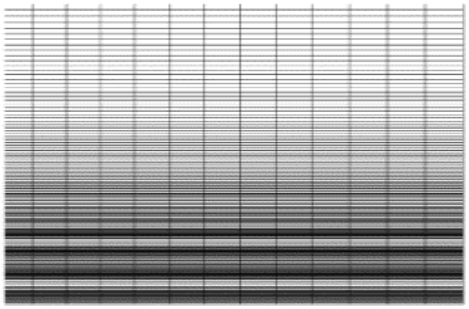

Velocity inlets

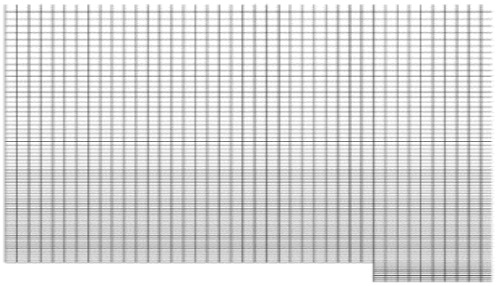

Film inlet

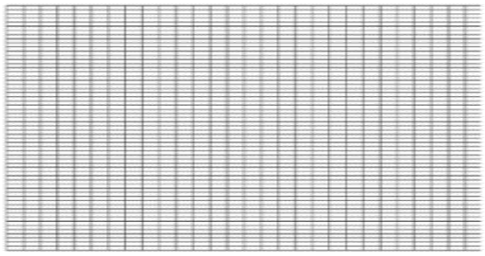

Main stream inlet

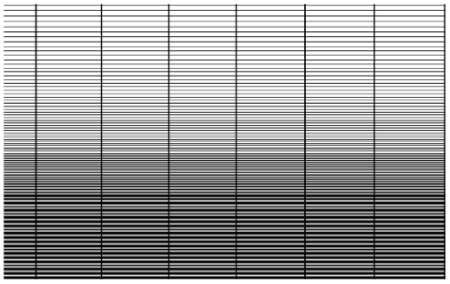

Pressure outlet

Figure 2: Grid at Different regions of the combustion chamber.

D. Boundary conditions

Figure 3 is predicting detail of boundary conditions. Steady planar simulation has been done for the present test case. Boundary conditions used for present test case are given below in table 1.

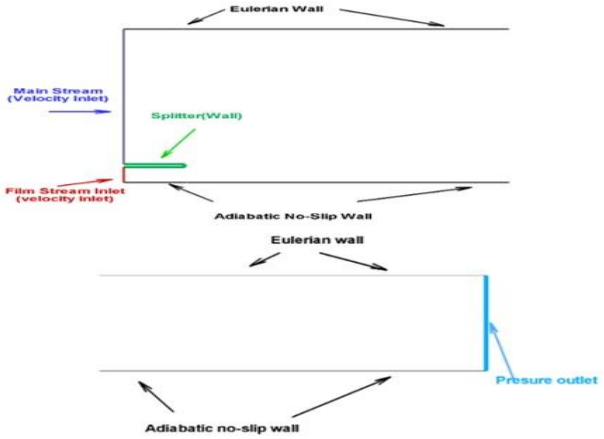

Fig. 3: Boundary conditions near velocity inlets and Outlet region.

Table 1: Boundary conditions values used for steady-state simulation

Boundary conditions	Mainstream	Film stream
Velocity (m/s)	11.10	24.70
Temperature (K)	462.92	296.33
Pressure (bar)	1.0	1.0

E. 3.4 Solver setup

The numerical simulation setup for the present test case [27] follows the following stepwise process. In this study, a steady 2D planar solver based on pressure is employed, with the velocity formulation set to absolute. A 2D axisymmetrical planar geometry has been used. A heat transfer problem is involved in this test case, thus the energy equation is enabled. Three different models are analyzed for turbulent flow, and they are compared with experimental results.

Specifically, these models are as follows:

- The SST k-omega model incorporates the option for viscous heating. In this model, $\alpha_\infty = 0.52$, $\beta^*_\infty = 0.09$, and $\zeta^* = 1.5$ are used as constants.
- A realizable k-epsilon model can be used with enhanced wall treatment and viscous heating. C_2-Epsilon, TKE Prandtle Number, TDR Prandtl Number, and Energy Prandtl Number, respectively, are set to 1.9, 1, 1.2, and 0.85.
- The Spalart-Allmaras model have option for viscous heating. In the model, the constants are $C_{b1} = 0.1355$, $C_{b2} = 0.622$, $C_{v1} = 7.11$, $C_{w2} = 0.3$

SST k-omega models are used for different grid resolutions, including medium, fine, and coarse. Solving the k-omega, k-epsilon, and Spalart-Allmaras models is achieved by means of a coupled pressure-velocity coupling scheme. The coupling scheme in all models is discretized using least squares cells. All of the models discussed above utilize second-order discretization for pressure. For momentum, turbulent kinetic energy, and specific dissipation rate, second-order upwind discretization is used. In order to calculate the turbulent dissipation rate, the k-epsilon model uses first-order upwind discretization. Modified turbulent viscosity is discretized using first-order upwind in the Spalart-Allmaras model, while energy is discretized using second-order. The solution is initialized using a hybrid initialization method. Each model is solved for a minimum of 10,000 iterations.

III. RESULT AND DISCUSSION

In the present study, a numerical simulation of film cooling efficiency has been performed over a flat plate in subsonic film cooling configuration (Multi-block computational domain). Pressure based steady state simulation has been done by applying SST k-ω, Realizable k-ε and Spalart-Allmaras model. Also by using SST k-ω with different grid levels, fine, medium and coarser simulation has been done. During the film process, air is used as the mainstream and as the film stream, with a temperature of 462.92 K and 296.33 K respectively. Computed results are validated and observed in the following manner.

F. Grid independent study

The SST k-ω model used for different grid levels to investigate the behavior of film cooling effectiveness. Fine, Medium and coarser grids level adopted in subsonic film cooling plate. Figure 4. display the dimensionless temperature profile (η) at slot exit (x/s). The dimensionless temperature profile or film Colling effectiveness of fine, medium and coarser grid levels obtain average at two location fist in interval (0, 2) and second in (6, 8). Figure 5 represents contour of static temperature (K) of medium, fine and coarser grids respectively. These contours are very similar to each other and display qualitative physical behavior of temperature fields. These contours show hot behavior in mainstream, change behavior at splitter location and depicts cold at adiabatic wall location. Figure 6 indicates stream wise velocity (m/s) profile contours, they depict low velocity magnitude at mainstream location and very high at adiabatic wall location. further they display average velocity magnitude at splitter location.

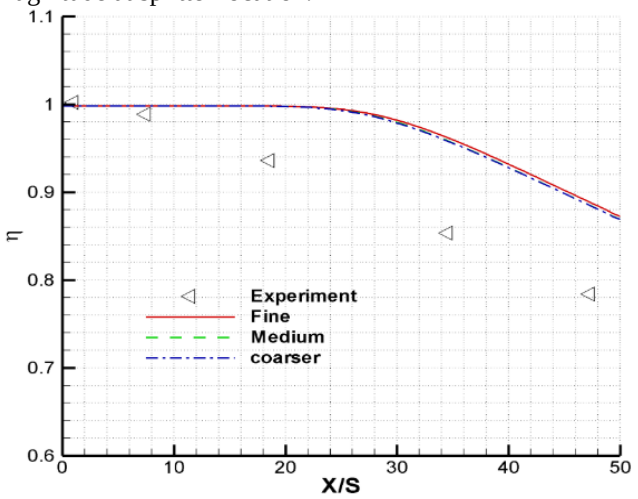

Fig. 4: film cooling efficiency (η) along bottom wall, CFD prediction with different mesh sizes models.

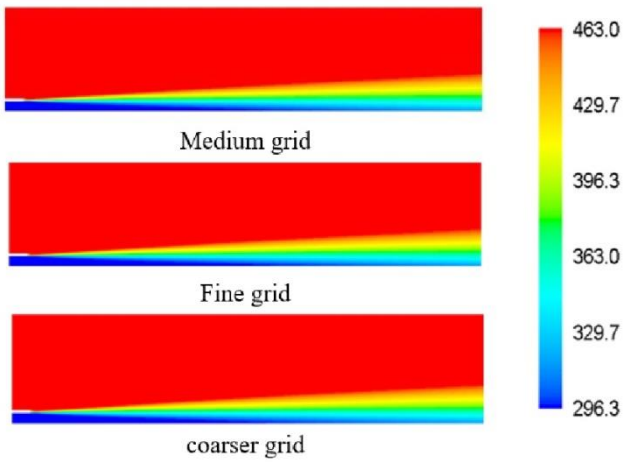

Fig. 5: Static temperature (K) contour SST k- ω models.

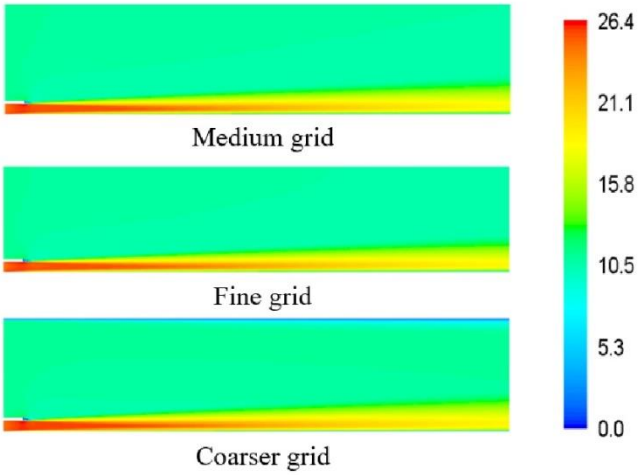

Fig. 6: Velocity magnitude (m/s) contour SST k- ω model.

G. Numerical simulation by different models

The SST k-ω, Realizable k-ε and S-A models are used to simulate film cooling efficiency over subsonic flat plate. In Figure 7 it is instantaneous realization of the film cooling efficiency (η) are averaged to obtain the mean film cooling effectiveness profiles at two locations downstream of the slot exit defined by x/s by all Models. But Realizable k-ε gives best agreements with experimental data it obtain averaged three location of the slot exit of film cooling effectiveness. Figure 8 represent temperature contour inside combustion chamber of realizable k-ε, S-A and SST k-ω models, they are depicting qualitative temperature physical behavior, they all display similar profiles with cold flow at adiabatic wall and hot flow in the mainstream. The temperature mingling layer increases stream-wise towards the wall with a resulting increase of the wall temperature. Figure 9 shows the field stream wise velocity contours, they all display boundary layer of velocity magnitude. Since the shear layer reaches the boundary layer of the wall, it is known as the film breaking point.

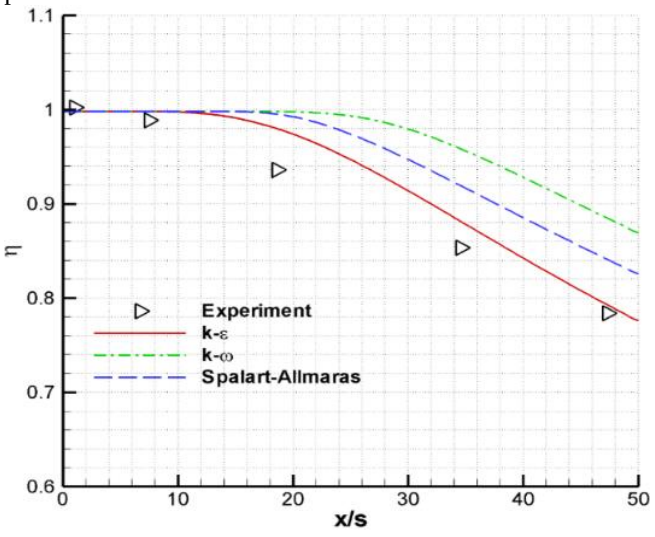

Fig. 7: Film cooling efficiency (η) along bottom wall, CFD simulation with different models vs experiment.

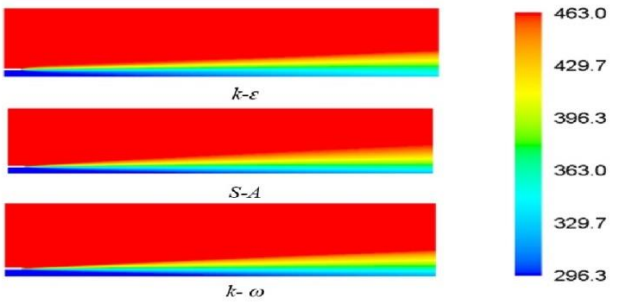

Fig. 8: Static temperature (K) contour SST model.

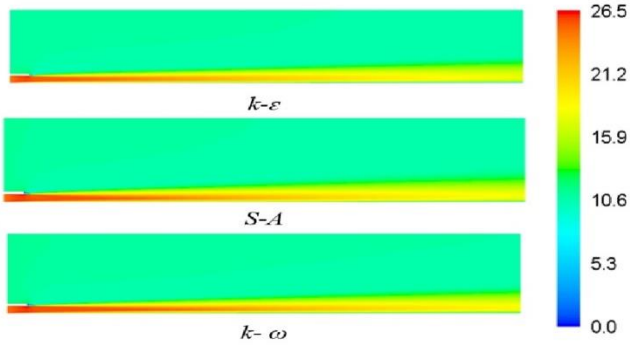

Fig. 9: Velocity magnitude (m/s) contour SST model.

IV. CONCLUSION

Measurements of the adiabatic effectiveness over subsonic flat plate has been simulated by CFD. Pressure based steady states simulation has been performed through solver by using different turbulent model and grid levels. Simulation results relatively reasonably agreed with experimental quantitatively and qualitatively. There is good agreement between numerical solutions and they are able to predict the slope of the efficiency decay even when they use different turbulence models. The present results are very promising and encourage the use of CFD to simulate and model liquid propellant rocket engine combustion chamber film cooling mechanisms. CFD methods are also more cost-effective than performing physical experiments. The results obtained can be used to optimize the design of the cooling systems and improve the efficiency of the rocket engine.

REFERENCES

[1] S. A. O'Briant, S. B. Gupta, and S. S. Vasu, "Laser ignition for aerospace propulsion," *Propuls. Power Res.*, vol. 5, no. 1, pp. 1–21, 2016.

[2] J. Linn and M. J. Kloker, "Numerical investigations of film cooling," in *RESPACE–Key Technologies for Reusable Space Systems: Results of a Virtual Institute Programme of the German Helmholtz-Association, 2003–2007*, Springer, 2008, pp. 151–169.

[3] K. H. Park, K. M. Yang, K. W. Lee, H. H. Cho, H. C. Ham, and K. Y. Hwang, "Effects of injection type on slot film cooling for a ramjet combustor," *J. Mech. Sci. Technol.*, vol. 23, pp. 1852–1857, 2009.

[4] J. Liu, S. Zhang, J. Wei, and O. J. Haidn, "RANS based numerical simulation of a GCH4/GO2 rocket engine combustion chamber with film cooling and improvement of wall heat flux prediction," *Appl. Therm. Eng.*, vol. 219, p. 119544, 2023.

[5] S.-J. Lee, I.-S. Moon, I.-Y. Moon, and S.-U. Ha, "Combustion test of oxidizer-rich single triplex injector preburner for staged combustion cycle rocket engine," in *Fluids Engineering Division Summer*

Meeting, American Society of Mechanical Engineers, 2015, p. V01AT09A010.

[6] M. Chiaverini, M. Malecki, J. Sauer, W. Knuth, and C. Hall, "Vortex combustion chamber development for future liquid rocket engine applications," in *38th AIAA/ASME/SAE/ASEE joint propulsion conference & exhibit*, 2002, p. 4149.

[7] T. A. Ward, *Aerospace propulsion systems*. John Wiley & Sons, 2010.

[8] A. A. Bhutto, M. Hussain, S. Feroz, A. Shah, and K. Harijan, "Computation of Vortex Driven Flow Instability through Unsteady RANS and Scale Resolving Simulation," *Inst. Sp. Technol.*, vol. 12, no. 1, pp. 14–22, 2022.

[9] A. Urbano *et al.*, "Exploration of combustion instability triggering using Large Eddy Simulation of a multiple injector liquid rocket engine," *Combust. Flame*, vol. 169, pp. 129–140, 2016, doi: https://doi.org/10.1016/j.combustflame.2016.03.020.

[10] K. Guo, Y. Ren, Y. Tong, W. Lin, and W. Nie, "Analysis of self-excited transverse combustion instability in a rectangular model rocket combustor," *Phys. Fluids*, vol. 34, no. 4, 2022.

[11] A. A. Bhutto, S. F. Shah, R. B. Khokhar, K. Harijan, and M. Hussain, "To Investigate Obstacle Configuration Effect on Vortex Driven Combustion Instability," 2023.

[12] A. A. Bhutto, K. Harijan, M. Hussain, S. F. Shah, and L. Kumar, "Numerical simulation of transient combustion and the acoustic environment of obstacle vortex-driven flow," *Energies*, vol. 15, no. 16, p. 6079, 2022.

[13] S. Luo, D. Xu, J. Song, and J. Liu, "A review of regenerative cooling technologies for scramjets," *Appl. Therm. Eng.*, vol. 190, p. 116754, 2021.

[14] M. Trotti, "Modelling of liquid film cooling in a GOX kerosene rocket combustion chamber," 2012.

[15] B. Betti, "Flow Field and Heat Transfer Analysis of Oxygen/Methane Liquid Rocket Engine Thrust Chambers," *2012*, 2012.

[16] W. L. Oberkampf and T. G. Trucano, "Verification and validation in computational fluid dynamics," *Prog. Aerosp. Sci.*, vol. 38, no. 3, pp. 209–272, 2002.

[17] C. Kirchberger *et al.*, "Prediction and analysis of heat transfer in small rocket chambers," in *46th AIAA Aerospace Sciences Meeting and Exhibit*, 2008, p. 1260.

[18] G. E. Bogin Jr *et al.*, "Modeling the Fuel Spray and Combustion Process of the Ignition Quality Tester with KIVA-3V," National Renewable Energy Lab.(NREL), Golden, CO (United States), 2010.

[19] H. Karimi and R. Mohammadi, "Modeling and simulation of a t wo combustion chambers liquid propellant engine," *Aircr. Eng. Aerosp. Technol.*, vol. 79, no. 4, pp. 390–397, 2007.

[20] Y. Daimon, H. Negishi, M. Koshi, and D. Suslov, "Numerical and experimental investigation of the methane film cooling in subscale combustion chamber," in *eucass-proceedings.eu*, 2016, pp. 129–144. doi: 10.1051/eucass/201608129.

[21] D. John and J. R. Anderson, "Computational fluid dynamics: the basics with applications," *Mech. Eng. Ser.*, 1995.

[22] H. K. Versteeg and W. Malalasekera, *An introduction to computational fluid dynamics: the finite volume method*. Pearson education, 2007.

[23] I. Ansys, "ANSYS Fluent Theory Guide; Ansys," *Inc. Canonsburg, PA, USA*, 2020.

[24] T.-H. Shih, W. W. Liou, A. Shabbir, Z. Yang, and J. Zhu, "A new k-epsilon eddy viscosity model for high Reynolds number turbulent flows: Model development and validation," 1994.

[25] S. SCOTTI, C. MARTIN, and S. LUCAS, "Active cooling design for scramjet engines using optimization methods," in *29th Structures, Structural Dynamics and Materials Conference*, 1988, p. 2265.

[26] C. A. Cruz and A. W. Marshall, "Surface and gas temperature measurements along a film cooled wall," *J. Thermophys. Heat Transf.*, vol. 21, no. 1, pp. 181–189, 2007.

[27] R. J. Goldstein, "Film Cooling," *Adv. Heat Transf.*, vol. 7, no. C, pp. 321–379, 1971, doi: 10.1016/S0065-2717(08)70020-0.

Balochistan Journal of Engineering & Applied Sciences (BJEAS) – (p-ISSN: 2518-2706
Volume 6, No.1

Assess the Impact of On-Farm Water Management Practices Regarding Agriculture Productivity for Sustainable Development in Balochistan

Jahanzaib Abdullazi Kakar[1], Atiq Ur Rehman[2], Arshad Hussain Hashmi[3]
[1] Project Engineer, Sabagzai Dam Irrigation Department, Government of Balochistan
[2] Executive Engineer, Irrigation Department, Government of Balochistan
[3]Registrar, Pakistan Institute of Development Economics. Islamabad, Pakistan
Corresponding author: jhanzaib1232@gmail.com

***Abstract*—In order to assess the impact of on-farm water management practices regarding agriculture productivity for sustainable development in three districts of Balochistan this research was conducted. Cross-sectional research design was applied. Quetta, Pishin and Mastung districts were chosen randomly. One hundred (100) farmers were selected. Sample random sampling was applied. Field information was recorded and put into the SPSS. Pearson Chi-Square test was run. Results show that most (45%) of growers are 19 to 40 years of age. Similarly, (45%) of growers obtained religious or Islamic education at Madrassa level. Vast majority (90%) of growers belonged to the joint family system. Majority (65%) of growers are getting married. So as to measure the on-farm water management practices the Pearson Chi-Square test applied. Statistically variations were observed in four out of five variables regarding on-farm water management practices. Thus, it was concluded that the perception differences remained regarding on-farm water management practices in three districts of Balochistan. It was recommended that a series of capacity building programs be arranged for farmers so that they could improve their sequential crop productivity methods and on- farm water management practices. Farmer's participation is encouraged within terms of on-farm water management practices for sustainable agriculture development.**

***Keywords*—** *Water management practices, Impact, Agriculture, Sustainable development, Balochistan.*

V. INTRODUCTION

Worldwide, water is a precious commodity and preliminary resource and input mostly used for domestic purposes, agricultural productivity, industrial sector and the like. Water is a fundamental sustainer about ecosystems (Brown et al., 2015). The timely availability of irrigation water for agriculture crops is part and parcel, an almost major bottleneck for agricultural productivity as well as food security at country level (Kang et al., 2009). Internationally, for agricultural productivity more than seventy (70 percent) groundwater is being used and extracted. Therefore, the agriculture sector is in the leading position for the consumption of water (DÖLL, 2009; and Siebert, 2010).
However, the groundwater is taken into account or regarded as a prime source of irrigation water for agricultural purposes. Globally, vast majority of nations are using and reliance on the ground water resources rather than rain or surface water. In the era of 1960s, the innovative water technologies and latest irrigation practices were used for agricultural purposes or crop productivity (Scanlon et al., 2012; and Schwartz & Ibaraki, 2011). However, for better crop yield and suitable crop productivity, the groundwater used is around 38% (113 million hectares) worldwide (Watto & Mugera, 2015; and Siebert, 2010).
It was observed that around 20% of farming land, their irrigation practices or water sources used to increase the yield and agricultural productivity around 40% within terms of food security (Douville, 2021; and EIB, 2023). Latest irrigation practices enhancing the crop production as a results the crop production increasing at a greater extent. Therefore, water reservoirs critically imperative regarding agricultural production. For better agriculture production, 65% of ground water and 90 percent of extracted groundwater is used in India (Chindarkar & Grafton, 2019; and NGWA, 2021).
Especially in arid countries, the ground water and latest irrigation practices are imperative resources for agricultural production as well as drinking water for human consumption. In this regard, the Arab regions are the most water-scarce region. Over mining of groundwater may affect agricultural production. In Iran the indiscriminate uses of groundwater affect agricultural production. Thus, the Iranian government developed private security to protect the groundwater assets in 2023 (UN, 2022).

A. Water resources management and their practices in Pakistan

As reported by the World Water Development Report (UN) during the period of 2000, the entire tangible renewable water assets improved at the rate of 2,961 m³ per capita (UNESCO, 2006). It was observed in Pakistan, an accessibility of water supply recorded more than 1,000 m³ per person, which indicates that Pakistan is falling in the high stress country category. Generally, during the years of 2004-05, the water availability has reduced at the rate of 1,101 m³ per capita as reported by the Planning and Development Division Government of Pakistan (GoP, 2007). Due to the rapid urbanization process, speedy industrialization advancement, quick demographic population growth factors are responsible for making the situation worse at the country level (Pakistan Economic Survey, 2007).
On the other hand, the process of rapid mining of groundwater continues depleting. In spite of a dropping the ground water table at country level, the rate of electric tube

wells increased at 6.7% and diesel tube wells increased 7.4% (ADB, 2004). Furthermore, contamination of the atmosphere at a very high rate, saltwater intrusion and saltation are limiting factors that restrict the water resources at country level. However, in this regard, 36% of ground water remains extremely salty or saline (GoP, 2008).

In Karachi and Islamabad cities and their urban premises, the surface water is used for domestic consumption. In the other cities of Pakistan, the groundwater supplies run by different Departments. Groundwater is used in most rural areas of Pakistan. However, on the other hand, canal irrigation used as the major sources for domestic water and agricultural water (GoP, 2005). Pakistan is blessed with a variety of environments. However, at country level 96% water used for agricultural purposes, 2% for domestic purposes and similar 2% for industrial purposes (Bridges, 2007).

Agriculture sector remains as the major source of livelihood options of the rural population, which contributes more than 25% of country GNP and constitutes the bulk of labor forces (65%), but agriculture remains as the major source of the economy which is based on water assets (GoP, 2002). However, the agriculture sector contributes 19% of the country's GDP (GoP, 2019).

At the country level, water is a basic and vital component for power generation for their masses. Around 29% electricity was generated through hydro-power that was based on water assets. On the other hand, Pakistan's world largest irrigation system is existing that is used for domestic, agricultural and industrial purposes. Total covered irrigated area was 181,000 km² in Pakistan (Pakistan Water Gateway, 2005). Likewise, water availability of rice growers is lower as compared to India and China (LEAD, 2016). Better agricultural water management practices and technologies are the major cause for better agricultural production and also responsible for per hectare yield increasing (Watto and Mugera, 2014).

A. On-Farm water management practices

On-farm water management project is enhancing the agricultural efficiency, yield, production, capacity and output through an efficient water system and well-mechanized system for better food security dimension. Major obstacles at country level is the non-availability of irrigation water, unreliability and inequality of water supply at farmer's field or grower's doorstep as a result the agricultural production is affected badly. Preliminary water supply by Indus Basin through canals under the supervision of Provincial Irrigation Department. While, on the other hand, construction of watercourse or watercourse operation and their maintenance is the sole responsibility of the growers. Due to the lack of financial resources, most of the watercourse were damaged as a result of 50% water conveyance losses. Therefore, the farmers did not get a better profit margin from their production or yield. In this context, a variety of research was carried out to solve this problem and to minimize these water losses or conveyance losses from up to 46% to 56%. On the other hand, the application losses at field level were also observed at country level. In order to stop the conveyance and water losses the government of Pakistan firstly implemented the 5-year pilot project. Afterward this program was converted almost immediately On Farm Water Management (OFWM) (GoP, 2016).

The silence features of program were given under:

- The Water Users Association is the basic component in this system. However, association and recordkeeping of WUA under work project administration so as to promote the water course and their improvement at district level.
- Develop the water user's associations based on cost sharing units.
- Application of water management practices and their plans run at district level by project administration.
- Increase the agricultural yield by using the optimal level of irrigation water.
- Watercourse, their renovation, their further improvement, precision of land leveling, plant protection measures, agronomy practices, irrigation application and the like run at district level through project management or authority.
- Agricultural farm machinery and their actual renting at approved rates given by authority.
- Render the capacity building program so that to strengthen the overall application of irrigation water and their efficiency.
- Develop the effective linkage mechanism between the agricultural department and farming community.
- Service matters, maintenance of physical infrastructure, purchasing of different items or capital goods and others related matters based on check and balance.
- Develop a superior coordination mechanism and well Monitoring and Evaluation (M&E) system.
- Promote the grower's contribution to irrigators' water distribution system.
- Improving agricultural productivity.
- Supporting the growers in diverse on-farm water management practices.
- Arranged the training for staff and growers regarding agricultural operation as well as maintenance of irrigation systems.
- Develop the well mechanism regarding farm planning or farm design.
- Reciprocal feedback for the entire project's business (GoP, 2016).

VI. PROBLEM STATEMENT

Balochistan region is considered as an under-privileged province of Pakistan. 85% of the province's population directly or indirectly depend on agriculture and allied agriculture activities. Therefore, agriculture and livestock remain as the major livelihood option of the rural farmers (Osbahr et al., 2008). Having the robust potential and huge land areas, the agriculture production is still limited due to the lack of better water management practices at farm level. Therefore, this research was carried out so as to assess the impact of water management practices regarding agriculture productivity for sustainable development in the selected district of Balochistan.

A. Study objectives

Current effort as following specific objectives:

[I]. To measure the socio-economic profile of the respondents.

[II]. To find out the limiting factors that are responsible for reducing agricultural productivity.

[III]. To identify the water management practices for agricultural productivity.

[IV]. To develop the need-based suggestions for future policy measures that will be supportive for water management practices.

B. Review of literature

Pakistan is the blessed country within terms of systemic irrigation system and prolonged history regarding the ground water resources and their utilization. In the early period, the karezes system, hand pump methods, open wells system with the help of rope/ buckets and Persian wheels were the most effective irrigation methods (Meckonnen et al., 2016; and Qureshi et al., 2009). In this era, pumping ground water systems were applied for irrigation systems as a result the water table decreased day by day. However, canal irrigation systems are regarded as the most effective method for supplies of water for drinking and agricultural purposes (Qureshi et al., 2008). In this context, around 17000 tube wells are put in functional so as to get rid of soil salinization risk (Mekonnen et al., 2016; and Qureshi et al., 2009). Ground water and water management practices were the prime source of irrigation at country level. Around fifty percent of the water requirement for agricultural purposes was dependent on ground water resources. Thus, the groundwater and water management practices were a major source of irrigation for farming communities because of its tractability availability (Watto and Mugera, 2015; and Shah, 2007).

C. Study design or methodology

In order to achieve the general objectives of present research (Trochim, 1989), the cross-sectional research design was applied (Campbell & Stanley, 1963) in order to assess the impact of cause and effects association between and among variables (Mady, 1982). Quetta, Pishin and Mastung districts were chosen for this research randomly. One hundred (100) farmers were selected for sample size and target population (Shaddish et al., 1991). Sample random sampling was applied in this research (Adcock & Collier, 2001). Closed-ended questions were developed. A structured questionnaire in this regard was developed. Socio-economic attribution based on assumption in this research was major independent variables (Campbell and Fiske, 1959). On the other hand, the table of McCall (1980) concerning "determining sample size from a given population" was carefully chosen. 5-point Likert Scaling as the major scaling that was used in this research (Wolcott, 1990; and Patten & Mildred, 2002). Thus, field information in this context, recorded and put into the SPSS (a computer software for social scientists) (Pyrczak, 2002). Pearson Chi-Square test was run in this research to detect the association and relationship among variables (Duffy, 1987). Alpha level was set at 0.05 level.

V. RESULTS

A. Socio-economic variables and their explanation

In this research the socio-economic variables were the vital independent variables. Therefore, in this research the variables were measured by using the statistical test.

Figure-1, Sample distribution about growers age

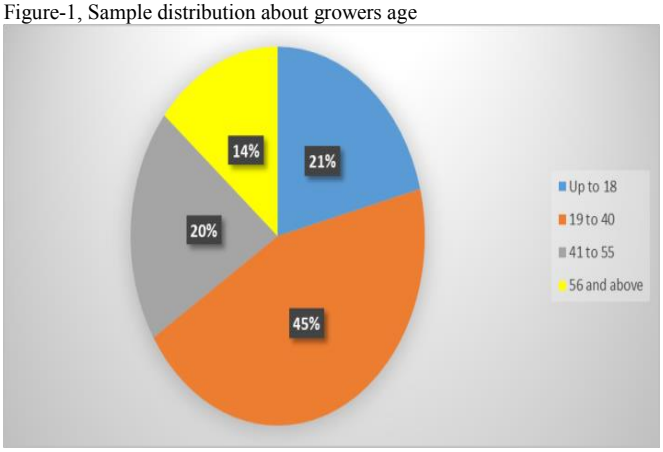

Age is the imperative component in this research, because due to age factor farmers gained the farming experiences more effectively as well as having sound decision making in any circumstances. Therefore, the age component is considered as shown in figure-1. Respondents were asked about their age composition. Most (45%) of growers are 19 to 40 years of age. While, 20-21% of growers have 41 to 50 and up to 18 years respectively.

Figure-2, Sample distribution about grower's educational level

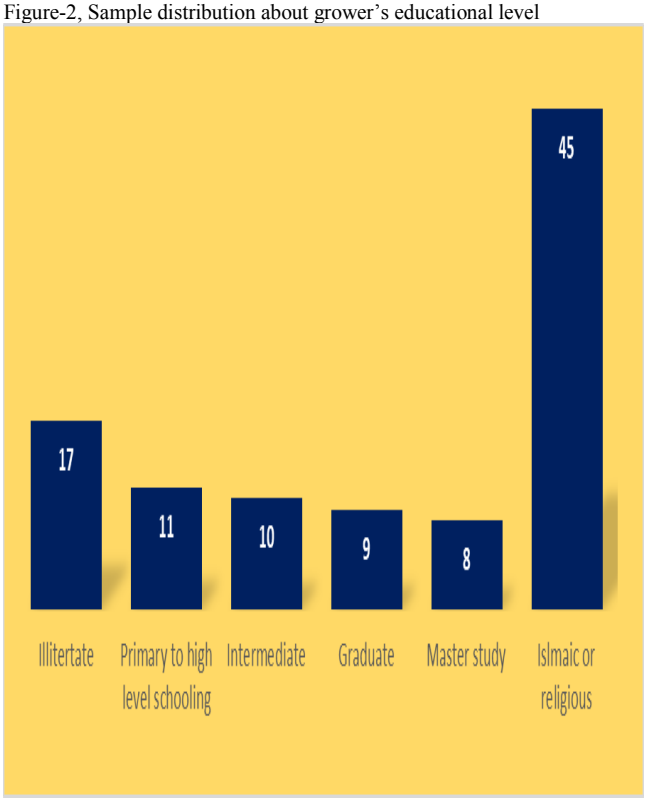

Figure-2 shows that most (45%) of growers obtained religious or Islamic education at Madrassa level. While most 17% of growers were uneducated. Whereas, most 11-10% of growers were getting the primary/ higher level of schooling to intermediate degree respectively.

Figure-3, Sample distribution about grower's family type

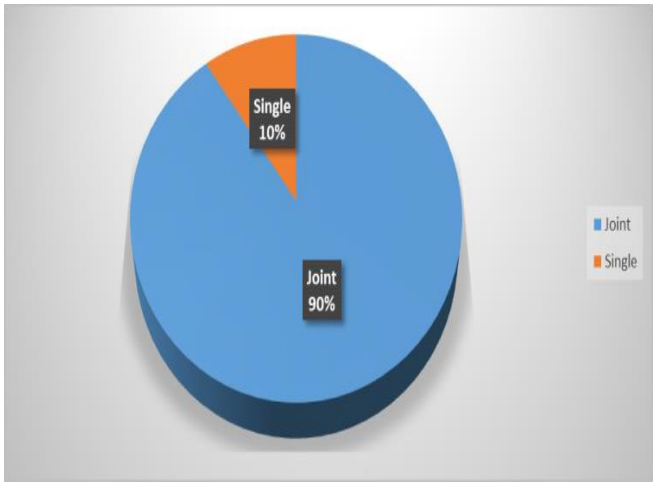

Sample distributions regarding the grower's family type are shown in figure-3. In this regard the data was gathered at field level. Vast majority (90%) of growers belonged to the joint family system. While, only 10% of growers belong from single family status.

Marital status growers of grower were determined and gauged as shown in figure-4. Majority (65%) of growers getting married or by status involved in marriage. While, 35% of growers did not get married and still have single status.

Figure-4, Sample distribution about grower's marital status

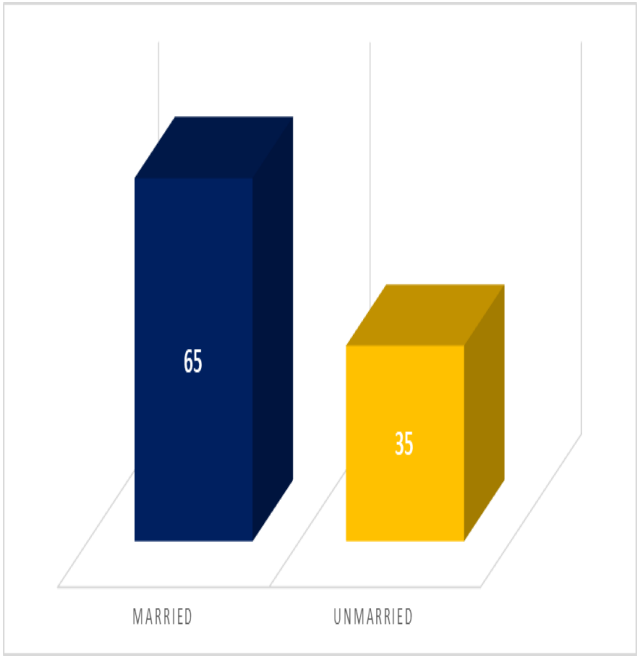

Table-1, Chi-square test about on-farm water management practices

On-farm water management practices	Value	df	Asymp: Sig. (2-sided)
Per hectare yield of various crop increased			
Pearson Chi-Square	46.137a	8	**.000****
Likelihood Ratio	52.274	8	.000
Linear-by-Linear Association	17.331	1	.000
Phi	.679	-	.000
Cramer's V	.480	-	.000
Farmers' knowledge concerning latest irrigation methods improved			
Pearson Chi-Square	15.456a	8	.051NS
Likelihood Ratio	19.325	8	.013
Linear-by-Linear Association	.119	1	.731
Phi	.393	-	.051
Cramer's V	.278	-	.051
Farmers income level improved			
Pearson Chi-Square	19.470a	8	.013*
Likelihood Ratio	25.655	8	.001
Linear-by-Linear Association	8.399	1	.004
Phi	.441	-	.013
Cramer's V	.312	-	.013
Farmer's participation level			
Pearson Chi-Square	31.192a	8	.000**
Likelihood Ratio	34.061	8	.000
Linear-by-Linear Association	10.088	1	.001
Phi	.559	-	.000
Cramer's V	.395	-	.000
Sustainable agriculture development retained due to water management practices			
Pearson Chi-Square	22.103a	8	.005*
Likelihood Ratio	28.115	8	.000
Linear-by-Linear Association	.362	1	.547
Phi	.470	-	.005
Cramer's V	.332	-	.005
No. of Valid Cases in this research= one hundred (100) growers *Statistically significant at zero point five alpha level			

Highly statistically discrepancies and differences found about various on-farm water management practices statements. Pearson Chi-Square was used in this research. Alpha level was calculated so as to determine the significant value Phi and Cramer's V respectively. However, on the other hand, p-value set on is .005 level (statistically significant).

In this research Pearson Chi-Square values are highly statistically significant, in statements like "per hectare yield of various crops increased" (Pearson Chi-Square=46.137a, Likelihood Ratio=52.274 and Linear-by-Linear Association=17.331) respectively. While, a statement such

as "farmer's participation level" (Pearson Chi-Square=31.192[a], Likelihood Ratio=34.061and Linear-by-Linear Association=10.088 respectively.

Only statistically significant observed statements like "farmer's income level improved: (Pearson Chi-Square=19.470[a], Likelihood Ratio=25.655 and Linear-by-Linear Association=8.399) respectively. And statements like: "sustainable agriculture development retained due to water management practices" (Pearson Chi-Square=22.103[a], Likelihood Ratio=28.115 and Linear-by-Linear Association = .362) respectively.

Thus, statistically non-significant found statement like "Farmers' knowledge concerning latest irrigation methods improved" (Pearson Chi-Square=15.456[a], Likelihood Ratio=19.325 and Linear-by-Linear Association=.119) respectively based on 0.05 alpha level about on-farm water management practices. Thus it was concluded that statistically significant observations.

D. Conclusion and recommendations

This research observed the present on-farm water management practices in three districts of Balochistan namely, Quetta, Pishin and Mastung. In this context, raw information or data was acquired at field level in respective districts of Balochistan province. Based on obtained results following recommendation was developed. Capacity building programs related with on-farm water management practices part and parcel and preliminary ingredients to empower the farmer's practical knowledge. Therefore, it should be recommended that a series of capacity building programs be arranged for farmers so that they can improve their sequential crop productivity methods and on- farm water management practices. Farmer's participation is encouraged within terms of on-farm water management practices for sustainable agriculture development.

REFERENCES

[1]. ADB, (2004). Balochistan Resource Management Program. Asian Development Bank. RRP: PAK 37135. pp. 11.

[2]. Adcock, R. & Collier, D. (2001). Measurement validity: A shared standard for qualitative and quantitative research. American Political Science Review 95: 529-546.

[3]. Bridges, G. (2007). Asian Water Development Outlook. Country Paper Pakistan. Asian Development Bank (2007). pp. 5.

[4]. Brown, C. M. Lund, J. R. Cai, X. Reed, P. M. Zagona, E. A. Ostfeld, A. Hall, J. Characklis, G.W. Yu, W. and Brekke, L. (2015). The future of water resources systems analysis: Toward a scientific framework for sustainable water management. Water Resource. Res. 51 6110-6124.

[5]. Campbell, D. T. and. Stanley, J. C. (1963). Experimental and quasi-experimental designs for research on teaching, Chicago: Rand McNally, 1963. 171-246. The seminal article on types of validity.

[6]. Campbell, D.T. & Fiske, D.W. (1959). Convergent and discriminant validation by the multi-trait-multimethod matrix. Psychological Bulletin, 56, 81-105.

[7]. Chindarkar, N. and Grafton, Q. (2019). India's depleting groundwater. When science meets policy. Asia & the Pacific Policy Studies. 6 (1): 108–124. doi:10.1002/app5.269.

[8]. Döll, P. (2009). Vulnerability to the impact of climate change on renewable groundwater resources: A global-scale assessment. Environmental Research Letters. 4.

[9]. Douville, H., Raghavan, K. Renwick, J. Allan, R.P. Arias, P.A. Barlow, M. Cerezo-Mota, R. Cherchi, A. Gan, T.Y. Gergis, J. Jiang, D. Khan, A. Pokam Mba, W. Rosenfeld, D. Tierney, J. and Zolina, O. (2021). Water Cycle Changes in Climate Change. Cambridge University Press, Cambridge, United Kingdom and New York, NY, US, pp. 1055–1210, doi:10.1017/9781009157896.010.

[10]. Duffy, M., E. (1987). Methodological Triangulation: A Vehicle for Merging Quantitative and Qualitative Research Methods. IMAGE: Journal of Nursing Scholarship,19(3), 130-133. http://www.georgetown.edu/departments/psychology/researchmethods/writing/webresearch.htm.

[11]. EIB, (2023). On Water. European Investment Bank.

[12]. GoP, (2002). Pakistan Water Sector Strategy. Ministry of Water and Power. Executive Summary Volume-1, pp. 6.

[13]. GoP, (2005). Water and Sanitation (Section 10). Medium Term Development Framework. Government of Pakistan. Ministry of Planning and Development. Section 10.2.

[14]. GoP, (2007). Government of Pakistan, Ministry of Economic Affairs and Statistics, Statistics Division. Overall Water Availability. Pakistan Statistical Year Book 2007. http://devdata.worldbank.org/query/.

[15]. GoP, (2008). Pakistan Water Gateway. The Pakistan Water Situational Analysis. pp. 4.

[16]. GoP, (2016). On-Farm Water Management. Government of the Punjab. Punjab Information Technology Board.

[17]. GoP. (2019). Agricultural Statistics of Pakistan 2018-19. Islamabad, Pakistan. Pakistan:

[18]. Kang, Y. Khan, S. and Ma. X. (2009). Climate change impacts on crop yield, crop water productivity and food security–a review Prog Nat. Sci. 19: 1665-1674.

[19]. LEAD, (2016). Groundwater Management in Pakistan: An Analysis of Problems and Opportunities. Pakistan: Learning and Knowledge Management Team, LEAD Pakistan.

[20]. Mady, D. (1982). Benefits of Qualitative and Quantitative methods in program evaluation, with illustrations. Educational Evaluation and Policy Analysis, 4, 223-236.

[21]. McCall, C. (1980). Sampling and statistics Handbook for research in Education. National Education Association: USA.

[22]. Mekonnen, D.K. Siddiqi, A. and Ringler, C. (2016). Drivers of groundwater use and technical efficiency of groundwater, canal water, and conjunctive use in Pakistan's Indus Basin Irrigation System. International Journal of Water Resources Development. 32: 17.

[23]. Ministry of Finance.

[24]. NGWA, (2021). Facts About Global Groundwater Usage. National Ground Water Association. Retrieved 29 March 2021.

[25]. Osbahr, H. Twyman, C. Neil, A. W. & Thomas, D. S. G. (2008). Effective livelihood adaptation to climate change disturbance: Scale dimensions of practice in Mozambique. Geoforum, 39(6), 1951-1964.doi: http://dx.doi.org/10.1016/j.geoforum.2008.07.010.

[26]. Pakistan Economic Survey (2007). Environment. Ministry of Finance. Chapter 16. Environment Pakistan., pp. 248.

[27]. Pakistan Water Gateway (2005). The Pakistan Water Situational Analysis. Retrieved 2008-05-28., pp. 6-9.

[28]. Patten, and Mildred, L. (2002). Understanding research methods: An Overview of the essentials (3rd ed.). Los Angeles: Pyrczak Publishing.

[29]. Pyrczak, F. (2002). Success at statistics: A Worktext with humor (2nd ed.). Los Angeles: Pyrczak Publishing.

[30]. Qureshi, A. S. McCornick, P. G. Qadir, M. and Aslam, M. (2008). Managing salinity and waterlogging in the Indus Basin of Pakistan. Agricultural Water Management 95:1-10.

[31]. Qureshi, A. S. Mccornick, P. G. Sarwar, A. and Sharma, B. R. (2009). Challenges and prospects of sustainable groundwater management in the Indus Basin, Pakistan. Water Resources Management. 24(8): 1551 -1569.

[32]. Scanlon, B. R. Faunt, C.C. Longuevergne, L. Reedy, R.C. Alley, W.M. Mcguire V.L. and Mcmahon. P.B. (2012). Groundwater depletion and sustainability of irrigation in the US High Plains and Central Valley. Proceedings of the National Academy of Sciences, 2012.

[33]. Schwartz, F.W. and Ibaraki. M. (2011). Groundwater: A Resource in Decline. Elements. 7: 175-179.

[34]. Shaddish, W, Cook, T. and Leviton, L. (1991). Foundations of Program Evaluation: Theories of Practice. SAGE Publishing Company. Newbury Park.

[35]. Shah, T. (2007). The groundwater economy of South-Asia: an assessment of size, significance and socio-ecological impacts: CABI Publications.

[36]. Siebert, S.E.A. (2010). Groundwater use for irrigation – a global inventory. Hydrol. Earth Syst. Sci. Discuss. 7: 3977-4021.

[37]. Trochim, W. (1989). An Introduction to Concept Mapping for Planning and Evaluation. Evaluation and Program Planning, 12, 1-16.

[38]. UN, (2022). The United Nations World Water Development Report 2022. Groundwater. Making the invisible visible. UNESCO, Paris Text was copied from this source, which is available under a Creative Commons Attribution 3.0 International License.

[39]. UNESCO, (2006). The 2nd UN World Water Development Report. United Nations Educational, Scientific and Cultural Organization. 'Water, a shared responsibility'. New York: UNESCO. ISBN 92-3-104006-5. pp. 134.

[40]. Watto, M.A. and Mugera. A.W. (2014). Measuring production and irrigation efficiencies of rice farms: Evidence from the Punjab province, Pakistan. Asian Economic Journal. 28: 301-322.

[41]. Watto, M.A. and Mugera. A.W. (2015). Irrigation water demand and implications for groundwater pricing in Pakistan. Water Policy. 18: 565-585.

[42]. Wolcott, H., R. (1990). Qualitative inquiry in education: The continuingdebate

Balochistan Journal of Engineering & Applied Sciences (BJEAS) – (p-ISSN: 2518-2706
Volume 6, No.1

Smart Streetlight Monitoring System using IoT

Arooj Sarfraz[1], Aamir Hussain[1], Akbar Khan[2], Shafi Ullah[2], Rehmat Ullah[2]
[1] Department of Computer Science MNS-University of Agriculture Multan, Pakistan
[2] Department of Computer Engineering, Balochistan University of Information Technology, Engineering, and Management Sciences (BUITEMS), Quetta, Pakistan
Correspondence Author: Aamir Hussain, Email: aamir.hussain@mnsuam.edu.pk

***Abstract*—Now a days Streetlights have become an important part of traffic safety. As a result, it is critical that we preserve energy as much as we can. A street light monitoring system is an automated system that improves efficiency. The paper will use the Internet of Things (IOT) as its primary technology. This paper main goal is to develop a Smart Streetlight Monitoring System that uses effective methods to reduce electricity consumption. The majority of places have automated street lights that identify when it's day or night and turn on and off in accordance. This paper is being expanded by adding a new constraint to turn on the light, which is that the streetlight will only turn on if there is darkness and someone is walking down the street. We also check the battery voltage and display it on the screen if the voltages are low, so the responsible person can troubleshoot the issue. We'll count the total number of vehicles passing by on a certain road or parked in a parking area. We also include a feature that allows the system to detect a fire in its early stages and send out an alert notification via alarm.**

Keywords*—*IoT, Smart Streetlight, Sensors, Energy consumption, Energy efficiency

I. INTRODUCTION

The streetlight monitoring system is one of the most important aspects of any city or small town. There is no way to overestimate the value of street lighting, however the current system has several drawbacks. Now, before the sun sets in the evening, street lights are turned on, and they are shut off the next morning when there is enough light for driving. Occasionally, the street light is left on throughout the day[1]. Another instance of waste is the full-blast lighting at midnight, even though there is little to no traffic[2]. When none of the objects are passed under the lights, a lot of energy is spent and wasted. Therefore, there is huge amount of wasted energy in the OPEN/OFF cycle. Streetlights that are out of service can potentially be a source of criminality on the roads and highways. One of the principle purposes behind changing to a free framework is that there is smaller amount electricity. One of the most serious issues is a road fire. There is currently no system in place that generates an alarm in the event of a fire. The best energy efficiency solution is presented in this paper. Additionally, the lighting system's manual operation has been entirely done away with. On the other hand, this system automatically turns on and off the lights. Only when there is someone passing through the street will the streetlight glow at full strength. It can also detect a fire in an area, sound an alarm, alert the system, and take appropriate safety measures depending on the circumstances. Reduce the number of people on the lead list. The proposed system could be used for other additional purposes, including lighting in industries, universities, parking lots, and supermarkets.

II. LITERATURE REVIEW

One of the consumable electricity sources that is necessary for daily life is street lighting. The present manually operated street lighting systems have a number of limitations. The recommended method makes use of a method that automatically dims street lights at night when nearby people or cars are present. A controller and many sensors are also required for a street lighting system to be considered intelligent [3]. The objective of this study is to develop a smart lighting system that uses less energy and can be controlled and monitored by mobile applications. A small-scale prototype that uses an Arduino board for control and automation has been created. It starts with establishing the circuit, recognizing the LDR sensor's input, and placing the PIR sensor [4]. This paper focuses on smart lighting communication protocols that can be used in smart cities to manage power effectively. In addition to providing a brief overview of the various IoT protocols used in various SLSs, we introduce a generic communication model for an SLS. Then, using a quick analysis of various lighting conditions, we also discuss the effects of SLS (indoor and outdoor) [5]. In this article, a traffic signal's timing is simply based on the number of cars parked along a road. In this model, a clustering algorithm based on the KNN algorithm is being used. A new model will be able to determine predicted timing using this technique based on the signal's inputs, which are the number of cars. How much time must be given and how many vehicles must be on each side of the road will determine this [6]. The main goal of this research is to create a street light that is automated and controlled to meet the needs of vehicles, pedestrians, and roads. A user-friendly control system that leverages IOT and LoRa can monitor and manage lighting systems from far-off places by using already-existing networks and unlicensed radio frequencies [7]. This research proposes an IoT-based smart street light system. When people are detected, the lights would turn on fully in this system; otherwise, they would turn on dimly or turn off. In our paper, we develop a system that makes use of IoT [8]and [19]. A study of streetlights with microcontroller-based control lighting. When no one is present, the lamps turn off or dim the brightness before the vehicles arrive. It will be challenging for pedestrians and automobiles to distinguish between smart street lamps and conventional street lights as all street lights switch on before they arrive [9]. The primary goal of the paper is proposed a system that would allow for the automation of street lights and the internet-based transfer of their data. Lights can be turned on

and off automatically depending on the surrounding conditions. Sensors measure light-dependent as well as humidity and temperature sensors to sense environmental conditions. An artificial power source, such as solar panels, may run the entire system [10]. This paper proposed a system that offers a remedy for regulating light intensity while taking traffic on the road into account. Instead of employing an IR sensor, this device uses a piezoelectric sensor to track the movement of objects on the street. An MSP430 microcontroller is in charge of the process [11].

III. MATERIAL AND METHODS

We propose a smart streetlight monitoring system to ensure, low power consumption. Our proposed system is divided into four modules based on its functionality

- Object Detection
- Vehicle Counting
- Fire Detection, Alarm and Send Notification
- Measure the voltage of battery

A. Object Detection

In first module lights are ON but dim, that consume less energy, after that any object passes under the lights that glows properly, when object move out of the range the lights

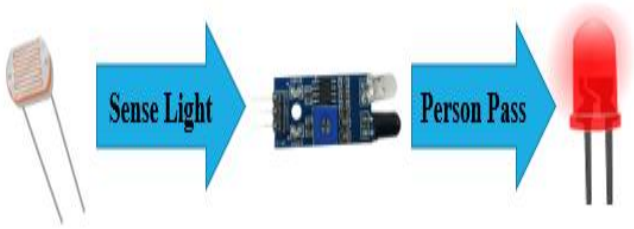

are in the normal form.

Figure 1 IR sensors for object detection

B. Vehicle Counting

In second module, we measure the total number of vehicles that passes through the specific road/parking area. All the vehicles that passes from the road are count and keep in the record.

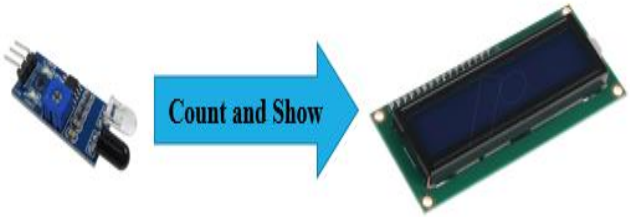

Figure 2 IR sensors for vehicle counting

C. Fire Detection, Alarm and Send Notification

In third module fire detection. We detect the fire, alert the surround by alarm, and send the notification to the admin viva mobile application. When there is any sort of fire in the surroundings between the ranges of the sensor, it alerts the surroundings as well as admin.

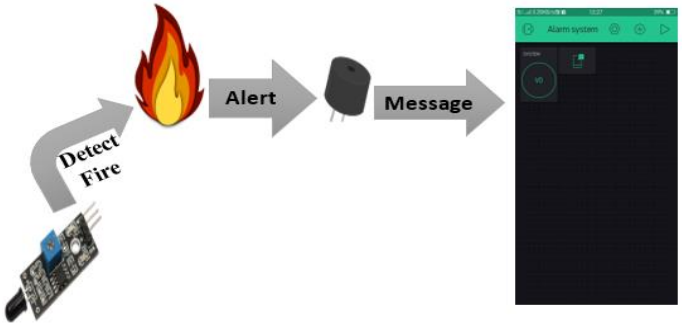

Figure 3 Flame sensor for fire detection

D. Measure the voltage of battery

In another module, we will measure the voltage that are used to glow the lights and send notification to the admin via application. If the voltages are low or high from the specific range, it alerts the admin that take specific action to avoid the major cause of the any failure.

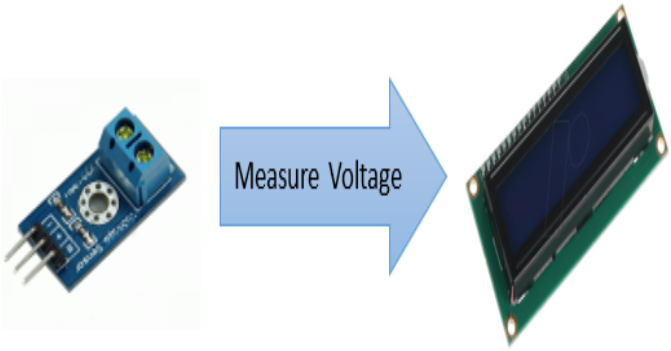

Figure 4 Measure the voltage of battery

A. Arduino IDE

Writing code and uploading it to a board are both made simple by the open source Arduino Software (IDE). In contrast to Windows, Mac OS, and Linux, it makes use of a distinct platform. It supports the programming languages C and C++. The environment is developed in Java, and it requires the installation of the IDE software before it can be used with any Arduino board [12 - 15].

B. C Programming language

C has structures that effectively translate to common machine instructions by design. It has been used for software ranging from supercomputers to PLCs and embedded devices.

C. Blynk Application

Blynk is a cutting-edge IoT platform that enables you to deploy your products at scale, connect any hardware to the

cloud, and create apps to manage it. [16 - 18]. This app is used to show the notification that is sent from the system using NodeMcu. We used Button to ON/OFF the fire detection system.

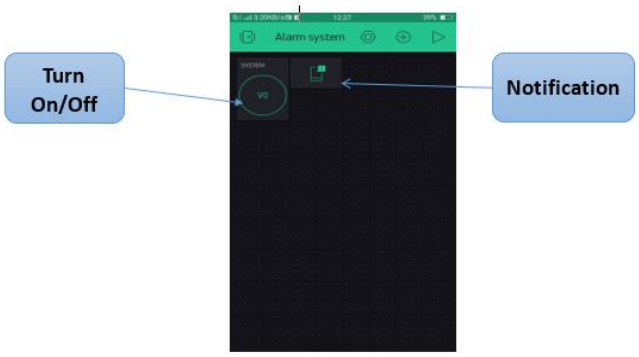

Figure 5 SSLMS Blynk Application

D. *LED's*

A light-emitting diode (LED) is an integrated diode that emits light when turned on. The electrons inside the LED can reconnect with holes, release energy in the form of photons, and generate light when we apply power to all of its tracks. As a result, the light source is a two-hour semiconductor light source. Our lighting system is made up of light-emitting diodes, and the quantity of light emitted is exactly the same as the amount of light emitted it nature, which means that when the outside light is less than the light emitted by LEDS, it has more power.

E. *LDR SENSOR*

The Light Dependent Resistor (LDR) is a type of sensor that detects light. The LDR is light-sensitive, and the quantity of light it receives affects how resistant it is. It is frequently utilized in electrical circuits, including those for automated lighting and contrast control.

F. *IR SENSORS*

An electrical gadget called an infrared sensor may identify things by detecting the infrared light those items emit. An IR LED transmitter takes in infrared light between 700nm and 1mm in wavelength. When a particular 30 volts are delivered to the LED transmitter, IR radiation is emitted. These photons strike an object, which then reflects the incident IR light back to the receiving photodiode.

G. *MEGA ARDUINO*

The ATmega2560 serves as a board for the Arduino Mega 2560 microcontroller. Connect it to a computer through USE, or power it using an AC-to-DC converter or battery. Several shields designed for the Uno and earlier Duemilanove boards work with the board.

H. *FLAME SENSOR*

The Flame Sensor module may recognize flames or strong lights. This sensor picks up infrared light from a flame or light source with a wavelength of 760 nm to 1100 nm. The YG1006 photo transistor sensor has great speed and sensitivity, and is used in fire sensors.

IV. WORKING FLOW

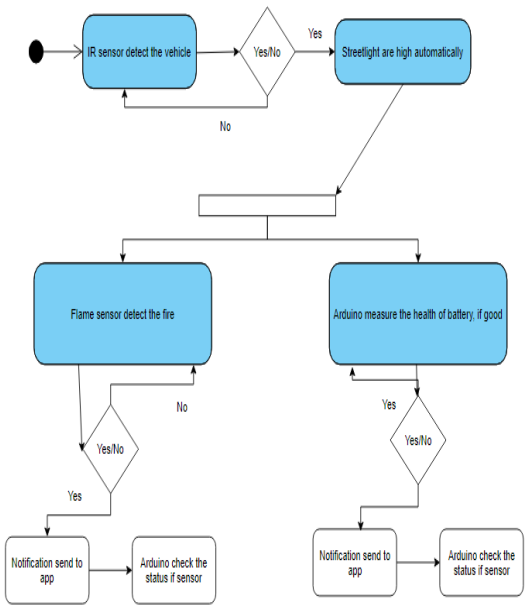

Fig. 6. Diagram of our proposed System

This diagram explains how the "smart streetlight monitoring system using IoT" work. It is powered by a battery, which is charged via a circuit that converts changing voltage into stable voltage. The Arduino then adjusts the power LED circuit in response to changes in the IR sensor and LDR. IR sensors detect the vehicles and measure the total number of vehicles that passes through the specific road/parking area. All the vehicles that passes from the road are count and keep in the record. Flame sensors are used to detect the fire, alert the surround by alarm, and send the notification to the admin viva mobile application. We also measure the voltage that are used to glow the lights and send notification to the admin via application. If the voltages are low or high from the specific range, it alerts the admin that take specific action to avoid the major cause of the any failure. The blink application is used to display the OUTPUT.

V. DISCUSSIONS AND RESULTS

In comparison to the traditional street light system, which keeps the lights on all night, the energy efficiency has increased. While strolling at night, it also assures traffic safety. One of the most serious issues is a road fire. It can also detect a fire in an area, sound an alarm, alert the system, and take appropriate safety measures depending on the circumstances. Power electronics are being used more and more often throughout many facets of modern life. Other smart applications explains in studies [20 - 23] may combine to design a smart city application. Sensors are one example of a component that has been utilized in an experiment that has become a crucial part of our daily lives. Energy may be effectively conserved using this system.

VI. CONCLUSION

By completing this project, we will be able to see how the smart streetlight monitoring system works and how it

benefits in energy conservation. The technical solution for setting up a smart street lighting system has been simplified. Provides cheap street lighting control infrastructure. It is possible to reduce the amount of energy used, which makes it more natural. Light errors in this system can be easily detected. The Municipal Organization will benefit greatly from this system.

In future work we use Machine Learning to detect the number plate of vehicles to accurate counting of vehicles and store the data of the vehicles that help in any sort of criminal activity. In module, we measure the voltage of battery and send notification to the control room to the specific patch of lights to detect the fault in battery to prevent from the damage of the system.

REFERENCES

[1] M. Saifuzzaman, N. N. Moon, and F. N. Nur, "IoT based street lighting and traffic management system," 5th IEEE Reg. 10 Humanit. Technol. Conf. 2017, R10-HTC 2017, vol. 2018-Janua, no. December, pp. 121–124, 2018, doi: 10.1109/R10-HTC.2017.8288921.

[2] S. Vani, R. Indumathi, V. Hindhu, and C. Engineering, "Iot Based Street Light Intensity Optimization and Air Pollution Monitoring System," vol. 8, no. 5, pp. 45–56, 2020.

[3] M. Caroline Viola Stella Mary, G. Prince Devaraj, T. Anto Theepak, D. Joseph Pushparaj, and J. Monica Esther, "Intelligent energy efficient street light controlling system based on IoT for smart city," Proc. Int. Conf. Smart Syst. Inven. Technol. ICSSIT 2018, no. Icssit, pp. 551–554, 2018, doi: 10.1109/ICSSIT.2018.8748324.

[4] Z. Baharum, A. S. Sabudin, E. M. M. Yusof, and N. A. Ahmad, "Mobile-Based Application: The Designation of Energy Saving Smart Light System for Monitoring and Controlling," Int. J. Interact. Mob. Technol., vol. 15, no. 18, pp. 90–103, 2021, doi: 10.3991/ijim.v15i18.24733.

[5] A. K. Sikder, A. Acar, H. Aksu, A. S. Uluagac, K. Akkaya, and M. Conti, "IoT-enabled smart lighting systems for smart cities," 2018 IEEE 8th Annu. Comput. Commun. Work. Conf. CCWC 2018, vol. 2018-Janua, pp. 639–645, 2018, doi: 10.1109/CCWC.2018.8301744.

[6] S. K. Janahan, M. R. M. Veeramanickam, S. Arun, K. Narayanan, R. Anandan, and S. J. Parvez, "IoT based smart traffic signal monitoring system using vehicles counts," Int. J. Eng. Technol., vol. 7, no. July, pp. 309–312, 2018, doi: 10.14419/ijet.v7i2.21.12388.

[7] J. Mathew, R. Rajan, and R. Varghese, "IOT BASED STREET LIGHT MONITORING & CONTROL WITH LoRa/LoRaWAN NETWORK," Int. Res. J. Eng. Technol., pp. 1173–1177, 2019, [Online]. Available: www.irjet.net

[8] N. Cm, V. Ts, M. Dakshayini, and P. Jayarekha, "IoT-Smart Street Light System," J. Inf. Technol. Sci., vol. 5, no. 1, pp. 7–10, 2019.

[9] U. M. PIYUSH SAINI, PRATEEK SAINI, AJAY KUMAR JANGID, "A Smart Street Light System With Auto Fault Detection," no. July, 2020.

[10] R. Majumdar, A. Srivastava, D. Tulsian, and V. P. Mishra, "IOT based Street Light Controlling Mechanism," Proc. 2019 Int. Conf. Comput. Intell. Knowl. Econ. ICCIKE 2019, no. December, pp. 433–436, 2019, doi: 10.1109/ICCIKE47802.2019.9004248.

[11] D. R. Parkash, Prabu V and P.G, "Internet of Things Based Intelligent Street Lighting System for Smart City," Int. J. Innov. Res. Sci. Eng. Technol., vol. 5, no. 5, pp. 7684–7691, 2018, doi: 10.15680/IJIRSET.2016.0505181.

[12] "Arduino Software Release Notes". Arduino Project. Retrieved September 25, 2019.

[13] Jean-Luc Aufranc (2021-03-03). "Arduino IDE 2.0 beta released with live debugger, revamped user interface". cnx-software.com. Retrieved 2021-03-04.

[14] Sulaman, M., Bazai, S. U., AKram, M., & Khan, M. A. (2022). The Deep Learning based Smart Navigational Stick for Blind People. UMT Artificial Intelligence Review, 2(2).

[15] "Arduino - FAQ". www.arduino.cc. Retrieved 2020-08-27.

[16] Barrie Jenkins, Peter Mullinger. 2011. Industrial and Process Furnaces: Principles, Design and Operation, Butterworth-Heinemann/IChemE series, p.329. Butterworth-Heinemann. ISBN 0080558062

[17] S. P. Bag. 1995. Fire Services in India: History, Detection, Protection, Management, Environment, Training and Loss Prevention, p. 49. Mittal Publications. ISBN 8170995981

[18] Chenebert, A.; Breckon, T.P.; Gaszczak, A. (September 2011). "A Non-temporal Texture Driven Approach to Real-time Fire Detection" (PDF). Proc. International Conference on Image Processing:1781–1784.CiteSeerX 10.1.1.228.875.doi:10.1109/ICIP.2011.6115796. ISBN 978-1-4577-1303-3.

[19] Jahangeer, A., Bazai, S. U., Aslam, S., Marjan, S., Anas, M., & Hashemi, S. H. (2023). A Review on the Security of IoT Networks: From Network Layer's Perspective. IEEE Access.

[20] Ullah, R., Bazai, S. U., Aslam, U., & Shah, S. A. A. (2023, May). Utilizing Blockchain Technology to Enhance Smart Home Security and Privacy. In Proceedings of International Conference on Information Technology and Applications: ICITA 2022 (pp. 491-498). Singapore: Springer Nature Singapore.

[21] Bhatti, U. A., Masud, M., Bazai, S. U., & Tang, H. (2023). Investigating AI-based smart precision agriculture techniques. Frontiers in Plant Science, 14.

[22] Ghafoor, M. I., Roomi, M. S., Aqeel, M., Sadiq, U., & Bazai, S. U. (2021, December). Multi-Features Classification of SMD Screen in Smart Cities using Randomised Machine Learning Algorithms. In 2021 2nd International Informatics and Software Engineering Conference (IISEC) (pp. 1-5). IEEE.

[23] Fakhar, S., Baber, J., Bazai, S. U., Marjan, S., Jasinski, M., Jasinska, E., ... & Hussain, S. (2022). Smart classroom monitoring using novel real-time facial expression recognition system. Applied Sciences, 12(23), 12134.

Balochistan Journal of Engineering & Applied Sciences (BJEAS) – (p-ISSN: 2518-2706
Volume 6, No.1

Adopting Homomorphic Encryption in Neural Networks: Issues and Future Directions

Mehmood Baryalai[1], Muhammad Imran Ghafoor[2], Zubair Zaland[3], Jahanzeb Bakhtiar[4], Muhammad Ashraf [5]
[1] Department of Information Technology, Balochistan University of Information Technology, Engineering, and Management Sciences (BUITEMS), Quetta, Pakistan
[2] Department of Engineering, Pakistan Television Corporation Lahore, Pakistan
[3] Department of Software Engineering, Balochistan University of Information Technology, Engineering, and Management Sciences (BUITEMS), Quetta, Pakistan
[4] Department of Computer Science, IIC University of Technology, Cambodia
[5] Department of Computer Engineering, Balochistan University of Information Technology, Engineering, and Management Sciences (BUITEMS), Quetta, Pakistan
Correspondence Author: Mehmood Baryalai, Email: mehmood.baryalai@buitms.edu.pk

***Abstract*—A cornerstone of intelligent information processing systems is categorizing data into its appropriate class with a similar pattern. Recommender systems all work on the principle of recognizing a pattern that has already been established. Data can be correlated from multiple sources using such systems, which is always beneficial. However, the adoption of intelligent classification technologies has led to one of the most controversial issues in recent years, namely, the threat to privacy associated with them. Not all sources can afford to compromise on the privacy of their data in processing environments for correlation or processing. Many technologies and methods are available to help achieve the best of both worlds by allowing in-telligent classification tasks to be performed in untrusted environments while protecting per-sonal information. However, despite the fact that homomorphic encryption appears to be the most promising of these methods, there is an urgent need to give answers to questions related to the classification of private information in untrusted environments based on the advance-ments made in homomorphic encryption and neural networks. Additionally, this paper presents important ideas and works relevant to classifying encrypted data using neural networks with the use of privacy-preserving homomorphic encryption techniques in order to highlight the gap for answering the questions posed.**

Keywords*—*Data privacy, homomorphic encryption, neural network, Data classification, secure classification.

I. INTRODUCTION

The internet is a facility to share data and information. But the widespread data-breaches and privacy violations have worried businesses as well as the average person to utilize the full potential of internet. Among the potential utilizations, intelligent data classification is progressively increasing throughout. Such intelligent data classifications are made on data that is already stored on the internet or uploaded temporarily for the sake of classification. There are instances in which the data items which needs to be uploaded may contain sensitive and private information. Due to this sensitive nature, such data items are kept back, and their classification is avoided altogether from the fear of data-breaches and privacy violations.

On the internet, entities can store and host their data in their own datacenters or on a third-party server. Maintaining private datacenters are expensive for many businesses and individuals because it requires financial, hardware, software, and human resources. So instead of owning a private datacenter, it is an ideal case if data is stored and hosted-up on third-party datacenters but only after encryption, for which relatively small amounts of rent will be paid. In the same way, if the data is hosted in a private datacenter, it still needs to be encrypted due to security concerns.
In both the cases of storing and hosting our encrypted data on a third-party or our private premises, it needs to be processed later at some point. And since the data is encrypted now, we either have to fully decrypt it (either on third-party or our private premises) or use an intelligent way to process without decryption. The intelligent way of processing without decryption is to use the homomorphic encryption schemes.

To stress the need for adopting a privacy-preserving classification mechanism, [1] has provided convincing cases. There are cases where we need to know the existence of certain objects or people in an image. This is done using object or face-recognition neural networks matching the required data points from the image like the facial elements with that of people in an existing database.

In classifying malware network traffic, a combination of techniques including neural networks are used. When dealing with medical data, there are multiple scenarios in which we must provide access to doctors or hospitals to our personal health reports. This data can be in the form of medical imagery like X-rays or CT scans, or it can be the records of our medical prescriptions. The combination of all this data is already used by Google's DeepMind project [2] to assist doctors in curing their patients. For a financial institute or a business, it is desirable to analyze market trend and predict the future. This becomes very accurate when their internal data can be consolidated and compared with that of other players in the market.

This paper examines the integration of homomorphic encryption in the inference stage of a classification task in neural networks. More concretely, this paper examines the technical aspects in each of them and presents a set of issues regarding their integration. The paper then discusses the attempts to solve each of the issues. And after discussing the

attempts, the paper also provides a roadmap of work that needs to be done.

The organization of the paper is, in introduction need for privacy-preserving classification and its prominent areas has been discussed. In the next section important and interrelated concepts for each of the neural networks and the homomorphic encryption will be discussed independently. Issues in performing classification tasks on homomorphically encrypted data will be detailed in section 3. The followed section 4 will provide an account of what has already been explored. And the subsequent section 5 will provide a general guideline of what needs to be explored further.

II. BASIC CONCEPTS

A. *Neural Network*

A neural network is essentially a computational structure which is very good in finding the closeness of an unknown observation of data to already known patterns [3]. The reader may think of identifying a face from an image in which instead of comparing the pixel values for equality with a known image, the neural network match the pattern in the pixel values with an already analyzed pattern from previously seen images of the same face. These (artificial) neural networks are originally inspired by the way biological neural cells operate in our nervous system. Several abstractions from the biological neural cells have been adopted into the present computational neural networks which are necessary to discuss.

Neural networks basically are a combination of interconnected neurons processing input values through a function f and then transmitting the output to the next neuron.

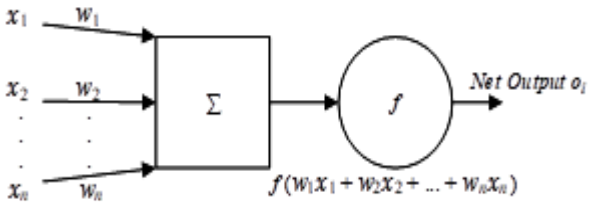

Fig. 1 An abstraction of a single neuron

The abstraction of a single neuron can be seen in Fig. 1. which shows n number of inputs shown by x_i. Each of these input connections to the neuron has an associated weight value shown by w_i. The incoming input x_i is multiplied by the corresponding weight w_i where both the values are expected to be real values. These incoming values obtained after multiplication are integrated at the neuron usually just by adding them all so that a net input is obtained. The net input (subjected to a threshold range) is then passed to the activation function f which triggers an output o_i.

B. *Homomorphic Encryption*

The aim of creating homomorphic encryption schemes is to perform arithmetic operations directly on the encrypted data. This exclusive property enables us to perform any arbitrary operations on the ciphertexts without the need of decryption. In the most recent homomorphic schemes, the supported arithmetic operations available are the addition and multiplication. Subtraction can be performed by negating the second number and adding to the first. The division operation however is not possible in a very straight forward way. In the same way, since comparison of two numbers is a logical task which is therefore also not straight forward.

In 2009, Gentry proposed the first fully homomorphic encryption (FHE) scheme [4]. An FHE scheme makes it possible to encrypt data and then carry out arbitrary computations on the encrypted data by operating on ciphertexts only without the need to decrypt the data first, and without knowledge of the secret decryption key. Prior to Gentry's work in 2009, PHE schemes showed how to compute a single type of homomorphic operation over the encrypted values. Among them, some did allow multiple types of operations but in a very limited way. Notable ones are shown against their supported type of encryption in Table 1 as follows:

Table 1: Partially Homomorphic Cryptosystems

PHE Cryptosystem	**Supported Homomorphic Encryption**
El Gamal [6]	Multiplicative
Paillier [7]	Additive
RSA [8]	Multiplicative
Goldwasser-Micali [9]	Additive, but it can encrypt only a single bit
Boneh-Goh-Nissim [10]	Unlimited number of additions but only one multiplication

As opposed to the recent Boolean circuit based evaluations, [5] discusses PHE schemes which have their plaintext messages and their corresponding ciphertexts contained in a related algebraic structure, often a group or a ring. This typically limits the function f to be an algebraic operation associated with the structure of the plaintexts. PHE schemes are more efficient than the later discussed SHE and FHE. Also, in such schemes it is not necessary to have a separate evk, the pk can be used in its place.

An example of SHE is the Brakerski, Gentry, and Vaikuntanathan (BGV) scheme [11] which bases its security on the Ring Learning With Errors (RLWE) problem. RLWE is considered to form a fundamental foundation for future public-key cryptography in a post-quantum computational world in which cryptanalysis of traditional problems, like integer factorization and discrete logarithm, will be much easier to solve. Although these schemes have no limit intrinsically on the manipulated ciphertext [5], the BGV showed that such schemes can be feasible to implement and adopt practically for relative efficiency and reasonably short ciphertexts [12]. SHE schemes also serve to build up later schemes like FHE and LHE, after modifications.

C. Related Work in Privacy-Preserving Classification

Several researchers have worked on preserving privacy of our data which includes adopting homomorphic encryption. In this regards, researchers have tried techniques like the differential privacy [14] and [16]. But the wider adoption of homomorphic encryption in neural networks is yet to come by developing more user-friendly code libraries and toolsets. However, several works exist to integrate HE with NN.

A recent implementation using FHE for classification tasks was presented by Bost et al. [1] in their library integrating building blocks for construction of classifiers. Their work consists of a set of protocols using homomorphic encryption and MPC through which they built three major classifiers i.e. Hyperplane Decisions, Naïve Bayes, and Decision trees. Their protocols, however, are only designed to accommodate two parties; the cloud with the classifiers and the client with the data. In such a scenario, the client needs to establish a continuous connection and participate in the computation process of the classifier with a constant connection.

Orlandi et al. [17] also explored the evaluation of a neural network by obscurity of the weights and the data transfer through homomorphic encryption among multiple parties, in which, they are leaking much of the information of weights of the network to the other party.

Another recent development by Dowlin et al. [18] introduces CryptoNets which demonstrates a levelled homomorphic encryption scheme applied in the execution of a trained NN. In their work the authors applied the levelled-homomorphic encryption scheme of Bos et al. [19], inspired by the original fully homomorphic encryption scheme suggested by Gentry [13]. Their method is applied to the 28×28 images of handwritten digits from Mixed National Institute of Standards and Technology (MNIST) dataset [20]. In their work, they avoided the heavy bootstrapping method of re-encryption in the original scheme and instead, they estimated the number of operations required in computing any arbitrary function homomorphically over encrypted data without the loss of accuracy in the final decrypted result.

D. Available Implementations

Practical implementations of PHE are common. A simple search on GitHub for "paillier" re-turned more than 90 results for repositories of project source codes in languages like Java, Py-thon, C, JavaScript etc. Similar was the case for other PHE schemes like "elgamal" which re-turned 161 repositories in various languages.

On the other hand, most of the FHE are of theoretical nature and exist only on paper today. Only two major implementations of FHE exists which are: Halevi and Shoup's HElib [21]; and Microsoft's SEAL [22].

HElib is an implementation of the HE schemes by Brakerski, Gentry, and Vaikuntanathan (BGV) [11], in which the library uses several optimizations like the ciphertext packing tech-niques for single instruction, multiple data (SIMD) [23] and the bootstrapping for FHE as de-tailed in [24]. Currently the HElib is meant for researchers working on HE having very low-level routines (e.g. shift, add, mul, etc) which are considered as the assembly language for HE. It is written in C++ and uses the NTL mathematical library often used with the GNU Multi-Precision library (GMP) for faster multiplications.

The Simple Encrypted Arithmetic Library (SEAL) is an implementation of the HE schemes by Fan and Vercauteren (FV) [25], in which, the security is again based on the Ring Learning With Errors (RLWE) problem like the BGV. RLWE is considered very strong, and the ciphertext size noise growth properties are claimed to be better mainly due to a smaller secret key size and secu-rity parameters.

A notable optimization library using CUDA GPU acceleration for SWH is the cuHE [26]. It is designed to boost homomorphic encryption schemes such as the BGV [11], López, Tromer, and Vaikuntanathan (LTV) [27] and Doröz, Hu, and Sunar (DHS) [28] by taking the advantage of the greater parallel computing power and high memory bandwidth offered by GPUs. It also takes advantage of an efficient implementation of the bootstrapping algorithm of [29] making it an ideal support for our work.

III. ISSUES IN PRIVACY-PRESERVING CLASSIFICATION

The classification task can be listed down as a set of arithmetic operations along with a few modifications to the neural network. In view of the discussion above, the following issues needs to be solved to achieve privacy-preserving classification:

A. Evaluating Activation Function

The crucial part in evaluating a single neuron is the evaluation of the activation function by using only the multiplication and the addition operations. This is problematic when we do not have support for the division operator.

Functions such as those presented in section 2.1. However, can be approximated by polynomial expressions using integer values, and do not necessarily need to be expressed in a bitwise manner. Some of the more efficient FHE schemes allow to encrypt polynomials that can encode such integer values. The advantage of this approach is that a single ciphertext now contains much more information than just a single bit of plaintext but restricts the possible operations to arithmetic circuits in these polynomials. Furthermore, these functions are often simple enough such that the expensive bootstrapping procedure can be avoided. Evaluating functions like the logistic sigmoid requires us to approximate it using Taylor series. This is because in the original equation we cannot raise the value of e (see equation 1) to an encrypted number x. So, the normal polynomial terms from McLaurin series (i.e. a case of Taylor series in the region near $x = 0$) for approximating the logistic sigmoid (shown in equation 1) are stated as:

$$f(x) = \frac{1}{2} + \frac{1}{4}x - \frac{1}{48}x^3 + \frac{1}{480}x^5 - \frac{17}{80640}x^7 + \frac{31}{1451520}x^9 - \cdots \quad (1)$$

The more the number of terms we use to approximate the function the more accurate will be the result, but more computational power will be needed.

B. Interpreting the Final Result

The output values from the neurons in the last layer are the confidence values of the network. These output neurons and their values correspond to the various classes it can predict about. Normally the last layer uses the softmax activation function which provides all the values in probabilities for each class. However, the probabilities are just a representational form to help in the understanding of the output.

Since homomorphic encryption cannot evaluate the softmax function and even if it is done then it will add further overhead. And because the output values represent the confidence of the network for each class, therefore for now, we can take the max of all the encrypted values and will know the predicted class. Several ways exist to find the max value for the encrypted results, it can be either of the following:

- Get the max in the binarized form of the encrypted result
- Send the values to the client to decrypt and get the result against each class.
- Use a multiparty computation protocol to find the maximum of the values.

C. Dual-Cloud Based Approach

A different approach of using non-colluding dual-cloud in evaluating a privacy-preserving neural network was given in [30]. The given approach worked by segregating the activation function to a second cloud in such a way that it will be computed in plaintext, whereas the first cloud hosts the weights and the topology of the neural network. The first cloud receives encrypted inputs from the client by using Paillier Cryptosystem which is an additively homomorphic scheme. The non-colluding nature of the two clouds and the computation mechanism of the neural network provides results after preserving the privacy of the client input data. Such a setup is very good in obtaining classification results without compromising on privacy, however the results will show that it is relatively slower.

The notable insight for the implementation was about the overall computing time of the neural network against different encryption key lengths as shown in Fig: 2. For this experiment Mixed National Institute of Standards and Technology (MNIST) [20] dataset was used having handwritten digits for the classification task. The dataset that was chosen contains digits in the form of labels along with pictorial images for training and 10,000 for testing and alike applications used in the studies [31] and [32]

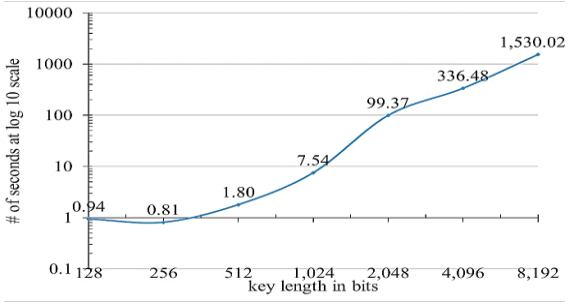

Fig. 2 Total Roundtrip Time until classification results against different key length

IV. FUTURE DIRECTION

Integrating homomorphic encryption within neural network classification faces two main hurdles. They are the hurdle of evaluating the classification result through limited support of operators and using integers, and the hurdle of heavy computation required due to homomorphic encryption.

For the purpose of evaluating the classification in a constrained environment, other activation functions like the Softsign activation function shown in equation 4 below:

$$f(x) = \frac{x}{1+|x|} \quad (2)$$

This function will not require us to approximate as like the logistic sigmoid. But we still need to solve two hurdles: the division operation; and possible negative numerator which is not supported in homomorphic encryption. if we are able to solve them then we will see a significant increase in the performance.

Since the homomorphic encryption is inherently slow, GPU-Based computation needs exploration for optimizing the homomorphic operations within a neural network. For this purpose we can use the software library of [26].
Recently introduced Binarized Neural Networks (BNNs) are also viable options if we can support or accommodate negative values. These networks are shown to be very efficient as they work by constraining the weights and activation functions to be either $\{0, 1\}$ or $\{-1, 1\}$. They actually reduce the computational complexity by using single bit exclusive-not-or (XNOR). The proposed approach of this study will be carried out for the studies [33 - 35].

V. CONCLUSION

Performing computation on encrypted data is termed as the holy grail of cryptography. In today's service-oriented nature of the internet, we have very mature neural networks that can help us in knowing about our data by classifying it to known classes. We discuss the integration of these two exceptional technologies together and get a resultant platform where we can be sure of the privacy of our data and still get valuable insight from it. This paper discusses the issues and gaps for privacy-preserving classification networks and suggests possible solutions in terms of implementation and practical adoption. In future, the proposed approach of this study will be carryout for [31] and [32].

REFERENCES

[1] Bost, R., Popa, R. A., Tu, S., & Goldwasser, S. (2014). Machine learning classification over encrypted data. Cryptology ePrint Archive.

[2] Hodson, H. (2016). Revealed: Google AI has access to huge haul of NHS patient data. New scientist, 29.

[3] Rojas, R. (2013). Neural networks: a systematic introduction. Springer Science & Business Media.

[4] Rivest, R. L., Adleman, L., & Dertouzos, M. L. (1978). On data

banks and privacy homomorphisms. Foundations of secure computation, 4(11), 169-180.

[5] Armknecht, F., Boyd, C., Carr, C., Gjøsteen, K., Jäschke, A., Reuter, C. A., & Strand, M. (2015). A guide to fully homomorphic encryption. Cryptology ePrint Archive.

[6] ElGamal, T. (1985). A public key cryptosystem and a signature scheme based on discrete logarithms. IEEE transactions on information theory, 31(4), 469-472.

[7] Paillier, P. (1999, May). Public-key cryptosystems based on composite degree residuosity classes. In International conference on the theory and applications of cryptographic techniques (pp. 223-238). Springer, Berlin, Heidelberg.

[8] Rivest, R. L., Shamir, A., & Adleman, L. (1983). A method for obtaining digital signatures and public-key cryptosystems. Communications of the ACM, 26(1), 96-99.

[9] Peng, K., Boyd, C., & Dawson, E. (2005, September). A multiplicative homomorphic sealed-bid auction based on Goldwasser-Micali encryption. In International Conference on Information Security (pp. 374-388). Springer, Berlin, Heidelberg.

[10] Boneh, D., Goh, E. J., & Nissim, K. (2005). Evaluating 2-DNF formulas on ciphertexts. ts. Theory of Cryptography: Proceedings of the 2nd Theory of Cryptology Conference (TCC'05), Feb 10− 12, 2005, Cambridge, MA, USA. LNCS 3378.

[11] Brakerski, Z., Gentry, C., & Vaikuntanathan, V. (2014). (Leveled) fully homomorphic encryption without bootstrapping. ACM Transactions on Computation Theory (TOCT), 6(3), 1-36.

[12] Cheon, J. H., Han, K., Kim, A., Kim, M., & Song, Y. (2018, August). A full RNS variant of approximate homomorphic encryption. In International Conference on Selected Areas in Cryptography (pp. 347-368). Springer, Cham.

[13] Chaudhary, P., Gupta, R., Singh, A., & Majumder, P. (2019, September). Analysis and comparison of various fully homomorphic encryption techniques. In 2019 International Conference on Computing, Power and Communication Technologies (GUCON) (pp. 58-62). IEEE.

[14] Yousuf, H., Lahzi, M., Salloum, S. A., & Shaalan, K. (2021). Systematic review on fully homomorphic encryption scheme and its application. Recent Advances in Intelligent Systems and Smart Applications, 537-551.

[15] Bazai, S. U., Jang-Jaccard, J., & Zhang, X. (2019). Scalable big data privacy with MapReduce. In Encyclopedia of big data technologies (pp. 1454-1462). Springer, Springer Nature..

[16] Bazai, S. U., Jang-Jaccard, J., & Zhang, X. (2017, July). A privacy preserving platform for MapReduce. In International Conference on Applications and Techniques in Information Security (pp. 88-99). Springer, Singapore.

[17] Orlandi, C., Piva, A., Barni, M.: Oblivious neural network computing via homomorphic encryption. Eurasip Journal on Information Security. 2007, (2007).

[18] Gilad-Bachrach, R., Dowlin, N., & Laine, K. Applying neural networks to encrypted data with high throughput and accuracy. In Proceedings of the International Conference on Machine Learning (pp. 201-210).

[19] Tan, W., Case, B. M., Hu, G., Gao, S., & Lao, Y. (2021). An ultra-highly parallel polynomial multiplier for the bootstrapping algorithm in a fully homomorphic encryption scheme. Journal of Signal Processing Systems, 93(6), 643-656.

[20] LeCun, Y., Cortes, C., Burges, C.J.C.: The MNIST database of handwritten digits, http://yann.lecun.com/exdb/mnist/.

[21] Halevi, S.: HElib - an implementation of homomorphic encryption, http://shaih.github.io/HElib/.

[22] Chen, H., Laine, K., & Player, R. (2017, April). Simple encrypted arithmetic library-SEAL v2. 1. In International conference on financial cryptography and data security (pp. 3-18). Springer, Cham.

[23] Smart, N., & Vercauteren, F. (2011). Fully homomorphic SIMD operations, cryptology ePrint archive. Report, 133, 2011.

[24] Halevi, S., & Shoup, V. (2021). Bootstrapping for helib. Journal of Cryptology, 34(1), 1-44.

[25] Migliore, V., Bonnoron, G., & Fontaine, C. (2018). Practical Parameters for Somewhat Homomorphic Encryption Schemes on Binary Circuits. IEEE Transactions on Computers, 67(11), 1550-1560.

[26] Mert, A. C., Öztürk, E., & Savaş, E. (2019). Design and implementation of encryption/decryption architectures for BFV homomorphic encryption scheme. IEEE Transactions on Very Large Scale Integration (VLSI) Systems, 28(2), 353-362.

[27] Yousuf, H., Lahzi, M., Salloum, S. A., & Shaalan, K. (2021). Systematic review on fully homomorphic encryption scheme and its application. Recent Advances in Intelligent Systems and Smart Applications, 537-551.

[28] Akavia, A., Oren, N., Sapir, B., & Vald, M. (2022). Compact storage for homomorphic encryption. Cryptology ePrint Archive.

[29] Pereira, H. V. L. (2021, May). Bootstrapping fully homomorphic encryption over the integers in less than one second. In IACR International Conference on Public-Key Cryptography (pp. 331-359). Springer, Cham.

[30] Baryalai, M., Jang-Jaccard, J., & Liu, D. (2016, December). Towards privacy-preserving classification in neural networks. In 2016 14th annual conference on privacy, security and trust (PST) (pp. 392-399). IEEE.

[31] Topbaş, A., Jamil, A., Hameed, A. A., Ali, S. M., Bazai, S., & Shah, S. A. (2021, October). Sentiment analysis for COVID-19 tweets using recurrent neural network (RNN) and bidirectional encoder representations (BERT) models. In 2021 International Conference on Computing, Electronic and Electrical Engineering (ICE Cube) (pp. 1-6). IEEE.

[32] Hameed, M., Yang, F., Bazai, S. U., Ghafoor, M. I., Alshehri, A., Khan, I., ... & Jaskani, F. H. (2022). Urbanization detection using lidar-based remote sensing images of Azad Kashmir using novel 3D CNNs. *Journal of Sensors*, *2022*, 1-9.

[33] Bazai, S. U., Jang-Jaccard, J., & Alavizadeh, H. (2021). A novel hybrid approach for multi-dimensional data anonymization for Apache spark. ACM Transactions on Privacy and Security, 25(1), 1-25.

[34] Bazai, S. U., Jang-Jaccard, J., & Alavizadeh, H. (2021). Scalable, high-performance, and generalized subtree data anonymization approach for Apache Spark. Electronics, 10(5), 589.

[35] Bazai, S. U., & Jang-Jaccard, J. (2020). In-memory data anonymization using scalable and high performance RDD design. Electronics, 9(10), 1732.

Balochistan Journal of Engineering & Applied Sciences (BJEAS) – (p-ISSN: 2518-2706
Volume 6, No.1

Performance Evaluation of Modified Iot Based Smart Irrigation System Installed At LUAWMS Experimental Olive Farm, Sukan

Sumaiya[1], Kashif Saghar[2], Tamoor Khan[1], Hafsa[1] Shahab Ud Din[2]
[1]Lasbela University of Agriculture, Water and Marine Sciences, Uthal
[2]Alhamd Islamic University Quetta.
Corresponding Author: sumaiyahanif1999@gmail.com

***Abstract*— Pakistan GDP directly depends on agriculture sectors. Scarcity of water and climate changes are the most important factors that severely effect the productivity of Agri-crops. Cultivable land in the country is more extensive but water reservoirs and other resources are very limited, smart agriculture may be more sustainable in these areas. Smart agriculture with integration of IoT and IoT based innovative ideas would bring a dynamic change in farming system of the country. Proposed research was design for bringing innovative change in typical IoT based Smart farming system, Therefore current research has been designed to improve traditional farming system with more intelligent IoT system. The performance of modified IoT based system was compared with manually operated Smart Irrigation System. The results showed that Maximum plant length of 40.90inches was recorded in the plants irrigated by modified IoT based irrigation system. Maximum root length of 8inches was recorded in plants irrigated by Internet of things (IoT) based SIS followed by Modified IoT based SIS with root length of 7.5 inches. Furthermore, The results revealed in this research showed that modified IoT based SIS used minimum level of water . The water used efficiency was 1.93 gallons, where as maximum water use 8.07 gallons were recorded in manually operated smart irrigation system. Furthermore the energy use was also minimum of 4amp by the plants of modified IoT based smart irrigation system. The energy use was minimum at 10.67amp by the plants irrigated by manually operated smart irrigation system. The recorded minimum cost effect were Rs. 153.33 in the plants irrigated by modified IoT based SIS during 6th month and maximum cost effect of Rs, 521.33 were recorded in plants irrigated by manually operated smart irrigation system.**

I. INTRODUCTION

The increased world population required high production of commodities to full fill demand of food in all sectors of life, particularly in agriculture where demand and supply are still not matching. Managing capital and labor is still a required challenge for maximizing productions of agricultural sector. High efficiency irrigation evolvement in smart agriculture farming provides a better solution for matching supply and demand chain, resource management and labor. Agriculture sector in Pakistan contributes a major source of income and more than 70% people depending for their lives to this sector. Agriculture provides 25% of GDP. The irrigation systems in Pakistan are operated manually by using traditional methods like flood and furrow irrigation etc. However in few areas these traditional techniques have replaced with smart irrigation system such as High efficiency irrigation systems (HEIS) like, drip , bubbler and sprinkler irrigation [7]. IoT refers to a latest technology which integrates different devices automation for the real time data evaluation being collected through various devices [6]. The accuracy and capabilities of collected data have increased significantly with the integration of the system. According to needs, various types of sensors could be employed for the data collection procedure. The collected data can be analyzed through the application of Data Science (DS). Data Sciene is an approach which make it possible to use predictive and prescriptive analysis to get beneficial information. [11].

Province of Baluchistan possesses five agro ecological zones. All types of Agricultural crops can be grown successfully in different pockets of the area. Majority of areas of province have irrigated by rains only few areas of Naseerabad division have irrigated by Indus River. No doubt, the cultivable land is more extensive but water reservoirs are very limited, smart agriculture may be more sustainable in these areas. Smart agriculture with efficient use of limited water not only provides much production under low water usage but it is also manageable by few labors. Integration and upgradation of formal IoT devices along with the help of cloud management system and units of their security for smart irrigation system would bring a dynamic change in farming system remote areas.[5]. Integration with high technology (IoT) with the farming practices would be better solution for high production within the limited resources. This would be based purely on the quantities approaches and statistical line which may bring best revolutionary changes in the traditional agriculture system of the area [1]. It is therefore has been planned to design an innovative intensive IoT system with inclusion of all required sensors and observatory devices (Camera) for intensive utilization of available resources. This research has been planned to integrate traditional farming system with more intelligent modified IoT system. The main objective of my work was to develop a self-operated irrigation system which would be economical and time saving by using Node based microcontroller modified with additional devices like, growth recording camera, environmental monitoring sensors for intensive utilization of water and growth performance. The modified IoT based system have integrated with smart irrigation system at LUAWMS olive farm, Sukkan for its performance evaluation.

II. RESEARCH METHOLODY

A. Research Design

This experiment was carried out on Olive experimental farm of Lasbela University of Agriculture, Water and Marine Sciences, Uthal during the year 2022-23. The selected olive plants were used for this experiment. There were two parallel functional components in this proposal**.** The IoT based (IoT Based and Modified IoT) system and the smart irrigation system (SIS

B. Data Collection & Variables of Study

B.A Comparison of efficiency of manually operated, IoT based and modified IoT based SIS

For evaluation of efficiency of modified IoT based SIS with Manually operated SIS and IoT based SIS following data were recorded. The recorded data were Agronomical (growth performance) data , water use efficiency, energy use efficiency and cost effect of subjected plants from the systems installed areas, The obtained data from three systems were compared with each other by using standard procedures for efficiency assessment. The o data were further analyzed statistically for significant effect of variances.

C. Installation and integration of IoT devices

IDE software (Integrated Development Environment), Arduino for writing the programme were used. Six moisture sensor were used for monitoring of moisture level of six olive plants. Humidity sensors were installed among the selected plants of IoT based and Modified Iot based system. Three weather/temperature sensors were used in the root zones of selected plants for Modified IoT system. For monitoring of plant, growth three growth-recording cameras have installed to focus and observe the growth of selected plants of modified IoT system. For each system the first olive plant were treated as replication one (R1), Plant two as R2 and plant three as R3. For recording of water consumption by the plants of each system three consumption meters were used. For energy use efficiency ampere meters were used. For integration of devices Node MCU (ESP8266) Wi-Fi Module were used.

Figure**.** Node MCU

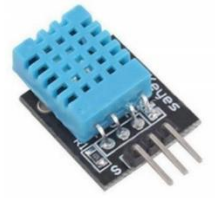

Figure**.** Digital temperature and

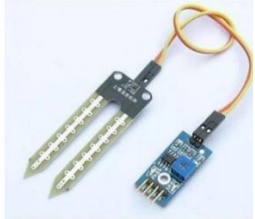

Fig. Moisture sensor humidity sensor

Fig. Growth monitoring camera

D. Installation of smart irrigation system and maintaining of water level in selected plants

Already installed Trickle irrigation system have used for integration of Iot based systems. The smart irrigation system were included with following components. Auto-controlled valves were used to maintain water requirement of all three systems. The source, main supply lines, sub-main lines, lateral lines and water emitters were used for every system. Each plant has watered with two pairs of paralleled emitters. They supply of water was uncontrolled with determine need in plants of manually operated system, where as in plants of IoT based system supply of water was controlled with controlled valves according to need on the basis of received information by moisture, humidity sensors. The supply of water was intensively controlled in plants of modified IoT system; it was completely based upon received information for installed sensors and growth recording cameras.

VI. EXPERIMENTS AND RESULT

Agriculture sector play's an important role in the economic development of a country. It contributes major part in GDP of the country like Pakistan. Scarcity of water and climate change are the most important factors that severely affect the productivity of agri-crops. In order to improve production and reduce production related factors, particularly for intensive management of limited water resources in the farming system of the area evolvement of intelligent agriculture with integration of innovative IoT (Internet of Things) are essential. In this regard, various innovative changes have made by various technologist in the field of IoT. The purpose of these innovative up gradations were to utilize limited Agri-Resources efficiently and intensively. Therefore the proposed research work was also designed to bring innovative modification in already available IoT based SIS particularly for olive plants. Further the objective of this research work was to design a system (modified IoT), which would be more effective and cost efficient as compared to already available system, In this regarded proposed system were designed initially for olive plants.

A. Description of experiment

Smart irrigation system.

The main components of installed Smart Irrigation System were, a source (Tube well), main supply unit, water consumption meter, main supply lines, sub-main supply lines, control valves, air vents, grommet take off, lateral lines and emitters (two pairs of emitter for each plant). The supply of irrigation water were managed by manually. The water need of plants were assess by visually observation basis. Thus the supply of water in this system was irregular and uncontrolled.


Fig. Author with main supply line

Fig. Controll valve

Fig. Lateral Lines

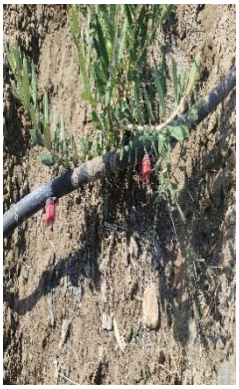

Fig. Emmetter

A. B. Modified IoT Based Smart Irrigation System

This was the actual designed work. The main objective of this research work was to develop and bring innovative change in typical IoT based SIS. Further, it was aimed to develop a system, which would be more efficient under low water consumption at intensive level, would also be low energy consuming and low cast as compared to other available systems. With this concept, typical IoT based system was modified with addition of soil temperature sensors and growth recording cameras. Purpose of Inclusion of soil temperature sensor was to monitor one of the core factor of plant growth and water holding capacity of soil, further this effect directly on plant growth and yield. Inclusion of growth recording camera was to monitor the growth of plant because the water use consumption is directly proportional to plant growth, in typical IoT based SIS, both these factor were ignored for monitoring and data collection. There were also two parts of this system, first designed smart irrigation water system and modified IoT system The smart irrigation system included a main source (Water Tank) for ensuring the continuous supply of irrigation according to need as per required time. The supply of irrigation water were ensured with main supply and sub-main and lateral lines. The main supply line were included with a automatic control valve operated by IoT system. A water consumption meter for measuring consumption of water daily and monthly basis, an air vent was also installed with main line for removing of air bubbles to save blockage of water flow. Whereas other part included IoT system. This system included various sensors, such as soil humidity sensor, soil moisture sensor, and environmental weather sensor. Soil temperature sensor and growth recording camera. IDE software (Integrated Development Environment), Arduino for writing the programme were used. For integration of devices Node MCU (ESP8266) Wi-Fi Module were used.

Fig. Main supply Tank

Fig. Water consumption meter

Fig. Moisture, Humidity Temperature. Weather sensors, camera

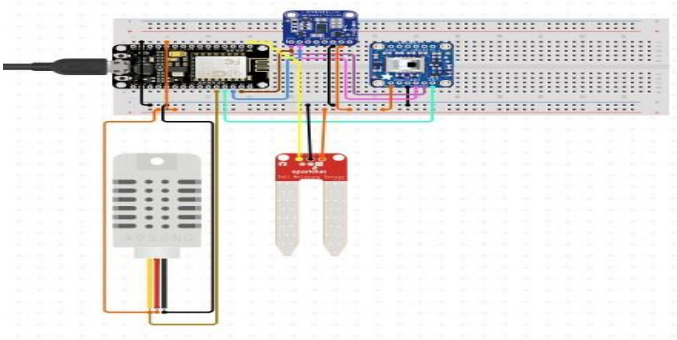

Fig. Circuit Diagrammed of the research

RESULTS

Three identical smart irrigation systems i.e. manually operated SIS, typical IoT based SIS and proposed modified IoT based SIS have installed at LUAWMS, olive farm, Sukan. The comparison of performance were evaluated on the basis of following parameters;

A. Growth performance among olive plants irrigated by three types of Smart irrigation systems

Table: Comparison of Olive growth performance irrigated by three systems

Parameters	Manually operated	IoT Based	Modified IoT Based	STD
Total Length	33.23bc	38.40c	40.90d	3.91

Root length	7.00a	8.00a	7.50a	0.50
Canopy of plant	11.50a	12.13b	12.00b	0.33
Big Branch	26.67b	11.67b	24.33c	8.07
Small Branch	52.33c	37.00c	112.33f	39.81
Leaf Small Branch	72.33d	151.00e	175.33g	53.84
Leaf Big Branch	22.33ab	46.67d	57.67e	18.08
LSD	**24.55**	**4.44**	**3.48**	

The growth performance among olive plants irrigated by three SIS has been depicted in Table 4.2. Significant differences were found among all three systems. The results showed maximum increase in all agronomic parameters of plant growth by the Modified IoT based SIS, whereas minimum growth performance were recorded in plants irrigated by manually operated SIS. Maximum plant length was reported in the plants irrigated by modified IoT based irrigation system i,e. 40.90 inches followed by IoT based SIS (30.40 inches) and Manually operated SIS (33. 23 inches). Maximum root length was recorded in plants irrigated by IoT based SIS i.e. 8 inches which were followed by Modified IoT based SIS (7.5 inches) and manually operated SIS (7 inches). Respectively, the maximum plant canopy of 12.13inches dia were recorded in plants irrigated by IoT based SIS, this is followed by 12 inches dia in plants irrigated by modified IoT based SIS and 11.5 inches dia in plants irrigated by manually operated smart irrigation system, Maximum number of small and big branches were exhibited by the plants irrigated by modified IoT based SIS i.e. 24 and 112, followed by plants irrigated by manually operated SIS were of 26 &52 and plants irrigated by IoT based SIS were of 11 and 37. Maximum number of leaves in small and big branches were recorded in plants irrigated by modified IoT based SIS i.e. 175 and 57, followed by plants irrigated by IoT based SIS were of 151 & 46 and plants irrigated by manually operated SIS were of 72 and 22 respectively.

The overall performance showed by these result were exhibited by the Plants irrigated by Modified IoT based SIS the obtained results are quite resembled to the results reported by [5]. The statistical analysis were also showed significant in variances. The bar chart also showing significant growth increase in plants irrigated by modified IoT based SIS.

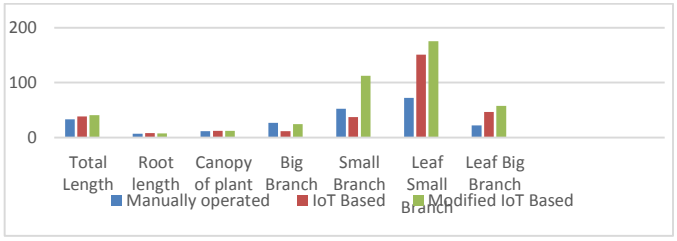

Fig. Bar Chart showing Olive growth performance irrigated by three systems

B. Water use efficiency in the olive plants among all three types of smart irrigation systems

Table: Comparison of Olive water use efficiency (glns) irrigated by three stems

Days	Manually operated	IoT Based	Modified IoT Based	STD
15 Days	7.17a	3.50a	2.20a	2.58
30 Days	7.17a	3.90a	3.17c	2.13
45 Days	7.00a	5.17c	2.10a	2.48
60 Days	8.07b	4.83b	2.27b	2.91
75 Days	7.00a	5.27c	2.40b	2.32
90 Days	7.43a	5.67c	1.93a	2.81
105 days	7.07b	4.27b	2.77b	2.18
LSD	**1.36**	**1.07**	**0.95**	

The comparison of water use efficiency by the plants among all three systems has been depicted Table-4.2. The overall results showed maximum water used efficiency during all 105 days, by the plants irrigated through manually operated SIS and minimum water use efficacy during all 105 days, were recorded in the plants irrigated by the modified IoT based SIS. The use of water by the olive plants irrigated through IoT based SIS were quit more than modified IoT based SIS and less than Manually operated SIS. The results revealed in this research showed that modified IoT based SIS used water at minimum and intensive levels. Maximum water use efficiency was recorded in the plants during the 60th day irrigated by manually operated SIS. The water use efficiency was 8.7 gallons, whereas minimum water use efficiency was recorded in plants during 90th days, irrigated through modified IoT based SIS. The water used efficiency was 1.93 gallons. Result of this research are comparatively better than the result reported by [12]. The results are also statistically significant. Same result can be seen in bar chart.

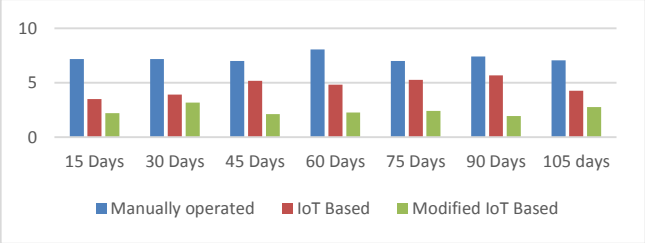

Fig. Bar Chart showing Water use efficiency (glns) for all three systems

C. Eight months energy use efficiency among all threes smart irrigation systems

Table: Comparison of Eight months energy use efficiency among all threes systems

Month	Manually operated	IoT Based	Modified IoT Based	STD
1st month	10.33ab	6.33b	4.67b	2.91
2nd month	11.00b	5.67a	5.00c	3.29
3rd month	11.00b	7.33c	4.00b	3.50
4th month	11.33c	6.67b	4.33b	3.56
5th month	11.00b	7.33c	4.00b	3.50
6th month	11.00b	7.00c	4.67b	3.20
7th month	10.67b	6.33b	3.67a	3.53
8th month	9.67a	5.67a	3.33a	3.21
LSD	**1.23**	**1.35s**	**1.30**	

The comparison of eight months energy use efficiency by the plants among all three systems has been depicted Table-4.3. The results revealed in this research showed maximum energy used to the plants irrigated by manually operated SIS. Whereas minimum energy was used by the plants irrigated by modified IoT based SIS. This showed that proposed (designed) system were more efficient in use of energy at minimum intensive levels. The results of this research are more significant than results recorded by [14], [8] and various other technologists. Maximum used energy was recorded in the plants irrigated by manually operated SIS.

During 7th month at 10.67 amperes. And minimum energy was used by the plants irrigated by modified IoT based SIS. The used energy was 4.00 amperes during 5th month. All variances of energy used efficiency between each system was statistically significant at probability level less than 0.05%. Efficient results by plant of modified IoT based SIS can be seen in bar chart.

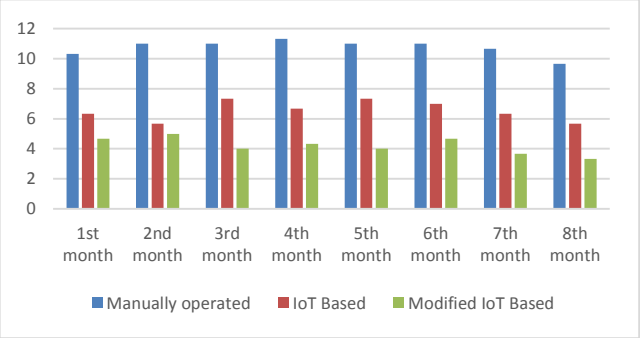

Fig. Bar Chart showing Eight months energy use efficiency for all three systems

D. Eight months cost effect for all three types of smart irrigation system.

Table: Comparison of Eight months cost effect (RS) for all three systems

Month	Manually operated	IoT Based	Modified IoT Based	STD
1st month	475.33	291.33	214.67	133.96
2nd month	506.00	260.67	230.00	151.27
3rd month	506.00	337.33	184.00	161.06
4st month	521.33	306.67	199.33	163.95
5st month	506.00	337.33	184.00	161.06
6st month	506.00	322.00	214.67	147.34
7st month	490.67	291.33	168.67	162.51
8st month	444.67	260.67	153.33	147.34
LSD	56.62	62.15	59.935	

Comparison of eight month cost effect among manually operated SIS, IoT based SIS and Modified IoT based SIS has been depicted in Table-4.4. The results showed that minimum cost effect were recorded by the plants irrigated through modified IoT based SIS, whereas maximum cost effect were shown by plants irrigated through manually operated SIS. The recorded minimum cost effect were Rs. 153.33 in the plants irrigated by modified IoT based SIS during 6th month. Maximum recorded cost effect was Rs 521 shown in plants irrigated by manually operated SIS during 4th month of experiment. Upon comparison the overall low cost effect were recorded by plants irrigated through modified IoT based SIS, the recorded cost from first month to eight months were Rs. 230-153.33, this was followed by Plants irrigated through IoT Based SIS the cost effect ranges were Rs 337.33-260.67. Maximum cost effect was recorded in plants irrigated by manually operated SIS with a range of cost effects from Rs. 521.33 to 444.67. The result showed that modified IoT based SIS preformed at lowest cost during same period this showed that proposed system is more efficient as compared other two systems. Same results were reported by [7]. The variances of the result are significant at probability level of less than 0.05%. The bar chart also expressed minimum efficient cost effect by plants of modified IoT based smart irrigation system.

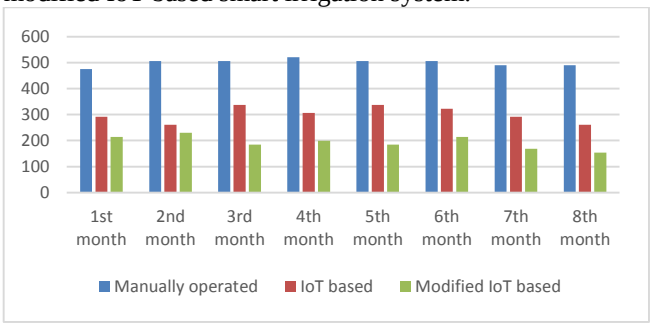

Fig-4.14. Bar Chart showing Eight months cost effect for all three system

VII. CONCLUSION AND RECOMMENDATIONS

A. Conclusion

The increased world population required high production of commodities to full fill demand of food in all sectors of life. Particularly in agriculture where demand and supply are not still matching. Agriculture sector play's an important role in the economic development of a country. Pakistan GDP directly depends agriculture. Scarcity of water and climate change are the most important factors. In order to improve production and reduce production related factor particularly intensive management of limited water resources in the farming system of the area evolvement of smart and efficient agriculture with integration of innovative IoT (Internet of things) is needed. In this regard various innovative changes have made by various technologist in the field of IoT. The purpose of current work was also an effort to bring innovative change in Traditional and typical IoT based SIS. The main objective of current research was to design a modified IoT based Smart irrigation system which would be more efficient, cost effective and resource saving. Hence proposed system were designed by inclusion of all possible data recording and monitoring devices for intensive utilization of available resources. Designed system were also compared with manually operated smart irrigation system and typical IoT based SIS for performance evaluation. In this regard following performance data (Plant Growth performance, Water use efficiency, Energy use efficiency and cost effect) were recorded for analysis. The result revealed in this research showed that maximum increase in all agronomic parameter of plant growth were seen in plants irrigated by the Modified Internet of Thing based SIS followed by Internet of Thing based SIS, whereas minimum growth performance were recorded in plants irrigated by manually operated smart irrigation system. The typical IoT based SIS also showed significant results as compared manually operated smart irrigation system. Hence, results in this research showed intensive level of water use efficiency by the plants irrigated through modified IoT based SIS. Furthermore, the energy use efficiency and cost effect were also minimum of plants irrigated by modified IoT based SIS, Maximum energy use efficiency and cost effect were showed by the plants irrigated through manually operated SIS, the energy use efficiency and cost effect were also significant of plants irrigated by IoT based SIS as compared to plants

irrigated by manually operated SIS. On the basis of overall results recorded by present research it is concluded that modified IoT based ANOVA for Eight months cost effect for modified IoT based SIS preformed more efficient as compared to two other systems both in best plant growth under lees resources use. This became possible due to intensive plant growth, environment and soil health monitoring devices. The plants irrigated by modified IoT based ANOVA for Eight months cost effect for modified IoT based SIS performed best under intensive utilization of resources. Concluding the Modified IoT based smart irrigation is more fit and most suitable for Olive crops to save water, energy and labor cost.

B. Recommendations

On the basis of revealed results of current research, Modified IoT based ANOVA for Eight months cost effect for modified IoT based SIS performed best under less resources utilization. The resources in Baluchistan province are quite limited for agriculture. For efficient utilization of limited resources at intensive level current designed is need of time. Therefore it is recommended that Modified IoT based ANOVA for Eight months cost effect for modified IoT based SIS can be successfully practiced in other crops orchard like, Chickoo, Apple, Pomegranate, Almond, Pistachaio etc, implementation of this type of system in said orchards will performed best under low water and energy use. The farming in such areas will also be cost effective.

REFERENCES

[1] Aakash, B., Parachi, B and Aakash R, (2021) "Research Article on Smart Irrigation System using IOT" *Int. Jr. for Res. in App. Science & Engineering Tech.* 9(12): 96-98.

[2] Abdulla K. (2019) "IoT-based Intelligent Irrigation Control System" *A Thesis submitted to German University carioc*. A net reference from www.reasearchgate.net.

[3] Anitha N. S., Sampath M. and Asha J. (2020) "Smart Irrigation system using Internet of Things" Sch .of. Inf. Tech. Eng. Vell. Inst. of. Tech, Tam. Nad. Ind. pp:1-7.

[4] Anonymous, (2020), "Agriculture statistic of Balochistan, 2019-20" Statistical department, Agri. Exten. Wing Baluy. pp: 278-79.

[5] Dankan G., Sandeep P., Ramesha. M., Jayashree M. and Ansuman S. (2021) "Smart Agriculture and Smart Farming using IoT Technology" *Journal of Physics,conference series.* pp:2089.

[6] Doukas C. (2012), "Building Internet of Things with the ARDUINO" CreateSpace Independent Publishing Platform USA. pp:200-221.

[7] Hemalatha R., Deepika G., Dhanalakshmi D., Dharanipriya K. and Divya M. (2016) "Internet of things (Iot) based smart irrigation" *Int. Jr. of Advanced Res. in Bio. Eng. Sci. and Tech*. 2(2):126-132.

[8] Jegathesh J. D., Amalraj S., Banumathi, and Jereena. J. J. (2019) "A Study On Smart Irrigation Systems For Agriculture Using Iot" Inte. Jour. of. Scii. &.tech. Res. 8:1-4.

[9] Jinyuan X.,Baoxing G.and.Guangzhao T.(2022)" agricultural IoT technology" *Col.of.Eng. Nan. Agri.Uni.Nan.210031.PR.Chi.* pp:11-22.

[10] Khanh Q., Nguyen V., Dang V., Nguyen M Q., Nguyen T B., Stefania L., Giovanni R. and Anselme M. (2022) "IoT-Enabled Smart Agriculture: Architecture, Applications, and Challenges" *Fac.of Inf. Tech .Hun. Yen. Uni. of Tech. and Edu*. pp :1-19.

[11] Krishna S., Samyak J., Varun A. and Shilpi S. (2019) "IoT Based Approach for Smart Irrigation System Suited to Multiple Crop Cultivation" *Int. Jr. of Eng.Res. and Tech.*12(3):357-363.

[12] Laura G., Lorena P., Jose M., J., Jaime L. and Pascal L. (2020) "IoT-Based Smart Irrigation Systems: An Overview on the Recent Trends on Sensors and IoT Systems for Irrigation in Precision Agriculture" *Inst. De. Inve. Pa. la. Gest. Int. de. zo. Cost. Uni. Pol. De. València, 46730 Grau de Gandia, Spain; laugarg2@teleco.upv.es (L.G.); lop.@.doc.upv.es (L.P.); joj.@.dcom.upv.es (J.M.J.).* pp:1-48.

[13] Qazi U. F., Muhammad T N., Abdelkader T A., and Bilal A. K (2021) "Optimization of Subsurface Smart Irrigation System for Sandy Soils of Arid Climate" Dep. of .Civ. Eng. Islm. Uni. of. Madi. Sau. Ara. pp: 1-15.

[14] Raquel G., Karina R., César M., Paola G. and Tanya R. (2019) "IoT Applications in Agriculture*" Esc. d. Ing .en.Com. e. Inf. Gua .Ecu.* pp:68–76.

[15] Shashi Kumar Bairam and Shivaji Chunchu.(2022)" iot in agriculture*" fac.of.sci.and.tech. Bou.Uni"* pp:123-128.

[16] Veerachamy R., Ramar R., Balasubramanian P., Irshad H., Abdulrazak H., Almaliki A A., Ashraf E. and Enas E H. (2022) "Exploiting IoT and Its Enabled Technologies for Irrigation Needs in Agriculture" Dep. of Comp. Sci. and Eng. Kala. Aca. of Res. And Edu. Kris. Indi. pp:1-20.

[17] Zongmei G. ,Yuanyuan S., Guantao X., Yongxian Y L., Xiang H., Zongmei G., Yuanyuan S., Guantao., Yongxian W., Yi L. and Xiang H. (2020) "Real-time hyperspectral imaging for the in-field estimation of strawberry ripeness with deep learning" Cen. for Pre. And Auto. Agri. Sys. Dep. Of Bio. Sys. Eng. USA. pp :31-38

Investigation of Deposit Formation on Exhaust Valve in Compression Ignition Engine

Faheem Ahmed Solangi[1], Liaquat Ali Memon[1], Saleem Raza Samo[1], Muhammad Ramzan Luhur[1], Altaf Alam Noonari[2], Ali Murtaza Ansari[1]
[1]Department of Mechanical Engineering, QUEST Nawabshah, Nawabshah 67450, Sindh, Pakistan
Institute of Enviromental Engineering And Management, Mehran University of Engineering and Technology, Jamshoro, Sindh, Pakistan
Corresponding Author: noonarialtaf@yahoo.com

***Abstract*— This work looked into the exhaust valve of a CIDI engine. The valve tends to stick when too much silt collects on the walls of the exhaust system, particularly when driving in urban settings, or when leaks in the vacuum or exhaust pipes occur. The engine ran at constant speed and load to know the deposition accumulation on exhaust valve. In this regard, A single cylinder, a diesel engine was selected and tested for 200 hours on each fuel sample to determine the effects of three tested fuels namely, DF, DF95WCO5, and DF20WCO20Pe20 on long run endurance test. According to the study's findings, the running surface of the exhaust valve had a very high level of damage. The findings showed that DF95WCO5, particularly on the exhaust valve, produced relatively larger amounts of deposits. Furthermore, when DF95WCO5 was utilized, the deposits generated on key engine components such as intake/exhaust valves, had a very different structure and elemental makeup than when DF and DF20WCO20Pe20 were used. However, it was observed that addition of n-pentanol as ternary blend resulted lessor deposits compared to both fuels. Overall, waste cooking oil inclusion rate revealed that deposits formed more frequently, particularly on the valves, and that these deposits also tended to be wet and brittle.**

I. INTRODUCTION

Many nations are currently working to develop a more sustainable, cleaner form of energy in order to address environmental issues [1]. Alternative fuels, particularly those that can replace diesel fuel entirely or in part, have recently risen to the top of researchers' priorities lists for this fuel type. Biodiesel is the most promising candidate as a diesel fuel substitute [2-4]. To achieve environmental sustainability, recycling is one of the most important factors [5]. Every year, the world discards numerous billion gallons of used cooking oil [6]. However, when WCO is not properly disposed of, it contains a major threat to the environment. Water passages may become clogged and contaminated by WCO. The WCO entered into waste water system can impede the regular operation of waste water treatment facilities [7]. A justifiable solution for both ecological well-being and energy security is to treat and recycle waste combustion products (WCO) for use in diesel engines [8]. WCO has the added benefit of being inexpensive, with all costs associated with collection and treatment [9]. Another promising way to lessen reliance on depleting fossil oil reserves is to recycle WCO as a renewable fuel for diesel locomotive. Although Rudolf Diesel, the creator of the diesel engine, initially intended for it to run on vegetable oils [10], Vegetable oil directly used in modern diesel engines can lead to issues like excessive engine wear, lubrication oil gelling, heavy carbon buildup in engine parts, injector coking, piston ring sticking, and fuel filter clogging [11]. Due to WCO's high viscosity and low volatility, diesel engines produce a lot of particulates due to poor fuel-air mixing, atomization, and vaporization. WCO reformulation using alcohols has stimulated attention of researchers because it approaches easy, practical, and cost-effective technique to reduce the viscosity of vegetable oils [12–18]. Regarding the analysis of n-pentanol and diesel mixtures, very few studies are available [19]. The group of high carbon alcohols includes n-pentanol, one of the most promising alcohols. Diesel engines have been tested with the five-carbon straight chain substance n-pentanol [20–27]. The main goal of this research is to conduct a comparative analysis of the exhaust valve deposits produced by 200-hour endurance tests on n-pentanol and waste cooking oil powered by diesel fuel, respectively.

ASTM	American society for testing and materials
C	Carbon
0_C	Degree centigrade
Cu	Copper
CI	Compression ignition
DF	Diesel fuel
DI	Direct injection
DF95-WCO5	Diesel fuel 95% + Waste cooking oil 5%
DF60-WCO20-Pe20	Diesel fuel 60% + Waste cooking oil 20% + N-pentanol 20%
EDX	Energy dispersive X-ray spectroscopy
Fe	Iron
IC	Internal combustion
Ni	Nickel
O	Oxygen
SEM	Scanning electron microscopy
Ni	Nickel
WCO	Waste cooking oil

II. MATERIAL AND METHODS

A. Fuel Preparation and Characterization

A restaurant provided the used cooking oil for collection. The additive n-pentanol was chosen to reduce viscosity of the used cooking oil. In a temperature range between 130 and 180 0C, the WCO was primarily used for frying activities. The oil was heated and strained before mixing to get rid of food particles and water dribbles. Since diesel abhors water and water can cause phase separation, it was crucial to adjust the strength of mixtures. The WCO was refined using a 4m filter. The test blend fuels(% vol.) were prepared. All test fuels had

stable engine operation and were miscible. When compared to test fuel characterization, Figure 1 depicts the appearance of diesel, used cooking oil, and n-pentanol.

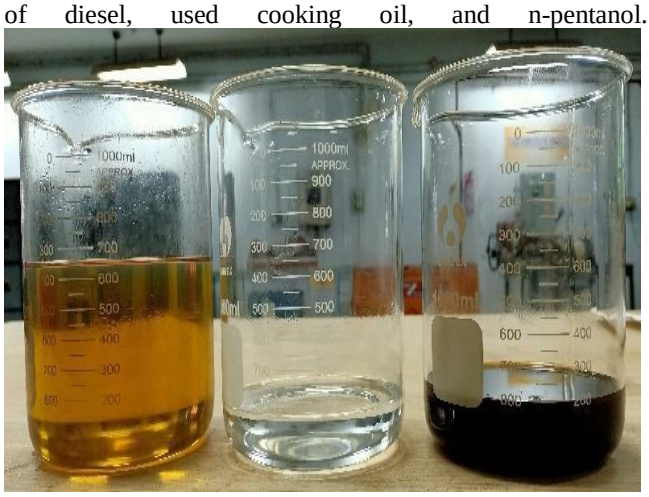

Fig. 1. Appearance of diesel,n-pentanol and waste cooking oil.

This was done by using a mechanical homogenizer machine and mixing all the fuel components together using the splash blending technique for 30 minutes at 4000 rpm. (1) DF (100% vol.) (2) D95WCO5 (95% volume diesel, WCO5% volume waste cooking oil) (3) D60WCO20Pe20 (60% volume diesel, 20% volume waste cooking oil, and 20% volume n-pentanol). The indispensable fuel characterization as per ASTM standard are given in table.1

Table 1. BLEND FUEL PROPERTIES

Properties	***D100***	***D95-WCO5***	***D60-WCO20-Pe20***	***Test Method***
Flash point ^{o}C	78	85	98	ASTM D-93
Viscosity 40 ^{o}C Cst	2.28	2.34	1.14	ASTM D- 7042
Cetane number	50	53	56	ASTM D- 6890
Density g/ml	0.85	0.89	0.83	ASTM D-7042
Heating valve MJ/Kg	42.5	39	41.5	ASTM D-5468

I. EXPERIMENTAL SET UP

The experimental investigation used a direct injection 1-cylinder, four-stroke diesel engine for this purpose. The dynamometer for eddy currents had the engine attached to it. The engine was stabilized by running for 10 minutes prior to any trials, and it was then run for 8 hours every day. To ensure precise and consistent measurements, each fuel sample underwent a separate testing procedure. The engine test rig schematic diagram is displayed below.

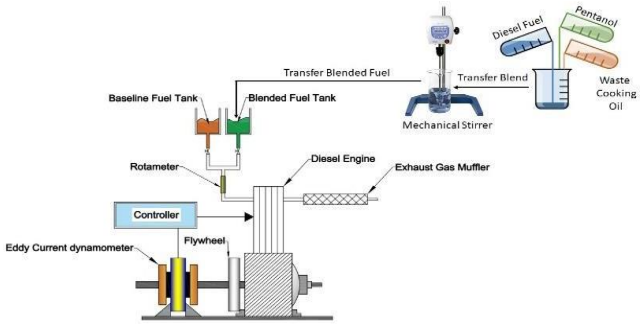

Fig. 2. The engine test rig schematic diagram.

On three test fuels: DF (diesel fuel) as the baseline, DF95-WCO5 (5% waste cooking oil, 95% diesel fuel), and n-pentanol DF60WCO20Pe20 (60% diesel fuel, 20% waste cooking oil, and 20% n-pentanol) respectively. The endurance test was conducted for 200 hours at 1300 rpm and constant load. Engine configurations are mentioned in table 2.

Table.2. Configurations.

Model	***Compression ignition indirect diesel engine***
Maximum engine torque	80 Nm
Maximum engine power	7.7 kW
Injection pressure	14.2 + 0.5 MPa
Valves clearance	Inlet valve 0.15-0.25mm
Piston mean speed	6.93 m/s
Cooling water consumption	1360 g/kW h
Specific fuel consumption	278.8 g/kW h
Compression ratio	21-23
Specific oil consumption	4.08 g/kW h
Means effective pressure	576 kPa
Stroke	80mm
Bore	75mm
Output (12 hours rating)	4.4kW/2600r/min
Displacement	0.353L

The locomotive was disassembled, and the exhaust valve was removed after the 200-hour endurance test. For each test fuel, the cycle was repeated in the same manner. Afterwards. In order to determine the deposits that had accumulated on each sample and their elemental composition, all exhaust valve samples were brought to the lab for scanning electron microscopy (SEM) and energy dispersive x-ray spectroscopy (EDS) tests.

II. Results and Discussion

A. Injector visual inspection

The deposits, or as they are commonly known, carbon accumulations in diesel engines are heterogenic combinations comprises of soot, carbon ash and the leftovers of oxygenated materials [28]. It has been claimed that measuring the temperature of the combustion chamber wall and the area of fuel impingement could be used to estimate the thickness of deposits [29-30]. Low wall temperature and unburned fuel may cause the engine chamber to accumulate more deposits [31]. In a 200-hour long-term endurance test on DF, DF60WCO20Pe20, and DF95WCO5 blends. As can be seen in Figure 3, photos of the exhaust valve were then taken. All of the valves' images were taken with a (DSLR) camera. Visual inspection following the completion of the procedure revealed a specific deposit buildup on the surfaces surrounding the exhaust for all fuel samples, as depicted in Figure 3. However, the exhaust valve was dirtier when using DF95WCO5 fuel than when using DF100 fuel. Evidently, compared to both fuels, the exhaust valve operated on DF60WCO20Pe20 demonstrated less deposit formation.

Fig. 3. Deposits on the valves via (a) Fresh valve (b) DF(c) DF95WCO5 (d) DF60WCO20Pe20.

B. SEM and EDS analysis

Low wall temperature and unburned fuel combined with low wall temperature can cause an increase in the amount of deposits that can form in the engine chamber [32]. Two parts of the engine's mechanism, the intake and exhaust valves, are located on the cylinder head. These valves control how much gas and liquid enters and exits the combustion chamber [33]. A lengthy endurance test was performed on a diesel engine that was powered by waste cooking oil (WCO), which is just waste cooking oil and diesel fuel. It has been asserted that determining the combustion chamber wall's temperature and the area of fuel impingement could be used to determine the thickness of deposits [34-35]. The combination of low wall temperature and unburned fuel could lead to more deposits forming in the engine chamber. After the long-term 200-hour endurance test using the test fuels DF, DF95WCO5, and DF60WCO20Pe20, the engine was partially disassembled and deposit formation on each exhaust valve was examined. Using SEM and EDS techniques, it was possible to comprehend how the deposit formed and what its associated composition was. To ascertain the chemical make-up of each test fuel, Figure 4 displays the SEM micrographs of deposits at a 25x magnification along with any related EDS.

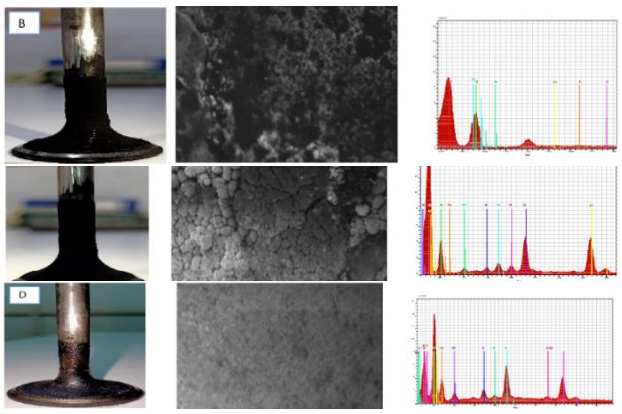

Fig.4. The SEM magnified micrographs of the deposited exhaust valves operated on DF, DF95WCO5 and DF60WCO20Pe20 related elemental analysis.

Fig. 4(B-D) show the SEM micrographs at 25_ magnifications in conjunction with EDS of deposits on exhaust valve fuelled with three blend fuels and compared to base line fuel respectively. It can be clearly seen from figure 4(b-d) that deposits with DF60WCO20Pe20 are substantially reduced compared to rest of two blends as well as base line fuel. Fig. 4(b-d) shows the SEM of deposits on exhaust valve fueled with DF (diesel fuel) at 25_ magnification and related elemental analysis by EDS on deposited surfaces as indicated to be on the top layer, which shows the amount of oxygen

(O) (52.66%). The top layer shows a concentration of oxygen (39.54) in case of DF95WCO5. However, the concentration of carbon (C) in these 44.63 % and 45.42 %, respectively. The deposited valves fuelled with DF60WCO20Pe20 on the surfaces have a lower concentration of carbon (9.96%) and lower concentrations of oxygen (24.81%). This suggests that the carbon concentration in the accumulation layer is low.

Results of the research exposed that higher quantity of deposit accumulation was detected in DF95WCO5 compared to DF.

III. Conclusions

The research findings are:

- The higher inclusion rate of waste cooking oil enhanced deposits accumulations on diesel engine parts, particularly on the exhaust valve.
- By using increase direct waste cooking oil inclusion rate, a tendency toward increased more deposit on the engine component was observed.
- DF fuel led to a large amount of deposits. More specifically, the use of DF95WCO5 showed excessive wetness in the exhaust valve. Thus making the DF95WCO5 caused deposits tend to be wet and brittle. However when using DF60WCO20Pe20 less deposit formation on the exhaust valve.
- Based on the deposits morphology, in every engine component, different shapes could be observed even by using the same fuel. By using different fuels, different deposit structures were detected in similar parts of the engine, especially in the injector tip, piston crown, and cylinder head. This was not observed in the exhaust valve.

- In the DF95WCO5 caused deposits, spherical patterns dominated the structures observed. This could be mainly attributed to the unburned fuel that failed to properly combust, and would later dominate the deposits structure. This deposit structure is similar to deposit structure observed in the piston groove.

It can also be stated that waste cooking oil/n-pentanol blend can easily be accepted as a substitute fuel in CIDI engines without any modifications.

REFERENCES

[1] Atmanli, A., & Yilmaz, N. (2018). A comparative analysis of n-butanol / diesel and 1- pentanol / diesel blends in a compression ignition engine. *Fuel*, *234*(July),161–169. https://doi.org/10.1016/j.fuel.2018.07.015

[2] M. A. Hanif, S. Nisar, and U. Rashid, "Supported solid and heteropoly acid catalysts for production of biodiesel," Catalysis Reviews - Science and Engineering. 59, 2 (2017) pp.165–188.

[3] K. Khiari, S. Awad, K. Loubar, L. Tarabet, R. Mahmoud, and M. Tazerout, "Experimental investigation of pistacia lentiscus biodiesel as a fuel for direct injection diesel engine," Energy Conversion and Management. 108, (2016) pp.392–399.

[4] H. Wu, J. Zhang, Y. Liu, J. Zheng, and Q. Wei, "Biodiesel production from Jatropha oil using mesoporous molecular sieves supporting K2 SiO3 as catalysts for transesterification," Fuel Processing Technology. 119, (2014) pp.114–120.

[5] Krishnamoorthy, V., Dhanasekaran, R., Rana, D., Saravanan, S., & Kumar, B. R. (2018). A comparative assessment of ternary blends of three bio-alcohols with waste cooking oil and diesel for optimum emissions and performance in a CI engine using response surface methodology. *Energy Conversion and Management*, *156*(September 2017), 337–357. https://doi.org/10.1016/j.enconman.2017.10.087.

[6] Hribernik A, Kegl B. Performance and exhaust emissions of an indirect-injection (IDI) diesel engine when using waste cooking oil as fuel. Energy Fuels 2009;23(3):1754–8. http://dx.doi.org/10.1021/ef800986w.

[7] Sabudak T, Yildiz M. Biodiesel production from waste frying oils and its quality control. Waste Manage 2010;30(5):799–803. http://dx.doi.org/10.1016/j.wasman. 2010.01.007.

[8] Senthil Kumar M, Jaikumar M. A comprehensive study on performance, emission and coKalam MA, Masjuki HH, Jayed MH, Liaquat AM. Emission and performance characteristics of an indirect ignition diesel engine fuelled with waste cooking oil. Energy 2011;36(1):397–402. http://dx.doi.org/10.1016/j.energy.2010.10.026.

[9] Agarwal D, Kumar L, Agarwal AK. Performance evaluation of a vegetable oil fuelled compression ignition engine. Renew Energy 2008;33(6):1147–56. http://dx.doi. org/10.1016/j.renene.2007.06.017.

[10] Bari S, Yu CW, Lim TH. Filter clogging and power loss issues while running a diesel engine with waste cooking oil. Proceedings of the Institution of Mechanical Engineers, Part D: J Automob Eng 2002;216(12):993–1001. http://dx.doi.org/10. 1243/095440702762508245.

[11] Atmanlı A, Yüksel B, İleri E. Experimental investigation of the effect of diesel–cotton oil– n-butanol ternary blends on phase stability, engine performance and exhaust emission parameters in a diesel engine. Fuel 2013;109:503–11. http://dx. doi.org/10.1016/j.fuel.2013.03.012.

[12] Sharon H, Jai Shiva Ram P, Jenis Fernando K, Murali S, Muthusamy R. Fueling a stationary direct injection diesel engine with diesel-used palm oil–butanol blends – An experimental study. Energy Convers Manage 2013;73:95–105. http://dx.doi. org/10.1016/j.enconman.2013.04.027.

[13] Lujaji F, Kristóf L, Bereczky A, Mbarawa M. Experimental investigation of fuel properties, engine performance, combustion and emissions of blends containing croton oil, butanol, and diesel on a CI engine. Fuel 2011;90(2):505–10. http://dx. doi.org/10.1016/j.fuel.2010.10.004.

[14] Atmanli A, İleri E, Yüksel B. Experimental investigation of engine performance and exhaust emissions of a diesel engine fueled with diesel–n-butanol–vegetable oil blends. Energy Convers Manage 2014;81:312–21. http://dx.doi.org/10.1016/j. enconman.2014.02.049.

[15] Atmanlı A, İleri E, Yüksel B. Effects of higher ratios of n-butanol addition to diesel– vegetable oil blends on performance and exhaust emissions of a diesel engine. J Energy Inst 2015;88(3):209–20. http://dx.doi.org/10.1016/j.joei.2014.09.008.

[16] Atmanli A. Effects of a cetane improver on fuel properties and engine characteristics of a diesel engine fueled with the blends of diesel, hazelnut oil and higher carbon alcohol. Fuel 2016;172:209–17. http://dx.doi.org/10.1016/j.fuel.2016.01.013.

[17] Atmanli A. Comparative analyses of diesel–waste oil biodiesel and propanol, nbutanol or 1-pentanol blends in a diesel engine. Fuel 2016;176:209–15. http://dx. doi.org/10.1016/j.fuel.2016.02.076.

[18] Atmanli, A., & Yilmaz, N. (2018). A comparative analysis of n-butanol / diesel and 1- pentanol / diesel blends in a compression ignition engine. *Fuel*, *234*(July), 161–169. https://doi.org/10.1016/j.fuel.2018.07.015.

[19] Yilmaz N, Atmanli A, Trujillo M. Influence of 1-pentanol additive on the performance of a diesel engine fueled with waste oil methyl ester and diesel fuel. Fuel 2017;207:461–9.

[20] Yilmaz N, Atmanli.. Quaternary blends of diesel, biodiesel, higher alcohols and vegetable oil in a compression ignition engine. Fuel 2018;212:462–9.

[21] Coughlin B, Hoxie A. Combustion characteristics of ternary fuel blends: pentanol, butanol and vegetable oil. Fuel 2017;196:488–96.

[22] Zhang ZH, Balasubramanian R. Investigation of particulate emission characteristics of a diesel engine fueled with higher alcohols/biodiesel blends. Appl Energy 2016;163:71–80.

[23] Atmanli A. Comparative analyses of diesel–waste oil biodiesel and propanol, nbutanol or 1-pentanol blends in a diesel engine. Fuel 2016;176:209–15.

[24] Yilmaz N, Atmanli A. Experimental assessment of a diesel engine fueled with diesel biodiesel-1-pentanol blends. Fuel 2017;191:190–7.

[25] Atmanli A. Effects of a cetane improver on fuel properties and engine characteristics of a diesel engine fueled with the blends of diesel, hazelnut oil and higher carbon alcohol. Fuel 2016;172:209–17.

[26] Yilmaz N, Ileri E, Atmanli A. Performance of biodiesel/higher alcohols blends in a diesel engine. Int J Energy Res 2016;40:1143–243.

[27] Diabya, M., Sablier, M., Negrateb, A. L., El Fassi, M., Bocquet, J., 2009. Understanding carbonaceous deposit formation resulting from engine oil degradation. Carbon 47, 355 – 366.

[28] Goldsworthy, L., 2006. Computational fluid dynamics modeling of residual fuel oil combustion in the context of marine diesel engines. Int. J. Engine. Res. 7(2), 181-199.

[29] Güralp, O., Hoffman, M., Assanis, D.N., Filipi, Z., Kuo, T.W., Najt, P. Rask, R., 2006. Characterizing the effect of combustion chamber deposits on a gasoline HCCI engine. SAE technical paper, No. 2006-01-3277.

[30] Suryantoro, M. T., Sugiarto, B., & Mulyadi, F. (2016). Growth and characterization of deposits in the combustion cham- ber of a diesel engine fueled with B50 and Indonesian biodiesel fuel (IBF). *12*, 521–527. https://doi.org/10.18331/BRJ2016.3.4.6

[31] Atmanli A. Effects of a cetane improver on fuel properties and engine characteristics of a diesel engine fueled with the blends of diesel, hazelnut oil and higher carbon alcohol.Fuel 2016;172:209–17. http://dx.doi.org/10.1016/j.fuel.2016.01.013.

Balochistan Journal of Engineering & Applied Sciences (BJEAS) – (p-ISSN: 2518-2706
Volume 6, No.1

Improved Catalytic Properties of Biochar Derived From Tamarind Seeds Through Sulfonation For Biodiesel Production

Sooraj Kumar[1], Suhail Ahmed Soomro[2], Khanji Harijan[3], Mohammad Aslam Uqaili[4]
[1]Department of Chemical Engineering, Mehran University of Engineering & Technology, Jamshoro 76090, Sindh, Pakistan
[2]Department of Mechanical Engineering, Mehran University of Engineering & Technology, Jamshoro 76090, Sindh, Pakistan
[3] Department of Electrical Engineering, Mehran University of Engineering & Technology, Jamshoro 76090, Sindh, Pakistan
Corresponding Author E-mail: soorajparhyar50@gmail.com

***Abstract*—Even though fossil fuels are finite and dwindling, their use to meet human needs seems relentless. To cater to our energy requirements without harming the environment, it's essential to tap into diverse renewable energy sources In this study, tamarind seeds were utilized in the production of heterogeneous acid catalysts that were next put to use in fatty acid esterification processes. Carbonization was followed by functionalization with concentrated sulfuric acid, utilizing a wide variety of different sulfonation conditions in order to produce the sulfonated biochar. The waste was carbonized in order to generate the sulfonated biochar. Biochar was characterized through analyzing techniques as; SEM, EDX and FTIR. As per results, the sulfonated biochar with enhanced properties was obtained at optimal temperature of 200 ^{0}C, contact time of 4 hours and maintaining the ratio of 1:10 solid to acid. Under ideal circumstances for the esterification reaction, a conversion of 97 % was accomplished using a catalyst concentration of 4%, a molar ratio of 10:1 for methanol to oleic acid, and a reaction time of 2 hours at a temperature of 80 ℃. The results of this study demonstrate that it may be possible to build a novel heterogeneous acid catalyst for use in the production of biodiesel by making use of biomass that is produced in vast quantities by the agricultural industry.**

Keyw ords*—*biochar; trans esterification; biomass based catalyst; biofuels; biodiesel

I. INTRODUCTION

Major issues with the use of fossil fuels include depleting oil reserves and the release of greenhouse gases, these elements drive research into renewable energy options. Biodiesel, an alternative fuel to diesel, has garnered a lot of interest in this sector in recent years. Biodiesel, which may be made from waste products like vegetable oil, animal fat, or edible oil, has useful properties such being non-toxic and biodegradable. It has similar physicochemical qualities to diesel made from petroleum and offers good combustion emission. Also, biodiesel can be used alone or mixed with regular diesel made from petroleum [1].

The price of raw materials is the key factor holding back progress in the biodiesel sector. Consequently, non-edible vegetable oils and discarded cooking oils, and numerous other acid oils are regarded as desirable raw material sources. Waste oils also have a number of benefits that increase the economic competitiveness of biodiesel. These advantages include the absence of competition with the food market, the recycling of residual oils, and a reduction in production costs [2].

The most prevalent process is the trans esterification reaction with homogeneous alkaline catalysts for producing biodiesel. However, when highly acidic oils are combined with basic catalysts, saponification reactions reduce production efficiency. Traditional homogeneous acid catalysts have a number of drawbacks, including undesirable side effects, equipment corrosion, and a substantial quantity of wastewater that must be treated, which increases environmental contamination. Therefore, heterogeneous acid catalysts are preferable for trans esterification reactions involving highly acidic lubricants. In addition, they have the benefit of being non-corrosive and readily recoverable and reusable [3].

Research has been conducted on heterogeneous acid catalysts such as zeolites, anion exchange resin, sulfated zirconia, and heteropoly acids. In comparison to other types of catalysts, Carbon-based catalysts offer benefits including minimal preparation costs and high catalytic efficiency. They are also accessible and inexpensive [4]. They are easy to functionalize, making them good biodiesel esterification catalysts. Heterogeneous acid catalysts are made from oilseed cake, glucose, bagasse, and other biomass. Biochar is a carbonaceous substance made from biomass wastes by incomplete carbonization. Biochar has 27–34% oxygen by mass, low in nitrogen and sulfur and high in phenolic and carboxylic acid groups. The scientific literature is dominated by studies of suffocated biochar (-SO3H groups) [5].

An intriguing phenomenon of different carbonized materials were evaluated by contrasting a variety of suffocated biochar catalysts' experimental results in esterification and trans esterification processes. combine acid groups -SO3H differently. Only a small portion of biomass utilized to make heterogeneous biodiesel catalysts has been studied, despite its central role in the process, according to the literature. Therefore, efforts in this area should center on finding ways to use more biomass waste and less conventional chemicals [6].

Tamarind (Tamarindus indica) is a tropical fruit tree that is well-known for its sour-sweet pulp used in various culinary and medicinal applications. The seeds are a byproduct once the pulp is extracted and have potential uses of their own. Tamarind trees can be found in the southern regions of Pakistan, especially in Sindh. They also grow in some parts of Punjab and Balochistan[7]. This study aims to produce an acid catalyst from tamarind seeds and to explore the sulfogoogle trannation procedures of the biochar synthesis

from this residue. Furthermore, its usage in the esterification process for biodiesel manufacturing is examined.

II. MATERIALS AND METHODS

Tamarind seed was obtained from Sanghar district, Sindh province, Pakistan. 98% sulfuric acid was used during the sulfonation process. using soybean, coconut, and palm fatty acid distillates from vegetable oils, 99.8% pure methanol, 99.8% oleic acid, 98.6% palmitic acid. 99% methyl heptadecanoate and 95% heptane were required for the calculation of methyl ester production. For the catalyst recovery in the purification step, we utilized ethanol at 99.8%. All chemicals were of Merck lab-grade quality.

B. Catalyst synthesis

The process of producing catalyst is made up of three steps, the tamarind seeds was used as the raw material for producing biochar. First, it was ground, and then it was put through sieves with mesh sizes of 35 and 120. Using a method adapted from Bora et al, The shell particles that were retained most (>35 mesh) underwent carbonization in an oven at 600 ℃ for an hour [8]. The biochar that resulted was sulfonated in a condenser-fitted round-bottom flask set over a hot plate, with constant stirring, variations were made in terms of time, temperature, and the ratio of biochar to concentrated H_2SO_4 (w/v) to understand their influence on the sulfonation process. When examined at 200°C with a biochar-to-acid ratio of 1:10 (w/v), the duration was varied between 1 to 8 hours. The temperature's impact was assessed between 120 and 200 ℃, keeping a constant sulfonation period of 4 hours and a 1:10 (w/v) solid-acid ratio. Lastly, with a fixed temperature of 200°C over 4 hours, the biochar-to-acid ratio was varied from 1:10 to 1:30 (w/v) [9].

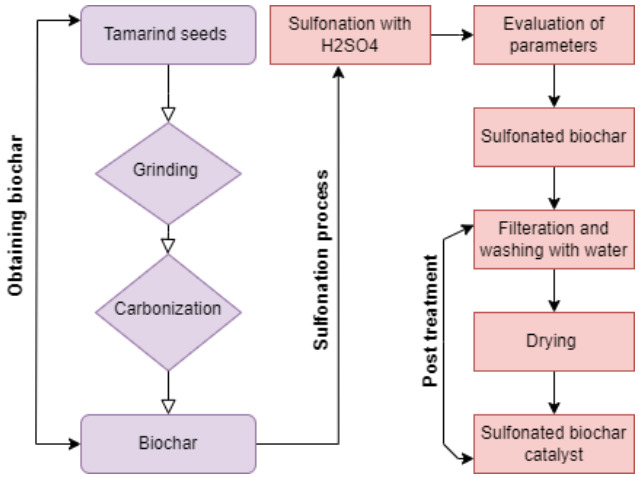

Fig. 1. Methods involved in producing biochar based catalyst

C. Catalyst characterization

Using a method adapted from Boehm et al, An acid-base reverse titration was used to measure the catalyst's overall acid density. One hour was spent agitating 0.1 g of the catalyst and 20 mL of a 0.1 mol/L NaOH solution. After centrifuging this mixture, the clear liquid on top was separated, and its acidity was measured with a 0.1 mol/L HCl solution containing phenolphthalein [10]. Scanning electron microscopy (SEM) was used to examine the catalyst's surface morphology. Using X-ray energy dispersion spectroscopy (EDS) and a microanalysis device, its surface elements were identified. Using Fourier transform infrared spectroscopy (FTIR), the functional groups of the catalyst were investigated [11], [12]. Spectra were collected between 4000 cm^{-1} and 400 cm^{-1} with an accuracy of 4 cm^{-1}. The solid particles were filtered in a vacuum, rinsed with deionized water until they attained a neutral pH, and then oven-dried at 60°C for one day to produce sulfonated biochar [13].

Esterification reacti

Sulfonated biochar's catalytic performance was measured by its ability to facilitate the esterification of oleic acid with methanol, synthesized under various sulfonation conditions. To comprehend the catalyst's effect on the reaction, esterification was also conducted with only the carbon support and the reactants (oleic acid and methanol) without any catalyst. The synthesis pathway for the catalyst is depicted in Figure 1. After the reactions, products were centrifuged to retrieve the catalyst, then decanted and rinsed with 90°C-heated distillate water to remove residual alcohol and water. These samples were desiccated in an 80°C oven overnight. The resultant biodiesel quantities were stored in vials for subsequent analyses. The acid values of the esterified products were compared to those of the original reactants in order to calculate the conversion rate of the reaction. Titration based to the AOCS Cd 3d-63 standard was used to determine this acid value. The following procedure outlined the steps required to ascertain the FFA conversion [14]–[16].

$$\text{FFA conversion \%} = \left(1 - \frac{AVf}{AVi}\right) x100\% \quad \text{(I)}$$

AVi is the fatty acid's acid value before the esterification reaction (in milligrams of KOH per gram), and AVf is the fatty acid's acid value after the procedure. Several variables, including the duration of the reaction (ranging from 0.5 to 2.5 hours), the amount of catalyst used (ranging from 1% to 5%), the molar ratio between methanol and oleic acid (ranging from 5:1 to 25:1), and the temperature range of the reaction (60°C to 120°C), were investigated to optimize the esterification parameters. Diverse feedstock's were utilized in order to evaluate the effectiveness of the catalyst under optimal conditions utilizing various fatty acid combinations in order to determine the catalyst's efficacy. This research utilized Soybean Fatty Acid Distillate (SFAD), Palm Fatty Acid Distillate (PFAD), and Coconut Fatty Acid Distillate (CFAD). Alongside palmitic acid, these substances were subjected to esterification procedures [17]–[19].

III. RESULTS AND DISCUSSION

A. Effect of the sulfonation conditions

Figure 2 shows catalyst synthesis as it relates to sulfonation factors including duration, temperature, and solid-acid ratio. All of these factors significantly altered the method. These materials' ability to catalyze esterification processes is evaluated by monitoring changes in the surface acid density and the rate at which free fatty acid is converted [20]. In order

to have a more comprehensive understanding of the functionalization process of biochar. The relationship between the functionalization of biochar and the period of sulfonation becomes more evident when examining Figure 1. The length of sulfonation appears to have a certain degree of influence on the functionalization of biochar. The acid density observed in unsulfated biochar was found to be 0.14 mmol g-1, indicating that the sulfonation process is likely responsible for the generation of acid sites in the catalysts. Nevertheless, with the prolongation of the sulfonation period, there was an observed augmentation in the acid density measurements, reaching a maximum of 4.2 mmol g-1 after a duration of 4 hours. But, post this zenith, a gradual decline was observed, plateauing to 2.9 mmol g^{-1} following 8 hours of sulfonation. After four hours of sulfonation, this result indicates that the functionalization process may have reached its maximum potential and that the pyrolyzed material may have degraded as a consequence. Despite this, all of the sulfonated catalysts demonstrated a high level of catalytic activity throughout the esterification events [21]–[23].

Sulfonation durations spanning from two to six hours yielded the most optimal results in terms of FFA conversion. At the four-hour time point, a significant peak was identified, characterized by a 98.5% conversion of free fatty acids (FFA) and the highest recorded value of total acid density at 4.2 mmol g-1. Remarkably, in spite of fluctuations in acid density, the results pertaining to FFA conversion exhibited a reasonably stable pattern. This observation indicates that the catalytic reaction reaches a saturation point under the experimental conditions, irrespective of variations in acid concentration. Previous studies have demonstrated similar results when employing carbon-based catalysts produced from corn chaff and a mixture of glucose and starch. In these studies, the optimal sulfonation times were determined to be 4 and 5 hours, respectively [24][25].

When it comes to sulfonation procedures involving biomass, the temperature is the primary factor that determines the level of functionalization achieved by the material.This characteristic is also proven in the current investigation, as shown in Figure 3, as the sulfonation temperature rises, total acid density values increase. This temperature increase could increase acid-biochar mass transfer, thus solidifying the sulfonation process, as studied by Niu et al [26]. The research conducted by Ngaosuwan, Goodwin, and Prasertdham has yielded results that are comparable. Using coffee grounds, a carbon-based heterogeneous acid catalyst was produced. Their research suggests that 200°C is the optimal temperature for the sulfonation procedure, which is consistent with the context of the present work [27].

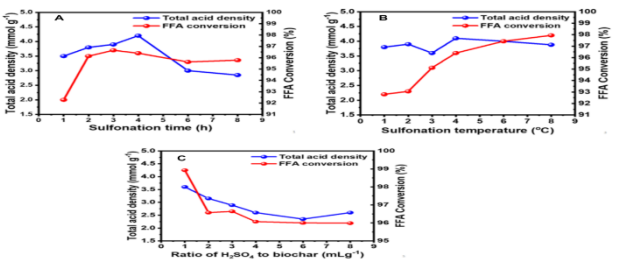

As shown in figure 2, sulfonated biochar's catalytic efficacy depends on sulfonation conditions. Esterification occurred at 90°C for 2 hours with a 20:1 methanol-to-oleic acid molar ratio and 5% catalyst load. The sulfonation process variables examined in this figure include: (a) Sulfonation time at 200 °Cwith a solid-acid ratio of 1:10. (b) The 4-hour sulfonation temperature with a 1:10 solid-acid ratio. (c) H2SO4/biochar at 200°C and 1:10 solid-acid ratio.

All of the sulfonated biochars showed impressive catalytic activity in esterification processes in the time-dependent research. This suggests that beyond a specific threshold, increasing the count of active sites doesn't proportionally enhance the FFA conversion during the catalyst's initial application. It underscores the idea that there may be a saturation point beyond which additional active sites might not significantly boost the esterification process. During the examination of the solid-acid ratio, it was discovered that an increase in the concentration of sulfuric acid did not favorably influence the sulfonation of the biochar (Fig. 2c), the decrease in acid density values was thereafter accompanied by a gradual degradation of the biochar. Starting from a weight-to-volume ratio of 1:10 and beyond, this phenomenon became evident. Consequently, one possible interpretation of this observation is that the functionalization is approaching, or nearing, its saturation point. This suggests that beyond this ratio, further increments might not contribute as effectively to enhancing the catalyst's performance [28].

Various biomass materials have been utilized in numerous investigations, including sources such as cassava bark, coconut shell, sawdust, and oleaginous seed cake, biochar sulfonation processes with a ratio of 1:10 (w/v) were found to be the most efficient. This prevalent ratio seems to be a common finding across multiple biomass materials, suggesting its potential optimality in the sulfonation process. In contrast to the findings related to this ratio, the results for the other variables examined showed that the FFA conversion rates in the esterification reactions remained notably high across all the catalysts explored in the current research [29], [30].

Both sulfonic acid sites and extra oxygenated acid sites are often produced during sulfonation reactions. The -SO3H groups were found to be the most catalytically active sites, as investigated by Zhang et al. It was also shown that the esterification process was facilitated by carboxyl groups, which enhanced the natural activity of the -SO3H groups [31]. Since the -SO3H group is quite acidic, its participation in the mechanism of the esterification reaction makes protonation of the methanol molecule more difficult. However, the rules of the game shift when a weaker acid group, such -COOH, is introduced. Methanol's -OH segment can create hydrogen bonds with the deprotonated COOH group. This imparted negative charge on oxygen boosts the methanol molecule's nucleophilic properties. Consequently, this enhancement benefits both the pace and conversion of the esterification reaction [31].

Without a catalyst, 6.8 % conversion to an ester was accomplished in the esterification reaction between methanol and oleic acid. Similar outcomes were attained when non-sulfonated biochar was used during the procedure, a slightly higher conversion rate of 7.3% was observed. However, this modest increase suggests that non-sulfonated biochar isn't particularly effective in significantly enhancing the FFA conversion in esterification. This finding highlights the possible increased activity of sulfated biochar, highlighting the significance and efficacy of the sulfonation process. More acid force density in a catalyst usually means better catalytic performance for making biodiesel. The catalyst containing

the highest concentration of acid, measuring 4.2 mmol of acid per gram, was chosen for further analysis in this investigation [32], [33]. The optimal sulfonation parameters for this chosen catalyst were identified as: a duration of four hours, a temperature setting of 200 ℃, and a ratio of one solid to ten acids (w/v) by weight. When compared with the data found in the published research on other types of sulfonated biomass, the values that were selected for the sulfonation process conditions that were used in the manufacture of biochar from murumuru kernel shells were found to be ideal. Lathiya, Bhatt, and Maheria investigated how to create a sulfonated carbon catalyst using orange peel byproducts. A 1:20 w/v (biochar to H2SO4) solid-to-acid ratio was required for their unique sulfonation method, coupled with an extended sulfonation duration of 24 hours, all maintained at a temperature of 200℃. When used in an esterification reaction with corn acid oil, this procedure achieved a remarkable 91.7% conversion efficiency as a final product. Bora et al conducted a study in which they turned waste from Mesua ferrea seed shells into a sulfonated activated carbon catalyst. Their research yielded an impressive conversion rate, with a peak of 95.6% for the oil examined. The optimal conditions under which these results were achieved involved a solid-to-acid ratio of 1:8 w/v (carbon to H_2SO_4), maintained at a temperature of 120℃ over a duration of 10 hours [34], [35].

B. Characterization Results

- Morphology analysis of biochar and catalyst

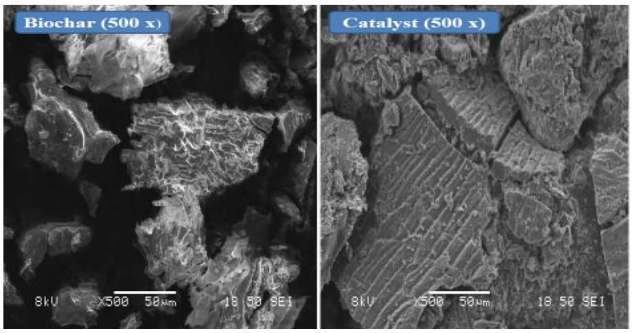

Fig. 3. SEM Images (A) Biochar (B) Catalyst

Scanning electron micrographs (SEM) of the catalyst and the unsulfonated biochar are shown in Figure 4, offering a close examination of their surface structures. The biochar's surface, as depicted in the figure, exhibits an irregular and varied texture, prominently displaying a highly-developed porous architecture — a characteristic often associated with carbonized organic refuse. Contrastingly, the SEM micrographs of the catalyst's surface reveal a decline in its porosity. The intense sulfonating agent employed during the biochar's functionalization led to the formation of minor cracks, contributed to partial oxidation, condensation, and even resulted in some loss of its inherent porous structure. Further scrutiny of the image indicates that the partial obstruction of the pores is attributed to the adherence of the –SO3H groups to the catalyst support, i.e., the biochar. This observation serves as compelling evidence of the effectiveness of the biochar sulfonation process. [36, 37].

- Elemental analysis of biochar and catalyst

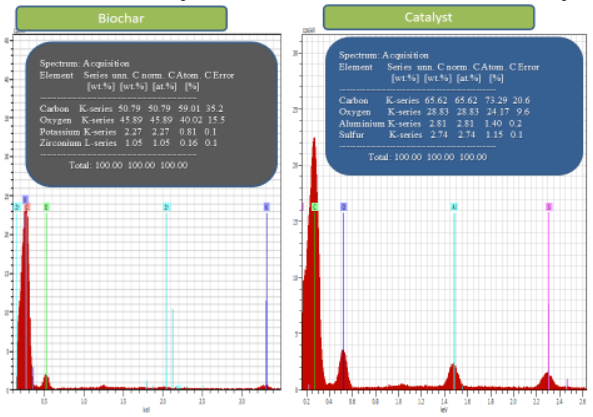

Fig. 4 EDS analysis catalyst

EDS analysis of the composition (shown in Fig. 5) showed a high carbon content, the result of the pyrolysis process. After the sulfonation procedure, however, the sample had a sulfur concentration of 2.74%, providing evidence of the successful incorporation of sulfonic groups. The increased amount of carbon shows the catalyst gone through further carbonization process as well as higher temperature sulfonation process enhanced carbon value.

- Functional group analysis of catalyst

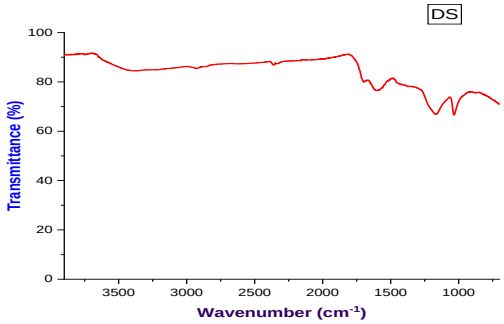

Fig. 5. FT-IR spectra of biochar catalyst

The FT-IR spectrum of biochar catalyst (Figure 6) reveals that the stretching and asymmetric vibration bands of -SO2 occurred at around 1020 and 1090 cm-1. The band seen at 3310 cm-1 (biochar catalyst) is due to phenolic OH groups and O-H stretching of -COOH. The frequency of 1680 cm-1 has been associated with the COOH C=O stretching. Sulfonating the biochar's surface with H_2SO_4 allowed the SO_3H groups to bind to the catalytic surface [38], [39].

C. *Biodiesel characterization*

The fuel's quality and effect on the engine are reflected in biodiesel's fuel characteristics. Biodiesel made from oleic acid was tested to ensure its purity by measuring its physicochemical parameters. The quality of the manufactured biodiesel is confirmed to be up to ASTM standards. The fuel's density and kinematic viscosity both play major roles in how the fuel is injected. High concentrations of these characteristics might clog the fuel injection system and cause deposits to form in the engine [40]. Biodiesel was discovered to have a density and kinematic viscosity of 0.889 g cm^{-3} and 4.7 mm2 s^{-1}, respectively. The "flash point," or the lowest temperature at which the fuel will begin to burn, is another

crucial quality. With a flash point of 173 degrees Celsius, biodiesel exceeds the standards of ASTM D6751. The capacity to maintain cold is especially important for ensuring adequate biodiesel fuel storage and for using biodiesel during the winter months in cold places. Therefore, the cold filter plugging point value that was discovered to be 1 ℃is deemed to be excellent [41], [42].

COMPARATIVE STUDY

C. TABLE II. COMPARATIVE STUDY

S. No.	Material	RM	Total acid density (mmol g^{-1})	Catalyst (wt%)	FFA Conversion (%)	Reference
1	Tamarind seeds	10:1	4.12	4	97.0	Present Study
2	Cow dung	18:1	16.6	4	96.5	[43]
3	Corn straw	7:1	2.6	7	93.0	[44]
4	Cacao shell	7:1		5	93.0	[45]
5	Sugar cane bagasse	18:1	2.4	1	94.4	[46]
6	Palm kernel shel	15:1	14.4	4	97.0	[47]

The catalytic effectiveness of tamarind seeds and sulfonated biochar produced from different biomass feedstock is shown in Table 4, used as a feedstock for biodiesel production via the esterification process. Different carbon sources can be evaluated for their catalytic potential by being subjected to the same synthetic processes (carbonization and sulfonation). The optimal reaction conditions for each catalyst used in the FFA conversion must also be verified. tamarind seeds use in heterogeneous acid catalysis for biodiesel synthesis is supported by the current study's findings, which demonstrate a similar pattern to that seen in the literature.

V. CONCLUSION

After conducting extensive research, the ideal parameters for sulfonating tamarind seeds in order to produce biochar have been determined. The findings indicate that the most favorable conditions consist of a solid-to-acid ratio of 1:10 (w/v) and a processing duration of 4 hours at a temperature of 200 °C. As a result of these conditions, the resulting catalyst exhibits an impressive total acid density of 4.2 mmol g-1. Similarly, the optimal conditions for the esterification of oleic acid and methanol have been identified. These conditions include a temperature of 90 °C, a reaction duration of 1.5 hours, a catalyst concentration of 5% (w/w), and a methanol to oleic acid molar ratio of 10:1. These conditions yielded an impressive FFA conversion rate of 97%. Such remarkable conversion rates in the esterification reactions underscore the potential viability of using agro-industrial by-products as alternate starting materials for producing a heterogeneous acid catalyst used for biodiesel synthesis. Furthermore, this study emphasize the feasibility of utilizing cost-effective residual acid oils as potential lipid sources in biodiesel production. The study strongly suggests that reintegrating discarded raw materials into the production process can lead to the derivation of high-value products, highlighting the concept of waste-to-wealth.

Acknowledgments

This research was funded by the Higher Education Commission (HEC) of Pakistan under the grant number 518-110288-2EG5-128 (50043375) for the Indigenous 5000 Ph.D. Fellowship Program Phase II project. The authors gratefully acknowledge Higher Education Commission (HEC) Islamabad, Pakistan, for its technical and financial assistance.

REFERENCES

[1] S. Kumar, S. A. Soomro, K. Harijan, M. A. Uqaili, and L. Kumar, "Advancements of Biochar-Based Catalyst for Improved Production of Biodiesel: A Comprehensive Review," Energies, vol. 16, no. 2, 2023, doi: 10.3390/en16020644.

[2] H. Soomro et al., "Assessment of Sustainable Biomass Energy Technologies in Pakistan Using the Analytical Hierarchy Process," Sustain., vol. 14, no. 18, 2022, doi: 10.3390/su141811388.

[3] X. Xiong, I. K. M. Yu, L. Cao, D. C. W. Tsang, S. Zhang, and Y. S. Ok, "A review of biochar-based catalysts for chemical synthesis, biofuel production, and pollution control," Bioresour. Technol., vol. 246, pp. 254–270, 2017, doi: 10.1016/j.biortech.2017.06.163.

[4] A. M. Dehkhoda, A. H. West, and N. Ellis, "Biochar based solid acid catalyst for biodiesel production," Appl. Catal. A Gen., vol. 382, no. 2, pp. 197–204, 2010, doi: 10.1016/j.apcata.2010.04.051.

[5] S. Anto et al., "Algae as green energy reserve: Technological outlook on biofuel production," Chemosphere, vol. 242, 2020, doi: 10.1016/j.chemosphere.2019.125079.

[6] R. Sharma et al., "A Comprehensive Review on Hydrothermal Carbonization of Biomass and its Applications," Chem. Africa, vol. 3, no. 1, 2020, doi: 10.1007/s42250-019-00098-3.

[7] S. Kumar, K. Harijan, M. Jeguirim, M. I. Soomro, J. D. Nixon, and M. A. Uqaili, "Assessment of energy potential of date palm residues in Khairpur district, Pakistan," Biofuels, vol. 12, no. 10, pp. 1267–1274, 2021, doi: 10.1080/17597269.2019.1610599.

[8] A. P. Bora, S. H. Dhawane, K. Anupam, and G. Halder, "Biodiesel synthesis from Mesua ferrea oil using waste shell derived carbon catalyst," Renew. Energy, vol. 121, pp. 195–204, 2018, doi: 10.1016/j.renene.2018.01.036.

[9] T. K. Choudhary, K. S. Khan, Q. Hussain, M. Ahmad, and M. Ashfaq, "Feedstock-induced changes in composition and stability of biochar derived from different agricultural wastes," Arab. J. Geosci., vol. 12, no. 20, 2019, doi: 10.1007/s12517-019-4735-z.

[10] H. P. Boehm, "Some aspects of the surface chemistry of carbon blacks and other carbons," Carbon N. Y., vol. 32, no. 5, pp. 759–769, 1994, doi: 10.1016/0008-6223(94)90031-0.

[11] S. X. Zhao, N. Ta, and X. D. Wang, "Effect of temperature on the structural and physicochemical properties of biochar with apple tree branches as feedstock material," Energies, vol. 10, no. 9, 2017, doi: 10.3390/en10091293.

[12] S. Chellappan, V. Nair, V. Sajith, and K. Aparna, "Experimental validation of biochar based green Bronsted acid catalysts for simultaneous esterification and transesterification in biodiesel production," Bioresour. Technol. Reports, vol. 2, pp. 38–44, 2018, doi: 10.1016/j.biteb.2018.04.002.

[13] F. Cheng and X. Li, "Preparation and application of biochar-based catalysts for biofuel production," Catalysts, vol. 8, no. 9, 2018, doi: 10.3390/catal8090346.

[14] S. Yu, L. Wang, Q. Li, Y. Zhang, and H. Zhou, "Sustainable carbon materials from the pyrolysis of lignocellulosic biomass," Mater. Today Sustain., vol. 19, 2022, doi: 10.1016/j.mtsust.2022.100209.

[15] A. W. Bhutto, K. Harijan, K. Qureshi, A. A. Bazmi, and A. Bahadori, "Perspectives for the production of ethanol from lignocellulosic feedstock - A case study," J. Clean. Prod., vol. 95, pp. 184–193, 2015, doi: 10.1016/j.jclepro.2015.02.091.

[16] Z. E. Tang, S. Lim, Y. L. Pang, H. C. Ong, and K. T. Lee, "Synthesis of biomass as heterogeneous catalyst for application in biodiesel production: State of the art and fundamental review," Renewable and Sustainable Energy Reviews, vol. 92. Elsevier Ltd, pp. 235–253, Sep. 01, 2018. doi: 10.1016/j.rser.2018.04.056.

[17] M. Li, Y. Zheng, Y. Chen, and X. Zhu, "Biodiesel production from waste cooking oil using a heterogeneous catalyst from pyrolyzed rice husk," Bioresour. Technol., vol. 154, pp. 345–348, 2014, doi: 10.1016/j.biortech.2013.12.070.

[18] R. V. Quah, Y. H. Tan, N. M. Mubarak, M. Khalid, E. C. Abdullah, and C. Nolasco-Hipolito, "An overview of biodiesel production using recyclable biomass and non-biomass derived magnetic catalysts," J. Environ. Chem. Eng., vol. 7, no. 4, Aug. 2019, doi: 10.1016/j.jece.2019.103219.

[19] N. Hossain, T. M. I. Mahlia, and R. Saidur, "Latest development in microalgae-biofuel production with nano-additives," Biotechnol. Biofuels, vol. 12, no. 1, 2019, doi: 10.1186/s13068-019-1465-0.

[20] A. M. Dehkhoda and N. Ellis, "Biochar-based catalyst for simultaneous reactions of esterification and transesterification," Catal. Today, vol. 207, pp. 86–92, 2013, doi: 10.1016/j.cattod.2012.05.034.

[21] A. M. Dehkhoda, A. H. West, and N. Ellis, "Biochar based solid acid catalyst for biodiesel production," Appl. Catal. A Gen., vol. 382, no. 2, pp. 197–204, Jul. 2010, doi: 10.1016/j.apcata.2010.04.051.

[22] A. W. Bhutto, A. A. Bazmi, and G. Zahedi, "Greener energy: Issues and challenges for Pakistan-Solar energy prospective," Renew. Sustain. Energy Rev., vol. 16, no. 5, pp. 2762–2780, 2012, doi: 10.1016/j.rser.2012.02.043.

[23] A. W. Bhutto, A. A. Bazmi, S. Karim, R. Abro, S. A. Mazari, and S. Nizamuddin, "Promoting sustainability of use of biomass as energy resource: Pakistan's perspective," Environmental Science and Pollution Research, vol. 26, no. 29. Springer Verlag, pp. 29606–29619, Oct. 01, 2019. doi: 10.1007/s11356-019-06179-7.

[24] C. Shulin, "Microalgal biodiesel production via a two-step process with carbon-based acidic catalyst," no. October 2016, 2013.

[25] S. Dora, T. Bhaskar, R. Singh, D. V. Naik, and D. K. Adhikari, "Effective catalytic conversion of cellulose into high yields of methyl glucosides over sulfonated carbon based catalyst," Bioresour. Technol., vol. 120, pp. 318–321, 2012, doi: 10.1016/j.biortech.2012.06.036.

[26] S. Niu, Y. Ning, C. Lu, K. Han, H. Yu, and Y. Zhou, "Esterification of oleic acid to produce biodiesel catalyzed by sulfonated activated carbon from bamboo," Energy Convers. Manag., vol. 163, pp. 59–65, 2018, doi: 10.1016/j.enconman.2018.02.055.

[27] K. Ngaosuwan, J. G. Goodwin, and P. Prasertdham, "A green sulfonated carbon-based catalyst derived from coffee residue for esterification," Renew. Energy, vol. 86, pp. 262–269, 2016, doi: 10.1016/j.renene.2015.08.010.

[28] E. Erdogan et al., "Characterization of products from hydrothermal carbonization of orange pomace including anaerobic digestibility of process liquor," Bioresour. Technol., vol. 196, pp. 35–42, 2015, doi: 10.1016/j.biortech.2015.06.115.

[29] K. Fakkaew, T. Koottatep, T. Pussayanavin, and C. Polprasert, "Hydrochar production by hydrothermal carbonization of faecal sludge," J. Water Sanit. Hyg. Dev., vol. 5, no. 3, pp. 439–447, 2015, doi: 10.2166/washdev.2015.017.

[30] X. Fu et al., "A microalgae residue based carbon solid acid catalyst for biodiesel production," Bioresour. Technol., vol. 146, pp. 767–770, 2013, doi: 10.1016/j.biortech.2013.07.117.

[31] H. Zhang et al., "Nanocarbon-based catalysts for esterification: Effect of carbon dimensionality and synergistic effect of the surface functional groups," Carbon N. Y., vol. 147, pp. 134–145, 2019, doi: 10.1016/j.carbon.2019.02.079.

[32] M. E. González et al., "Functionalization of biochar derived from lignocellulosic biomass using microwave technology for catalytic application in biodiesel production," Energy Convers. Manag., vol. 137, pp. 165–173, 2017, doi: 10.1016/j.enconman.2017.01.063.

[33] U. Kumar, S. Joseph Paul, and S. Jain, "Biochar: A source of nano catalyst in transesterification process," in Materials Today: Proceedings, Elsevier Ltd, 2020, pp. 5501–5505. doi: 10.1016/j.matpr.2020.09.248.

[34] D. R. Lathiya, D. V. Bhatt, and K. C. Maheria, "Synthesis of sulfonated carbon catalyst from waste orange peel for cost effective biodiesel production," Bioresour. Technol. Reports, vol. 2, pp. 69–76, 2018, doi: 10.1016/j.biteb.2018.04.007.

[35] A. E. Harman-Ware et al., "Microalgae as a renewable fuel source: Fast pyrolysis of Scenedesmussp.," Renew. Energy, vol. 60, pp. 625–632, 2013, doi: 10.1016/j.renene.2013.06.016.

[36] R. Mathiarasi, C. Mugesh kanna, and N. Partha, "Transesterification of soap nut oil using novel catalyst," J. Saudi Chem. Soc., vol. 21, no. 1, pp. 11–17, Jan. 2017, doi: 10.1016/j.jscs.2013.07.006.

[37] L. E. Hernandez-Mena, A. A. B. Pecora, and A. L. Beraldo, "Slow pyrolysis of bamboo biomass: Analysis of biochar properties," Chem. Eng. Trans., vol. 37, pp. 115–120, 2014, doi: 10.3303/CET1437020.

[38] T. M. Huggins, J. J. Pietron, H. Wang, Z. J. Ren, and J. C. Biffinger, "Graphitic biochar as a cathode electrocatalyst support for microbial fuel cells," Bioresour. Technol., vol. 195, pp. 147–153, 2015, doi: 10.1016/j.biortech.2015.06.012.

[39] C. Italiano, A. Vita, C. Fabiano, M. Laganà, and L. Pino, "Bio-hydrogen production by oxidative steam reforming of biogas over nanocrystalline Ni/CeO2 catalysts," Int. J. Hydrogen Energy, vol. 40, no. 35, pp. 11823–11830, 2015, doi: 10.1016/j.ijhydene.2015.04.146.

[40] K. Hasni, Z. Ilham, S. Dharma, and M. Varman, "Optimization of biodiesel production from Brucea javanica seeds oil as novel non-edible feedstock using response surface methodology," Energy Convers. Manag., vol. 149, pp. 392–400, 2017, doi: 10.1016/j.enconman.2017.07.037.

[41] J. M. Jung, J. I. Oh, K. Baek, J. Lee, and E. E. Kwon, "Biodiesel production from waste cooking oil using biochar derived from chicken manure as a porous media and catalyst," Energy Convers. Manag., vol. 165, pp. 628–633, 2018, doi: 10.1016/j.enconman.2018.03.096.

[42] M. M. El-Dalatony et al., "Whole conversion of microalgal biomass into biofuels through successive high-throughput fermentation," Chem. Eng. J., vol. 360, pp. 797–805, Mar. 2019, doi: 10.1016/j.cej.2018.12.042.

[43] S. H. Jien, "Physical characteristics of biochars and their effects on soil physical properties," Biochar from Biomass Waste Fundam. Appl., pp. 21–35, 2018, doi: 10.1016/B978-0-12-811729-3.00002-9.

[44] P. Planning et al., "Faculty of Industrial," pp. 1–44.

[45] S. Gunukula, A. Daigneault, A. A. Boateng, C. A. Mullen, W. J. DeSisto, and M. C. Wheeler, "Influence of upstream, distributed biomass-densifying technologies on the economics of biofuel production," Fuel, vol. 249, pp. 326–333, Aug. 2019, doi: 10.1016/j.fuel.2019.03.079.

[46] M. Hamza et al., "A review on the waste biomass derived catalysts for biodiesel production," Environmental Technology and Innovation, vol. 21. Elsevier B.V., Feb. 01, 2021. doi: 10.1016/j.eti.2020.101200.

Balochistan Journal of Engineering & Applied Sciences (BJEAS) – (p-ISSN: 2518-2706
Volume 6, No.1

Simulation based Analysis of Numerical Relay for Power Transformer Protection

Abdul Hameed Soomro[1], Saeed Ahmed Shaikh[1], Rahbar Hussain[3] , Suresh Kumar[3], Rohit3, Sajid Ahmed[3], Najaf Ali[3]
[1]Faculty, Department of Electrical Engineering, Quaid-e-Awam University of Engineering Science and Technology Nawabshah Campus Larkana, Sindh Pakistan

[2]Students, Department of Electrical Engineering, Quaid-e-Awam University of Engineering Science and Technology Nawabshah Campus Larkana, Sindh Pakistan

Correspondence Author: Abdul Hameed Soomro, E-mail: abdul.hameed@quest.edu.pk

***Abstract*—Numerical relays have become an essential component in modern power systems for providing accurate and reliable protection to critical equipment, including power transformers. Power transformers play a crucial role in power transmission and distribution networks, and their failure can lead to significant financial losses and even power outages. Numerical relays for power transformer protection are designed to detect faults and abnormal conditions in the transformer's primary and secondary windings and provide quick and precise tripping signals to disconnect the transformer from the power grid. These relays use advanced algorithms to measure various electrical parameters, such as current, voltage, phase angle, and frequency, to detect faults such as over-current, overvoltage, under-voltage, and differential current. Numerical relays for power transformer protection offer several advantages over traditional electro-mechanical relays, including faster response times, increased accuracy, and more comprehensive protection capabilities. This paper reviews the key features of numerical relays for power transformer protection and their significance in ensuring the reliable and safe operation of power systems. In this research study the MATLAB software is utilized to get the efficiency of protective relay under unbalance conditions**.

Index Terms: *Numeric Relay, Power Transformer*

I. INTRODUCTION

A power transformer is a type of electrical transformer that is designed to transfer electrical energy between circuits at different voltage levels [1]. Power transformers are essential components in the transmission and distribution of electrical power, as they enable the efficient and safe transfer of electrical energy over long distances [2]. Power transformer protection is critical for ensuring the reliability and safety of power systems [3]. A power transformer failure can lead to significant financial losses, power outages, and even damage to equipment or human life [4]. Over the years, several protection methods have been developed to detect and mitigate transformer faults [5-8]. R. H. Alrashidi et al. (2019) proposed a new protection scheme for power transformers based on wavelet transform and support vector machine (SVM) [9]. L. Zheng et al. (2019) proposed a protection method for power transformers based on the hybrid model of artificial neural network (ANN) and ant colony optimization (ACO). The proposed method was tested on a 220 kV transformer. S. Zhang et al. (2019) developed a transformer protection method based on the deep belief network (DBN) [10]. The proposed method was tested on a 110 kV transformer. F. Li et al. (2019) proposed a protection method for power transformers based on a fuzzy clustering algorithm and a novel decision-making approach [11]. The proposed method was tested on a 110 kV transformer. Guo et al. (2019) proposed a protection method for power transformers based on a kernel density estimator (KDE) and a support vector machine (SVM) [12]. The proposed method was tested on a 220 kV transformer. F. Xie et al. (2020) proposed a protection method for power transformers based on the artificial immune system (AIS) and principal component analysis (PCA) [13]. The proposed method was tested on a 220 kV transformer. R. Zhao et al. (2020) proposed a transformer protection method based on the ensemble empirical mode decomposition [14] and the extreme learning machine (ELM). The proposed method was tested on a 110 kV transformer. H. Li et al. (2020) proposed a protection method for power transformers based on the hybrid model of fuzzy clustering and adaptive resonance theory (ART) [15]. The proposed method was tested on a 220 kV transformer. S. S. Islam et al. (2020) proposed a transformer protection method based on the frequency response analysis (FRA) and the support vector machine (SVM) [16]. The proposed method was tested on a 33 kV transformer. M. R. Hasan et al. (2021) proposed a protection method for power transformers based on the hybrid model of the genetic algorithm (GA) and the SVM [17]. The proposed method was tested on a 380 kV transformer. K. Wu et al. (2021) proposed a protection method for power transformers based on a novel feature extraction method and a support vector machine (SVM) [18]. The proposed method was tested on a 110 kV transformer. These protection schemes were utilized individually as discussed literature which increases the cost of protection and complexity of the system [6].

In this paper, we will primarily focus on power transformer and presented the numerical relay. Numerical relays for power transformer protection are designed to detect faults and abnormal conditions in the transformer's primary and secondary windings and provide quick and precise tripping signals to disconnect the transformer from the power grid [19]. These relays use advanced algorithms to measure various electrical parameters, such as current, voltage, phase angle, and frequency, to detect faults such as over-current,

overvoltage, under-voltage, and differential current [20]. Numerical relays for power transformer protection offer several advantages over traditional electro-mechanical relays, including faster response times, increased accuracy, and more comprehensive protection capabilities [21]. This paper reviews the key features of numerical relays for power transformer protection and their significance in ensuring the reliable and safe operation of power systems. The numerical relay is shown in Fig. 1 [19].

In this research paper the MATLAB Simulink software is utilized to analyze the performance of numeric relay under over-current, overvoltage, and under voltage.

Section 2 describes the Power Transformer,
Section 3 describe the Numerical Relay,
Section 4 describes the Methodology,
Section 5 describes the Results and Discussions,
Section 5 describes the Conclusions.

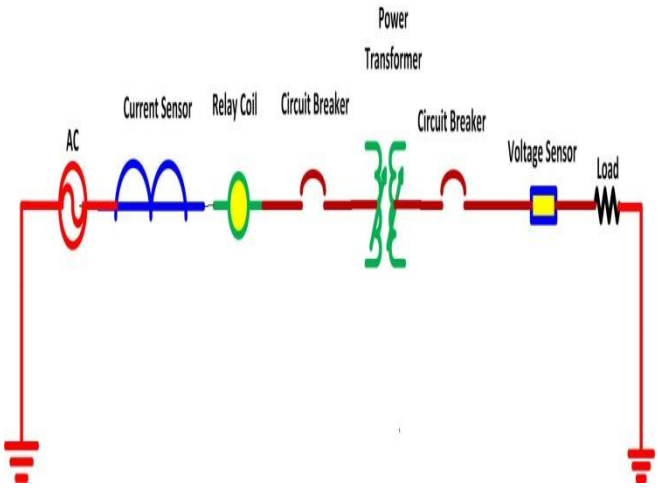

Fig. 1 One Line Diagram of Numerical Relay

II. POWER TRANSFORMER

Power transformers are critical components in the electrical power industry, serving a vital role in the safe and efficient transfer of electrical energy [[1]. Their applications are widespread, ranging from power plants and substations to industrial facilities and commercial buildings [22]. With the continuous growth in demand for electrical power, the significance of power transformers in the generation, transmission, and distribution of electrical power will become increasingly crucial [23]. One of the primary functions of a power transformer is to adjust the voltage of the electrical power being transferred, either by stepping up or stepping down the voltage [24], this is achieved through changing the turns ratio in the primary and secondary windings. Power transformers can transfer electrical power at varying voltage levels, from low voltage levels used in households to high voltage levels employed in power transmission lines [25]. The fundamental structure of a power transformer comprises a magnetic core around which two or more coils of wires are wound [26], The primary winding is the coil linked to the electrical power source, while the secondary winding is the coil linked to the load. When primary winding is energized then it produces a magnetic field that induces a voltage in the secondary winding [26]. The power transformer is shown in Fig. 2 [25].

Fig. 2 Power Transformer at Grid Station

III. NUMERICAL RELAY

Numerical relays are digital devices that have been increasingly used in power systems for protection and control applications compared to their electromechanical and static counterparts, numerical relays provide faster and more accurate protection, as well as more advanced control and monitoring features [20], and has led to their widespread adoption in power systems around the world. The primary advantages of numerical relays are their ability to perform complex algorithms and logic functions in real-time [19], this allows them to provide faster and more accurate protection for power system equipment, such as transformers, generators, and transmission lines. Additionally, numerical relays can perform advanced control functions, such as voltage regulation and reactive power compensation [21]. Numerical relays can be classified based on their functionality, such as distance protection, differential protection, and over-current protection [27]. In addition to their protection and control functions, numerical relays can also provide valuable data for power system analysis and monitoring [28]. The working parts of Numerical relay are shown in Fig. 3 [19].

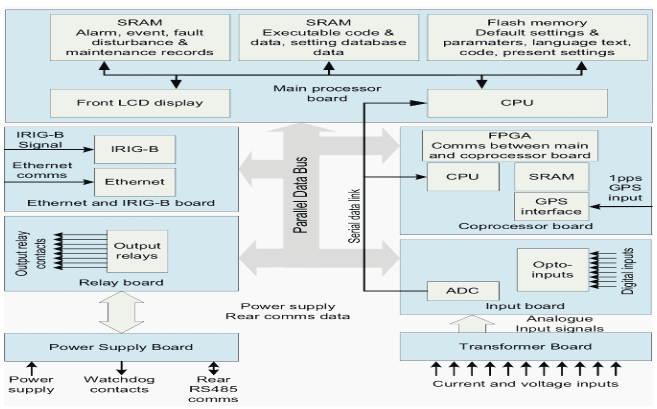

Fig. 3 Parts of Numerical Relay

The structure of a numerical relay is consists of the Input Module, CPU, Memory, Multiplexer, Analog to Digital Converter, Output Module, and Digital Input/Communication Module [29]. The Input Module is responsible for managing the analog parameters of the power system [21]. The analog signals with high-powered are firstly stepped down through current and potential transformers and then passed onto the numerical relay, which uses a low-pass filter to remove any noise resulting from corona or induction effects from nearby high voltage lines [30]. The CPU functions as the central processing unit of the system, acting as the "brain" that processes all data protection algorithms and digital inputs, and also performing filtering tasks [31]. The Numerical Relay contains two types of memory Random Access Memory (RAM) and Read-Only Memory (ROM). The RAM stores input data and processes it during compilation, while the ROM functions as a storage unit for software and other data related to events and disturbances [32], making it crucial for fault analysis and troubleshooting. To facilitate the CPU in processing the analog signals received from the current and potential transformers, an Analog to Digital Converter is employed [33]. A numerical relay has an output module consists of digital contacts that become operational when CPU sends a trip command, these contacts generate pulses, which serve as response signals, and their response time can be adjusted as per the specific relay applications. The Numerical Relay is equipped with serial and parallel ports, similar to a computer, enabling its connection to control and communication systems within the substation [34], [35].

The equation representing a typical numerical relay is expressed as follows [19].

$$I_{a^2} + I_{b^2} + I_{c^2} = I_{p^2} \quad (1)$$

Where

Ia, Ib, and Ic are the phase currents of the power system and Ip is the pickup current threshold of the relay. This equation is used to detect a fault in the power system. If the sum of the square of the three phase currents ($I_{a^2} + I_{b^2} + I_{c^2}$) exceeds the pickup current threshold (I_{p^2}), the relay will trip the circuit breaker to isolate the fault and prevent damage to the power system [2]. The pickup current threshold can be adjusted to provide the desired level of protection and sensitivity to the relay.

IV. METHODOLOGY

The research study utilized MATLAB Simulink software to analyze the performance of numerical relay under over-current, overvoltage, and under voltage. The simulation results were obtained using the parameters listed in Table 1. The Fig. 4 shows the one line diagram of proposed system [2].

Table I. Simulation Parameters

S.No	Parameters	Value
System Parameters		
1	Grid Voltage	132 KV
2	Power Transformer (S/D)	20 MVA/11 KV
3	Line Parameters	R=0.01 Ohm, L= 16.89 e-6 Henry
4	Frequency	50Hz
Over-current Relay		
5	Relay setting	100%
6	CT ratio	300/5
7	Fault time	0.04 Seconds
8	Relay Operating Time	0.065 Seconds
Overvoltage Relay		
9	Relay setting	10%
10	Delay Time	0.2 Seconds
11	Fault time	0.1 Seconds
12	Relay Operating Time	0.35 Seconds
Under-voltage Relay		
13	Relay setting	10%
14	Delay Time	0.2 Seconds
15	Fault time	0.1 Seconds
16	Relay Operating Time	0.33 Seconds

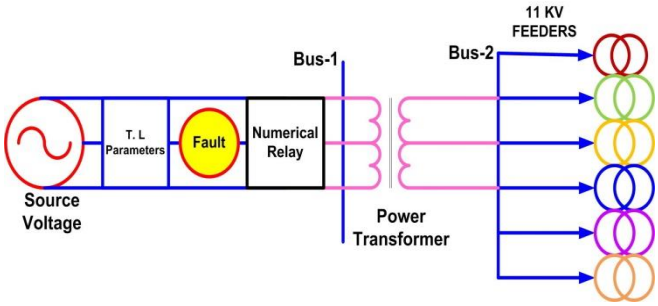

Fig. 4 Proposed System with Numerical Relay

V. RESULTS AND DISCUSSIONS

A. Power Transformer Protection under Over-current fault condition

Under this fault condition the fault occurs in all three phases and switching time of relay was initiated from 0.065 seconds with sampling time of 0.5 Seconds. It has seen that the feeder voltage has dropped and feeder current has increased to 3000 Ampere as shown in figures 5(a) and 5(b). The relay coil of numerical relay is energized and initiates the operation of circuit breaker to isolate the power transformer form the system as shown in figure 5(c).

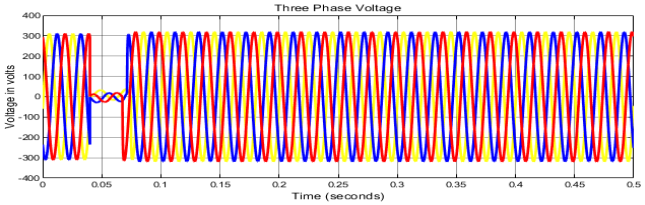

Fig. 5(a) Feeder Voltage under Fault Condition

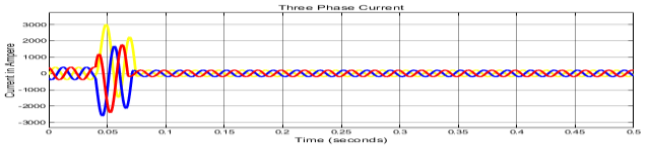

Fig. 5(b) Feeder Current under Fault Condition

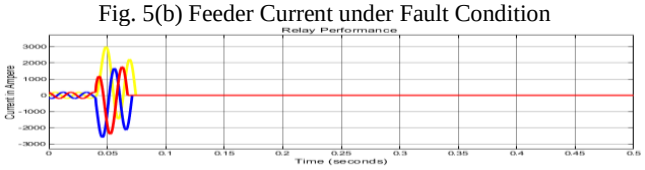

Fig. 5(c) Numerical Relay Performance under Fault Condition

B. Power Transformer Protection under Over-voltage fault condition

Under this fault condition the voltage in all phases was increased and switching time of relay was initiated from 0.35 seconds with sampling time of 0.5 Seconds. It has seen that the feeder voltage has increased up to 25% of normal value as shown in figures 6(a). The relay coil of numerical relay is energized and initiates the operation of circuit breaker to isolate the power transformer form the system as shown in figure 6(b).

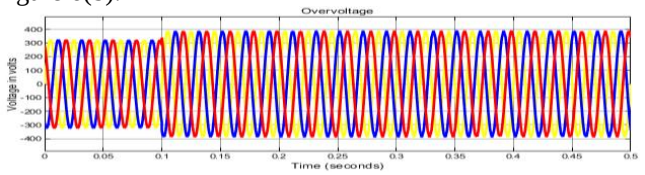

Fig. 6(a) Overvoltage Fault Condition

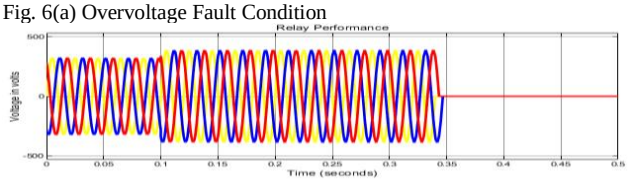

Fig. 6(b) Numerical Relay Performance under Overvoltage

A. Power Transformer Protection during under-voltage fault condition

Under this fault condition the voltage in all phases was decreased and switching time of relay was initiated from 0.33 seconds with sampling time of 0.5 Seconds. It has seen that the feeder voltage has decreased upto 12% of normal value as shown in figures 7(a). The relay coil of numerical relay is energized and initiates the operation of circuit breaker to isolate the power transformer form the system as shown in figure 7(b).

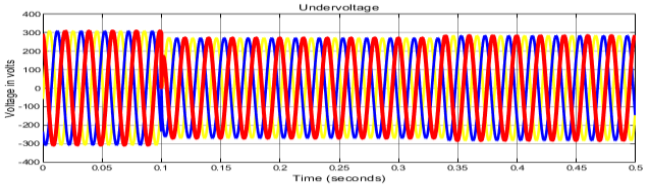

Fig. 7(a) Under-voltage Fault Condition

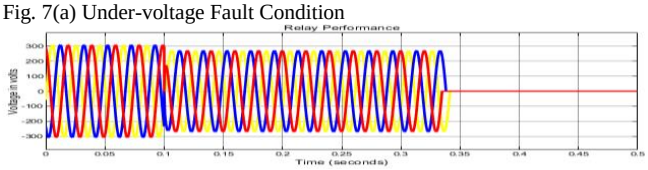

Fig. 7(b) Numerical Relay Performance under Under-voltage

C. Discussion

This study is carried out to analyze the performance of protective device for Power transformer under unbalance conditions. It has been seen that the numerical is the best selection to provide protection to transformer under different unbalance conditions. This type of relay reduces the cost of protection because multiple protections can be achieved through single device. Without protective devices the equipment's may damage or failure which give huge financial loss to the utility company and also reliability of power is badly affected.

VI. CONCLUSIONS

Numerical Relays are critical in the protection of power transformers in modern electrical systems. They are designed to detect and isolate faults that may occur in the transformer, preventing damage and ensuring the reliability of the system. The architecture of a numerical relay includes various modules such as Input, CPU, Memory, Multiplexer and Analog to Digital Converter, Output, and Digital Input/Communication. The ability to store and analyze data related to events and disturbances is essential for effective troubleshooting and maintenance of the transformer. Numerical Relays provide highly accurate and sensitive protection for power transformers, enabling quick and precise detection of faults. The use of advanced algorithms and software ensures reliable and efficient operation of the relay, reducing the risk of false tripping or failure to detect faults. In addition, the ability to customize the relay settings to match the specific requirements of the transformer enhances the effectiveness of the protection system. Overall, the use of Numerical Relays for power transformer protection is essential for ensuring the safe and reliable operation of modern electrical systems. With their advanced features and capabilities, numerical relays provide highly effective protection for power transformers, reducing the risk of damage and improving the overall efficiency and reliability of the system.

REFERENCES

[1] M. S. Ali, A. Omar, A. S. A. Jaafar, and S. H. Mohamed, "Conventional methods of dissolved gas analysis using oil-immersed power transformer for fault diagnosis: A review," *Electric Power Systems Research*, vol. 216, p. 109064, 2023.

[2] X. Miao, P. Jiang, F. Pang, Y. Tang, H. Li, G. Qu, *et al.*, "Numerical analysis and experimental research of vibration and noise characteristics of oil-immersed power transformers," *Applied Acoustics*, vol. 203, p. 109189, 2023.

[3] E. Baker, S. V. Nese, and E. Dursun, "Hybrid Condition Monitoring System for Power Transformer Fault Diagnosis," *Energies*, vol. 16, p. 1151, 2023.

[4] V. A. Thiviyanathan, P. J. Ker, Y. S. Leong, F. Abdullah, A. Ismail, and M. Z. Jamaludin, "Power transformer insulation system: A review on the reactions, fault detection, challenges and future prospects," *Alexandria Engineering Journal*, 2022.

[5] Z. Li, Z. Jiao, A. He, and N. Xu, "A denoising-classification neural network for power transformer protection," *Protection and Control of Modern Power Systems*, vol. 7, pp. 1-14, 2022.

[6] A. R. Abbasi, "Fault detection and diagnosis in power transformers: A comprehensive review and classification of publications and

methods," *Electric Power Systems Research*, vol. 209, p. 107990, 2022.

[7] M. Tajdinian, H. Samet, and Z. M. Ali, "A Sub-Cycle phase angle distance measure algorithm for power transformer differential protection," *International Journal of Electrical Power & Energy Systems*, vol. 137, p. 107880, 2022.

[8] A. J. Patil, A. Singh, and P. Scholar, "A literature review: Traditional and advanced protection schemes of power transformer," *International Journal of Engineering Research and General Science*, vol. 7, pp. 1-19, 2019.

[9] L. D. Simões, H. J. Costa, M. N. Aires, R. P. Medeiros, F. B. Costa, and A. S. Bretas, "A power transformer differential protection based on support vector machine and wavelet transform," *Electric Power Systems Research*, vol. 197, p. 107297, 2021.

[10] W. Zhang, X. Yang, Y. Deng, and A. Li, "An inspired machine-learning algorithm with a hybrid whale optimization for power transformer PHM," *Energies*, vol. 13, p. 3143, 2020.

[11] J. Zhu, S. Li, and H. Dong, "Running status diagnosis of onboard traction transformers based on kernel principal component analysis and fuzzy clustering," *IEEE Access*, vol. 9, pp. 121835-121844, 2021.

[12] E. Sadrfaridpour, T. Razzaghi, and I. Safro, "Engineering fast multilevel support vector machines," *Machine Learning*, vol. 108, pp. 1879-1917, 2019.

[13] P. Li, X. Wang, and J. Yang, "Short- term wind power forecasting based on two- stage attention mechanism," *IET Renewable Power Generation*, vol. 14, pp. 297-304, 2020.

[14] J. R. Huerta-Rosales, D. Granados-Lieberman, J. P. Amezquita-Sanchez, D. Camarena-Martinez, and M. Valtierra-Rodriguez, "Vibration signal processing-based detection of short-circuited turns in transformers: A nonlinear mode decomposition approach," *Mathematics*, vol. 8, p. 575, 2020.

[15] S. R. Thomas, V. Kurupath, and U. Nair, "A passive islanding detection method based on K-means clustering and EMD of reactive power signal," *Sustainable Energy, Grids and Networks*, vol. 23, p. 100377, 2020.

[16] Z. Zhao, J. Liu, C. Tang, Q. Zhou, and Y. Gui, "Classification of transformer winding deformation fault types by FRA polar plot and multiple SVM classifiers," in *2020 IEEE International Conference on High Voltage Engineering and Application (ICHVE)*, 2020, pp. 1-4.

[17] V. K. Sahu, "A review of various protection schemes of power transformers," *Turkish Journal of Computer and Mathematics Education (TURCOMAT)*, vol. 12, pp. 3220-3228, 2021.

[18] Z. Li, J. Cheng, and A. Abu-Siada, "Classification and Location of Transformer Winding Deformations using Genetic Algorithm and Support Vector Machine," *Recent Advances in Electrical & Electronic Engineering (Formerly Recent Patents on Electrical & Electronic Engineering)*, vol. 14, pp. 837-845, 2021.

[19] E. Awada, E. Radwan, M. Nour, A. Al-Qaisi, and A. Y. Al-Rawashdeh, "Modeling of power numerical relay digitizer harmonic testing in wavelet transform," *Bulletin of Electrical Engineering and Informatics*, vol. 12, pp. 659-667, 2023.

[20] S. Nikolovski, M. Havranek, and P. Marić, "Numerical relay protection coordination using simulation software," in *2013 36th International Convention on Information and Communication Technology, Electronics and Microelectronics (MIPRO)*, 2013, pp. 869-873.

[21] A. Abdelmoumene and H. Bentarzi, "A review on protective relays' developments and trends," *Journal of Energy in Southern Africa*, vol. 25, pp. 91-95, 2014.

[22] J. H. Harlow, *Electric power transformer engineering*: CRC press, 2003.

[23] A. C. Franklin and D. P. Franklin, *The J & P transformer book: a practical technology of the power transformer*: Elsevier, 2016.

[24] D. Wang, C. Mao, J. Lu, S. Fan, and F. Peng, "Theory and application of distribution electronic power transformer," *Electric power systems research*, vol. 77, pp. 219-226, 2007.

[25] J. Winders, *Power transformers: principles and applications*: CrC Press, 2002.

[26] H. Wrede, V. Staudt, and A. Steimel, "Design of an electronic power transformer," in *IEEE 2002 28th Annual Conference of the Industrial Electronics Society. IECON 02*, 2002, pp. 1380-1385.

[27] M. P. Ransick, "Numeric protective relay basics," in *Conference Record of 1998 IEEE Industry Applications Conference. Thirty-Third IAS Annual Meeting (Cat. No. 98CH36242)*, 1998, pp. 2342-2347.

[28] P. McLaren, G. Swift, Z. Zhang, E. Dirks, R. Jayasinghe, and I. Fernando, "A new directional element for numerical distance relays," *IEEE Transactions on Power Delivery*, vol. 10, pp. 666-675, 1995.

[29] M. Sachdev, T. Sidhu, and P. McLaren, "Issues and opportunities for testing numerical relays," in *2000 Power Engineering Society Summer Meeting (Cat. No. 00CH37134)*, 2000, pp. 1185-1190.

[30] M. M. Saha and R. Pfistner, "The state of the art of numerical relaying," *International Journal of Electrical Power & Energy Systems*, vol. 13, pp. 91-99, 1991.

[31] P. K. Gangadharan, T. S. Sidhu, and G. J. Finlayson, "Current transformer dimensioning for numerical protection relays," *IEEE transactions on Power Delivery*, vol. 22, pp. 108-115, 2006.

[32] J. Rahebi and M. M. S. Al-Shalah, "Design, Modeling and Implementation of Multi-Function Protective Relay with Digital Logic Algorithm," *Avrupa Bilim ve Teknoloji Dergisi*, pp. 549-565, 2020.

[33] A. A. Elbaset, Y. S. Mohamed, and A. N. A. Elghaffar, "IEC 61850 Communication Protocol with the Protection and Control Numerical Relays for Optimum Substation Automation System," *Journal of Engineering Science & Technology Review*, vol. 13, 2020.

[34] M. Andreev, "Investigation of processes in the measuring part of digital devices of relay protection in the MATLAB software package," *Russian Electrical Engineering*, vol. 90, pp. 530-537, 2019.

[35] S. Mitra and P. Chattopadhyay, "Design and implementation of flexible Numerical Overcurrent Relay on FPGA," *International Journal of Electrical Power & Energy Systems*, vol. 104, pp. 797-806, 2019.